UNIVERSITÁ DEGLI STUDI DI FIRENZE

Scuola di Dottorato

Progetto e Costruzione di Macchine

XIX ciclo

ING IND-14

Ph.D. Thesis

NOISE AND VIBRATION ANALYSIS IN THE MID-FREQUENCY RANGE

Prof. Giovanni Nerli Ph.D. Coordinator

Prof. Marco Pierini Ph.D. Tutor

Candidate

ALESSANDRO PRATELLESI

Florence, December 2006

UNIVERSITÁ DEGLI STUDI DI FIRENZE

Scuola di Dottorato

Progetto e Costruzione di Macchine
XIX ciclo

ING IND-14

Ph.D. Thesis

NOISE AND VIBRATION ANALYSIS IN THE MID-FREQUENCY RANGE

Prof. Giovanni Nerli Ph.D. Coordinator _____

Prof. Marco Pierini Ph.D. Tutor _____

Candidate

Alessandro Pratellesi _____

Florence, December 2006

Sapeva ascoltare, e sapeva leggere.
Non i libri, quelli sono buoni tutti, sapeva leggere la gente.
Alessandro Baricco, Novecento.

Abstract

The transmission of structure-borne noise in an automobile typically involves the dynamic interactions of a large number of substructures. In order to model structure-borne noise it is therefore necessary to describe the dynamic behavior of each structure, as well as the connectivity and dynamic interactions between the various substructures. To investigate the vibro-acoustic behavior of complex structures in the low and the high frequency range, efficient formulations are available, FEM, BEM and SEA. The most problematic frequency range is the middle one: in this frequency range vibro-acoustic behavior of complex structures express both low and high frequency characteristics, so a formulation which is able to correctly predict the behavior of a complex structure is actually needed. A number of methods have been proposed for predicting vibro-acoustic response of complex structures in the mid-frequency range, and some of them are reported in this thesis.
The aim of this work is to develop a formulation which is able to treat the vibrational behavior of a structure over the complete frequency range, while focusing especially on mid-frequency aspects.

The starting point of this work is the Smooth Integral Formulation developed by M.Viktorovitch. The Smooth Integral Formulation SIF is able to treat the vibrational behavior of a structure on the complete frequency range. This feature is due to the fact that the underlying assumptions of this formulation are very general, and are linked rather to the material description of the structure than to the frequency field of investigation. Nevertheless, this formulation shall not be utilized in the low frequency domain because the assumptions of the method have no influence in this range and moreover the number of unknowns is greater than for a classical Boundary element Method. In the high frequency field (the domain where all the subsystems have a high frequency behavior), the SIF is suitable and can be used to describe the behavior of the complete structure in a much more convenient way than it could be carried out with a classical FEM or BEM. In the mid-frequency field (the domain where some of the subsystems have a high frequency behavior and the others show a low frequency behavior), the SIF can be utilized to describe the whole structure.

In mid-frequency domain the key point is the development of hybrid formulations, where the low frequency behaving subsystems are treated with classical kinematic formulations, whereas the high frequency behaving subsystems are treated with high frequency methods. The steps from the SIF formulation and its application, towards the development of the hybrid formulation and its application, are reported in this thesis. Initially simple and isolated structures are analyzed to test the capabilities of SIF formulation, and different modelling problematics are undertaken. Then the SIF is coupled to deterministic methods, FEM and BEM, to analyze mid-frequency structures.

Summary

This work is focused on the development of a mid-frequency formulation for the vibro-acoustic analysis of complex systems.

The manuscript is organized as follows: the first chapter is an introductive part on the important of frequency analysis for structure design and in particular for the automotive structures. Also a very general overview on the structure behavior as a function of frequency is given. The second chapter is a review of the principal and widely used methods for the frequency analysis in the low- and high-frequency range. For each method, advantages and drawbacks are presented.

Chapter three is dedicated to the mid-frequency problem, introducing the behavior of mid-frequency structures and the state of the art of the development of mid-frequency formulations. In this chapter the objectives of this research project and the procedure that we have decided to follow to achieve those tasks are explained.

Chapters four and five deal with the SIF formulation which constitute the central feature of all the work. In chapter four, the theory of SIF formulation is illustrated, while in chapter five the results of the application of SIF to some simple structures are reported.

Chapters six and seven are about the use of SIF for mid-frequency predictions, the uptakes that we need to use in modelling are presented together with numerical validations. In chapter eight a new formulation for the mid-frequency analysis, based on the results of chapter seven, is developed and tested. This hybrid formulation couples FEM and SIF.

Up to chapter eight the formulations have been tested for simple 1D structures. In chapter nine the SIF formulation is extended toward 2D applications, in particular to deal with acoustic domains. The SIF is then coupled with BEM to investigate a 2D mid-frequency structure in order to evaluate the efficiency and feasibility of the hybrid method.

Chapter ten is about the final development of the hybrid method to be consistent and applicable to complex structure which vibrates in the mid-frequency range. The method is tested for FEM-SIF and BEM-SIF applications, on fluid-structure systems, and acoustical domains.

In chapter eleven there are the concluding remarks and the future perspectives.

Acknowledgements

Questo lavoro è stato realizzato all'interno del gruppo di Progetto e Costruzione di Macchine del Dipartimento di Meccanica e Tecnologie Industriali di Firenze. Desidero in particolare ringraziare il Prof. Giovanni Nerli Coordinatore del Dottorato per la costanza e la disponibilità con cui ha svolto la direzione del corso.

Ringrazio tanto il Prof. Marco Pierini, mio tutor, per la fiducia e l'entusiasmo che ha dimostrato nei miei confronti fin dall'inizio del dottorato. I suoi consigli ed il suo supporto sono stati davvero preziosi.

Vorrei ringraziare vivamente anche l'Ing. Niccolò Baldanzini, che mi ha seguito in tutti i passi della ricerca, con preziosi consigli e offrendomi importanti momenti di confronto sull'attività.

Ringrazio gli altri membri del gruppo PCM ed in particolare le persone che in questi anni hanno fatto e fanno parte del laboratorio, il mitico Bread&Fox Office.

Desidero ringraziare la RIETER Automotive di Winterthur, in quanto finanziatrice della mia borsa di Dottorato, in particolare l'Ing. Maurizio Mantovani responsabile del settore CoE Vehicle Acoustics per la fiducia e l'interesse dimostrato per il lavoro da me svolto. Ringrazio anche il Dr. Claudio Bertolini per i preziosi consigli ed i momenti di confronto sulle basi scientifiche del lavoro.

Ringrazio davvero tanto il Dr. Michel Viktorovitch, che ha avuto la pazienza e la costanza di seguirmi in modo attento ed efficace. Il suo modo di fare cordiale e la sua competenza hanno permesso che il dottorato si svolgesse in modo proficuo e sereno.

Ringrazio la mia famiglia che mi ha supportato in questi anni di studio, che ha sempre dimostrato una grande fiducia in me, e mi ha trasmesso entusiasmo e voglia di fare.
Infine vorrei ringraziare i miei amici e le persone a me vicine che non mi hanno mai fatto mancare il loro affetto e la loro stima.

Table of Contents

Chapter 1

Introduction

Vehicle manufacturers are continuously searching for ways in which vehicle refinement can be improved and its cost reduced. This involves the study of a wide range of noise sources from engine structure-borne noise to airborne tyre noise. Consumers now expect high levels of comfort and refinement from all passenger cars and no longer just in executive class models. In response, car manufacturers are placing vehicle refinement at the heart of their product development strategies with the consequence of a need of efficient, fast and reliable vibro-acoustic tools.

1.1 The sound quality

Car buyers have long been slamming car doors as one way to subjectively judge the quality of a vehicle. But as overall vehicle quality has improved, consumers have become more discerning, and the important acoustic characteristics of a vehicle today go well beyond the sounds of door slams. Increasingly, automotive interior noise levels and the "acoustic signature" of a vehicle – the way the car sounds to its occupants under various operating conditions – are becoming competitive differentiators for automakers. A sports car driver wants to hear the throaty roar of a powerful engine under heavy acceleration, for example. And for high-end vehicles, interior acoustics that enable easy conversation between front seat and back seat passengers can provide a higher perception of quality and luxury. "As basic issues such as reliability are better addressed by all of the car makers, then companies start looking for other ways to differentiate their products, and trying to give the consumer an unusually quiet or pleasing product acoustically is one of those," notes Bob Baker, staff development engineer responsible for acoustics at the General Motors Technical Center (Warren, MI).

Car companies must meet stricter environmental regulations for exterior noise and increased customer expectations for noise, vibration, ride, handling, and the overall feel, comfort and sound of the vehicle. These attributes constitute the strategically important brand value of the vehicle that differentiate competitors. A Jaguar has a certain ride, for example, while a BMW has a unique feel in the way it handles and a Harley has a distinctive sound riders want to hear from classic heavyweight motorcycles. Since noise and vibration represent such a significant contribution to the brand image of a vehicle, OEMs are vitally concerned with getting these attributes right. Developing components, subsystems and the complete vehicle to the required levels of noise and vibration characteristics by using computer-based simulation, testing and analysis tools is referred to as

NVH (noise, vibration, harshness) engineering, representing one of the most complex and strategically important aspects of automotive development.
Some aspects of the NVH engineering are listed below:

- Automotive interior noise levels declined from an average of 72 decibels in 1980 in a vehicle traveling at 55 mph to 66 decibels in 2000.

- Light weight, sound absorbing fibers and foams are replacing traditional, heavy sound barrier materials in automotive floor and dash systems.

- OEMs and suppliers are relying heavily on software simulation tools for predictive acoustic modeling that cuts the time required to develop new acoustic materials and systems.

- Major effort is aimed at tuning interior systems to eliminate extraneous noise in the 300 to 3,400 hertz voice band of human speech, as a way to make in-vehicle conversation easier.

1.2 The importance of frequency analysis

With the steadily increasing customer demands and competitive nature of the market, engineers face the challenging but complex problem of meeting the ever expanding but often conflicting design criteria. To accomplish this difficult task, the industry has become aware and convinced that a major imperative for getting insight in the sensitivity of the design criteria to the different design parameters and for making any advance beyond the very timeconsuming and expensive prototype testing approach is to apply appropriate predictive engineering methods in all stages of the design process. Along with the tightening of the legal regulations on noise emission levels and human exposure to noise, the acoustic properties of a product are often awarded a high priority on the list of design criteria. The acoustic properties are often determined by structure-borne noise, which is induced by the dynamic displacements of a mechanical structure. Since the pressure waves also cause a mechanical load on the structure and hence influence the mechanical vibrations, there is a mutual fluids-structure coupling interaction. Especially for dynamic systems in which a small acoustic cavity is enclosed by a thin-walled mechanical structure, this structural-acoustic coupling interaction cannot be neglected. Vibro-acoustic effects play a dominant role in the sound quality of transportation means such as cars, aircraft, buses and trains, as well as in industrial, environmental and domestic noise levels. It becomes apparent from the above that there is a strong need for reliable prediction tools for vibroacoustic analysis and optimal design of noise control measures [1].

1.3 Dynamic structural behavior of complex structure as a function of frequency

Generally, a complex mechanical structure can be defined as a system made of a large number of different components which exhibit large differences in terms of material and geometrical properties, and consequently have very different vibro-acoustic behaviour.

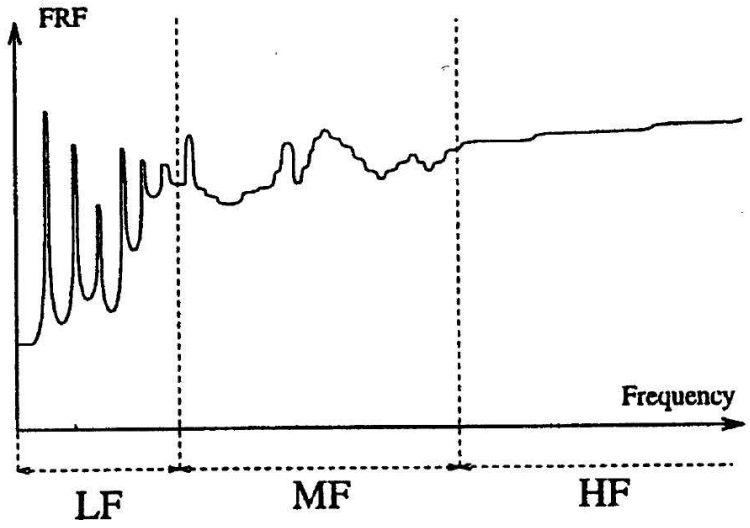

Figure 1.1: From [2], a "qualitative diagram" illustrating structural response in the low-frequency (LF), mid-frequency (MF), and high-frequency (HF) ranges.

The automotive industry is used to divide the vibro-acoustics problematic in three separate domains, according to the frequency range. The low-frequency (LF) range is identified as the domain for which the dynamic behaviour of a complex structure can be expressed in terms of magnitude and phase of the response at discrete frequencies and locations. The dimensions of the subsystems may be considered short with respect to the wavelength (short members). On the other hand, the high-frequency (HF) field is defined as the frequency range for which the components of a system are long with respect to the wavelength (long members). This range is characterized by high modal density, strong modal overlap, and an attendant smoothing effect in the frequency response. This is depicted in fig. 1.1, [2].

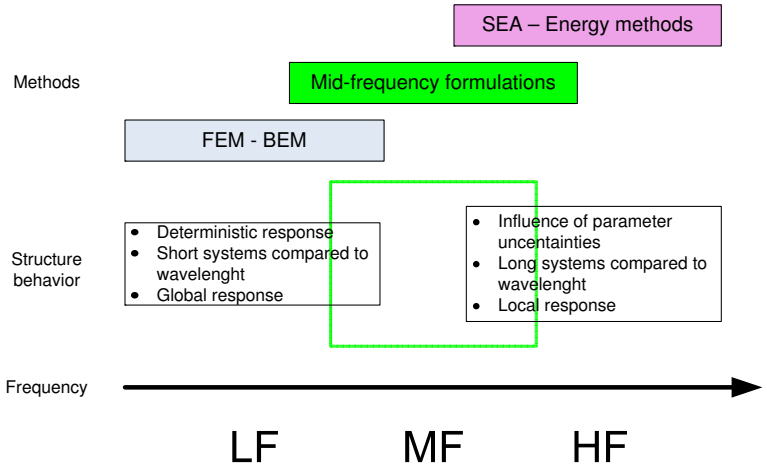

Figure 1.2: Vibro-acoustic field and methods

The low-frequency range is characterized by well-spaced modes and distinct resonant

peaks in the frequency response function. Methods which discretize the structures and solve them in terms of finite elements are used. The results obtained are accurate and it's possible to describe the vibroacoustic behavior even of complex structure, fig. 1.2.
As the frequency of analysis increases, difficulties arises. The wavelength decreases, and becomes difficult to have a model of the complex structure which is able to predict the vibroacoustic behavior. In particular the response of the system becomes sensitive to small details in its construction, its properties and its boundary conditions, which are not know to sufficient accuracy. This is due to the fact that as the frequency increases wavelength becomes comparable to the uncertainties in physical properties of the structure, which are not known exactly, so the results of model could be unrepresentative of the physical structure. The effect of this sensitiveness can be seen in figure 1.3. The FRFs of a plane plate, obtained with a Monte Carlo simulation, varying the geometrical and physical paramenters (length, thickness, width, Young modulus, density), show that above 100Hz it is no more possible to have a precise and defined response, but a spread of results, [3]. Another reason

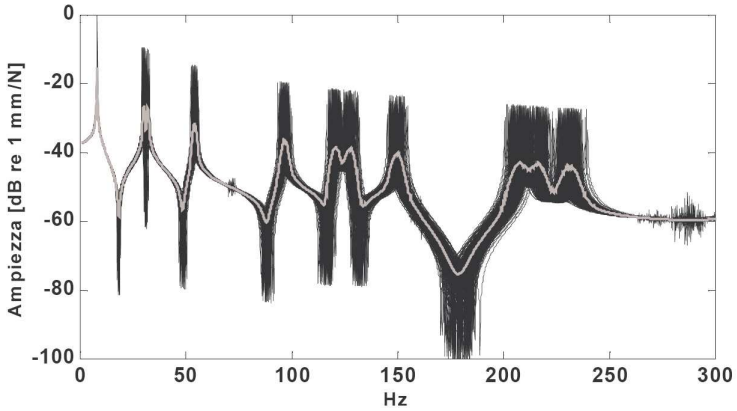

Figure 1.3: From [3], FRFs functions of a plane plate, varying the geometrical and physical parameters. Mean value (grey line) and spread (black).

is that wavelength is small in high frequency range, so using i.e. FEM method to solve the system requires elements dimensions to be small, at least six elements per wavelength should be used to produce an accurate response. The computational model becomes heavy and time to solution increases. To overcome those problems statistical methods were developed, like SEA, which give results in terms of mean value of the variables in frequency and space, so they're not influenced by structural uncertainties [4].
Finally, the mid-frequency (MF) domain is defined as a transition region. In this field, the structure is constituted of two classes of subsystems, respectively exhibiting simultaneously a LF and a HF behaviour.

Chapter 2

Review of methods for predicting the vibro-acoustic response of a complex structure

This chapter provides a qualitative description of the classical methods for the frequency analysis in the low- and high-frequency range, [1, 4, 5]. For each methods the main features are presented and the advantages are compared to the others in order to provide a useful review to better understand the mid-frequency problem which will be introduced in the next chapter, chap.3.

2.1 Deterministic FEM

The deterministic approach is based on classical mechanics. The response of each substructure is described in terms of a set of basis functions and linear equations are formulated which describe the precise coherent interactions of the various degrees of freedom in a model. Finite Element approach, [6], is effective at low frequencies (and low wavenumber) where a small number of degrees of freedom can be used to describe the response and where the precise coherent relationship between the various degrees of freedom is relatively insensitive to perturbations.
However, as the frequency increases, the finite element mesh must be refined in order to capture shorter-wavelength vibration, which can lead to a large number of DOF in a finite element model. Even without pushing the limits of fine meshes, large-scale models such as automotive vehicles can have millions of DOF, making it unwieldy to compute even the first few modes with FEA. Thus, cost is a major limiting factor for using FEA in the mid-frequency range.
In a typical FE model it is assumed that a very detailed and precise description of each substructure is necessary in order to describe its dynamic behavior. The solution of an FE model is then concerned with finding a precise coherent relationship between the response of every degree of freedom in a model as a function of frequency. At mid to high frequencies the relationship is extremely sensitive to small changes in:

1. the properties of the substructures and their boundary conditions,
2. the way in which the substructures are connected,
3. the spatial distribution of the excitation,

4. the frequency content of the excitations.

This traditional and widely used method become less useful in the presence of large amount of uncertainty.

*A*dvantages:

- Use of existing (low frequency) CAE process and software tools
- Amount of detail which can be included in the analysis

*D*isadvantages:

- Difficulty in interpreting results at higher frequencies
- Lack of insight into best choice for design changes
- Computational expenses
- Sensitivity of response not accounted for in analysis
- Amount of detail which is needed in the analysis

An obstacle for the deterministic methods, like FEM, to be applied in the mid- and high-frequency range deals with the inevitable variability in the physical realisation of (vibro-acoustic) systems. Inherent, even small, variations in geometrical component dimensions, material properties and assembly tolerances imply large variations in the mid- and high-frequency response, so that one single deterministic prediction model with nominal system property values is no longer representative for the mid- and high-frequency dynamic behaviour of all possible physical realisations of the system under study. It is more appropriate to consider a (large) population of nominally identical systems and to provide information on the ensemble averaged dynamic response and the associated confidence levels [1].

2.2 Boundary Element Method

The BEM distinguish itself as a boundary method, meaning that the numerical discretization is conducted at reduced spatial dimension. For example, for problems in three spatial dimensions, the discretization is performed on the bounding surface only; and in two spatial dimensions, the discretization is on the boundary contour only, figure 2.1. This reduced dimension leads to smaller linear systems, less computer memory requirements, and more efficient computation. This effect is most pronounced when the domain is unbounded. Unbounded domain needs to be truncated and approximated in domain methods. The BEM, on the other hand, automatically models the behavior at infinity without the need of deploying a mesh to approximate it, [7, 8, 9].
Depending on the complexity of geometry and load case, this can lead to important time saving in the creation and modification of the mesh.
A basic feature of all Boundary Element Methods is their use of fundamental solutions, which are analytically free space solutions of the governing differential equation under the action of point source. The fact that they are exact solutions accounts for some of the advantages of the BEM, viz., the improved accuracy in the calculation of stresses and exterior problems.

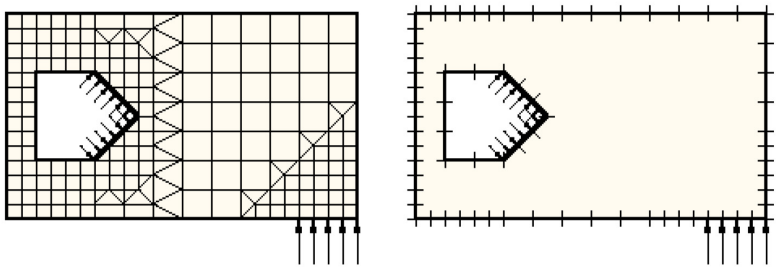

Figure 2.1: Discretisation of a FEM model (left) and of a BEM model (right)

*A*dvantages:

- Discretization of the boundary only
- Simplified pre-processing, e.g., data input from CAD can be discretised directly
- Improved accuracy in stress concentration problems.
- Simple and accurate modeling of problems involving infinite and semi-infinite domains.
- Simplified treatment of symmetrical problems (no discretisation needed in the plane of symmetry).

*D*isadvantages:

- Non-symmetric, fully populated system of equations in collocation BEM.
- Requires the knowledge of a suitable fundamental solution.
- Frequency dependent fundamental solution.
- Treatment of inhomogeneous and non-linear problems.

2.3 Spectral Elements, Waveguide Analysis

One of the main problem with a FE model (which employs elements based on low order polynomials) is that the basis function used in analysis are not well suited to describing short wavelength behavior. The response of certain substructures can be represented more efficiently using exponential shape functions. This is typically the case if a subsystem is long in one direction (in comparison with the wavelength of deformation). The subsystem can then be described as a one-dimensional waveguide which supports various propagating and evanescent wavetypes. If the deformation of the cross-section can be described analytically then an exact representation of the response of the waveguide is possible, at a given frequency of interest [10]. The extension of the approach to higher dimensional substructures (such as arbitrarily shaped plates, shells and acoustic cavities) is problematic. The approach lacks of generality, and can be characterized as a deterministic low frequency/low wavenumber method.

*A*dvantages:

- Less computational expense than a (traditional) FE model
- Provides physical insight into the dynamic behavior of various substructures (types of propagating waves, cut-on frequencies, dispersion properties ...)

*D*isadvantages:

- Does not provide a general approach for all substructures
- Lack of insight into best choice for design changes
- Computational expenses
- Sensitivity of response not accounted for in analysis

2.4 Energy Influence Coefficients and Energy Flow models

If the excitations applied to various substructures are uncorrelated then an alternative way to describe the response of a system is in terms of a relationship between the total energy contained in each substructure, and the external power input to each substructure. For a linear system is always possible to write this relationship as a matrix whose entries vary as a function of frequency so that $E = AP_{in}$. The matrix A is referred to as a matrix of energy influence coefficients, [11]. Since the energy influence coefficients provide information about the way in which energy flows (or is distributed) through a system, the approach is often referred to as an energy flow model. In general the matrix A is fully populated and asymmetric. In order to provide a complete description of a given system it is therefore necessary to compute all entries of the matrix A as a function of frequency. The energy influence coefficients can be measured experimentally, or they can be determined from a detailed FE model [12, 13].
An FE computed Energy Flow Model can be viewed as a postprocessing operations which provides insights into the influence of various uncorrelated excitations on the response in certain regions of a system. The approach is still based on a deterministic description of the system and is therefore a deterministic low frequency/low wavenumber method.

*A*dvantages:

- Use of existing (low frequency) CAE process and software tools
- Amount of details which can (in principle) be included in the analysis
- Insight into the influence of various excitations on overall response.

*D*isadvantages:

- Energy Influence Coefficients not directly related to physical parameters used in design (ie. effects of isolations, local damping modifications ...)
- Entire matrix of Energy Influence Coefficients needs to be recomputed when a design change is made
- Sensitivity of response not accounted for in analysis
- Amount of details which is needed in the analysis

- Computational expense

In an attempt to improve upon the heat conduction approximation, Le Bot and Jezequel recently introduced a local energy flow approach. This is a wave-based approach, in which it is assumed that the energy density is a sum of the energy quantities of each propagative field. In addition, the Huygens principle is used, so that the energy is assumed to be a superposition of the direct field and the reverberant field. The direct field is created by primary (actual) sources in the domain. The reverberant field is considered to be created by secondary (fictive) sources located at the boundary of the domain. Based on this approach, the local energy results are found to be "a direct prediction of the mean values of expected dynamical levels". The local energy flow approach has been applied to coupled plates [15, 16].

2.5 Statistical Energy Analysis (SEA)

The Statistical Energy Analysis (SEA) is widely employed for solving high-frequency problems [10, 14, 17, 18, 19]. SEA is a sub-structuring analysis method which is aimed at predicting the energy levels space and frequency averaged. SEA is generally used for structure-borne or air-borne excitations, even though the former set of applications might not be straightforward, depending on the complexity of the modelled structure (definition of junctions, power inputs...). Employing relevantly the SEA requires to verify some hypotheses: the structure shall be non-zero damped, input powers shall be uncorrelated and the subsystems weakly coupled, the system shall present a reverberant field. Furthermore, the modal density of each subsystem shall be high; usually those requirements are not completely verified for realistic industrial structures.
The SEA method considers the relationship between the input power and the subsystem energy which is given by $P_{in} = HE$. This relationship holds for any linear system with non-zero damping and uncorrelated input powers. If the substructures are assumed to be represented by various "subsystem" of weakly coupled local modes, then it can be shown that the entries of H take on a particular physical significance and can be related to parameters which describe :

(i) the local dissipation of energy within a subsystem (represented by by damping loss factor parameter),

(ii) the energy storage capacity of a subsystem (modal density), and

(iii) the rate at which energy flows between adjacent subsystem (coupling loss factor CLF).

Typically, statistical estimates of these parameters are used to define the entries of H.
If the subsystem are weakly coupled [20] then the flow of energy between adjacent subsystems is typically only a function of the local properties of the subsystems and the various junction in a model. Statistical estimates of the coupling loss factors can therefore be obtained by considering the way in which the waves incident on a local junction are scattered into adjacent subsystems. Such analysis are available for calculating the coupling loss factors for (canonical) point, line and area junctions [21, 22]. The modal loss factor calculations can be automated in software and an SEA model of a general system obtained from a fairly coarse description of the system.
The computational expense of a deterministic analysis is therefore reduced in SEA by considering the ensemble average dynamic behavior of a collection of subsystems.

*A*dvantages:

- Use of existing (low frequency) CAE process and software tools
- Very little detail required to describe (ensemble average) dynamic behavior
- Highly efficient and requires very little computational expense
- Accounts for uncertainty in the properties of the system
- Provides direct into effects of design changes (ie. effect of isolation, local damping modifications . . .)

*D*isadvantages:

- In some instances CLFs of simplified canonical junctions do not capture the detailed dynamic behavior of a given complex junction
- An analytical SEA model assumes certain form for the matrix H (ie. no indirect CLFS, symmetry of modal CLF matrix), which is only guaranteed to be exact if the system is weakly coupled. A system is typically weakly coupled at high frequencies but may not necessarily be weakly coupled at mid and low-frequencies
- The strength of the coupling is a function of how a system is discretized into subsystems. At mid and low frequencies the most appropriate choice of subsystems can be problematic (and require the use of expert knowledge, prior experience and, in some instances, empiricism).

2.6 Continuum Thermal Analogies

The flow of vibrational energy between weakly coupled subsystems in SEA is analogous to the way in which heat flows between two bodies of different temperature in a thermal analysis. So it has been postulated that the heat conduction equation can be used to model the flow of vibrational energy in a continuum, [23, 24, 25, 12]. It is certainly tempting to adopt a thermal analogy from an implementation point of view since the heat conduction equation is easier to solve than the wave equation and presents less numerical challenges. Such an approach has been referred as '*the energy finite element method*', '*power flow finite elements*', '*the energy boundary element method*'.
However, the main drawback of this approach concerns the validity of its theoretical background when dealing with two and three dimensional systems [26, 27].
The heat conduction equation arises from the application of statistical mechanics to dynamic systems in which the response of adjacent degrees of freedom are weakly correlated (The conduction of heat in a body relates to the incoherent transfer of momentum between vibrating molecules). The spatial incoherence of the response is therefore a central assumption of the analysis. One of the main motivations for applying the energy finite element method appears to be to predict spatial gradients in the energy density in a reverberant field. However, one of the findings of room acoustics is that the energy density in a reverberant field is generally spatially uniform [28]. When local concentrations of energy occur, they are primarily due to coherent interactions of the reverberant field with known boundary conditions [29]. Such gradients are not predicted by the energy finite element method and one is therefore led to question what spatial variations are in fact being predicted.

*A*dvantages:

- Ease of implementation

*D*isadvantages:

- No rigorous theoretical basis for 2D or 3D wavefields
- Does not recover the direct field of sources or the coherent scattering that occurs at junctions/boundaries
- Requires calculation of the same junction CLFs as SEA
- Cannot capture the resonant effects in the behavior of a system comprised of short and long members.

In the energy methods, the amount of power transferred between members at a joint is estimated in terms of coupling loss factors (SEA) or power transfer coefficients (in EFEA). The value of coupling loss factors or the power transfer coefficients are computed from analytical solutions of semi-infinite members, [10]. The computations are meaningful when the connected members are long, thus the power transfer characteristics of the long members can be considered the same with the power transfer characteristics of the semi-infinite members. The requirement for high modal overlap is necessary because the information produced by the analytical solutions of the semi-infinite members captures the exchange of power flow between members when there is an equal amount of coupling between the normal modes of the members. If large difference exist in the power flow due to the distinct resonant behavior of the short members, then the power transfer characteristics cannot be estimated properly from analytical solutions of semi-infinite members [30].

Chapter 3

The Mid-Frequency range

The mid-frequency (MF) domain is defined in this work as a transition region. In this field, the structure is constituted of two classes of subsystems, respectively exhibiting a LF and a HF behaviour. A proper method for this range should be able to account for all the different vibrational contributions exhibited by the system, it is necessary to account for both the coherent global and incoherent local motion of a system. None of the methods listed in chapter 2 satisfy this requirements. The deterministic methods (FEM, BEM and Waveguide Analysis) can provide a good description of the strongly coherent behavior of certain subsystems, but provide a poor description of the weakly coherent behavior of other subsystems. Similarly, SEA provides a good description of the weakly coherent behavior of certain subsystems but provides a poor description of the strongly coherent behavior of other subsystems.

In this chapter the mid frequency problem is presented , sec. 3.1, and some interesting mid-frequency methods which have been developed recently, sec. 3.2.

Finally, sec. 3.3, it is presented the point of view of the authors about the possible solution to the mid-frequency problem, and the chosen strategy is introduced.

3.1 The Mid-Frequency problem

Consider now the problem of predicting the dynamic response of a complex system which consists of a large number of coupled structural-acoustic subsystems, some of which may be "statistical" and some of which may be deterministic. If all the subsystems are statistical then the transmission of energy throughout a system is typically well characterized using SEA model (the transmission of energy tends to be dominated by the local interactions of the various subsystem). If all the subsystems are (well) below their acoustic limits (the acoustic limit represents a saturation point in the statistics of the natural frequencies of a subsystem, above the acoustic limit, the statistics of the natural frequencies can be defined using simple probability laws based on the expected modal density of a given subsystem) and each has an extremely small statistical overlap then the response is typically well characterized using a global FE modal.

The frequency range over which the subsystem are neither completely deterministic nor completely statistical is termed the "mid-frequency range". The problem of predicting the dynamic response of a system in the mid-frequency range is termed the "mid-frequency problem" [31].

In the mid-frequency range some members in a system are long while other members are

short. In the mid-frequency range the FEA method requires a prohibiting large number of elements to perform an analysis due to the presence of the long members. In addition, high computational resources are required in order to produce frequency-averaged FEA results that constitute a meaningful representation of the ensemble-average response of a system with uncertainty. The energy methods (SEA and EFEA) contain assumptions that are valid when all components of a system are long. Employing relevantly the SEA requires to verify some hypotheses: the structure shall be non-zero damped, input powers shall be uncorrelated and the subsystems weakly coupled, the system shall present a reverberant field. Furthermore, the modal density of each subsystem shall be high. It is generally recognized that, in addition to other conditions, each subsystem must ideally contain a great number of resonant modes over the analysis band of interest. One implication of this condition is that the wavelength of the subsystem deformation must be of the same order as, or less then, the dimensions of the subsystem. In some cases this requirement may be only partially met: for example, in-plane waves in a plate are generally of much longer wavelength than bending waves, so that while the bending motion might meet the SEA requirement, the in-plane motion might not. Such difficulties can, in some cases, be overcome by employing problem specific modeling techniques within SEA, [32]. The so-called structural SEA aims at treating the structure-borne contribution of a car from a few hundred Hertz upward, by means of the SEA. For this purpose, the authors developed a methodology to define in a reliable way the subsystems of a structure without violating the basic assumptions of the SEA. Beside these specific modeling techniques, it is true to say that a general approach is lacking [33]. The assumption of a small wavelength with respect to the dimension of a member in the EFEA is similar to the assumption of high modal overlap in SEA. The requirement for small wavelength in the EFEA allows to neglect the near-field effects in the wave solution and allows to consider a reverberant behavior for all the members in a system during the development of the governing differential equations. Thus the energy methods cannot capture the resonant effects in the behavior of a system in the mid-frequencies, the resonant effect are generated from the presence of short members, [30]. Therefore SEA and FEA, while both are extremely useful in their respective frequency regions, can leave an empty gap in the mid-frequency range, where the modal density is not high enough for frequency averaging to give reliable results, but where a number of modes are present which can make the FEA unwieldy.

3.2 Mid-Frequency methods

In view of some characteristic properties of the mid-frequency dynamic behaviour of vibro-acoustic systems, the prediction techniques should meet the following requirements:

- The prediction techniques must be applicable for general, real-life vibro-acoustic engineering applications.
- In contrast with SEA models, in which all local information is lost, the prediction techniques should still provide detailed information on the spatial distribution of the mid-frequency response variables within the various components of the considered vibro-acoustic system.
- The prediction techniques must account for the effects of product and process variability and provide ensemble statistics of the mid-frequency dynamic behaviour.
- Many engineering structures, especially built-up structures such as vehicles, trains, truck cabins, etc., have a particular mid-frequency dynamic behaviour: parts of

the structure consist of stiff and strongly connected components that still exhibit long wavelength dynamic deformations in the mid-frequency range, while other parts exhibit already a highly resonant behaviour with short wavelength deformations. The mid-frequency prediction techniques should enable a hybrid modelling approach in which the long wavelength components are modelled deterministically, while the short wavelength components are described in a probabilistic manner.

Three main approaches are used to deal with the mid-frequency range:

1. Pushing low-frequency analysis higher
2. Pulling the high-frequency analysis lower
3. Specialized and hybrid techniques.

3.2.1 Pushing low-frequency analysis higher

A first methodology consists of developing a deterministic technique with an enhanced computational efficiency compared to the conventional element based techniques. In this way, the practical frequency limitation can be shifted towards the mid-frequency range and statistical information on the prediction results can be obtained through efficient Monte Carlo simulations or through special-purpose stochastic procedures.

A popular approach for generating reduced order models systematically from finite element models is component mode synthesis. In component mode synthesis (CMS), a complex structure is partitioned into several component structures or substructures. (In this study, the terms "components," "component structures," and "substructures" are used interchangeably). The vibration of the full complex structure is represented by a set of modes selected for each component structure, plus a set of vectors that are used to couple the components at their interfaces. The CMS approach has several advantages. Through substructuring, the model sizes for the required finite element calculations are reduced from the order of system DOF to the order of component DOF. Another clear computational advantage is that the final system model can be significantly smaller than the original finite element model while retaining excellent accuracy for a frequency range of interest. Furthermore, since the component models are separated, the components can be designed and re-designed separately before being assembled in the dynamic analysis. The most popular CMS method seems to be the Craig-Bampton method [34]. It is an exceptionally efficient and stable method, and it has been implemented in many commercial software programs.

3.2.2 Pulling the high-frequency analysis lower

A second methodology consists of improving the applicability of probabilistic techniques towards mid-frequency modelling by relaxing some of the most stringent assumptions of conventional SEA, as is proposed in the Wave Intensity Analysis [35]. Langley examined the assumption of equipartition of vibration energy among the resonant modes, which is equivalent to assuming diffuse wavefields in each structural component. He noted that the diffuse wavefield assumption of SEA can lead to poor results due to the filtering effect of interfaces between components. Langley relaxed this assumption by modeling the vibrational wave intensity with a Fourier series. By taking a single Fourier term, the conventional SEA formulation is found.

There have been many other efforts toward improving SEA estimates of coupling loss factors and power flow. Simmons [36] used finite element models to calculate coupling loss factors and power flow through plate junctions. Maxit and Guyader [37, 38] have also presented a method for using finite element models to determine SEA coupling loss factors. Also Scippa et al. [39] developed a method to complement the modelling capabilities and overcome the main limitations of the current and purely analytical methods employed to derive CLF values. An hybrid approach is used which integrates travelling wave and finite element analysis (FEA). Yan et al. [40] implemented this type of combined FEA/SEA approach in commercial software. They used NASTRAN to calculate impedance matrices at every driving frequency, and post-processed them to obtain coupling loss factors. These coupling loss factors were then used in AutoSEA, the commercial SEA code, to find the system response in the mid-frequency range.

3.2.3 Specialized and hybrid techniques

In this section, techniques that specifically target the mid-frequency range are covered. These methods are notable in that they employ hybrid techniques and/or new approaches to the modeling and analysis of mid-frequency vibration in complex structures.
A large part of this section is dedicated to Langley and Vlahopoulos formulations because they are actually the most studied, applied and promising formulations for the mid-frequency range. They have been implemented (or being implemented actually) in commercial software. Moreover the key concept introduced by those formulations an the one of Soize are very important to understand easily and properly the formulations developed in this work.

Fuzzy structure theory

C.Soize

Fuzzy Structure Theory was introduced by Soize et al. in 1986 [41] as a way to handle the mid-frequency dynamic analysis of systems with structural complexity. Since then, further developments have been presented by Soize [2, 42] and by Soize and Bjaoui [43]. The basic approach is to treat a structure as a combination of a primary structure and a number of secondary structures and attachments. The primary structure is called the master structure, and it is the part of the structure that can be modeled deterministically using conventional techniques such as finite element analysis. The complement to the master structure consists of substructures having complexities that cannot be easily modeled and/or properties that are not precisely known. For this reason, they are referred to as fuzzy substructures. The entire system, consisting of the master structure plus fuzzy substructures, is called a fuzzy structure.

The key concept in fuzzy structure analysis is that fuzzy substructures act like vibration absorbers due to high modal density above their first resonant frequency, and the corresponding transfer of energy from the master structure to the fuzzy substructures acts like added damping for the overall structural response.

The objective of the method is to predict the effect of fuzzy substructures on the response of the master structure-the response of the fuzzy substructures is not sought. The model thus employs a random boundary impedance operator, $\mathbf{Z}_{fuz}(\omega)$, which represents the effect of the fuzzy substructures on the master structure. This impedance is a sum of

the impedances for the L fuzzy substructures:

$$\mathbf{Z}_{fuz}(\omega) = \sum_{l=1}^{L} \mathbf{Z}^{l}_{fuz}(\omega) \tag{3.1}$$

The equations of motion for the fuzzy structure are written as:

$$i\omega(\mathbf{Z}(\omega) + \mathbf{Z}_{fuz}(\omega))\mathbf{U}(\omega) = \mathbf{f}(\omega) \tag{3.2}$$

where $\mathbf{Z}$, $\mathbf{U}$, and $\mathbf{f}$ are the impedance, displacement, and forcing for the master structure. The fuzzy substructures do not add degrees of freedom to the model. Soize developed a recursive method to find the random solution [42]. Alternatively, a solution can be found using Monte Carlo simulation.

Hybrid FEA/SEA formulation - Vibro-Acoustic Analysis of complex systems

P.J.Shorter, R.S.Langley

In order to bridge the gap between FEA and SEA, it seems reasonable to seek a hybrid method in which some components are modeled by FEA and some by SEA. In 1999, [33] introduced an approach to modeling mid-frequency vibration that combines both a low-frequency deterministic approach for the global structure and a high-frequency SEA approach for certain substructures. In addition, elements of fuzzy structure theory [42] and Belyaev's smooth function approach [44, 45] are incorporated. Further developments of this hybrid technique have been reported by Shorter and Langley [46, 47].
The following part belongs to the recent article of Langley and Shorter, [47].

The hybrid FEA/SEA method is based on partitioning the response of the system into global and local components. The distinction between the two types of components is based on their corresponding wavelengths of the response. The global component was intended to capture long wavelength deformations, whereas the local component was related to short wavelength deformations. The solution method consisted of a deterministic model of the global response and an SEA model of the local response. The global equations of motion included a contribution to the dynamic stiffness matrix and the forcing vector arising from the presence of the local response. The main effect of the local mode dynamics was to add damping and effective mass to the global modes, similar to the fuzzy structure theory. The local mode response was computed using SEA. This equation included an input power term which originated from the presence of the global modes. The proposed method provides a flexible way to account for necessary deterministic details in a vibro-acoustic analysis without requiring that an entire system be modeled deterministically.
The term complex is used to indicate that the properties of certain subsystems of a system are not known to a high enough level of precision to justify (or warrant) the use of a deterministic analysis. Such subsystems typically support several propagating wave-types (with many directions of propagation) and are large in comparison with a wavelength.

Consider the Vibro-Acoustic system illustrated in fig. 3.1. The system consists of a number of coupled subsystems excited by a spatially distributed load. Each subsystem consists of a domain Ω and a boundary Γ. It is assumed that the boundary of each subsystem can be decomposed into a region that is known precisely (termed the deterministic boundary), and a region that is known imprecisely (termed the reverberant boundary).

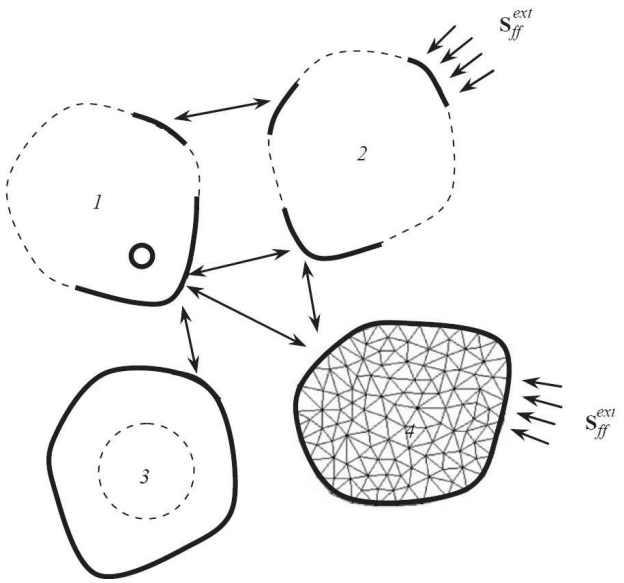

Figure 3.1: From [47], a system that comprises of a number of coupled subsystems: solid line indicates deterministic boundary, dashed line indicates random boundary, double arrow indicates a junction, single arrow indicates a distributed excitation (mesh used to indicate that a subsystem is entirely deterministic).

Regions of the boundary that allow energy to be transferred into a subsystem (due to external excitations or coupling to adjacent subsystems), are termed connection regions. The connection regions of a subsystem form part of the deterministic boundary. For example, the deterministic boundary might be defined to be the region of the boundary that lies within a few wavelengths of the connection regions of a subsystem (in a given frequency range of interest). In some instances, the deterministic boundary of a subsystem might represent the entire subsystem boundary; the subsystem is then said to be deterministic. Subsystems which are not deterministic are said to be statistical. The connection regions of different subsystems are coupled together by various junctions. Each junction typically involves several connection regions. It is assumed that all connection regions associated with a given junction are coincident and have compatible displacement fields (this assumption is not essential but simplifies the description of a junction). The junctions can be separated into three types: (*i*) those that involve only deterministic subsystems, (*ii*) those that involve a mix of deterministic and statistical subsystems and (*iii*) those that involve only statistical subsystems. These junctions are referred to as: (*i*) deterministic junctions, (*ii*) hybrid junctions and (*iii*) statistical junctions, respectively.
A set of generalized coordinates with degrees of freedom $\mathbf{q}_1$ can be chosen to describe the displacement response of the deterministic subsystems. The degrees of freedom $\mathbf{q}_1$ therefore also describe the displacement fields across the deterministic and hybrid junctions. In order to describe the displacement field across the statistical junctions in a model, it is necessary to define an additional set of generalized coordinates with degrees of freedom $\mathbf{q}_2$. The degrees of freedom $\mathbf{q}_1$ and $\mathbf{q}_2$ may be combined to form a single set of degrees of freedom $\mathbf{q}$, where $\mathbf{q}_1 = [\mathbf{q}_1^T \quad \mathbf{q}_2^T]^T$. The degrees of freedom $\mathbf{q}$ are deterministic and fully define the displacement field across all deterministic subsystems and across all connection regions within a system.

The contribution to the global dynamic stiffness matrix arising from the deterministic subsystems can be obtained at a given frequency of interest ω (using, for example, a finite or boundary element model), and written as $\mathbf{D}_d(\omega)$. In general, the deterministic subsystems will be non-conservative and the dynamic stiffness matrix $\mathbf{D}_d(\omega)$ will therefore be complex. The uncoupled equations of motion for the deterministic subsystems can then be written as

$$\mathbf{D}_d\mathbf{q} = \mathbf{f}_d \tag{3.3}$$

where $\mathbf{f}_d$ is a vector of generalized forces applied to the deterministic degrees of freedom $\mathbf{q}$. Consider a statistical subsystem, it is shown that the response of a statistical subsystem with an uncertain boundary can be described in terms of the superposition of: (i) a direct field and (ii) a reverberant field. The direct field describes the outgoing displacement field associated with a prescribed displacement of the deterministic boundary, in the absence of the random boundary. The reverberant field satisfies: (i) a blocked boundary condition across the deterministic boundary and (ii) the prescribed boundary condition across the random boundary, when added to the direct field. The direct field is independent of the properties of the random boundary; the reverberant field is extremely sensitive to the properties of the random boundary.
The uncoupled equations of motion for the mth statistical subsystem can be derived using a direct boundary element method and written as [46]:

$$\mathbf{D}_{dir}^{(m)}\mathbf{q} = \mathbf{f} + \mathbf{f}_{rev}^{(m)} \tag{3.4}$$

where $\mathbf{D}_{dir}^{(m)}$ is the direct field dynamic stiffness matrix for the m^{th} statistical subsystem $\mathbf{f}$ is a vector of generalized forces and $\mathbf{f}_{rev}^{(m)}$ is the blocked reverberant force on the connection degrees of freedom. The direct field dynamic stiffness matrix describes the force on the connection degrees of freedom due to the generation of a direct field in the mth subsystem (in the absence of the random boundary).
Assembling the equations of motion for the statistical and deterministic subsystems. eqs. (3.3) and (3.4), gives:

$$\mathbf{D}_{tot}\mathbf{q} = \mathbf{f}_{ext} + \sum_m \mathbf{f}_{rev}^{(m)} \tag{3.5}$$

where $\mathbf{f}_{ext}$ is the vector of generalized forces applied to the coupled system arising from external excitation, and where

$$\mathbf{D}_{tot}\mathbf{q} = \mathbf{D}_d + \sum_m \mathbf{D}_{dir}^{(m)} \tag{3.6}$$

The total dynamic stiffness matrix for the system $\mathbf{D}_{tot}$ is found by adding the dynamic stiffness of the deterministic subsystems to the direct field dynamic stiffness of the statistical subsystems, eq. (3.6).
Writing eq.(3.5) in crossspectral form and averaging over an ensemble of random boundaries gives

$$\langle \mathbf{S}_{qq} \rangle = \mathbf{D}_{tot}^{-1} \langle \mathbf{S}_{ff} \mathbf{D}_{tot}^{-H} \rangle \tag{3.7}$$

It can be shown [46] that as the amount of uncertainty regarding the properties of the random boundaries of the statistical subsystems increases, the blocked force in eq.(3.7) tends to the following limit

$$\langle \mathbf{S}_{ff} \rangle = \mathbf{S}_{ff}^{ext} + \sum_m \mathbf{S}_{ff}^{(m),rev} \tag{3.8}$$

where the cross-spectrum of the blocked reverberant force associated with the reverberant field of the mth subsystem is given by

$$\mathbf{S}_{ff}^{(m),rev} = \alpha_m Im\mathbf{D}_{dir}^{(m)} \tag{3.9}$$

The constant of proportionality α_m is related to the (ensemble average) incident power in the reverberant field of the mth subsystem.
Inserting eqs.(3.8) and (3.9) into eq.(3.7) gives

$$\langle \mathbf{S}_{qq} \rangle = \mathbf{D}_{tot}^{-1} \Big(\mathbf{S}_{ff}^{ext} + \sum_m \alpha_m Im\mathbf{D}_{dir}^{(m)} \Big) \mathbf{D}_{tot}^{-H}. \tag{3.10}$$

Eq.(3.10) is an exact expression for the ensemble average response of a system of coupled subsystems with uncertain boundaries (that possess the statistics discussed previously). In order to solve eq.(3.10), it is necessary to determine the (ensemble average) amplitudes α_m of the reverberant fields in the statistical subsystems. However, the amplitudes of the reverberant fields are functions of the response $\langle \mathbf{S}_{qq} \rangle$; eq.(3.10) does not therefore contain enough information for an explicit calculation of the response. The additional information that is needed to solve eq.(3.10) is introduced by considering conservation of energy in the reverberant fields of the statistical subsystems, when averaged across the ensemble. The ensemble average amplitudes of the reverberant fields am can then be found by solving a set of linear simultaneous equations (similar in form to the symmetric SEA equations).
The solution procedure for the method derived previously is summarized below:

System definition

1. A system is partitioned into a set of coupled subsystems. Connection regions are specified on each subsystem.

2. The boundary of each subsystem is partitioned into a deterministic region and a reverberant region. This definition (along with the choice of sub-structuring) explicitly defines the parts of a system that are assumed to be known deterministically. Typically, the decomposition of the boundary is based on an estimate of the propagating wavelengths within a given subsystem (in many instances this step may simply consist of a statement that subsystems smaller than a wavelength are modelled deterministically).

3. Degrees of freedom are specified for: (a) the deterministic subsystems and (b) the statistical junctions in a system.

Assembly of direct field equations

4. The dynamic stiffness matrix for the deterministic subsystems $\mathbf{D}_d$ is obtained at a given frequency of interest using, for example, a finite or boundary element analysis. The excitation applied to the system is specified in terms of a cross-spectral matrix at a given frequency of interest $\mathbf{S}_{ff}^{ext}$.

5. The direct field dynamic stiffness matrix $\mathbf{D}_{dir}^{(m)}$ is calculated for each statistical subsystem. In general, this dynamic stiffness can be found from a boundary element analysis; however, in many instances the dynamic stiffness can be found analytically for canonical point, line and area connections to common subsystems (with an assumption that the response of distant connections to the same subsystem are incoherent).

6. The total dynamic stiffness matrix for the system is then assembled

$$\mathbf{D}_{tot}\mathbf{q} = \mathbf{D}_d + \sum_m \mathbf{D}_{dir}^{(m)} \tag{3.11}$$

Assembly of reverberant field equations

7. The input power to each statistical subsystem due to the external excitation is calculated using equation

$$P_{in,0}^{(m)} = \frac{\omega}{2} \sum_{jk} Im\{D_{dir}^m\}_{jk} (\mathbf{D}_{tot}^{-1} \mathbf{S}_{ff}^{ext} \mathbf{D}_{tot}^{-H})_{jk}. \tag{3.12}$$

8. The power transfer coefficients (or coupling loss factors) are then calculated using equation

$$h_{nm} = \frac{2}{\pi} \sum_{jk} Im\{D_{dir}^m\}_{jk} (\mathbf{D}_{tot}^{-1} Im\{\mathbf{D}_{dir}^{(n)}\} \mathbf{D}_{tot}^{-H})_{jk}. \tag{3.13}$$

   (looping over the excited and receiving statistical subsystems).

9. The total power transfer coefficients are calculated for each statistical subsystem using equation

$$h_{tot,m} = \frac{2}{\pi} \sum_{jk} Im\{D_{tot}\}_{jk} (\mathbf{D}_{tot}^{-1} Im\{\mathbf{D}_{dir}^{(n)}\} \mathbf{D}_{tot}^{-H})_{jk}. \tag{3.14}$$

10. The modal overlap factors are calculated for each statistical subsystem using equation

$$M_m = \omega n_m \eta_m. \tag{3.15}$$

11. The reverberant power balance equations are assembled for the statistical subsystems using equation

$$\begin{bmatrix} M_1 + h_{tot,1} - h_{11} & \dots & -h_{1m} \\ \vdots & \ddots & \\ -h_{m1} & & M_m + h_m^{\alpha} + \sum_{n \neq 1} h_{m1} \end{bmatrix} \begin{bmatrix} \frac{E_1}{n_1} \\ \vdots \\ \frac{E_m}{n_m} \end{bmatrix} = \begin{bmatrix} P_{in,0}^{(1)} \\ \vdots \\ P_{in,0}^{(m)} \end{bmatrix}, \tag{3.16}$$

and the external input powers found at step 7.

Solution for reverberant response and response recovery

12. The reverberant power balance equations in equation (3.16) are solved to find the ensemble average modal energy density in the reverberant field of each statistical subsystem.

13. The reverberant energy levels are inserted into equations

$$\langle \mathbf{S}_{qq} \rangle = \mathbf{D}_{tot}^{-1} \Big(S_{ff}^{ext} + \sum_{m} \alpha_m Im\{\mathbf{D}_{dir}^{(m)}\} \Big) \mathbf{D}_{tot}^{-H}, \tag{3.17}$$

and

$$\alpha_m = \frac{4E_m}{\pi \omega n_m}, \tag{3.18}$$

to find the ensemble average cross-spectral response $\langle \mathbf{S}_{qq} \rangle$.

14. The total energy of each statistical subsystem is found by adding the energy in the direct and reverberant fields (in many instances the former is small compared with the latter and can be neglected).

15. The previous analysis is repeated for various discrete frequencies of interest.

Numerical application

Consider the structure illustrated in fig. 3.2. Two thin aluminum plates are connected to a z-section frame via five point connections; the first plate is excited and interest lies in predicting the transverse response of the second plate across a frequency range from 15 Hz to 1.5 kHz. The first plate is assumed to be excited by a transverse point force whose precise location within the subsystem is unknown; The results obtained using the hybrid method are compared to those obtained with a Monte Carlo simulation. The Monte Carlo simulation was performed for 500 separate realizations of the ensemble. The energy responses in the source and receiving subsystems are shown in fig. 3.3 for each member of the ensemble. The variance in the response is clearly evident, even at relatively low frequencies. The ensemble average response is also plotted in the Figure. It can be seen that distinct fluctuations remain in the ensemble average response of the structure. For example, around 950 Hz a significant amount of energy is transmitted through the frame into the receiving plate across the ensemble (the peak response being approximately 10 dB higher than the response at neighboring frequencies). The increase of energy in the receiving plate is accompanied by a slight reduction in the energy of the source plate (approximately 2−3 dB at 950 Hz).

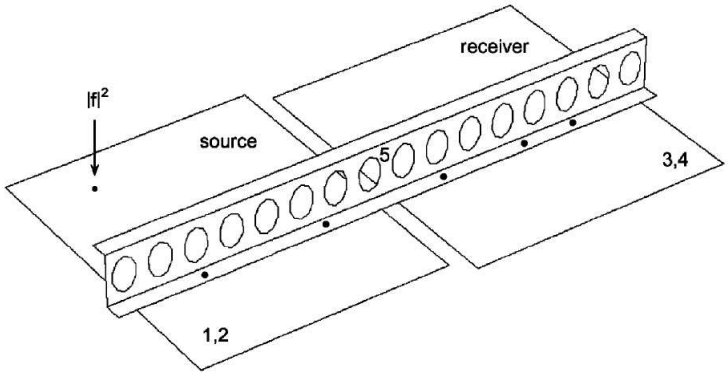

Figure 3.2: From [47], a complex structural system consisting of two statistical subsystems (the flexural wavefields of the two plates) point connected to various deterministic subsystems (the z-section frame and the in-plane wavefields of the two plates).

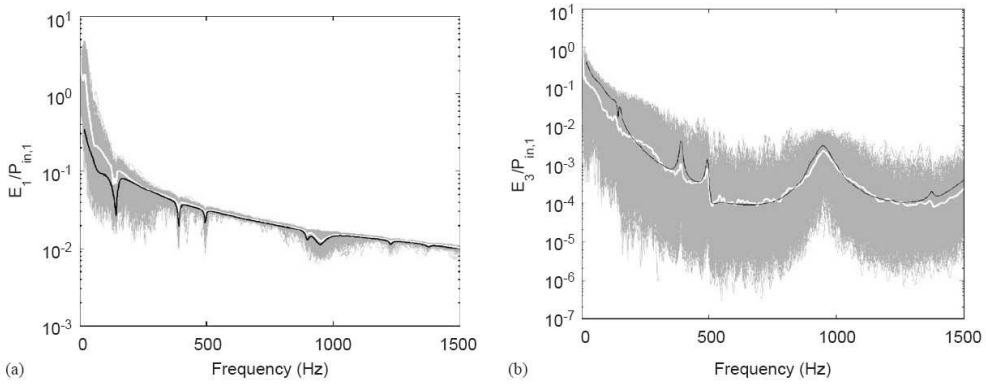

Figure 3.3: From [47], energy in flexural wavefields of (a) source plate and (b) receiving plate, per unit input power computed using: (i) an FE Monte Carlo simulation and (ii) the Hybrid approach. Gray lines, computed using Monte Carlo approach for 500 realizations of ensemble; white line, ensemble average of FE results; black line, ensemble average computed using Hybrid approach.

Hybrid Finite Element Formulation

N. Vlahopoulos, X. Zhao

In 1999, Vlahopoulos and Zhao [48, 49] presented a hybrid conventiona/energy FEA method for mid-frequency structural vibration. In this hybrid formulation, it is assumed that a complex structure is divided into "long" components that have relatively high-frequency vibration, and "short" components that have relatively low-frequency vibration. The terms "long" and "short" refer to the scale of the characteristic length of the component relative to the wavelength of vibration: a short component has only a few wavelengths over its length, while a long component has many wavelengths. The approach was then extended by the authors by allowing for the case of excitation applied on short members [50], beams connected at an arbitrary angle [51] and to complex systems comprised of flexible plates spot-welded to a stiff frame structure made of tubular beams [52].

The hybrid FEA approach combines conventional FEA with EFEA to achieve a numerical solution for systems comprised by stiff and flexible members. Stiff and flexible members are modeled by conventional FEA and EFEA, respectively. The EFEA is selected to be coupled with the low-frequency methods because it is based on a spatial discretization of the system that is being modeled. Thus, it is possible to develop appropriate interface conditions at the joints between the primary variables of the EFEA models of the flexible members and the FEA models of the stiff members.
The effect of the flexible members on the behavior of the stiff members is modeled by adding damping elements in the FEA model of the stiff members. The values of the damping elements are evaluated from the driving point impedance of the flexible members. The latter is computed by applying a CMS approach. The vibration of the stiff members and the amount of power flow to the flexible members through the spot-welded connections are obtained first. The latter comprises the excitation for the EFEA analysis which determines the amount of bending energy in the plate members. The computational procedure of the hybrid FEA is outlined in fig. 3.4.

Results for the box structure

A box with main dimension of 1.2m wide, 2m long, and 1m height is analyzed fig. 3.5. It is comprised by plate members spot-welded connected to a frame made of tubular beam members [52]. An excitation force oriented along the x direction is applied at one of the lower corners of the box structure. The locations on the stiff members where vibration results are compared from the FEA and the hybrid computations are identified in fig. 3.5. The plates for which bending energy results are presented are also identified in fig. 3.5. The velocities computed at nodes 1 and 2 by the FEA and the hybrid FEA are compared in fig. 3.6. The results demonstrate that the vibration of the stiff members is captured correctly by the hybrid method and that the interaction between stiff and flexible members is accounted properly by the addition of the damping elements.

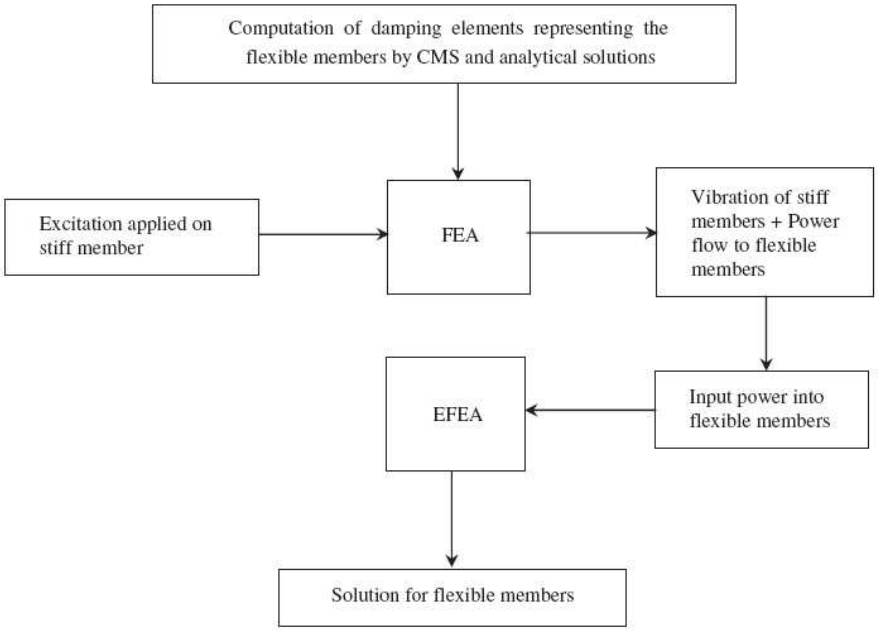

Figure 3.4: From [52], flow chart of the hybrid FEA computational process.

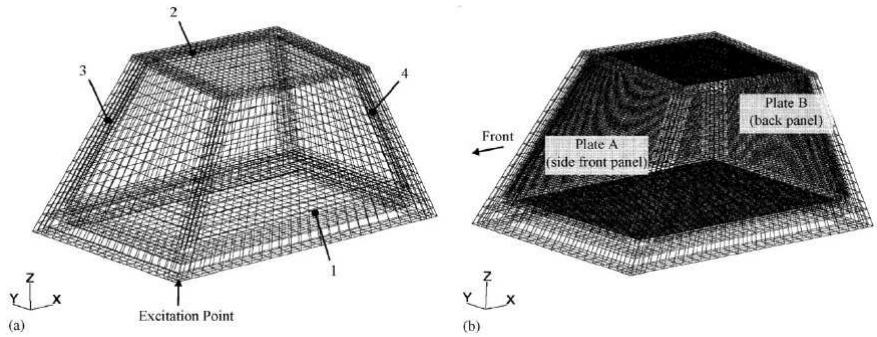

Figure 3.5: From [52], box structure comprised by multiple plates and beams for (a) hybrid FEA: 18,034 dof, (b) FEA: 218,419 dof.

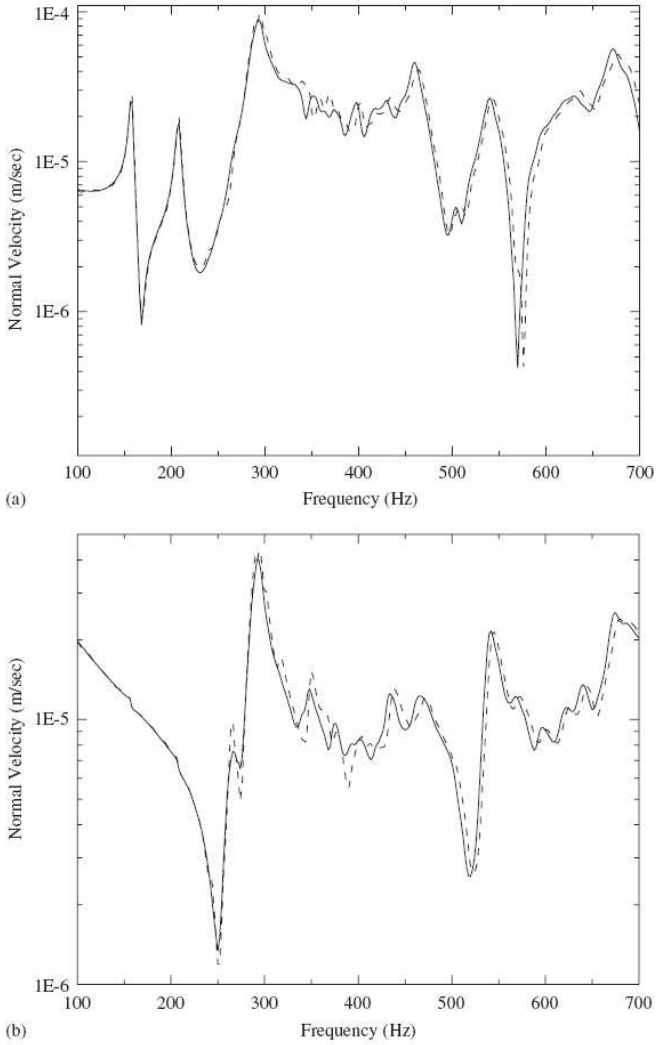

Figure 3.6: From [52], velocity at points 1 (a) and 2 (b) on the frame of the box structure when external excitation is applied in the x-directional excitation. —— Hybrid FEA, - - - - conventional FEA.

3.3 Objective of this research project

There are main challenges dealing with the mid-frequency range [5]:

- The wave-mode duality of structural vibration is especially important in the mid-frequency range. Incompatibilities between a modal approach and a wave- or energy-based approach must be resolved if one is to consider hybrid methods that employ both types of analysis. Even if a hybrid approach is not taken, each interface between components involves vibration, wave, and energy transmission issues that are not easily resolved. Furthermore, complicated and/or jointed connections require specialized modeling. In terms of problem formulation, the partitioning of the model into appropriate substructures is a crucial step and may not always be obvious or convenient.

- There is a critical accuracy versus efficiency trade-off in the mid- frequency range. From a low-frequency perspective, refining a finite element mesh, running the finite element analysis, and extracting key results from the analysis can be prohibitively expensive as frequency increases. Therefore, approximate methods must be adopted. From a high-frequency perspective, the situation is reversed. The simplifying assumptions that enable efficient analysis methods in the high-frequency range may not be appropriate for the mid-frequency range, leading to a quantitative and even qualitative breakdown in modeling accuracy as frequency decreases.

- As the frequency of vibration increases from the low- to mid-frequency range, parameter uncertainties have a greater influence on the response, especially as the wavelength decreases to the scale of random structural variations (e.g., manufacturing tolerances). At some point in the mid-frequency range, a deterministic model represents at best one member in the population of structures with the same nominal design, such that uncertainty in the system must be considered in order to predict the response. Estimated parameters and unmodeled structural complexities provide additional sources of uncertainty. Furthermore, from an engineering perspective, it is important not only to predict the response for a particular design, but also to predict the effect of design changes on that response.

The aim of this work is to develop and test a formulation which is suited for the mid-frequency range, and is able to account for all the different contributions. It is the view of the authors that the crux of the mid-frequency problem is not associated with the development of entirely new methods for describing the dynamic behavior of a system. In our opinion, the solution to the mid-frequency problem requires the development of a hybrid method which can consistently and rigorously combine deterministic and statistical descriptions of the dynamic behavior of a system in a given analysis. Such a hybrid method must provide a clear separation between the deterministic and statistical portions of a model that avoids duplication or omission of any dynamic behavior. Furthermore, the method must fully account for all interactions that occur between the statistical and deterministic portions of the model.

The starting point of this work is the Smooth Integral Formulation developed by M.Viktorovitch [53, 54, 55]. The Smooth Integral Formulation SIF is able to treat the vibrational behavior of a structure on the complete frequency range. This feature is due to the fact that the underlying assumptions of this formulation are very general, and are

linked more to the material description of the structure than to the frequency field of investigation. Nevertheless, this formulation shall not be utilized in the low frequency domain because the assumptions of the method have no influence in this range and moreover the number of unknowns to treat are greater than for a classical Boundary element Method, for instance. In the high frequency field (the domain where all the subsystems have a high frequency behavior), the SIF is suitable and can be used to describe the behavior of the complete structure in a much more convenient way than it could be carried out with a classical FEM or BEM. In the mid-frequency field (the domain where some of the subsystems have a high frequency behavior and the other show a low frequency behavior), the SIF can be utilized for describing the whole structure, even if the randomness introduced to the description of the geometry of the "low frequency" subsystems does not bring relevant information at the end.
In this frequency domain the key point is to develop hybrid formulations, where the low frequency behaving subsystems are treated with classical kinematic formulations, whereas the high frequency behaving subsystems are treated utilizing high frequency methods.
The steps from the theory of the SIF formulation and its application, towards the development of the hybrid formulation and its application, are reported in the following chapters. Initially simple and isolated structures are analyzed to test the capabilities of SIF formulation, and different modelling problematics are undertaken. Then the SIF is coupled to deterministic methods, FEM and BEM, to analyze more complex mid-frequency structures. A final validation of the formulation is realized and also some consideration about computational efforts are carried out.

The SIF has been chosen to model the high-frequency parts of the structures because of its flexibility, because it provides a response which it is not averaged over the frequency band or the spatial domain, like SEA. Another reason is that wanting to create a hybrid method, there is the need to couple the boundary quantities like force and displacement, or energy at the interface between a long and a short subsystem which are modelled with different formulation. This problem doesn't exist in the chosen methodology because both FEM (or BEM) and SIF variables are expressed, for instance, in terms of force and displacement, therefore they are homogeneous and can be easily coupled.

Chapter 4

The Smooth Integral Formulation Theory

The starting point of this work is a formulation developed by M.Viktorovitch et al. [53, 54, 55] in the late Nineties, so-called the Smooth Integral Formulation (SIF). It is based on a boundary integral formulation coupled with a statistical approach to account for uncertainties in the structural parameters. The underlying idea is that a structure always encounters physical uncertainties which play an increasing role when the frequency increases. According to Fahy [56], the differences among systems which share the same design characteristics, and the effects of these differences on vibrational behavior are individually unpredictable in the HF, therefore a probabilistic model is appropriate. Thus, introducing randomness to the geometrical or/and material properties of the structure leads to a precise description of the deterministic LF response and a smooth response in the high-frequency field corresponding to the "average" of the strongly oscillating vibratory response. In between, a transition zone is observed in which the response gradually shifts from the deterministic to the average response. In order to solve the problem, some fundamental assumptions dealing with the correlation among the unknowns of the formulation are introduced. Those assumptions allows to obtain a close system solution of the SIF which does not requires a recursive method.
The stochastic characterization of the boundaries allows to give a consistent vibro-acoustic description of structures on the whole frequency range.

4.1 High-frequency modelling thanks to the Smooth Integral Formulation (SIF)

In the high-frequency field, the vibrational response of a structure is dramatically sensitive to small perturbations of its geometrical and material properties. This phenomenon has been illustrated by Keane and Manohar [57, 58] who calculated the successive probability density functions of the eigenfrequencies of a beam, for which a random parameter is introduced in the definition of its mass density. Thus, solving the usual constitutive equations describing the vibrational behaviour of the structure, by means of a usual numerical solver is generally meaningless. To overcome this problem, randomness is introduced to the description of the geometry of the structure and a formulation exhibiting explicitly the expectations of the usual kinematic unknowns, with respect to the randomness, is derived. This randomness should not affect the response in the low-frequency field, on the other

hand, the aim is to obtain a smooth response in the high-frequency field highlighting the overall trend of the fast varying deterministic behaviour.
In other respect, writing a first order moment formulation is useless since these variables vanish to zero when the frequency rises. Therefore, the formulation must be written on the second order unknowns.

The constitutive equations of the SIF derived in papers [53, 54] and Ph.D. Thesis [55] are reminded in what follows.

4.2 The random formulation for isolated structures

The initial stage for deriving the SIF equations is a direct boundary integral formulation [7]. The formulation is very general and stands for one-, two- and three-dimensional problems. The integral representation for a homogeneous, isotropic and linear mechanical system of domain Ω and smooth boundary $\partial\Omega$, subjected to a harmonic loading f, may be written:

$$\begin{aligned} c \cdot u(\boldsymbol{\xi}) &= \int_{\Omega_f} f(\mathbf{y}) \cdot G(\mathbf{y}, \boldsymbol{\xi}) \mathrm{d}\Omega \\ &+ \int_{\partial\Omega} \Big(u(\mathbf{x}) \cdot dG(\mathbf{x}, \boldsymbol{\xi}) - T(\mathbf{x}) \cdot G(\mathbf{x}, \boldsymbol{\xi}) \Big) \mathrm{d}\partial\Omega. \end{aligned} \tag{4.1}$$

The integral representation is completed with the following boundary conditions:

$$\left\{ \begin{array}{ll} u(\mathbf{x}) = \hat{u}(\mathbf{x}) & \text{on} \quad \partial\Omega_u \\ T(\mathbf{x}) = \hat{T}(\mathbf{x}) & \text{on} \quad \partial\Omega_T \end{array} \right. \quad \text{and} \quad \left\{ \begin{array}{ll} c = \frac{1}{2} & \boldsymbol{\xi} \in \partial\Omega \\ c = 0 & otherwise \end{array} \right.$$

where $u(\mathbf{x})$ is the kinematic unknown (e.g. pressure, displacement), T is the boundary force unknown, G denotes the Green kernel, dG is the first order derivative of the Green kernel with respect to the variable $\mathbf{x}$, $\partial\Omega_u$ and $\partial\Omega_T$ constitute a partition of $\partial\Omega$.

The random parameters are introduced on the geometrical description of the structures, the boundary parameter are supposed to be randomly known and are written:

$$\widetilde{x}_i = x_i + \epsilon_i \tag{4.2}$$

where x_i is the deterministic value of the parameter, while ϵ_i is the zero mean random variable. To solve the formulation a statistic probability distribution should be introduced, a Gaussian normal distribution has been chosen (any other probabilistic law can be chosen), with standard deviation equal to σ and density function f_{ϵ_i}:

$$f_{\epsilon_i} = \big(1/\sigma\sqrt{2\pi}\big) exp[-\epsilon_i^2/2\sigma^2]. \tag{4.3}$$

Even if the position of the boundaries are assumed to be random parameter, the boundary conditions are deterministic; so ie. for the case of a clamped boundary we have zero-displacement $w(\widetilde{x}) = 0$.
A randomness is then applied to the locations of the loading and the boundary of the structure. These two new random parameters are respectively denoted by $\tilde{\Omega}_f$ and $\partial\tilde{\Omega}$. Accordingly, the partition of the boundary becomes $\partial\tilde{\Omega} = \partial\tilde{\Omega}_T \cup \partial\tilde{\Omega}_u$.
The explicit expression of $\langle G(\widetilde{x}_i, \widetilde{x}_j) \rangle$, for $i \neq j$ is:

$$\langle G(\widetilde{x}_i, \widetilde{x}_j) \rangle = \int_{\infty}^{\infty} \int_{-\infty}^{\infty} G(\widetilde{x}_i, \widetilde{x}_j) f_{\epsilon_i \epsilon_j}(\epsilon_i, \epsilon_j) d\epsilon_i d\epsilon_j. \tag{4.4}$$

For the calculation of the expectation of a generic exponential function, please refer to Appendix A.

N_u and N_T are respectively the number of boundary elements defined for $\partial\tilde{\Omega}_u$ and $\partial\tilde{\Omega}_T$. The collocation method is employed which enables the transformation of the integral equations, eqs. (4.1), into a discrete set of equations. As an illustration, the equation evaluated at point $\tilde{\boldsymbol{\xi}} \in \partial\tilde{\Omega}_u$ is reported. $\tilde{u}_j$ is the boundary random unknown at element j.

$$\begin{aligned}\frac{1}{2}u_\xi &= \int_{\tilde{\Omega}_f} f(\mathbf{y}) \cdot G(\mathbf{y}, \tilde{\boldsymbol{\xi}}) \mathrm{d}\Omega \\ &+ \sum_{j=1}^{N_T} \int_{\partial\tilde{\Omega}_j} [u_j \cdot dG(\mathbf{x}, \tilde{\boldsymbol{\xi}}) - \hat{T}_j \cdot G(\mathbf{x}, \tilde{\boldsymbol{\xi}})] \mathrm{d}\partial\Omega \\ &+ \sum_{k=1}^{N_u} \int_{\partial\tilde{\Omega}_k} [\hat{u}_k \cdot dG(\mathbf{x}, \tilde{\boldsymbol{\xi}}) - T_k \cdot G(\mathbf{x}, \tilde{\boldsymbol{\xi}})] \mathrm{d}\partial\Omega. \end{aligned} \tag{4.5}$$

The goal of this work is to derive an integral representation whose unknowns are the expectations of the cross-products of the force and displacement unknowns. Therefore, for any boundary location $\tilde{\boldsymbol{\xi}} \in \partial\tilde{\Omega}$, the right- and left-hand sides of the Eq. (4.5) are multiplied by the conjugate of the random boundary unknown at the same spatial position. The expectations of the equations are finally considered. They are represented by $\langle - \rangle$.
Finally, $N_u + N_T$ boundary element equations are obtained.

4.3 Limiting the unknowns and final formulation

To solve the $N_u + N_T$ equations some statistical assumptions for limiting the number of unknowns are defined. These assumptions govern the correlation of the different variables appearing in the equations above. They are based on a physical interpretation of the integral equations. They were detailed in the previously mentioned publications [53, 54].

The first assumption deals with the statistical behaviour of the different sources.

Assumption 1: *The contributions of two sources are statistically independent when the positions of the sources or the target points of the contributions are distinct.*

At this stage, two types of sources are distinguished; the external loadings which are called primary sources and the boundary sources (on which no loading is applied) which are called secondary sources. The latter are constituted by the multiple wave reflections of the waves stemming from the loadings.

The second assumption governs the random behaviour of the force and displacement variables.

Assumption 2: *It is considered that a force or a displacement variable expressed at any point of the structure, is only correlated with the contributions of the primary sources at that point.*

As an illustration, if we consider the term related to the contribution of the external force at point $\tilde{\mathbf{x}}_i$, $\left\langle \tilde{u}_i^* \cdot \int_{\tilde{\Omega}_f} f(\mathbf{y}) \cdot G(\mathbf{y}, \tilde{\mathbf{x}}_i)\, \mathrm{d}\Omega \right\rangle$ it cannot be split because f is a primary source for $\tilde{\mathbf{x}}_i$. Instead if we consider the contribution at $\tilde{\mathbf{x}}_i$ of source located at $\tilde{\mathbf{x}}_j$,

$$\left\langle \tilde{u}_i^* \cdot \sum_{\substack{j=1 \\ j\neq i}}^{N_T} \tilde{u}_j \int_{\partial\tilde{\Omega}_j} dG(\mathbf{x}, \tilde{\mathbf{x}}_i)\, \mathrm{d}\partial\Omega \right\rangle$$

according to assumptions 1-2 this can be split as follows

$$\langle \tilde{u}_i^* \rangle \cdot \sum_{\substack{j=1 \\ j \neq i}}^{N_T} \langle \tilde{u}_j \rangle \Big\langle \int_{\partial \tilde{\Omega}_j} dG(\mathbf{x}, \tilde{\mathbf{x}}_i)\, \mathrm{d}\partial\Omega \Big\rangle.$$

For assembled systems, we should classify the sources in a different way:
Assumption 3: *The boundaries connecting two substructures, of which one contains a primary source, become primary sources for the other substructure.*
This assumption enables one to express the correlation between an external loading located on a subsystem and a force displacement unknown on another substructure.

4.4 The fundamental equations of the SIF

Finally, applying the first two assumptions, the fundamental equations of the formulation may be written:

◇ $\tilde{\mathbf{x}}_i \in \partial\tilde{\Omega}_i$, $i \in [1, N_T]$:

$$\begin{aligned}
\frac{1}{2}\langle |\tilde{u}_i|^2 \rangle \quad &= \Big\langle \tilde{u}_i^* \cdot \int_{\tilde{\Omega}_f} f(\mathbf{y}) \cdot G(\mathbf{y}, \tilde{\mathbf{x}}_i)\, \mathrm{d}\Omega \Big\rangle \\
&+ \langle \tilde{u}_i^* \rangle \cdot \sum_{\substack{j=1 \\ j \neq i}}^{N_T} \langle \tilde{u}_j \rangle \Big\langle \int_{\partial \tilde{\Omega}_j} dG(\mathbf{x}, \tilde{\mathbf{x}}_i)\, \mathrm{d}\partial\Omega \Big\rangle \\
&- \langle \tilde{u}_i^* \rangle \cdot \sum_{j=1}^{N_T} \Big\langle \int_{\partial \tilde{\Omega}_j} \hat{T}_j \cdot G(\mathbf{x}, \tilde{\mathbf{x}}_i)\, \mathrm{d}\partial\Omega \Big\rangle \\
&+ \langle \tilde{u}_i^* \rangle \cdot \sum_{k=1}^{N_u} \Big\langle \int_{\partial \tilde{\Omega}_k} \hat{u}_k \cdot dG(\mathbf{x}, \tilde{\mathbf{x}}_i)\, \mathrm{d}\partial\Omega \Big\rangle \\
&- \langle \tilde{u}_i^* \rangle \cdot \sum_{k=1}^{N_u} \langle \tilde{T}_k \rangle \Big\langle \int_{\partial \tilde{\Omega}_k} G(\mathbf{x}, \tilde{\mathbf{x}}_i)\, \mathrm{d}\partial\Omega \Big\rangle \\
&+ \langle |\tilde{u}_i|^2 \rangle \cdot \Big\langle \int_{\partial \tilde{\Omega}_i} dG(\mathbf{x}, \tilde{\mathbf{x}}_i)\, \mathrm{d}\partial\Omega \Big\rangle. \qquad (4.6)
\end{aligned}$$

◇ $\tilde{\mathbf{x}}_i \in \partial\tilde{\Omega}_i$, $i \in [1, N_u]$:

$$\begin{aligned}
\frac{1}{2}\langle \tilde{T}_i^* \rangle \cdot \hat{u}_i \quad &= \Big\langle \tilde{T}_i^* \cdot \int_{\tilde{\Omega}_f} f(\mathbf{y}) \cdot G(\mathbf{y}, \tilde{\mathbf{x}}_i)\ \mathrm{d}\Omega \Big\rangle \\
&+ \langle \tilde{T}_i^* \rangle \cdot \sum_{j=1}^{N_T} \langle \tilde{u}_j \rangle \Big\langle \int_{\partial \tilde{\Omega}_j} dG(\mathbf{x}, \tilde{\mathbf{x}}_i)\, \mathrm{d}\partial\Omega \Big\rangle \\
&- \langle \tilde{T}_i^* \rangle \cdot \sum_{j=1}^{N_T} \Big\langle \int_{\partial \tilde{\Omega}_j} \hat{T}_j \cdot G(\mathbf{x}, \tilde{\mathbf{x}}_i)\, \mathrm{d}\partial\Omega \Big\rangle \\
&+ \langle \tilde{T}_i^* \rangle \cdot \sum_{k=1}^{N_u} \Big\langle \int_{\partial \tilde{\Omega}_k} \hat{u}(\mathbf{x}) \cdot dG(\mathbf{x}, \tilde{\mathbf{x}}_i)\, \mathrm{d}\partial\Omega \Big\rangle
\end{aligned}$$

$$-\langle \tilde{T}_i^* \rangle \cdot \sum_{\substack{k=1 \\ k \neq i}}^{N_u} \langle \tilde{T}_k \rangle \Big\langle \int_{\partial \tilde{\Omega}_k} G(\mathbf{x}, \tilde{\mathbf{x}}_i) \, \mathrm{d}\partial\Omega \Big\rangle$$
$$-\langle |\tilde{T}_i|^2 \rangle \cdot \Big\langle \int_{\partial \tilde{\Omega}_i} G(\mathbf{x}, \tilde{\mathbf{x}}_i) \, \mathrm{d}\partial\Omega \Big\rangle. \tag{4.7}$$

Eqs. (4.6) and (4.7) are the fundamental relationships of the Smooth Integral Formulation. Studying these equations one can observe that the number of unknowns is equal to $3(N_u + N_T)$. These unknowns are:

- First order moments: $\langle \tilde{u}_i \rangle$ and $\langle \tilde{T}_i \rangle$.
- Second order moments: $\langle |\tilde{u}_i|^2 \rangle$ and $\langle |\tilde{T}_i|^2 \rangle$.
- Expectation of kinematic variable multiplied by the contribution of the primary source: $\langle \tilde{u}_i^* \cdot \int_{\tilde{\Omega}_f} f(\mathbf{y}) \cdot G(\mathbf{y}, \tilde{\mathbf{x}}_i) \, \mathrm{d}\Omega \rangle$ and $\langle \tilde{T}_i^* \cdot \int_{\tilde{\Omega}_f} f(\mathbf{y}) \cdot G(\mathbf{y}, \tilde{\mathbf{x}}_i) \, \mathrm{d}\Omega \rangle$.

In order to obtain a consistent set of equations, $2(N_u + N_T)$ supplementary equations are added to the formulation [53, 54]. These $(N_u + N_T)$ equations are the expectation of the basic equation evaluated in $\tilde{\boldsymbol{\xi}} = \tilde{\mathbf{x}}_i \in \partial\tilde{\Omega}_i$, $i = 1, ..., N_u + N_T$. The remaining equations come from the basic equation multiplied by the conjugate of the contribution of the external force $\int_{\tilde{\Omega}_f} f^*(\mathbf{y}) \cdot G^*(\mathbf{y}, \tilde{\mathbf{x}}_i) \, \mathrm{d}\Omega$, evaluated in $\tilde{\boldsymbol{\xi}} = \tilde{\mathbf{x}}_i \in \partial\tilde{\Omega}_i$, $i = 1, 2, ..., N_u + N_T$.

4.5 Discussion

The SIF formulation constitute the central feature of this work. It is initially used to analyse the response of simple random structures, like isolated rods and beams. Then the SIF is used for more complex structures, made of several coupled subsystems, for which is possible to simulate a mid-frequency behavior. Finally it is coupled to deterministic methods to have a hybrid approach for the mid-frequency range.
It is really important to understand the capabilities of this statistical method in order to proceed to the development of a hybrid method, and on this purpose an entire chapter is dedicated to SIF applications.

Chapter 5

Applications of the SIF formulation to 1D systems

In this section the SIF formulation is applied to simple monodimensional structures, made of isolated and coupled systems like a simple rod, beam, or two coupled rods. Those applications have already been solved and reported by M.Viktorovitch in his publications and Ph.D. thesis [53, 54, 55].
They are here simply recalled because they provide the starting point for the development of the hybrid formulation which is the main topic of this Ph.D. research.

5.1 Rod

The boundary integral representation of the simple rod is formulated in this section. One of the possible formulations to obtain the integral equations is derived from the dynamic reciprocal theorem: if two distinct elastic equilibrium states exist in a boundary region, then the work done by the forces and moments of the first system on the displacement and slope of the second is equal to the work done by the forces and moments of the second system on the displacement and slope of the first one. The first system is the actual state of displacements, slopes, body and boundary forces and moments, and the second one corresponds to a unit force system in an infinite solid [7].
The equation of motion for the rod in the frequency domain, can be written [59]:

$$\frac{\partial^2 w}{\partial^2 x} + k^2 w = \frac{-F_0}{ES} \tag{5.1}$$

where $w(x)$ is the longitudinal displacement, $E = E_0(1 + i\eta)$ is the complex modulus of elasticity, η is the loss damping factor, ρS is the mass density per unit length, S is the cross section area, F_0 is the longitudinal loading, k is the wave number:

$$k^2 = \omega^2 \rho / E_0(1 + i\eta) \approx k_0^2(1 - i\eta) \tag{5.2}$$

ω is the circular frequency of vibration.
The solution for a unit force excitation in an infinite rod is given by the Green Kernel G:

$$G(x, \xi) = (1/2ik)e^{-ik|\xi - x|} \tag{5.3}$$

where ξ is the loading location, and x is the spatial position.
Equation for the rod evaluated at point x:

$$\begin{aligned} w(x) &= \frac{F_0}{ES}G(x-x_f) + \frac{\partial w(x_2)}{\partial x}G(x-x_2) - \frac{\partial w(x_1)}{\partial x}G(x-x_1) \\ &\quad - w(x_2)\frac{\partial G(x-x_2)}{\partial x} + w(x_1)\frac{\partial G(x-x_1)}{\partial x}. \end{aligned} \tag{5.4}$$

5.1.1 BEM application: rod

The BEM formulation as been applied to a simple rod, figure 5.1. The mechanical

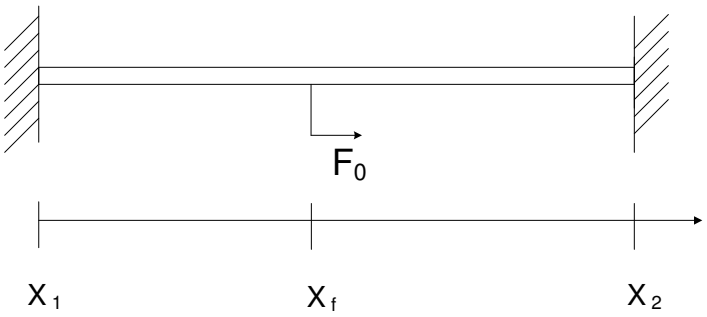

Figure 5.1: Structure made of an isolated rod

system is considered to be homogeneous, isotropic, linear, elastic, and the hypothesis of small displacement is taken into account. The points x_1 and x_2 are the boundaries of the rod which is excited by an external longitudinal harmonic force, F_0, located in x_f. The boundary conditions are clamped/clamped, $w(x_1) = w(x_2) = 0$. Using eq. (5.4) to evaluate the response at x_1 and x_2 we obtain:

$$\begin{aligned} 0 &= \frac{F_0}{ES}G(x_1-x_f) + \frac{\partial w(x_2)}{\partial x}G(x_1-x_2) - \frac{\partial w(x_1)}{\partial x}G(x_1-x_1), \\ 0 &= \frac{F_0}{ES}G(x_2-x_f) + \frac{\partial w(x_2)}{\partial x}G(x_2-x_2) - \frac{\partial w(x_1)}{\partial x}G(x_2-x_1). \end{aligned} \tag{5.5}$$

Rod physical properties and geometry:

- Configuration n.1
  The physical properties of configuration n.1 are reported in table 5.1 and results in figure 5.2.

	length [m]	x_f [m]	E [N/m^2]	S [m^2]	η [%]	ρ [kg/m^3]
Rod n.1	3.60	2.50	$2.1 \cdot 10^{11}$	10^{-4}	2	7800

Table 5.1: BEM application. Parameters of the rod, configuration n.1

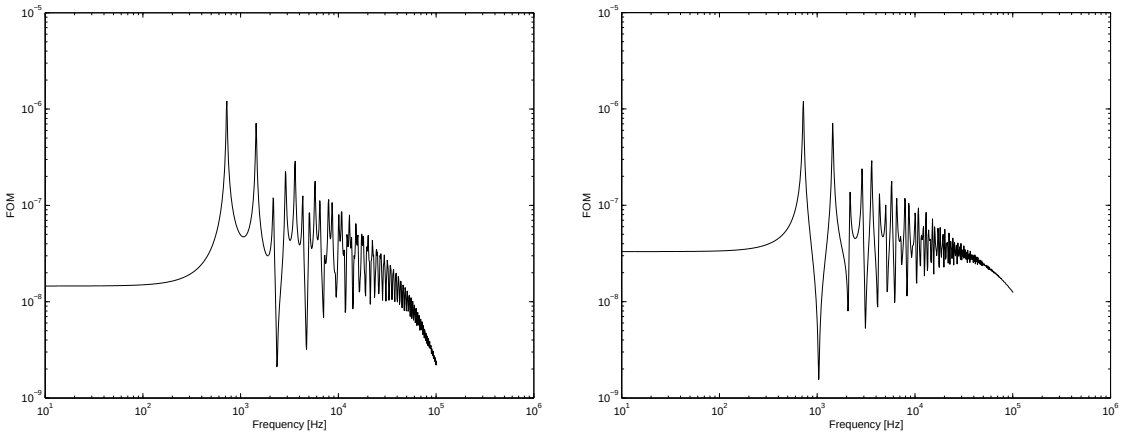

(a) (b)

Figure 5.2: BEM single rod. Frequency evolution of the modulus of the first order moment $\partial w/\partial x$ at x_1 (a) and x_2 (b). Configuration n.1.

- Configuration n.2
  The physical properties of configuration n.2 are reported in table 5.2 and results in figure 5.3.

	length [m]	x_f [m]	E [N/m^2]	S [m^2]	η [%]	ρ [kg/m^3]
Rod n.2	2.30	1.98	$2.1 \cdot 10^{11}$	10^{-4}	3	7800

Table 5.2: BEM application. Parameters of the rod, configuration n.2

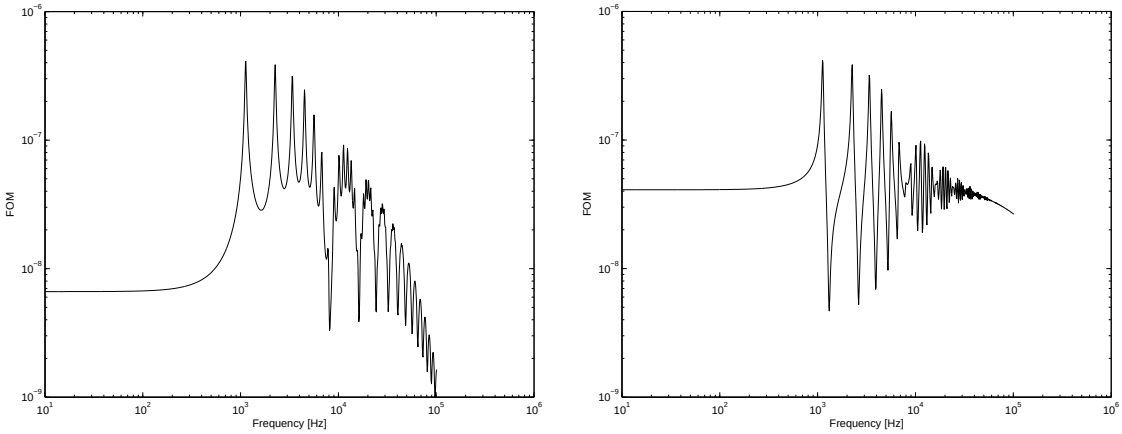

(a) (b)

Figure 5.3: BEM single rod. Frequency evolution of the modulus of the first order moment $\partial w/\partial x$ at x_1 (a) and x_2 (b). Configuration n.2.

- Configuration n.3 - FEM results comparison
  The physical properties of configuration n.3 are reported in table 5.3 and results in

figure 5.4.
BEM is able to model properly the vibrational behavior of a clamped/clamped rod, as we can see from the comparison between the results obtained using BEM (evaluating the response of the rod in different points along the structure and then superposing all the curves), and the results obtained with FEM (using Nastran FEM solver), fig. 5.4.

	length [m]	x_f [m]	E [N/m^2]	S [m^2]	η [%]	ρ [kg/m^3]
Rod n.3	6.00	1.48	$2.1 \cdot 10^{11}$	10^{-4}	4	7800

Table 5.3: BEM application. Parameters of the rod, configuration n.3

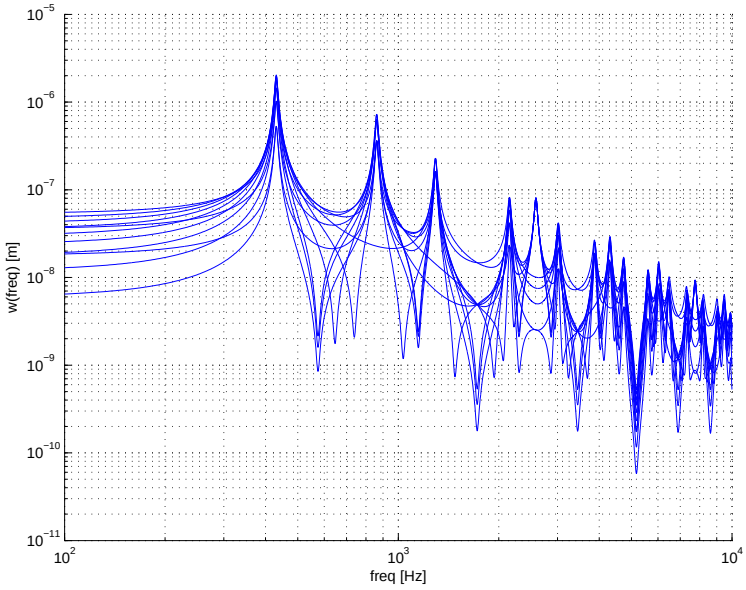

(a)

Number	Nat.Freq. [Hz]
1	431
2	862
3	1293
4	(1724)
5	2155
6	2585
7	3016
8	(3447)
9	3878
10	4309
11	4740
12	(5157)

(b)

Figure 5.4: BEM single rod. Comparison of the value of the natural frequencies for a BEM calculation (a) and FEM calculation (b). Response of BEM calculated at different points along the structure. The modes in brackets are the anti-resonant modes.

As we can see from the previous results, the response of a rod subjected to a longitudinal harmonic excitation mainly depends from the length of the structure, and from the physic parameter, Young modulus and mass density, while is independent from the cross sectional area.

5.1.2 SIF application: single rod

In this section the SIF formulation for the clamped-clamped rod will be developed and applied. With respect to the BEM formulation, a randomness is used in the geometrical description of the boundary locations, fig. 5.5.

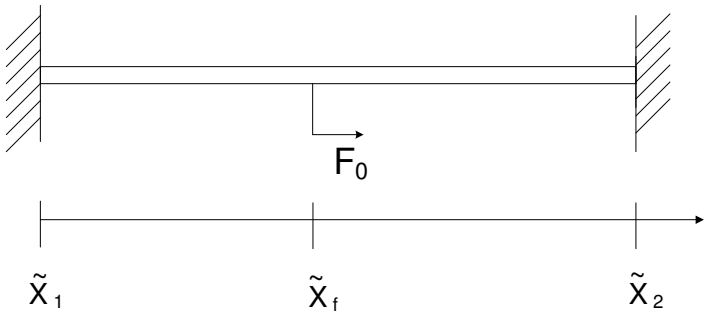

Figure 5.5: Single rod structure with random boundaries.

SIF single rod: deriving the equations

The boundary equations for a clamped/clamped rod established in sec. 5.1.1 are recalled, in the case of a point loading F_0:

$$\begin{aligned} w(x_1) &= \frac{F_0}{ES}G(x_1,x_f) + \frac{\partial w(x_2)}{\partial x}G(x_1,x_2) - \frac{\partial w(x_1)}{\partial x}G(x_1,x_1) \\ w(x_2) &= \frac{F_0}{ES}G(x_2,x_f) + \frac{\partial w(x_2)}{\partial x}G(x_2,x_2) - \frac{\partial w(x_1)}{\partial x}G(x_2,x_1) \end{aligned} \tag{5.6}$$

The geometrical parameters encountered in equations (5.6) are x_1, x_2 and x_f, corresponding to the positions of the boundaries and the location of the loading. These parameters are considered to be randomly known and are written:

$$\tilde{x}_1 = x_1 + \varepsilon_1, \qquad \tilde{x}_2 = x_2 + \varepsilon_2, \qquad \tilde{x}_f = x_f + \varepsilon_f, \tag{5.7}$$

where ε_1, ε_2 and ε_f are assumed to be independent zero mean random variables. Even if the positions of the boundaries are assumed to be random parameters, the boundary conditions are deterministic; that is to say for the case of the clamped/clamped rod: $w(\tilde{x}_1) = w(\tilde{x}_2) = 0$. Using the random notations, eq. (5.7), the integral formulation of the rod, equations (5.6), becomes:

$$\begin{aligned} 0 &= \frac{F_0}{ES}G(\tilde{x}_1,\tilde{x}_f) + \frac{\partial w(\tilde{x}_2)}{\partial x}G(\tilde{x}_1,\tilde{x}_2) - \frac{\partial w(\tilde{x}_1)}{\partial x}G(\tilde{x}_1,\tilde{x}_1) \\ 0 &= \frac{F_0}{ES}G(\tilde{x}_2,\tilde{x}_f) + \frac{\partial w(\tilde{x}_2)}{\partial x}G(\tilde{x}_2,\tilde{x}_2) - \frac{\partial w(\tilde{x}_1)}{\partial x}G(\tilde{x}_2,\tilde{x}_1) \end{aligned} \tag{5.8}$$

The random boundary formulation is obtained by multiplying each side of the first equation (respectively the second equation) of (5.8), by the conjugate of the unknown boundary kinematic variable, $\partial w^*(\tilde{x}_1)/\partial x$ (respectively $\partial w^*(\tilde{x}_2)/\partial x$). The expectations with respect to $\tilde{x}_1$, $\tilde{x}_2$ and $\tilde{x}_f$ (represented by the symbol $\langle - \rangle$) of the two sides of the equations are then taken into account. Using the assumptions of section 4.3 one obtains:

$$\begin{aligned} 0 \;=\; & \frac{F_0}{ES}\Big\langle \frac{\partial w^*(\tilde{x}_1)}{\partial x}G(\tilde{x}_1,\tilde{x}_f)\Big\rangle \\ & + \Big\langle \frac{\partial w^*(\tilde{x}_1)}{\partial x}\Big\rangle\Big\langle \frac{\partial w(\tilde{x}_2)}{\partial x}\Big\rangle\Big\langle G(\tilde{x}_1,\tilde{x}_2)\Big\rangle - \Big\langle \Big|\frac{\partial w(\tilde{x}_1)}{\partial x}\Big|^2\Big\rangle G(\tilde{x}_1,\tilde{x}_1) \end{aligned}$$

$$
\begin{aligned}
0 &= \frac{F_0}{ES}\Big\langle \frac{\partial w^*(\tilde{x}_2)}{\partial x} G(\tilde{x}_2,\tilde{x}_f)\Big\rangle \\
&\quad + \Big\langle \Big|\frac{\partial w(\tilde{x}_2)}{\partial x}\Big|^2\Big\rangle G(\tilde{x}_2,\tilde{x}_2) - \Big\langle \frac{\partial w^*(\tilde{x}_2)}{\partial x}\Big\rangle\Big\langle \frac{\partial w(\tilde{x}_1)}{\partial x}\Big\rangle\Big\langle G(\tilde{x}_2,\tilde{x}_1)\Big\rangle
\end{aligned} \tag{5.9}
$$

Equations (5.9) contain six unknowns:

$$
\begin{gathered}
\Big\langle w(\tilde{x}_1)\Big\rangle, \Big\langle w(\tilde{x}_2)\Big\rangle, \Big\langle \Big|w(\tilde{x}_1)\Big|^2\Big\rangle, \Big\langle \Big|w(\tilde{x}_2)\Big|^2\Big\rangle \\
\Big\langle \frac{\partial w^*(\tilde{x}_1)}{\partial x} G(\tilde{x}_1,\tilde{x}_f)\Big\rangle, \Big\langle \frac{\partial w^*(\tilde{x}_2)}{\partial x} G(\tilde{x}_2,\tilde{x}_f)\Big\rangle
\end{gathered}
$$

Four more equations must be added to the formulation in order to estimate the six unknowns. Two equations are obtained by considering the expectation of the classical boundary integral equations (5.8). The same random assumptions are applied to these two equations. The final expression of the different equations have the following form:

$$
\begin{aligned}
0 &= \frac{F_0}{ES}\Big\langle G(\tilde{x}_1,\tilde{x}_f)\Big\rangle + \Big\langle \frac{\partial w(\tilde{x}_2)}{\partial x}\Big\rangle\Big\langle G(\tilde{x}_1,\tilde{x}_2)\Big\rangle - \Big\langle \frac{\partial w(\tilde{x}_1)}{\partial x}\Big\rangle G(\tilde{x}_1,\tilde{x}_1) \\
0 &= \frac{F_0}{ES}\Big\langle G(\tilde{x}_2,\tilde{x}_f)\Big\rangle + \Big\langle \frac{\partial w(\tilde{x}_2)}{\partial x}\Big\rangle G(\tilde{x}_2,\tilde{x}_2) - \Big\langle \frac{\partial w(\tilde{x}_1)}{\partial x}\Big\rangle\Big\langle G(\tilde{x}_2,\tilde{x}_1)\Big\rangle
\end{aligned} \tag{5.10}
$$

The last two relationships are obtained by multiplying each side of the conjugate of the first equation (respectively the second equation) of (5.8) by $G(\tilde{x}_1,\tilde{x}_f)$ (respectively by $G(\tilde{x}_2,\tilde{x}_f)$).

$$
\begin{aligned}
0 &= \Big(\frac{F_0}{ES}\Big)^*\Big\langle \Big|G(\tilde{x}_1,\tilde{x}_f)\Big|^2\Big\rangle + \Big\langle \frac{\partial w^*(\tilde{x}_2)}{\partial x}\Big\rangle\Big\langle G^*(\tilde{x}_1,\tilde{x}_2)\Big\rangle\Big\langle G(\tilde{x}_1,\tilde{x}_f)\Big\rangle \\
&\quad - \Big\langle \frac{\partial w^*(\tilde{x}_1)}{\partial x} G(\tilde{x}_1,\tilde{x}_f)\Big\rangle G^*(\tilde{x}_1,\tilde{x}_1) \\
0 &= \Big(\frac{F_0}{ES}\Big)^*\Big\langle \Big|G(\tilde{x}_2,\tilde{x}_f)\Big|^2\Big\rangle + \Big\langle \frac{\partial w^*(\tilde{x}_2)}{\partial x} G(\tilde{x}_2,\tilde{x}_f)\Big\rangle G^*(\tilde{x}_2,\tilde{x}_2) \\
&\quad - \Big\langle \frac{\partial w^*(\tilde{x}_1)}{\partial x}\Big\rangle\Big\langle G^*(\tilde{x}_2,\tilde{x}_1)\Big\rangle\Big\langle G(\tilde{x}_2,\tilde{x}_f)\Big\rangle
\end{aligned} \tag{5.11}
$$

In order to completely solve the problem, one must finally consider six equations given by the three sets of relationships (5.9)-(5.11). If a high frequency response is required, the evaluation of the first order moments of the boundary unknowns is not compulsory and there values may be set to zero. Therefore, the two equations (5.10) may be suppressed within this context.

SIF single rod: results

The results obtained with the SIF formulation at the boundaries $\tilde{x}_1$ and $\tilde{x}_2$ are compared to those obtained with BEM for the same nominal system with no randomness. In both configurations, 1 and 2, we have assumed to have a uniform randomness on the boundary parameters, $\sigma_1 = \sigma_2 = \sigma_f = 0.03$.

Rod physical properties and geometry:

- Configuration n.1
  The physical properties of configuration n.1 are reported in table 5.4 and results in

	length [m]	x_f [m]	E [N/m^2]	S [m^2]	η [%]	ρ [kg/m^3]
Rod n.1	3.60	2.50	$2.1 \cdot 10^{11}$	10^{-4}	2	7800

Table 5.4: SIF application. Parameters of the rod, configuration n.1

figures 5.6 and 5.7.

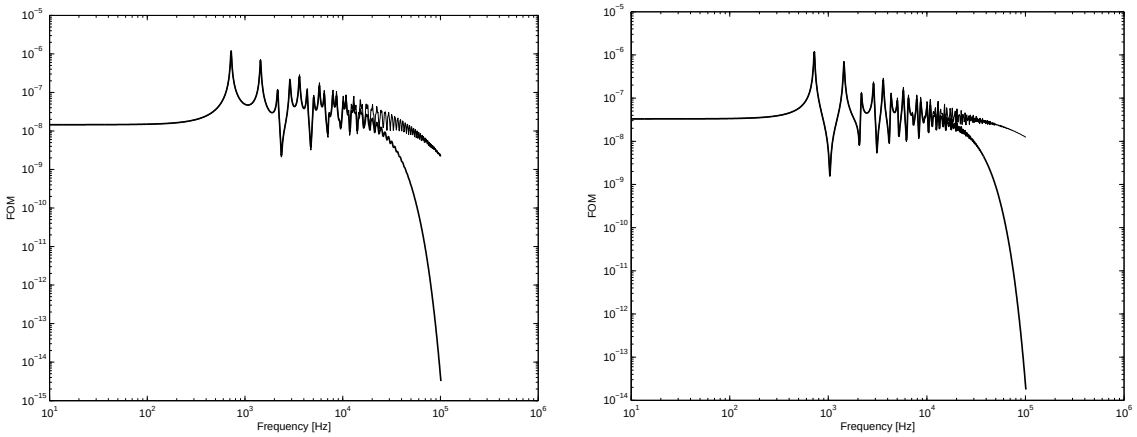

(a) (b)

Figure 5.6: SIF single rod. Frequency evolution of the modulus of the first order moment $\langle \partial w/\partial x \rangle$ at x_1 (a) and x_2 (b). Configuration n.1. —— SIF —— BEM.

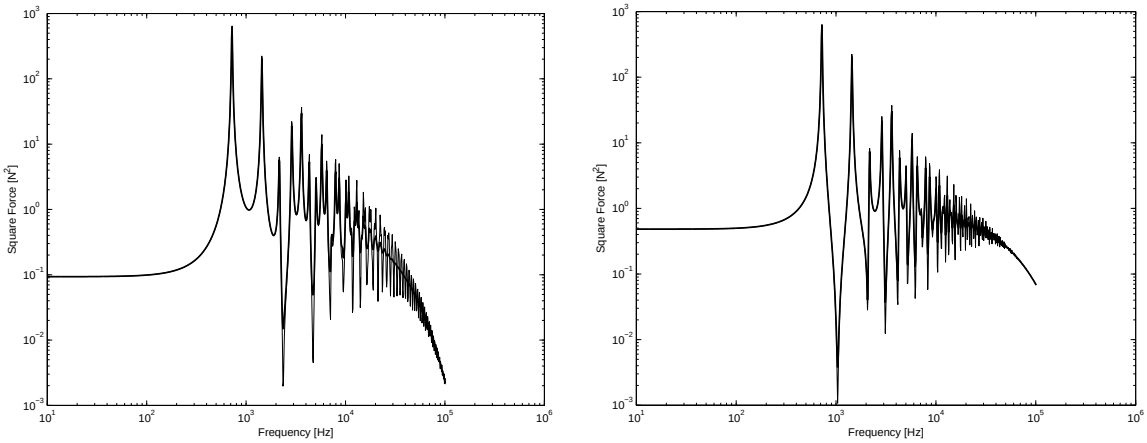

(a) (b)

Figure 5.7: SIF single rod. Frequency evolution of the modulus of the second order moment $\langle |\partial w/\partial x|^2 \rangle$ at x_1 (a) and x_2 (b). Configuration n.1. —— SIF —— BEM.

- Configuration n.2
  The physical properties of configuration n.2 are reported in table 5.5 and results in

figures 5.8 and 5.9.

	length [m]	x_f [m]	E [N/m^2]	S [m^2]	η [%]	ρ [kg/m^3]
Rod n.2	2.30	1.98	$2.1 \cdot 10^{11}$	10^{-4}	3	7800

Table 5.5: SIF application. Parameters of the rod, configuration n.2

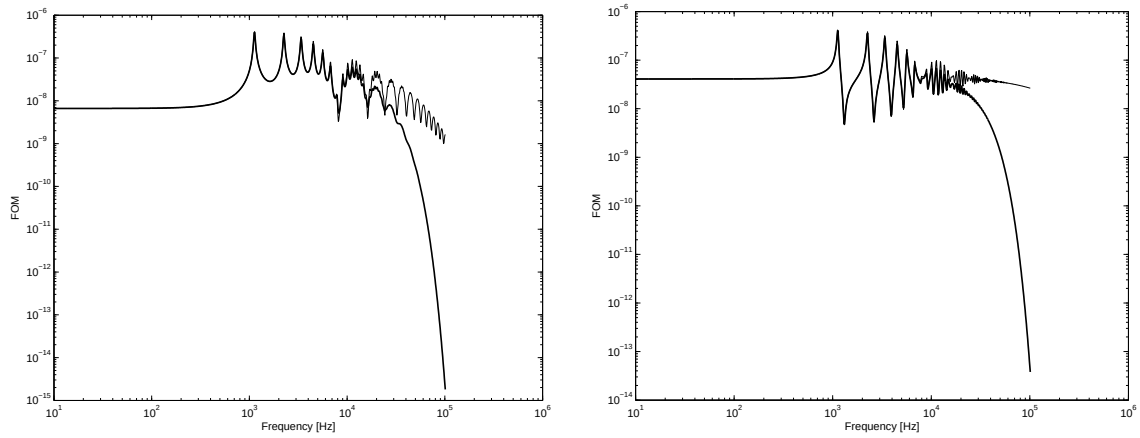

(a) (b)

Figure 5.8: SIF single rod. Frequency evolution of the modulus of the first order moment $\langle \partial w/\partial x \rangle$ at x_1 (a) and x_2 (b). Configuration n.2. —— SIF —— BEM.

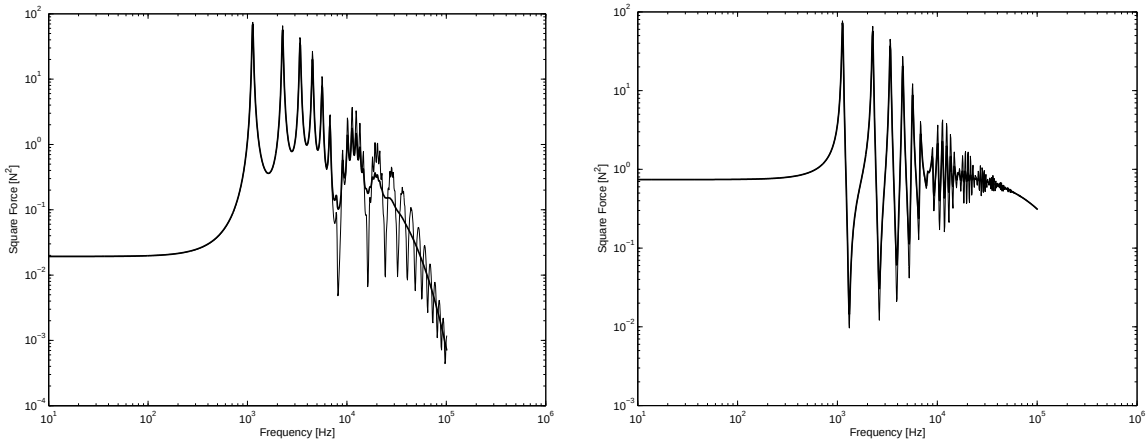

(a) (b)

Figure 5.9: SIF single rod. Frequency evolution of the modulus of the second order moment $\langle |\partial w/\partial x|^2 \rangle$ at x_1 (a) and x_2 (b). Configuration n.2. —— SIF —— BEM.

The frequency evolution of two first order moment variables can be seen in figures 5.6 and 5.8. The evaluation of these variables provides some information on the behaviour

of the structure, only in the low frequency field range for which the random parameters do not greatly disturb the unknowns. When the frequency increases, the expectations with respect to the geometrical random parameters of the variables vanish to zero, as expected. Therefore, a first order moment stochastic formulation may only be used to model a structural complexity (described by the random parameter) in the low frequency range. In order to evaluate the high frequency behaviour of the structures, it is necessary to deal with the second order moments of the different variables. The interest of the second order moment description is shown by figures 5.7 and 5.9. The expectations of the square displacement variables are in good agreement with the modal description in the low frequency range (the size of the range depends on the value of the standard deviation), and a smooth asymptotic behaviour in the high frequency field is obtained.

5.2 Beam

Considering an homogeneous, isotropic, linear, elastic beam transversally loaded by a harmonic force, and assuming small displacements, write its equation of motion in the frequency domain can be written [59]:

$$\frac{\partial^4 w}{\partial x^4} - k^4 w = \frac{q(x)}{EI} \tag{5.12}$$

where I denotes the moment of inertia, and $w(x)$ is the flexural displacement in y axis direction, while x axis is along the beam axis. The parameter k represents the wave number and may be written:

$$k^4 \;=\; \omega^2 \rho S/EI(i+i\eta) \approx k_0^4(1-i\eta) \tag{5.13}$$

where $k_0^4 = \omega^2 \rho S/EI$.
For the beam, G has the following expression:

$$G(\xi,x) = -(1/4k^3)[ie^{-ik|\xi-x|} + e^{-k|\xi-x|}] \tag{5.14}$$

In relation to the beam, two equations are required in order to solve the entire set of boundary unknowns.
Equations for the beam evaluated at point ξ:

$$\begin{aligned} w(\xi) \;=\; & \int_{x_1}^{x_2} \frac{q(x)}{EI} G(\xi,x)dx - \Big[\frac{\partial^3 w(x)}{\partial x^3} G(\xi,x)\Big]_{x_1}^{x_2} + \Big[\frac{\partial^2 w(x)}{\partial x^2}\frac{\partial G(\xi,x)}{\partial x}\Big]_{x_1}^{x_2} \\ & - \Big[\frac{\partial w(x)}{\partial x}\frac{\partial^2 G(\xi,x)}{\partial x^2}\Big]_{x_1}^{x_2} + \Big[w(x)\frac{\partial^3 G(\xi,x)}{\partial x^3}\Big]_{x_1}^{x_2} \end{aligned} \tag{5.15}$$

$$\begin{aligned} \frac{\partial w(\xi)}{\partial \xi} \;=\; & \int_{x_1}^{x_2} \frac{q(x)}{EI}\frac{\partial G(\xi,x)}{\partial \xi} dx - \Big[\frac{\partial^3 w(x)}{\partial x^3}\frac{\partial G(\xi,x)}{\partial \xi}\Big]_{x_1}^{x_2} + \Big[\frac{\partial^2 w(x)}{\partial x^2}\frac{\partial^2 G(\xi,x)}{\partial x \partial \xi}\Big]_{x_1}^{x_2} \\ & - \Big[\frac{\partial w(x)}{\partial x}\frac{\partial^3 G(\xi,x)}{\partial x^2 \partial \xi}\Big]_{x_1}^{x_2} + \Big[w(x)\frac{\partial^4 G(\xi,x)}{\partial x^3 \partial \xi}\Big]_{x_1}^{x_2} \end{aligned} \tag{5.16}$$

For a clamped/clamped beam, the boundary conditions become: $w(x_1) = w(x_2) = 0$ and $\partial w(x_1)/\partial x = \partial w(x_2)/\partial x = 0$.

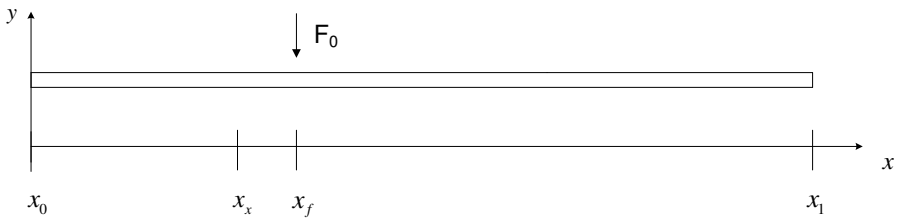

Figure 5.10: Single beam structure.

5.2.1 BEM application: beam

The BEM formulation as been applied to a simple beam, figure 5.10. The mechanical system is considered to be homogeneous, isotropic, linear, elastic, and the hypothesis of small displacement is taken into account.
The points x_1 and x_0 are the boundaries of the beam which is excited by an external shear harmonic force, F_0, located at x_f. The boundary conditions are free-free

$$\frac{\partial^3 w(x_0)}{\partial x^3} = \frac{\partial^3 w(x_1)}{\partial x^3} = 0, \qquad \frac{\partial^2 w(x_0)}{\partial x^2} = \frac{\partial^2 w(x_1)}{\partial x^2} = 0.$$

The geometrical and mechanical characteristics of the beam are given in table 5.6.
The response is evaluated in terms of slope and displacement at the boundary points x_0, fig. 5.11 and x_1, fig. 5.12. Also the displacement at an internal point, $x_x = 0.13$m is reported, fig. 5.13.

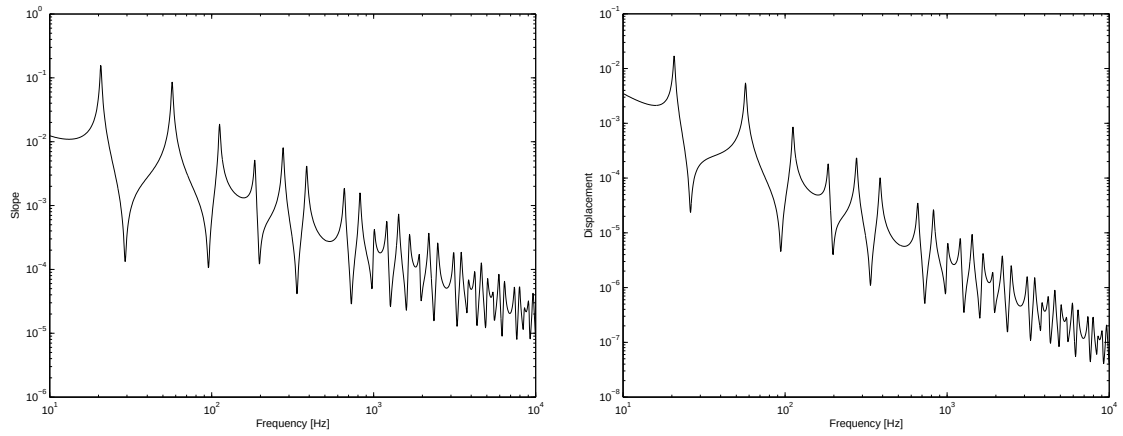

(a) (b)

Figure 5.11: BEM single beam. Frequency evolution of the modulus of the slope (a) and displacement (b) at x_0.

	length [m]	x_f [m]	E [N/m^2]	S [m^2]	I_z [m^4]	η [%]	ρ [kg/m^3]
Beam	0.50	0.15	$2.1 \cdot 10^{11}$	10^{-4}	$3.80 \cdot 10^{-12}$	2	7800

Table 5.6: BEM application. Parameters of the beam.

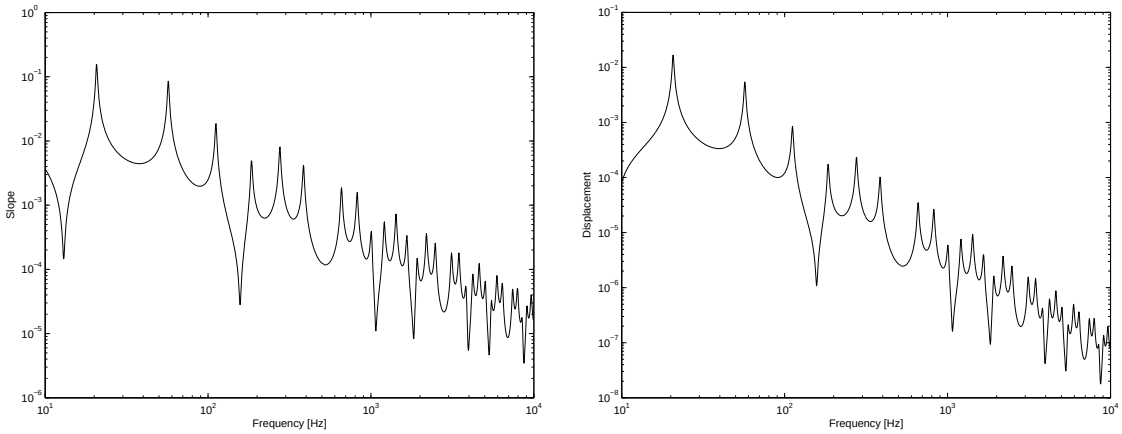

(a) (b)

Figure 5.12: BEM single beam. Frequency evolution of the modulus of the slope (a) and displacement (b) at x_0.

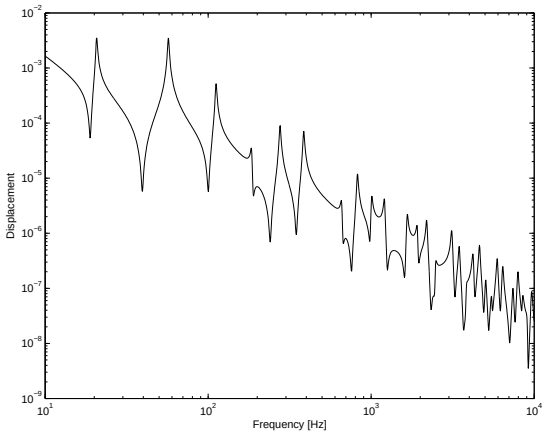

Figure 5.13: BEM single beam. Frequency evolution of the modulus of the displacement at x_x.

Those results obtained using the BEM formulation can be compared to the natural frequencies obtained with an analytical calculation [59] for a free-free beam, fig. 5.14.

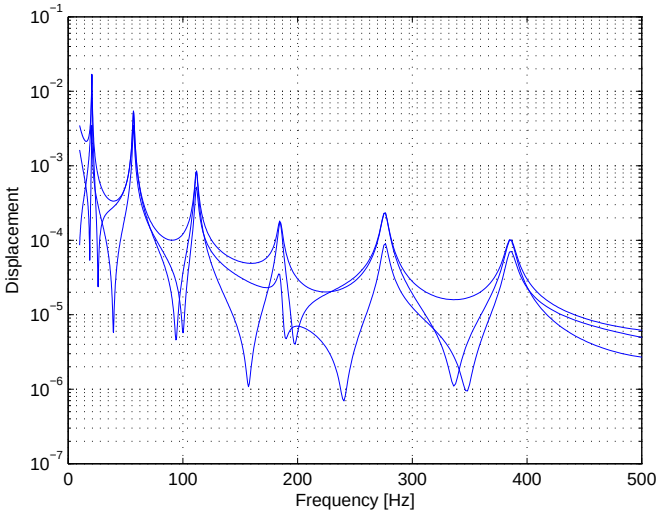

(a)

Number	Nat.Freq. [Hz]
1	20,2
2	55,7
3	109,1
4	180,4
5	269,5
6	376,4
7	501,0

(b)

Figure 5.14: BEM single beam. Comparison of the value of the natural frequencies with BEM (a) and analytical calculation (b).

We can say that there is a good agreement between the results obtained with the two different methods. This will be important in the following section because the BEM results for the beam will be used as references results to illustrate the capabilities and features of SIF.

5.2.2 SIF application: beam

In this section the SIF formulation for the free-free beam will be developed and applied. With respect to the BEM formulation, a randomness is used in the geometrical description of the boundary locations, fig. 5.15.

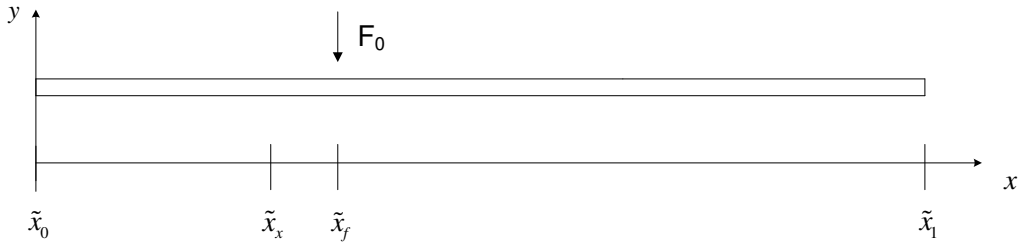

Figure 5.15: Single beam structure with random boundaries.

SIF single beam: deriving the equations

The SIF equations are obtained from eqs.(5.15)-(5.16) using the procedure reported in chapter 4. The basic BEM equations are randomized, introducing a random parameter at

boundary locations, x_0 and x_1, and also on the force location x_f. Then eq.(5.15), evaluated in $\tilde{x}_0$, is multiplied by the conjugate of $w(\tilde{x}_0)$, and eq.(5.16), evaluated in $\tilde{x}_0$, is multiplied by the conjugate of $\partial w^*(\tilde{x}_0)/\partial x$. An analogous procedure is used for $\tilde{x}_1$.

$$\begin{aligned}
\Big\langle \Big| w(\tilde{x}_0) \Big|^2 \Big\rangle &= \frac{F_0}{EI} \Big\langle w^*(\tilde{x}_0) G(\tilde{x}_0, \tilde{x}_f) \Big\rangle - \Big\langle w^*(\tilde{x}_0) \Big\rangle \Big\langle \frac{\partial w(\tilde{x}_1)}{\partial x} \Big\rangle \Big\langle \frac{\partial^2 G(\tilde{x}_0, \tilde{x}_1)}{\partial x^2} \Big\rangle \\
&+ \Big\langle w^*(\tilde{x}_0) \frac{\partial w(\tilde{x}_0)}{\partial x} \Big\rangle \frac{\partial^2 G(\tilde{x}_0, \tilde{x}_0)}{\partial x^2} + \Big\langle w^*(\tilde{x}_0) \Big\rangle \Big\langle w(\tilde{x}_1) \Big\rangle \Big\langle \frac{\partial^3 G(\tilde{x}_0, \tilde{x}_1)}{\partial x^3} \Big\rangle \\
&- \Big\langle \Big| w(\tilde{x}_0) \Big|^2 \Big\rangle \frac{\partial^3 G(\tilde{x}_0, \tilde{x}_0)}{\partial x^3} \qquad (5.17)
\end{aligned}$$

$$\begin{aligned}
\Big\langle \Big| w(\tilde{x}_1) \Big|^2 \Big\rangle &= \frac{F_0}{EI} \Big\langle w^*(\tilde{x}_1) G(\tilde{x}_1, \tilde{x}_f) \Big\rangle - \Big\langle w^*(\tilde{x}_1) \frac{\partial w(\tilde{x}_1)}{\partial x} \Big\rangle \frac{\partial^2 G(\tilde{x}_1, \tilde{x}_1)}{\partial x^2} \\
&+ \Big\langle w^*(\tilde{x}_1) \Big\rangle \Big\langle \frac{\partial w(\tilde{x}_0)}{\partial x} \Big\rangle \Big\langle \frac{\partial^2 G(\tilde{x}_1, \tilde{x}_0)}{\partial x^2} \Big\rangle + \Big\langle \Big| w(\tilde{x}_1) \Big|^2 \Big\rangle \frac{\partial^3 G(\tilde{x}_1, \tilde{x}_1)}{\partial x^3} \\
&- \Big\langle w^*(\tilde{x}_1) \Big\rangle \Big\langle w(\tilde{x}_0) \Big\rangle \Big\langle \frac{\partial^3 G(\tilde{x}_1, \tilde{x}_0)}{\partial x^3} \Big\rangle \qquad (5.18)
\end{aligned}$$

$$\begin{aligned}
\Big\langle \Big| \frac{\partial w(\tilde{x}_0)}{\partial x} \Big|^2 \Big\rangle &= \frac{F_0}{EI} \Big\langle \frac{\partial w^*(\tilde{x}_0)}{\partial x} \frac{\partial G(\tilde{x}_0, \tilde{x}_f)}{\partial \xi} \Big\rangle - \Big\langle \frac{\partial w^*(\tilde{x}_0)}{\partial x} \Big\rangle \Big\langle \frac{\partial w(\tilde{x}_1)}{\partial x} \Big\rangle \Big\langle \frac{\partial^3 G(\tilde{x}_0, \tilde{x}_1)}{\partial x^2 \partial \xi} \Big\rangle \\
&+ \Big\langle \Big| \frac{\partial w(\tilde{x}_0)}{\partial x} \Big|^2 \Big\rangle \frac{\partial^3 G(\tilde{x}_0, \tilde{x}_0)}{\partial x^2 \partial \xi} + \Big\langle \frac{\partial w(\tilde{x}_0)}{\partial x} \Big\rangle \Big\langle w(\tilde{x}_1) \Big\rangle \Big\langle \frac{\partial^4 G(\tilde{x}_0, \tilde{x}_1)}{\partial x^3 \partial \xi} \Big\rangle \\
&- \Big\langle \frac{\partial w^*(\tilde{x}_0)}{\partial x} w(\tilde{x}_0) \Big\rangle \frac{\partial^4 G(\tilde{x}_0, \tilde{x}_0)}{\partial x^3 \partial \xi} \qquad (5.19)
\end{aligned}$$

$$\begin{aligned}
\Big\langle \Big| \frac{\partial w(\tilde{x}_1)}{\partial x} \Big|^2 \Big\rangle &= \frac{F_0}{EI} \Big\langle \frac{\partial w^*(\tilde{x}_1)}{\partial x} \frac{\partial G(\tilde{x}_1, \tilde{x}_f)}{\partial \xi} \Big\rangle - \Big\langle \Big| \frac{\partial w(\tilde{x}_1)}{\partial x} \Big|^2 \Big\rangle \frac{\partial^3 G(\tilde{x}_1, \tilde{x}_1)}{\partial x^2 \partial \xi} \\
&+ \Big\langle \frac{\partial w^*(\tilde{x}_1)}{\partial x} \Big\rangle \Big\langle \frac{\partial w(\tilde{x}_0)}{\partial x} \Big\rangle \Big\langle \frac{\partial^3 G(\tilde{x}_1, \tilde{x}_0)}{\partial x^2 \partial \xi} \Big\rangle + \Big\langle \frac{\partial w^*(x_1)}{\partial x} w(\tilde{x}_1) \Big\rangle \frac{\partial^4 G(\tilde{x}_1, \tilde{x}_1)}{\partial x^3 \partial \xi} \\
&- \Big\langle \frac{\partial w^*(\tilde{x}_1)}{\partial x} \Big\rangle \Big\langle w(\tilde{x}_0) \Big\rangle \Big\langle \frac{\partial^4 G(\tilde{x}_1, \tilde{x}_0)}{\partial x^3 \partial \xi} \Big\rangle \qquad (5.20)
\end{aligned}$$

Equations (5.17)-(5.20) are the fundamental equations of SIF for the beam, with free-free boundary conditions. The number of unknowns of this application is 16 and they are reported below.

$$\begin{aligned}
&\Big\langle \Big| w(\tilde{x}_0) \Big|^2 \Big\rangle, \Big\langle \Big| w(\tilde{x}_1) \Big|^2 \Big\rangle, \Big\langle \Big| \frac{\partial w(\tilde{x}_0)}{\partial x} \Big|^2 \Big\rangle, \Big\langle \Big| \frac{\partial w(\tilde{x}_1)}{\partial x} \Big|^2 \Big\rangle \\
&\Big\langle w(\tilde{x}_0) \frac{\partial w^*(\tilde{x}_0)}{\partial x} \Big\rangle, \Big\langle w^*(\tilde{x}_0) \frac{\partial w(\tilde{x}_0)}{\partial x} \Big\rangle, \Big\langle w(\tilde{x}_1) \frac{\partial w^*(\tilde{x}_1)}{\partial x} \Big\rangle, \Big\langle w^*(\tilde{x}_1) \frac{\partial w(\tilde{x}_1)}{\partial x} \Big\rangle \\
&\Big\langle w^*(\tilde{x}_0) G(\tilde{x}_0, \tilde{x}_f) \Big\rangle, \Big\langle w^*(\tilde{x}_1) G(\tilde{x}_1, \tilde{x}_f) \Big\rangle, \Big\langle \frac{\partial w^*(\tilde{x}_0)}{\partial x} G(\tilde{x}_0, \tilde{x}_f) \Big\rangle, \Big\langle \frac{\partial w^*(\tilde{x}_0)}{\partial x} G(\tilde{x}_0, \tilde{x}_f) \Big\rangle \\
&\Big\langle w^*(\tilde{x}_0) \frac{\partial G(\tilde{x}_0, \tilde{x}_f)}{\partial \xi} \Big\rangle, \Big\langle w^*(\tilde{x}_1) \frac{\partial G(\tilde{x}_1, \tilde{x}_f)}{\partial \xi} \Big\rangle, \\
&\Big\langle \frac{\partial w^*(\tilde{x}_0)}{\partial x} \frac{\partial G(\tilde{x}_0, \tilde{x}_f)}{\partial \xi} \Big\rangle, \Big\langle \frac{\partial w^*(\tilde{x}_1)}{\partial x} \frac{\partial G(\tilde{x}_1, \tilde{x}_f)}{\partial \xi} \Big\rangle
\end{aligned}$$

Four of the missing twelve equations are obtained multiplying the basic equations (5.15) and (5.16) evaluated at x_0 respectively by the conjugate of $\partial w(\tilde{x}_0)/\partial x$ and $w(\tilde{x}_0)$; the same procedure is used for boundary x_1. The remaining eight equations are obtained multiplying the conjugate of the basic equations at $\tilde{x}_0$ and $\tilde{x}_1$ by the contributions of the primary force F_0, like $F_0/EI \cdot G(\tilde{x}_0, \tilde{x}_f)$ and $F_0/EI \cdot \partial G(\tilde{x}_0, \tilde{x}_f)/\partial \xi$.

After the evaluation of the boundary unknowns, it is possible to write an equation giving the expectations of the square unknowns in the whole domain. The spatial position $\tilde{\xi}$ is considered random and the latter assumptions are used. The random assumptions are utilized in the following equation. One obtains:

$$
\begin{aligned}
\Big\langle \Big| w(\tilde{\xi}) \Big|^2 \Big\rangle \;=\; & \Big|\frac{F_0}{EI}\Big| \Big\langle \Big| G(\tilde{\xi},\tilde{x}_f) \Big|^2 \Big\rangle \\
& + \Big\langle \Big| \frac{\partial w(\tilde{x}_1)}{\partial x} \Big|^2 \Big\rangle \Big\langle \Big| \frac{\partial^2 G(\tilde{\xi},\tilde{x}_1)}{\partial x^2} \Big|^2 \Big\rangle + \Big\langle \Big| \frac{\partial w(\tilde{x}_0)}{\partial x} \Big|^2 \Big\rangle \Big\langle \Big| \frac{\partial^2 G(\tilde{\xi},\tilde{x}_0)}{\partial x^2} \Big|^2 \Big\rangle \\
& + \Big\langle \Big| w(\tilde{x}_1) \Big|^2 \Big\rangle \Big\langle \Big| \frac{\partial^3 G(\tilde{\xi},\tilde{x}_1)}{\partial x^3} \Big|^2 \Big\rangle + \Big\langle \Big| w(\tilde{x}_0) \Big|^2 \Big\rangle \Big\langle \Big| \frac{\partial^3 G(\tilde{\xi},\tilde{x}_0)}{\partial x^3} \Big|^2 \Big\rangle \\
& + 2\mathrm{Re}\Big\{ -\Big(\frac{F_0}{EI}\Big)^* \Big\langle G^*(\tilde{\xi},\tilde{x}_f) \Big\rangle \Big\langle \frac{\partial w(\tilde{x}_1)}{\partial x} \Big\rangle \Big\langle \frac{\partial^2 G(\tilde{\xi},\tilde{x}_1)}{\partial x^2} \Big\rangle \\
& + \Big(\frac{F_0}{EI}\Big)^* \Big\langle G^*(\tilde{\xi},\tilde{x}_f) \Big\rangle \Big\langle \frac{\partial w(\tilde{x}_0)}{\partial x} \Big\rangle \Big\langle \frac{\partial^2 G(\tilde{\xi},\tilde{x}_0)}{\partial x^2} \Big\rangle \\
& + \Big(\frac{F_0}{EI}\Big)^* \Big\langle G^*(\tilde{\xi},\tilde{x}_f) \Big\rangle \Big\langle w(\tilde{x}_1) \Big\rangle \Big\langle \frac{\partial^3 G(\tilde{\xi},\tilde{x}_1)}{\partial x^3} \Big\rangle \\
& - \Big(\frac{F_0}{EI}\Big)^* \Big\langle G^*(\tilde{\xi},\tilde{x}_f) \Big\rangle \Big\langle w(\tilde{x}_0) \Big\rangle \Big\langle \frac{\partial^3 G(\tilde{\xi},\tilde{x}_0)}{\partial x^3} \Big\rangle \Big] \\
& - \Big\langle \frac{\partial w^*(\tilde{x}_1)}{\partial x} \Big\rangle \Big\langle \frac{\partial^2 G^*(\tilde{\xi},\tilde{x}_1)}{\partial x^2} \Big\rangle \Big\langle \frac{\partial w(\tilde{x}_0)}{\partial x} \Big\rangle \Big\langle \frac{\partial^2 G(\tilde{\xi},\tilde{x}_0)}{\partial x^2} \Big\rangle \\
& + \Big\langle \frac{\partial w^*(\tilde{x}_1)}{\partial x} \Big\rangle \Big\langle \frac{\partial^2 G^*(\tilde{\xi},\tilde{x}_1)}{\partial x^2} \Big\rangle \Big\langle w(\tilde{x}_0) \Big\rangle \Big\langle \frac{\partial^3 G(\tilde{\xi},\tilde{x}_0)}{\partial x^3} \Big\rangle \Big] \\
& - \Big\langle w(\tilde{x}_1) \frac{\partial w^*(\tilde{x}_1)}{\partial x} \Big\rangle \Big\langle \frac{\partial^3 G(\tilde{\xi},\tilde{x}_1)}{\partial x^3} \frac{\partial^2 G^*(\tilde{\xi},\tilde{x}_1)}{\partial x^2} \Big\rangle \\
& + \Big\langle w(\tilde{x}_0) \frac{\partial w^*(\tilde{x}_0)}{\partial x} \Big\rangle \Big\langle \frac{\partial^3 G(\tilde{\xi},\tilde{x}_0)}{\partial x^3} \frac{\partial^2 G^*(\tilde{\xi},\tilde{x}_0)}{\partial x^2} \Big\rangle \\
& + \Big\langle w(\tilde{x}_1) \Big\rangle \Big\langle \frac{\partial w^*(\tilde{x}_0)}{\partial x} \Big\rangle \Big\langle \frac{\partial^2 G^*(\tilde{\xi},\tilde{x}_0)}{\partial x^2} \Big\rangle \Big\langle \frac{\partial^3 G(\tilde{\xi},\tilde{x}_1)}{\partial x^3} \Big\rangle \\
& - \Big\langle w(\tilde{x}_0) \Big\rangle \Big\langle w^*(\tilde{x}_1) \Big\rangle \Big\langle \frac{\partial^3 G(\tilde{\xi},\tilde{x}_0)}{\partial x^3} \Big\rangle \Big\langle \frac{\partial^3 G^*(\tilde{\xi},\tilde{x}_1)}{\partial x^3} \Big\rangle \Big\} \qquad (5.21)
\end{aligned}
$$

SIF single beam: results

The geometrical and mechanical characteristics of the beam, fig. 5.15, are given in table 5.7. The results obtained with the SIF formulation at the boundaries $\tilde{x}_0$ and $\tilde{x}_1$ and at the internal point $\tilde{x}_x = 0.13$m are compared with those obtained with BEM for the same nominal system with no randomness.

	length [m]	x_f [m]	E [N/m^2]	S [m^2]	I_z [m^4]	η [%]	ρ [kg/m^3]	σ
Beam	0.50	0.15	$2.1 \cdot 10^{11}$	10^{-4}	$3.80 \cdot 10^{-12}$	2	7800	0.01

Table 5.7: SIF application. Parameters of the beam.

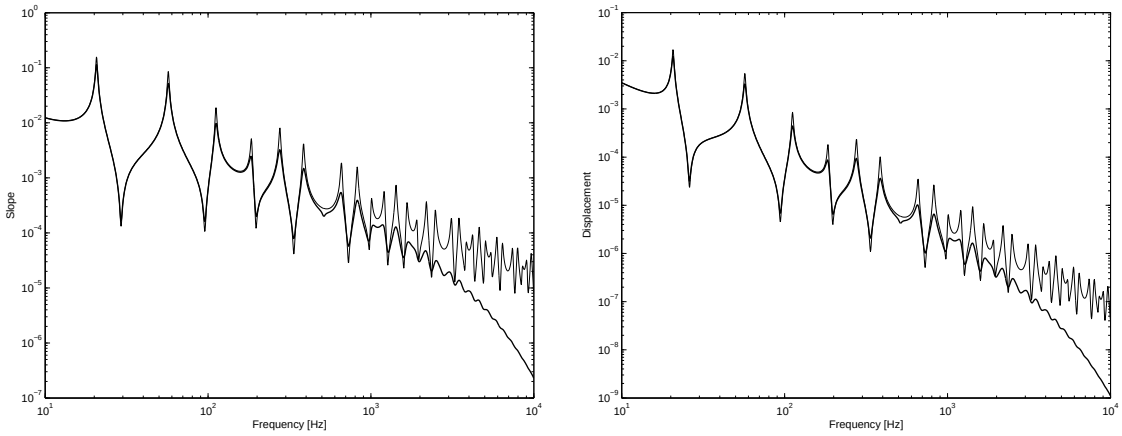

(a) (b)

Figure 5.16: SIF single beam. First order moment solution. Frequency evolution of the modulus of the slope (a) and displacement (b) at x_0. —— SIF BEM

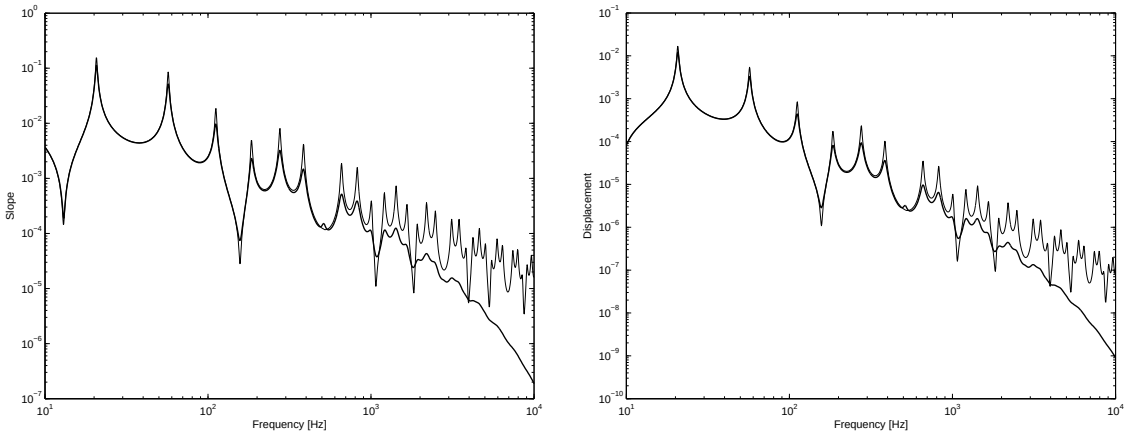

(a) (b)

Figure 5.17: SIF single beam. First order moment solution. Frequency evolution of the modulus of the slope (a) and displacement (b) at x_1. —— SIF BEM

The frequency evolution of two first order moment variables is shown in figures 5.16 and 5.17. The evaluation of these variables provides some information on the behaviour of the structure, only in the low frequency range for which the random parameters do not greatly disturb the unknowns. When the frequency increases, the expectations with respect to the geometrical random parameters of the variables vanish to zero.

The second order results are reported in figures 5.18 and 5.19. The results in terms of displacement and velocity at point $\tilde{x}_x$, the internal point, are depicted in fig. 5.20. The same observations as for the case of the rod can be made. The low frequency response is reached accurately while a smooth behaviour, corresponding to the general trend of the deterministic result, is given in the high frequency domain.

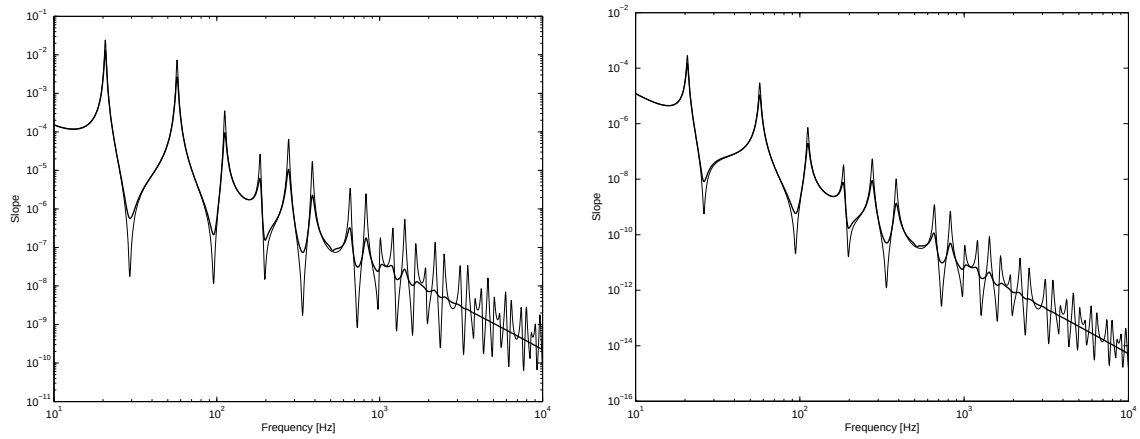

(a) (b)

Figure 5.18: SIF single beam. Second order moment solution. Frequency evolution of the square modulus of the slope (a) and displacement (b) at x_0. —— SIF —— BEM

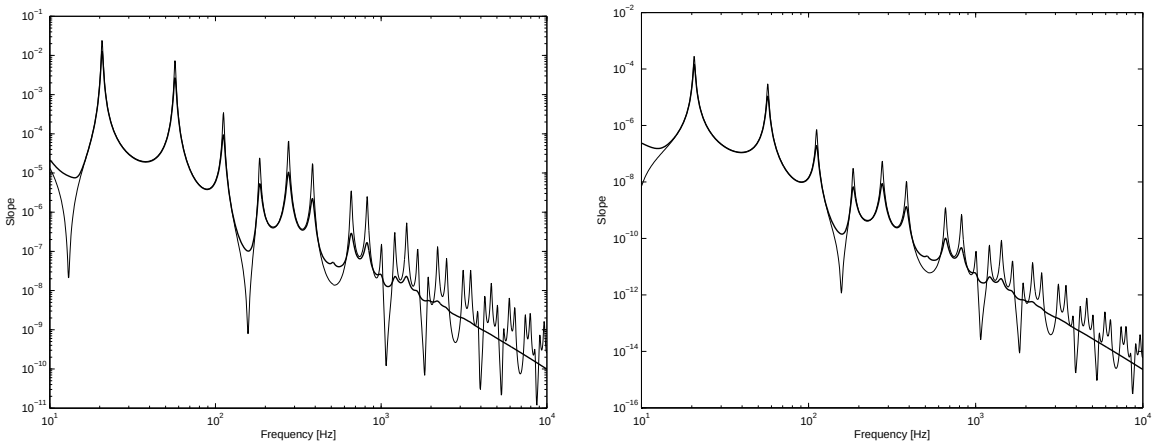

(a) (b)

Figure 5.19: SIF single beam. Second order moment solution. Frequency evolution of the square modulus of the slope (a) and displacement (b) at x_1. —— SIF —— BEM

5.2.3 SIF single beam: validation of results

The SIF results for a single beam have been validated with an experimental test. The experimental results, obtained performing a classical laser FRF measurement on an excited beam, figure 5.10, have been compared to those obtained with a classical deterministic formulation BEM, and with SIF. The geometrical and physical properties of the beam are reported in table 5.8.

	length [m]	x_f [m]	E [N/m^2]	S [m^2]	I_z [m^4]	η [%]	ρ [kg/m^3]
Beam	0.50	0.15	$2.1 \cdot 10^{11}$	$4.85 \cdot 10^{-5}$	$3.80 \cdot 10^{-12}$	2	7800

Table 5.8: SIF validation: Geometrical and physical properties of the beam.

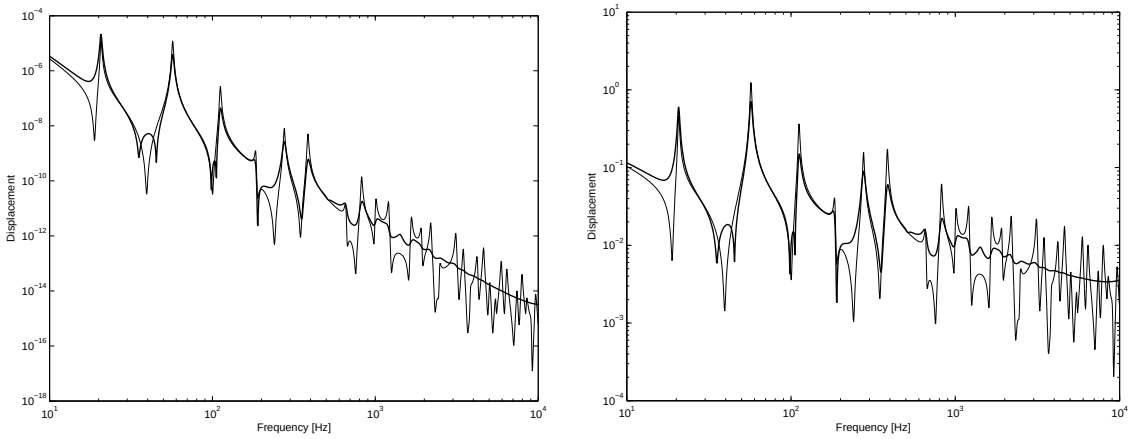

(a) (b)

Figure 5.20: SIF single beam. Second order moment solution. Frequency evolution of the square modulus of the displacement (a) and velocity (b) at point x_x. —— SIF —— BEM

The beam is excited by an external shear force, F_0 located at $x_f = 0.15$m, and the FRF is evaluated at point $x_x = 0.13$m.
The results are reported in figure 5.21. In the low frequency range we have a good agreement between the BEM and the experimental results, even if probably the value of the structural damping can be adjusted. But as the frequency increases we have no more a good agreement and this can be due to the errors in measurements and in characterizing the experimental sample. We can see in figure 5.22 that the response of a flexural beam is very sensitive to small changes in the physical properties as the frequency increase. In figure 5.22 are reported the results of the FRF at x_x modifying the length of the beam by 2%. Thus it is necessary to have a very precise and detailed characterization of the sample.

The SIF formulation gives good results, which fits with the experimental one in the low-frequency range, and then, as the frequency increases is able to correctly predict the trend of the FRF. From this simple example we can understand the advantage of the SIF formulation against a deterministic formulation. With a classical characterization of the sample and with only one run of the program, the SIF is able to give a result which is representative of a population of structures over the whole frequency range.

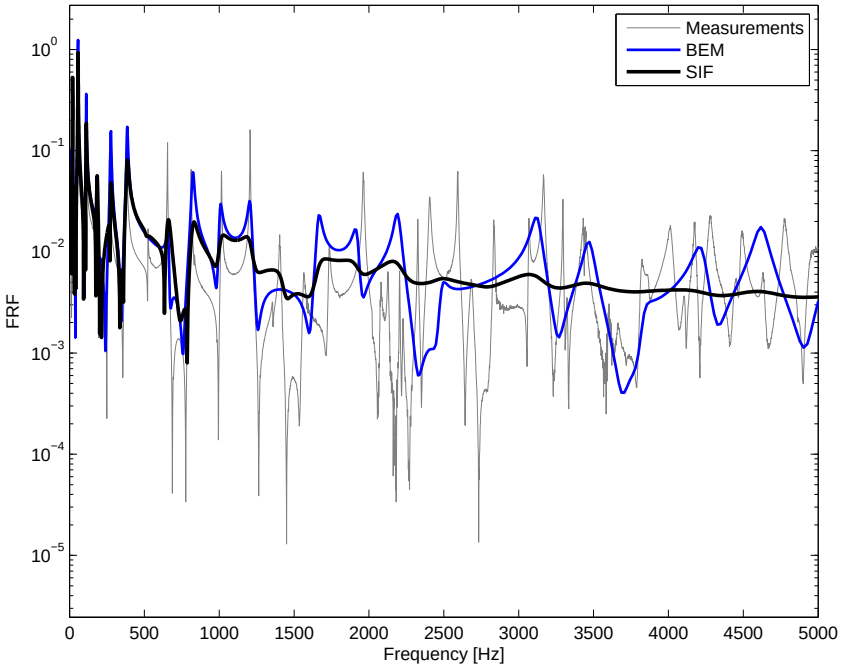

Figure 5.21: SIF beam validation. Second order moment solution. Frequency evolution of the FRF function at x_x. —— measurements, —— BEM solution, ——— SIF solution

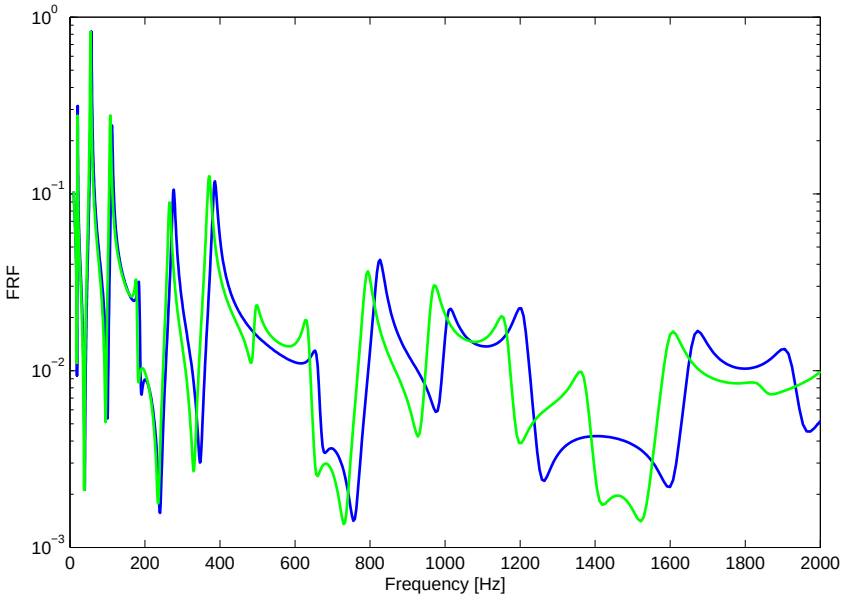

Figure 5.22: SIF beam validation. Shift in the frequency evolution of the FRF function at x_x modifying the length of 2%.

5.3 Two coupled rods

In this section the SIF formulation is applied to a structure made of two coupled parts: two rods. It is a simple structure, but it allows us to test the SIF for assembled systems.

5.3.1 BEM two coupled rods: deriving the equations

Two coupled rods with different geometrical and mechanical characteristics are considered, fig. 5.23: The mechanical system is considered to be homogeneous, isotropic, linear,

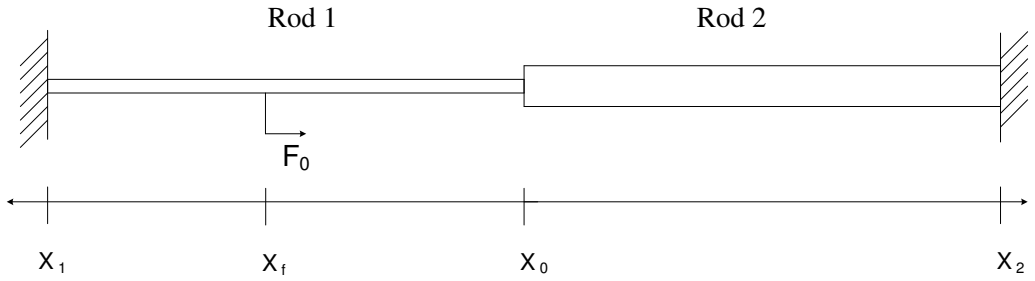

Figure 5.23: BEM application: two coupled rods

elastic, and the hypothesis of small displacement is taken into account.
The points x_1 and x_0 are the boundaries of rod 1, x_0 and x_2 of rod 2. The point x_0 is the coupling point.
Two different reference coordinate systems are used to describe the structure, both centered in x_0, the coupling point, and with opposite direction.
Rod 1 is excited by an external longitudinal harmonic force, F_0. The boundary conditions are clamped- clamped, $w(x_1) = w(x_2) = 0$. The deterministic integral representation for two coupled rods may be written:

$$\begin{aligned} w(\xi_1) &= \frac{F_0}{E_1 S_1} G_1(\xi_1 - x_f) + \frac{\partial w(x_1)}{\partial x} G_1(\xi_1 - x_1) - \\ &\quad - \frac{\partial w^{(1)}(x_0)}{\partial x} G_1(\xi_1 - x_0) + w^{(1)}(x_0) \frac{\partial G_1(\xi_1 - x_0)}{\partial x} \\ w(\xi_2) &= \frac{\partial w(x_2)}{\partial x} G_2(\xi_2 - x_2) - \frac{\partial w^{(2)}(x_0)}{\partial x} G_2(\xi_2 - x_0) + \\ &\quad + w^{(2)}(x_0) \frac{\partial G_2(\xi_2 - x_0)}{\partial x} \end{aligned} \tag{5.22}$$

Evaluating the equations (5.22) at the boundary points for the two rods, we obtain the boundary equations for this structure:
Rod 1

$$\begin{aligned} 0 &= \frac{F_0}{E_1 S_1} G_1(x_1 - x_f) + \frac{\partial w(x_1)}{\partial x} G_1(x_1 - x_1) \\ &\quad - \frac{\partial w^{(1)}(x_0)}{\partial x} G_1(x_1 - x_0) + w^{(1)}(x_0) \frac{\partial G_1(x_1 - x_0)}{\partial x} \\ 0 &= \frac{F_0}{E_1 S_1} G_1(x_0 - x_f) + \frac{\partial w(x_1)}{\partial x} G_1(x_0 - x_1) \end{aligned}$$

$$-\frac{\partial w^{(1)}(x_0)}{\partial x}G_1(x_0-x_0)+w^{(1)}(x_0)\Big(\frac{\partial G_1(x_0-x_0)}{\partial x}-1\Big) \tag{5.23}$$

Rod 2

$$\begin{aligned} 0 &= \frac{\partial w(x_2)}{\partial x}G_2(x_2-x_2)-\frac{\partial w^{(2)}(x_0)}{\partial x}G_2(x_2-x_0) \\ &\quad +w^{(2)}(x_0)\frac{\partial G_2(x_2-x_0)}{\partial x} \\ 0 &= \frac{\partial w(x_2)}{\partial x}G_2(x_0-x_2)-\frac{\partial w^{(2)}(x_0)}{\partial x}G_2(x_0-x_0) \\ &\quad +w^{(2)}(x_0)\Big(\frac{\partial G_2(x_0-x_0)}{\partial x}-1\Big) \end{aligned} \tag{5.24}$$

Coupling equations (continuity of displacement and traction at the junction):

$$w^{(1)}(x_0)=-w^{(2)}(x_0) \tag{5.25}$$

$$E_1S_1\frac{\partial w^{(1)}(x_0)}{\partial x}=E_2S_2\frac{\partial w^{(2)}(x_0)}{\partial x} \tag{5.26}$$

List of the unknowns:
Rod 1

$$\frac{\partial w(x_1)}{\partial x},\frac{\partial w^{(1)}(x_0)}{\partial x},w^{(1)}(x_0)$$

Rod 2

$$\frac{\partial w(x_2)}{\partial x},\frac{\partial w^{(2)}(x_0)}{\partial x},w^{(2)}(x_0)$$

Linear system solution:

$$\begin{bmatrix} G_1(x_1-x_1) & -G_1(x_1-x_0) & \frac{\partial G_1(x_1-x_0)}{\partial x} & 0 & 0 & 0 \\ G_1(x_0-x_1) & -G_1(x_0-x_0) & \frac{\partial G_1(x_0-x_0)}{\partial x} & 0 & 0 & 0 \\ 0 & 0 & 0 & G_2(x_2-x_2) & -G_2(x_2-x_0) & \frac{\partial G_2(x_2-x_0)}{\partial x} \\ 0 & 0 & 0 & G_2(x_0-x_2) & -G_2(x_0-x_0) & \frac{\partial G_2(x_0-x_0)}{\partial x} \\ 0 & 0 & 1 & 0 & 1 & 0 \\ 0 & E_1S_1 & 0 & -E_2S_2 & 0 & 0 \end{bmatrix} \cdot \begin{bmatrix} \frac{\partial w(x_1)}{\partial x} \\ \frac{\partial w^{(1)}(x_0)}{\partial x} \\ w^{(2)}(x_0) \\ \frac{\partial w(x_2)}{\partial x} \\ \frac{\partial w^{(2)}(x_0)}{\partial x} \\ w^{(2)}(x_0) \end{bmatrix} = \begin{bmatrix} -\frac{F_0}{E_1S_1}G_1(x_1-x_f) \\ -\frac{F_0}{E_1S_1}G_1(x_0-x_f) \\ 0 \\ 0 \\ 0 \\ 0 \end{bmatrix} \tag{5.27}$$

5.3.2 BEM two coupled rods: results

- Configuration n.1
  The physical properties of configuration n.1 are reported in table 5.9 and results in figures 5.24 and 5.25.

	length [m]	x_f [m]	E [N/m^2]	S [m^2]	η [%]	ρ [kg/m^3]
Rod 1	2.45	1.50	$2.1 \cdot 10^{11}$	10^{-4}	2	7800
Rod 2	3.20		$2.1 \cdot 10^{11}$	10^{-4}	2	7800

Table 5.9: BEM application. Parameters of the two rods, configuration n.1

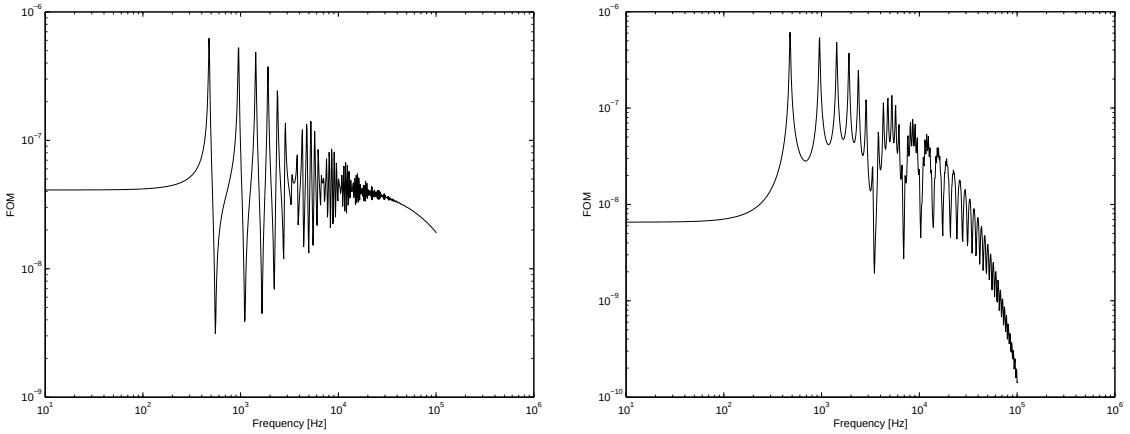

(a) (b)

Figure 5.24: BEM two coupled rods. Frequency evolution of the modulus of the first order moment $\partial w/\partial x$ at x_1 (a) and x_2 (b). Configuration n.1.

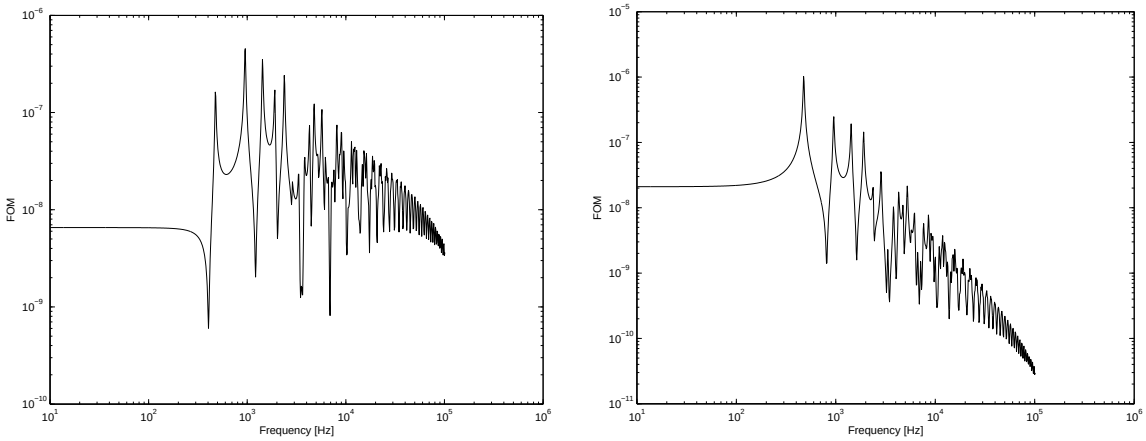

(a) (b)

Figure 5.25: BEM two coupled rods. Frequency evolution of the modulus of the first order moment $\partial w/\partial x$ (a) and w (b) at x_0. Configuration n.1.

- Configuration n.2
  The physical properties of configuration n.2 are reported in table 5.10 and results in figures 5.26 and 5.27.

	length [m]	x_f [m]	E [N/m^2]	S [m^2]	η [%]	ρ [kg/m^3]
Rod 1	1.67	0.48	$2.1 \cdot 10^{11}$	10^{-3}	2	7800
Rod 2	8.92		$2.1 \cdot 10^{10}$	10^{-5}	2	7800

Table 5.10: BEM application. Parameters of the two rods, configuration n.2

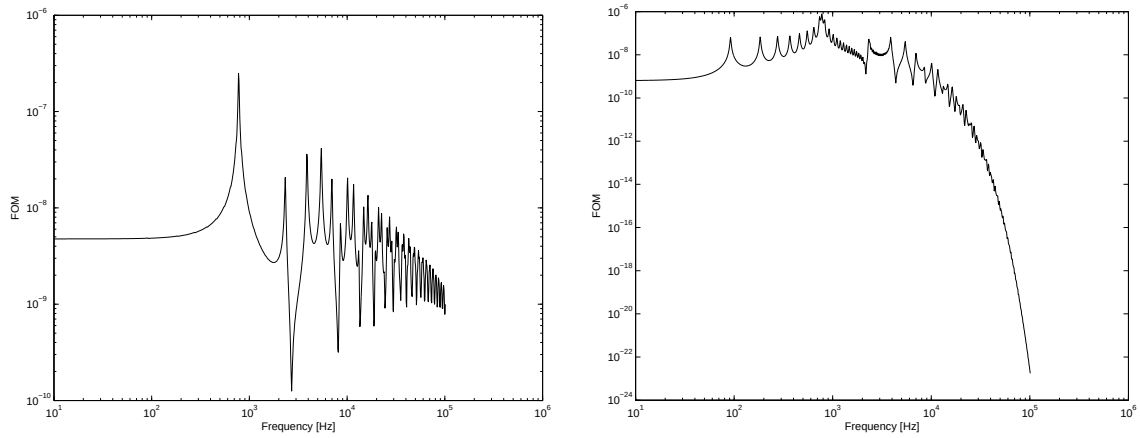

(a) (b)

Figure 5.26: BEM two coupled rods. Frequency evolution of the modulus of the first order moment $\partial w/\partial x$ at x_1 (a) and x_2 (b). Configuration n.2.

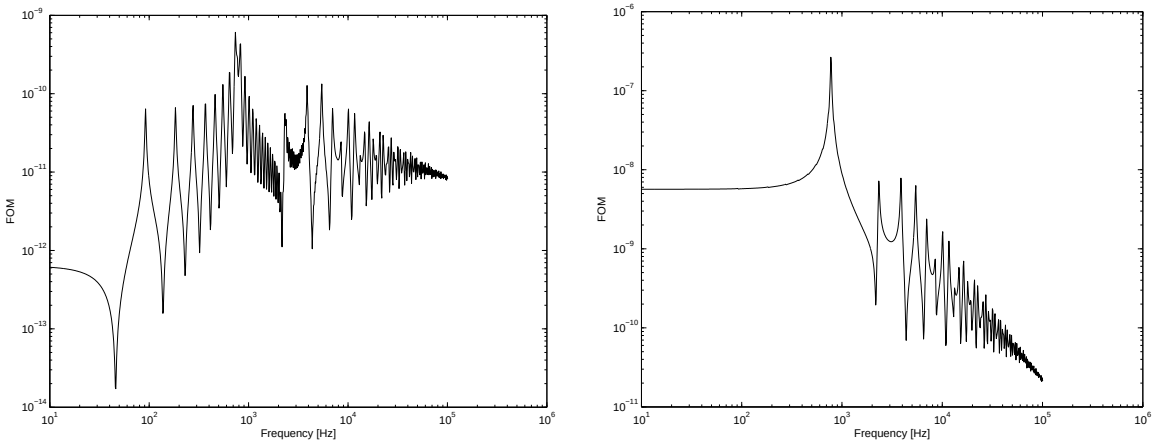

(a) (b)

Figure 5.27: BEM two coupled rods. Frequency evolution of the modulus of the first order moment $\partial w/\partial x$ (a) and w at x_0 (b). Configuration n.2.

- Configuration n.3
  The physical properties of configuration n.3 are reported in table 5.11 and results in figures 5.28 and 5.29.

	length [m]	x_f [m]	E [N/m^2]	S [m^2]	η [%]	ρ [kg/m^3]
Rod 1	8.12	2.50	$2.1 \cdot 10^{10}$	10^{-4}	3	7800
Rod 2	2.33		$2.1 \cdot 10^{11}$	10^{-3}	2	7800

Table 5.11: BEM application. Parameters of the two rods, configuration n.3

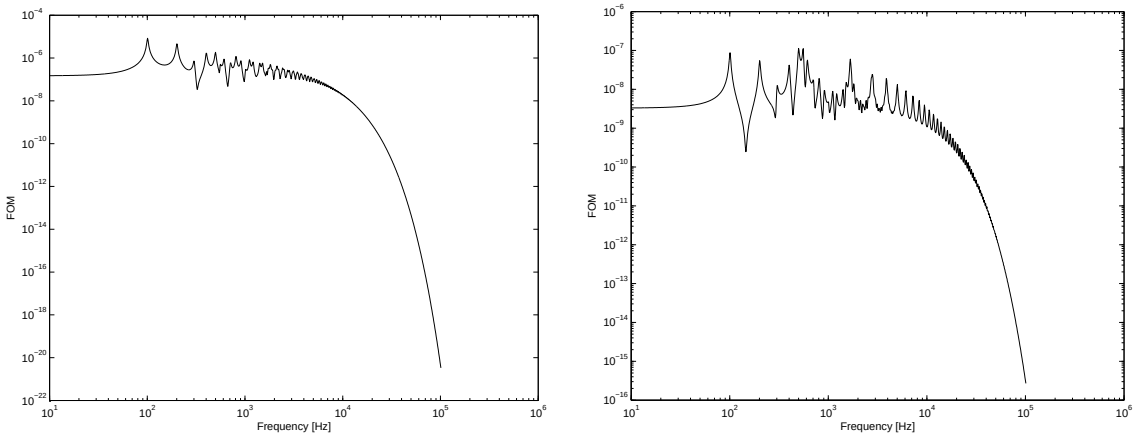

(a) (b)

Figure 5.28: BEM two coupled rods. Frequency evolution of the modulus of the first order moment $\partial w/\partial x$ at x_1 (a) and x_2 (b). Configuration n.3.

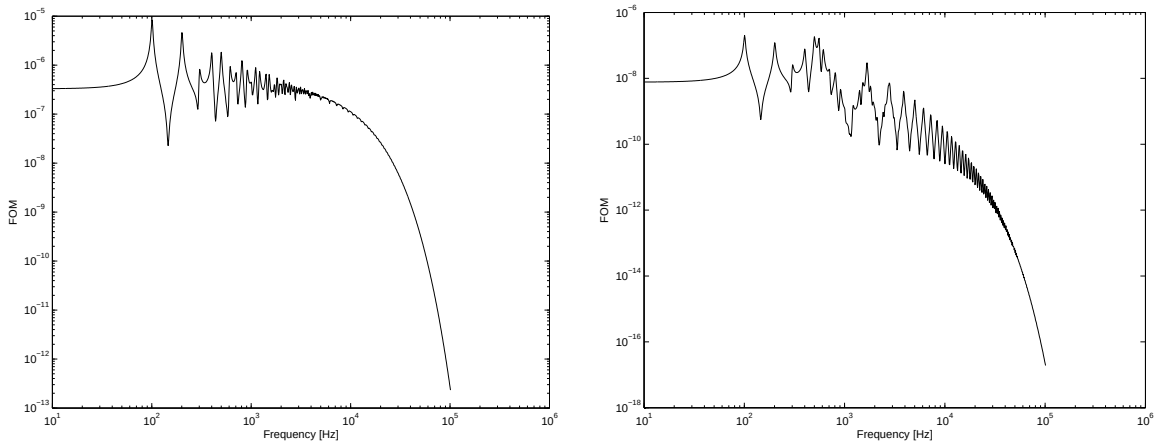

(a) (b)

Figure 5.29: BEM two coupled rods. Frequency evolution of the modulus of the first order moment $\partial w/\partial x$ (a) and w at x_0 (b). Configuration n.3.

5.3.3 Discussion

The two configurations for the coupled rods highlight the different behavior of the structure. In configuration n.2, the rod 1 is typically a low frequency behavior rod as we can see from figures 5.26 and 5.27; rod 2 instead is a high frequency rod, due to the

fact that is longer and more flexible than rod 1. The modes of rod 2 appears at very low frequency, but their influence decrease as the frequency raises, and modes of rod 1 become predominant.
It is also important to notice that the values of traction in the boundary point go to zero as the frequency increases, and this is as much evident as the rod is high frequency. This agree with the high frequency theory, as SEA, that states that a subsystem becomes independent from boundary conditions as the frequency becomes high.

5.3.4 SIF two coupled rods: deriving the equations

In this configuration two coupled rods with different geometrical and mechanical characteristics are considered, fig. 5.30: The mechanical system is considered to be homogeneous,

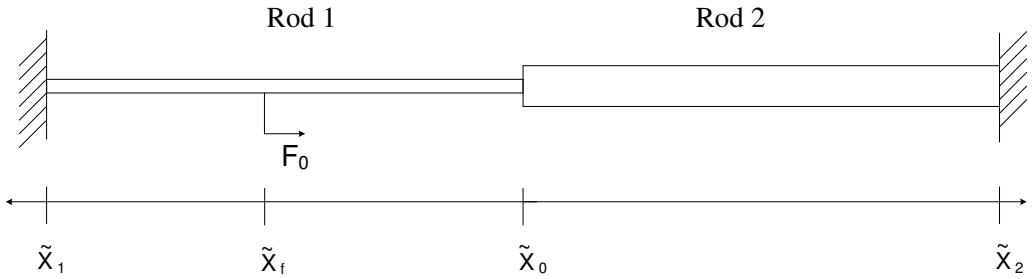

Figure 5.30: SIF application: two coupled rods with random boundaries

isotropic, linear, elastic, and the hypothesis of small displacement is taken into account.
Different configurations in terms of geometrical and physical properties are considered in this section, in order to investigate the efficiency of this formulation.
The points x_1 and x_0 are the boundaries of rod 1, x_0 and x_2 of rod 2. The point x_0 is the coupling point.
Rod 1 is excited by an external longitudinal harmonic force, F_0. The boundary conditions are clamped-clamped, $w(x_1) = w(x_2) = 0$.

Deriving the SIF equations

Boundary element equations for two coupled rods:
Rod 1:

$$\begin{aligned} 0 &= \frac{F_0}{E_1 S_1} G_1(x_1 - x_f) + \frac{\partial w(x_1)}{\partial x} G_1(x_1 - x_1) \\ &\quad - \frac{\partial w^{(1)}(x_0)}{\partial x} G_1(x_1 - x_0) + w^{(1)}(x_0) \frac{\partial G_1(x_1 - x_0)}{\partial x} \qquad (5.28) \\ 0 &= \frac{F_0}{E_1 S_1} G_1(x_0 - x_f) + \frac{\partial w(x_1)}{\partial x} G_1(x_0 - x_1) \\ &\quad - \frac{\partial w^{(1)}(x_0)}{\partial x} G_1(x_0 - x_0) + w^{(1)}(x_0) \Big(\frac{\partial G_1(x_0 - x_0)}{\partial x} - 1 \Big) \qquad (5.29) \end{aligned}$$

Rod 2:

$$
\begin{aligned}
0 &= \frac{\partial w(x_2)}{\partial x} G_2(x_2 - x_2) - \frac{\partial w^{(2)}(x_0)}{\partial x} G_2(x_2 - x_0) \\
&\quad + w^{(2)}(x_0) \frac{\partial G_2(x_2 - x_0)}{\partial x} \qquad (5.30) \\
0 &= \frac{\partial w(x_2)}{\partial x} G_2(x_0 - x_2) - \frac{\partial w^{(2)}(x_0)}{\partial x} G_2(x_0 - x_0) \\
&\quad + w^{(2)}(x_0) \Big(\frac{\partial G_2(x_0 - x_0)}{\partial x} - 1 \Big) \qquad (5.31)
\end{aligned}
$$

Coupling equations (continuity of displacement and traction):

$$w^{(1)}(x_0) = -w^{(2)}(x_0) \qquad (5.32)$$

$$E_1 S_1 \frac{\partial w^{(1)}(x_0)}{\partial x} = E_2 S_2 \frac{\partial w^{(2)}(x_0)}{\partial x} \qquad (5.33)$$

Introducing randomness at the boundaries, x_1, x_2, x_0, x_f, in equations (5.28)-(5.31):
Rod 1:

$$
\begin{aligned}
0 &= \frac{F_0}{E_1 S_1} G_1(\tilde{x}_1 - \tilde{x}_f) + \frac{\partial w(\tilde{x}_1)}{\partial x} G_1(\tilde{x}_1 - \tilde{x}_1) \\
&\quad - \frac{\partial w^{(1)}(\tilde{x}_0)}{\partial x} G_1(\tilde{x}_1 - \tilde{x}_0) + w^{(1)}(\tilde{x}_0) \frac{\partial G_1(\tilde{x}_1 - \tilde{x}_0)}{\partial x} \qquad (5.34) \\
0 &= \frac{F_0}{E_1 S_1} G_1(\tilde{x}_0 - \tilde{x}_f) + \frac{\partial w(\tilde{x}_1)}{\partial x} G_1(\tilde{x}_0 - \tilde{x}_1) \\
&\quad - \frac{\partial w^{(1)}(\tilde{x}_0)}{\partial x} G_1(\tilde{x}_0 - \tilde{x}_0) + w^{(1)}(\tilde{x}_0) \Big(\frac{\partial G_1(\tilde{x}_0 - \tilde{x}_0)}{\partial x} - 1 \Big) \qquad (5.35)
\end{aligned}
$$

Rod 2:

$$
\begin{aligned}
0 &= \frac{\partial w(\tilde{x}_2)}{\partial x} G_2(\tilde{x}_2 - \tilde{x}_2) - \frac{\partial w^{(2)}(\tilde{x}_0)}{\partial x} G_2(\tilde{x}_2 - \tilde{x}_0) \\
&\quad + w^{(2)}(\tilde{x}_0) \frac{\partial G_2(\tilde{x}_2 - \tilde{x}_0)}{\partial x} \qquad (5.36) \\
0 &= \frac{\partial w(\tilde{x}_2)}{\partial x} G_2(\tilde{x}_0 - \tilde{x}_2) - \frac{\partial w^{(2)}(\tilde{x}_0)}{\partial x} G_2(\tilde{x}_0 - \tilde{x}_0) \\
&\quad + w^{(2)}(\tilde{x}_0) \Big(\frac{\partial G_2(\tilde{x}_0 - \tilde{x}_0)}{\partial x} - 1 \Big) \qquad (5.37)
\end{aligned}
$$

Coupling equations:

$$w^{(1)}(\tilde{x}_0) = -w^{(2)}(\tilde{x}_0) \qquad (5.38)$$

$$E_1 S_1 \frac{\partial w^{(1)}(\tilde{x}_0)}{\partial x} = E_2 S_2 \frac{\partial w^{(2)}(\tilde{x}_0)}{\partial x} \qquad (5.39)$$

List of the unknowns:

Rod 1 (10 unknowns)

$$\Big\langle \frac{\partial w(\tilde{x}_1)}{\partial x} \Big\rangle, \Big\langle \frac{\partial w^{(1)}(\tilde{x}_0)}{\partial x} \Big\rangle, \Big\langle w^{(1)}(\tilde{x}_0) \Big\rangle,$$
$$\Big\langle \Big| \frac{\partial w(\tilde{x}_1)}{\partial x} \Big|^2 \Big\rangle, \Big\langle \Big| \frac{\partial w^{(2)}(\tilde{x}_0)}{\partial x} \Big|^2 \Big\rangle, \Big\langle \Big| w^{(1)}(\tilde{x}_0) \Big|^2 \Big\rangle,$$
$$\Big\langle w^{(1)}(\tilde{x}_0) \cdot \frac{\partial w^{(1)*}(\tilde{x}_0)}{\partial x} \Big\rangle, \Big\langle w^{(1)*}(\tilde{x}_0) \cdot \frac{\partial w^{(1)}(\tilde{x}_0)}{\partial x} \Big\rangle,$$
$$\Big\langle \frac{\partial w^*(\tilde{x}_1)}{\partial x} \cdot G_1(\tilde{x}_1 - \tilde{x}_f) \Big\rangle, \Big\langle \frac{\partial w^{(1)*}(\tilde{x}_0)}{\partial x} \cdot G_1(\tilde{x}_0 - \tilde{x}_f) \Big\rangle, \Big\langle w^{(1)*}(\tilde{x}_0) \cdot G_1(\tilde{x}_0 - \tilde{x}_f) \Big\rangle.$$

Rod 2 (9 unknowns)

$$\Big\langle \frac{\partial w(\tilde{x}_2)}{\partial x} \Big\rangle, \Big\langle \frac{\partial w^{(2)}(\tilde{x}_0)}{\partial x} \Big\rangle, \Big\langle w^{(2)}(\tilde{x}_0) \Big\rangle,$$
$$\Big\langle \Big| \frac{\partial w(\tilde{x}_2)}{\partial x} \Big|^2 \Big\rangle, \Big\langle \Big| \frac{\partial w^{(2)}(\tilde{x}_0)}{\partial x} \Big|^2 \Big\rangle, \Big\langle \Big| w^{(2)}(\tilde{x}_0) \Big|^2 \Big\rangle,$$
$$\Big\langle w^{(2)}(\tilde{x}_0) \cdot \frac{\partial w^{(2)*}(\tilde{x}_0)}{\partial x} \Big\rangle, \Big\langle w^{(2)*}(\tilde{x}_0) \cdot \frac{\partial w^{(2)}(\tilde{x}_0)}{\partial x} \Big\rangle,$$
$$\Big\langle \frac{\partial w^{(2)}(\tilde{x}_0)}{\partial x} \cdot G_2(\tilde{x}_2 - \tilde{x}_0) \cdot \frac{\partial w^*(\tilde{x}_2)}{\partial x} \Big\rangle, \Big\langle w^{(2)}(\tilde{x}_0) \cdot \frac{\partial G_2(\tilde{x}_2 - \tilde{x}_0)}{\partial x} \cdot \frac{\partial w^*(\tilde{x}_2)}{\partial x} \Big\rangle.$$

SIF equations of rod 1:

The first equation, (5.40) is obtained by multiplying the first basic equation (5.34), by the conjugate of $\partial w(\tilde{x}_1)/\partial x$ and getting the expectation with respect to $\tilde{x}_1$, $\tilde{x}_0$ and $\tilde{x}_f$; while the second and the third equations, (5.41) and (5.42), are obtained by multiplying the second equation (5.35)respectively by the conjugate of $\partial w^{(1)}(\tilde{x}_0)/\partial x$ and $w^{(1)}(\tilde{x}_0)$.
The fourth and fifth equations, (5.43) and (5.44), are obtained getting the expectation of the basic equations (5.34) and (5.35).
The sixth, (5.45), equation is obtained by multiplying the conjugate of the first basic equation by $F_0/Y_1S_1 \cdot G_1(\tilde{x}_1 - \tilde{x}_f)$; the seventh, (5.46), multiplying the conjugate of the second basic equation by $F_0/Y_1S_1 \cdot G_1(\tilde{x}_0 - \tilde{x}_f)$.

$$\begin{aligned}
0 &= \frac{F_0}{E_1S_1}\Big\langle \frac{\partial w^*(\tilde{x}_1)}{\partial x} G_1(\tilde{x}_1 - \tilde{x}_f) \Big\rangle + \Big\langle \Big| \frac{\partial w(\tilde{x}_1)}{\partial x} \Big|^2 \Big\rangle G_1(\tilde{x}_1 - \tilde{x}_1) \\
&\quad - \Big\langle \frac{\partial w^{(1)}(\tilde{x}_0)}{\partial x} \Big\rangle \Big\langle \frac{\partial w^*(\tilde{x}_1)}{\partial x} \Big\rangle \Big\langle G_1(\tilde{x}_1 - \tilde{x}_0) \Big\rangle \\
&\quad + \Big\langle w^{(1)}(\tilde{x}_0) \Big\rangle \Big\langle \frac{\partial w^*(\tilde{x}_1)}{\partial x} \Big\rangle \Big\langle \frac{\partial G_1(\tilde{x}_1 - \tilde{x}_0)}{\partial x} \Big\rangle, \qquad (5.40) \\
0 &= \frac{F_0}{E_1S_1}\Big\langle \frac{\partial w^{(1)*}(\tilde{x}_0)}{\partial x} G_1(\tilde{x}_0 - \tilde{x}_f) \Big\rangle + \Big\langle \frac{\partial w(\tilde{x}_1)}{\partial x} \Big\rangle \Big\langle \frac{\partial w^{(1)*}(\tilde{x}_0)}{\partial x} \Big\rangle \Big\langle G_1(\tilde{x}_0 - \tilde{x}_1) \Big\rangle \\
&\quad - \Big\langle \Big| \frac{\partial w^{(1)}(\tilde{x}_0)}{\partial x} \Big|^2 \Big\rangle G_1(\tilde{x}_0 - \tilde{x}_0) \\
&\quad + \Big\langle w^{(1)}(\tilde{x}_0) \frac{\partial w^{(1)*}(\tilde{x}_0)}{\partial x} \Big\rangle \Big(\frac{\partial G_1(\tilde{x}_0 - \tilde{x}_0)}{\partial x} - 1 \Big), \qquad (5.41) \\
0 &= \frac{F_0}{E_1S_1}\Big\langle w^{(1)*}(\tilde{x}_0) G_1(\tilde{x}_0 - \tilde{x}_f) \Big\rangle + \Big\langle \frac{\partial w(\tilde{x}_1)}{\partial x} \Big\rangle \Big\langle w^{(1)*}(\tilde{x}_0) \Big\rangle \Big\langle G_1(\tilde{x}_0 - \tilde{x}_1) \Big\rangle \\
&\quad - \Big\langle \frac{\partial w^{(1)}(\tilde{x}_0)}{\partial x} w^{(1)*}(\tilde{x}_0) \Big\rangle G_1(\tilde{x}_0 - \tilde{x}_0)
\end{aligned}$$

$$+\Big\langle\Big|w^{(1)}(\tilde{x}_0)\Big|^2\Big\rangle\Big(\frac{\partial G_1(\tilde{x}_0-\tilde{x}_0)}{\partial x}-1\Big), \tag{5.42}$$

$$0 = \frac{F_0}{E_1S_1}\Big\langle G_1(\tilde{x}_1-\tilde{x}_f)\Big\rangle+\Big\langle\frac{\partial w(\tilde{x}_1)}{\partial x}\Big\rangle G_1(\tilde{x}_1-\tilde{x}_1)$$
$$-\Big\langle\frac{\partial w^{(1)}(\tilde{x}_0)}{\partial x}\Big\rangle\Big\langle G_1(\tilde{x}_1-\tilde{x}_0)\Big\rangle+\Big\langle w^{(1)}(\tilde{x}_0)\Big\rangle\Big\langle\frac{\partial G_1(\tilde{x}_1-\tilde{x}_0)}{\partial x}\Big\rangle, \tag{5.43}$$

$$0 = \frac{F_0}{E_1S_1}\Big\langle G_1(\tilde{x}_0-\tilde{x}_f)\Big\rangle+\Big\langle\frac{\partial w(\tilde{x}_1)}{\partial x}\Big\rangle\Big\langle G_1(\tilde{x}_0-\tilde{x}_1)\Big\rangle$$
$$-\Big\langle\frac{\partial w^{(1)}(\tilde{x}_0)}{\partial x}\Big\rangle G_1(\tilde{x}_0-\tilde{x}_0)+\Big\langle w^{(1)}(\tilde{x}_0)\Big\rangle\Big(\frac{\partial G_1(\tilde{x}_0-\tilde{x}_0)}{\partial x}-1\Big), \tag{5.44}$$

$$0 = \Big(\frac{F_0}{E_1S_1}\Big)^*\Big\langle\Big|G_1(\tilde{x}_1-\tilde{x}_f)\Big|^2\Big\rangle+\Big\langle\frac{\partial w^*(\tilde{x}_1)}{\partial x}G_1(\tilde{x}_1-\tilde{x}_f)\Big\rangle G_1^*(\tilde{x}_1-\tilde{x}_1)$$
$$-\Big\langle\frac{\partial w^{(1)*}(\tilde{x}_0)}{\partial x}\Big\rangle\Big\langle G_1(\tilde{x}_1-\tilde{x}_f)\Big\rangle\Big\langle G_1^*(\tilde{x}_1-\tilde{x}_0)\Big\rangle$$
$$+\Big\langle w^{(1)*}(\tilde{x}_0)\Big\rangle\Big\langle G_1(\tilde{x}_1-\tilde{x}_f)\Big\rangle\Big\langle\frac{\partial G_1^*(\tilde{x}_1-\tilde{x}_0)}{\partial x}\Big\rangle, \tag{5.45}$$

$$0 = \Big(\frac{F_0}{E_1S_1}\Big)^*\Big\langle\Big|G_1(\tilde{x}_0-\tilde{x}_f)\Big|^2\Big\rangle+\Big\langle\frac{\partial w^*(\tilde{x}_1)}{\partial x}\Big\rangle\Big\langle G_1(\tilde{x}_0-\tilde{x}_f)\Big\rangle\Big\langle G_1^*(\tilde{x}_0-\tilde{x}_1)\Big\rangle$$
$$-\Big\langle\frac{\partial w^{(1)*}(\tilde{x}_0)}{\partial x}G_1(\tilde{x}_0-\tilde{x}_f)\Big\rangle G_1^*(\tilde{x}_0-\tilde{x}_0)$$
$$+\Big\langle w^{(1)*}(\tilde{x}_0)G_1(\tilde{x}_0-\tilde{x}_f)\Big\rangle\Big(\frac{\partial G_1^*(\tilde{x}_0-\tilde{x}_0)}{\partial x}-1\Big). \tag{5.46}$$

SIF equations of rod 2:

The first equation, (5.47), is obtained by multiplying the first basic equation (5.36), by the conjugate of $\partial w(\tilde{x}_2)/\partial x$ and getting the expectation with respect to $\tilde{x}_2$ and $\tilde{x}_0$; while the second and the third equations, (5.48) and (5.49), are obtained by multiplying the second equation (5.37) respectively by the conjugate of $\partial w^{(2)}(\tilde{x}_2)/\partial x$ and $w^{(2)}(\tilde{x}_0)$ then getting the expectation.
The fourth and fifth equations, (5.50) and (5.51), are obtained getting the expectation of the basic equations (5.36) and (5.37).
The sixth equation, (5.52), is obtained by multiplying the conjugate of the first basic equation by $\partial w(\tilde{x}_2)/\partial x \cdot G_2(\tilde{x}_2-\tilde{x}_0)$; while the seventh, (5.53), multiplying by $w^{(2)}(\tilde{x}_0)\cdot \partial G_2(\tilde{x}_2-\tilde{x}_0)/\partial x$ then getting the expectation. The first basic equation has to be used because following the BEM theory, we have to consider the equation calculated in the point which we want to evaluate the influence of the primary source.

$$0 = \Big\langle\Big|\frac{\partial w(\tilde{x}_2)}{\partial x}\Big|^2\Big\rangle G_2(\tilde{x}_2-\tilde{x}_2)-\Big\langle\frac{\partial w^{(2)}(\tilde{x}_0)}{\partial x}\frac{\partial w^*(\tilde{x}_2)}{\partial x}\,G_2(\tilde{x}_2-\tilde{x}_0)\Big\rangle$$
$$+\Big\langle w^{(2)}(\tilde{x}_0)\frac{\partial w^*(\tilde{x}_2)}{\partial x}\frac{\partial G_2(\tilde{x}_2-\tilde{x}_0)}{\partial x}\Big\rangle, \tag{5.47}$$

$$0 = \Big\langle\frac{\partial w(\tilde{x}_2)}{\partial x}\Big\rangle\Big\langle\frac{\partial w^{(2)*}(\tilde{x}_0)}{\partial x}\Big\rangle\Big\langle G_2(\tilde{x}_0-\tilde{x}_2)\Big\rangle-\Big\langle\Big|\frac{\partial w^{(2)}(\tilde{x}_0)}{\partial x}\Big|^2\Big\rangle G_2(\tilde{x}_0-\tilde{x}_0)$$
$$+\Big\langle w^{(2)}(\tilde{x}_0)\frac{\partial w^{(2)*}(\tilde{x}_0)}{\partial x}\Big\rangle\Big(\frac{\partial G_2(\tilde{x}_0-\tilde{x}_0)}{\partial x}-1\Big), \tag{5.48}$$

$$0 = \Big\langle\frac{\partial w(\tilde{x}_2)}{\partial x}\Big\rangle\Big\langle w^{(2)*}(\tilde{x}_0)\Big\rangle\Big\langle G_2(\tilde{x}_0-\tilde{x}_2)\Big\rangle-\Big\langle\frac{\partial w^{(2)}(\tilde{x}_0)}{\partial x}w^{(2)*}(\tilde{x}_0)\Big\rangle G_2(\tilde{x}_0-\tilde{x}_0)$$

$$+\Big\langle\Big|w^{(2)}(\tilde{x}_0)\Big|^2\Big\rangle\Big(\frac{\partial G_2(\tilde{x}_0-\tilde{x}_0)}{\partial x}-1\Big), \tag{5.49}$$

$$\begin{aligned}0 &= \Big\langle\frac{\partial w(\tilde{x}_2)}{\partial x}\Big\rangle G_2(\tilde{x}_2-\tilde{x}_2)-\Big\langle\frac{\partial w^{(2)}(\tilde{x}_0)}{\partial x}\Big\rangle\Big\langle G_2(\tilde{x}_2-\tilde{x}_0)\Big\rangle\\ &\quad+\Big\langle w^{(2)}(\tilde{x}_0)\Big\rangle\Big\langle\frac{\partial G_2(\tilde{x}_2-\tilde{x}_0)}{\partial x}\Big\rangle,\end{aligned} \tag{5.50}$$

$$\begin{aligned}0 &= \Big\langle\frac{\partial w(\tilde{x}_2)}{\partial x}\Big\rangle\Big\langle G_2(\tilde{x}_0-\tilde{x}_2)\Big\rangle-\Big\langle\frac{\partial w^{(2)}(\tilde{x}_0)}{\partial x}\Big\rangle G_2(\tilde{x}_0-\tilde{x}_0)\\ &\quad+\Big\langle w^{(2)}(\tilde{x}_0)\Big\rangle\Big(\frac{\partial G_2(\tilde{x}_0-\tilde{x}_0)}{\partial x}-1\Big),\end{aligned} \tag{5.51}$$

$$\begin{aligned}0 &= \Big\langle\frac{\partial w^*(\tilde{x}_2)}{\partial x}w^{(2)}(\tilde{x}_0)\frac{\partial G_2(\tilde{x}_2-\tilde{x}_0)}{\partial x}\Big\rangle\, G_2^*(\tilde{x}_2-\tilde{x}_2)\\ &\quad-\Big\langle\frac{\partial w^{(2)*}(\tilde{x}_0)}{\partial x}w^{(2)}(\tilde{x}_0)\Big\rangle\Big\langle\frac{\partial G_2(\tilde{x}_2-\tilde{x}_0)}{\partial x}G_2^*(\tilde{x}_2-\tilde{x}_0)\Big\rangle\\ &\quad+\Big\langle\Big|w^{(2)}(\tilde{x}_0)\Big|^2\Big\rangle\Big\langle\Big|\frac{\partial G_2(\tilde{x}_2-\tilde{x}_0)}{\partial x}\Big|^2\Big\rangle,\end{aligned} \tag{5.52}$$

$$\begin{aligned}0 &= \Big\langle\frac{\partial w^*(\tilde{x}_2)}{\partial x}\frac{\partial w^{(2)}(\tilde{x}_0)}{\partial x}G_2(\tilde{x}_2-\tilde{x}_0)\Big\rangle G_2^*(\tilde{x}_2-\tilde{x}_2)-\\ &\quad\Big\langle\Big|\frac{\partial w^{(2)}(\tilde{x}_0)}{\partial x}\Big|^2\Big\rangle\Big\langle\Big|G_2(\tilde{x}_2-\tilde{x}_0)\Big|^2\Big\rangle\\ &\quad+\Big\langle w^{(2)*}(\tilde{x}_0)\frac{\partial w^{(2)}(\tilde{x}_0)}{\partial x}\Big\rangle\Big\langle G_2(\tilde{x}_2-\tilde{x}_0)\frac{\partial G_2^*(\tilde{x}_2-\tilde{x}_0)}{\partial x}\Big\rangle.\end{aligned} \tag{5.53}$$

Coupling equations:

$$\Big\langle w^{(1)}(\tilde{x}_0)\Big\rangle=-\Big\langle w^{(2)}(\tilde{x}_0)\Big\rangle \tag{5.54}$$

$$Y_1S_1\Big\langle\frac{\partial w^{(1)}(\tilde{x}_0)}{\partial x}\Big\rangle=Y_2S_2\Big\langle\frac{\partial w^{(2)}(\tilde{x}_0)}{\partial x}\Big\rangle \tag{5.55}$$

$$\Big(Y_1S_1\Big)^*\Big\langle w^{(1)}(\tilde{x}_0)\frac{\partial w^{(1)*}(\tilde{x}_0)}{\partial x}\Big\rangle=-\Big(Y_2S_2\Big)^*\Big\langle w^{(2)}(\tilde{x}_0)\frac{\partial w^{(2)*}(\tilde{x}_0)}{\partial x}\Big\rangle \tag{5.56}$$

$$\Big\langle\Big|w^{(1)}(\tilde{x}_0)\Big|^2\Big\rangle=\Big\langle\Big|w^{(1)}(\tilde{x}_0)\Big|^2\Big\rangle \tag{5.57}$$

$$\Big|Y_1S_1\Big|^2\Big\langle\Big|\frac{\partial w^{(1)}(\tilde{x}_0)}{\partial x}\Big|^2\Big\rangle=\Big|Y_2S_2\Big|^2\Big\langle\Big|\frac{\partial w^{(2)}(\tilde{x}_0)}{\partial x}\Big|^2\Big\rangle \tag{5.58}$$

$$Y_1S_1\Big\langle w^{(1)*}(\tilde{x}_0)\frac{\partial w^{(1)}(\tilde{x}_0)}{\partial x}\Big\rangle=-Y_2S_2\Big\langle w^{(2)*}(\tilde{x}_0)\frac{\partial w^{(2)}(\tilde{x}_0)}{\partial x}\Big\rangle \tag{5.59}$$

Solving the problem

Green Kernel expectation
Green Kernel expression for the rod:

$$G(\tilde{\xi}-\tilde{x})=\frac{1}{2ik_0\big(1-i\eta/2\big)}e^{-ik_0\big(1-i\eta/2\big)|\tilde{\xi}-\tilde{x}|}$$

Calculations of the expectations:

$$\Big\langle G(\tilde{\xi}-\tilde{x})\Big\rangle = \begin{cases} \frac{1}{2ik_0\left(1-i\eta/2\right)} & \text{if } \xi = x \\ \frac{1}{2ik_0\left(1-i\eta/2\right)} e^{-ik_0\left(1-i\eta/2\right)|\tilde{\xi}-\tilde{x}|} e^{k_0^2\frac{\eta^2}{4}\left(\frac{\sigma_\xi^2+\sigma_x^2}{2}\right)} & \\ \qquad \cdot e^{-k_0^2\left(\frac{\sigma_\xi^2+\sigma_x^2}{2}\right)} e^{ik_0^2\frac{\eta}{2}\left(\sigma_\xi^2+\sigma_x^2\right)} & \text{else} \end{cases} \tag{5.60}$$

$$\Big\langle \frac{\partial G(\tilde{\xi}-\tilde{x})}{\partial x}\Big\rangle = \begin{cases} \frac{1}{2} & \text{if } \xi > x \text{ and } \xi \to x \\ -\frac{1}{2} & \text{if } \xi < x \text{ and } \xi \to x \\ \frac{1}{2}\frac{|\xi-x|}{\xi-x} e^{-ik_0\left(1-i\eta/2\right)|\tilde{\xi}-\tilde{x}|} e^{k_0^2\frac{\eta^2}{4}\left(\frac{\sigma_\xi^2+\sigma_x^2}{2}\right)} & \\ \qquad \cdot e^{-k_0^2\left(\frac{\sigma_\xi^2+\sigma_x^2}{2}\right)} e^{ik_0^2\frac{\eta}{2}\left(\sigma_\xi^2+\sigma_x^2\right)} & \text{else} \end{cases} \tag{5.61}$$

$$\Big\langle \Big|\frac{\partial G(\tilde{\xi}-\tilde{x})}{\partial x}\Big|^2\Big\rangle = \begin{cases} \frac{1}{4} & \text{if } \xi = x \\ \frac{1}{4} e^{-k_0\eta|\tilde{\xi}-\tilde{x}|} e^{k_0^2\eta^2\left(\frac{\sigma_\xi^2+\sigma_x^2}{2}\right)} & \text{else} \end{cases} \tag{5.62}$$

$$\Big\langle \Big|G(\tilde{\xi}-\tilde{x})\Big|^2\Big\rangle = \begin{cases} \frac{1}{k_0^2\left(\eta^2-4\right)} & \text{if } \xi = x \\ \frac{1}{k_0^2\left(\eta^2-4\right)} e^{-k_0\eta|\tilde{\xi}-\tilde{x}|} e^{k_0^2\eta^2\left(\frac{\sigma_\xi^2+\sigma_x^2}{2}\right)} & \text{else} \end{cases} \tag{5.63}$$

$$\Big\langle G(\tilde{\xi}-\tilde{x})\frac{\partial G^*(\tilde{\xi}-\tilde{x})}{\partial x}\Big\rangle = \begin{cases} \frac{1}{4ik_0\left(1-i\eta/2\right)} & \text{if } \xi > x \text{ and } \zeta \to x \\ -\frac{1}{4ik_0\left(1-i\eta/2\right)} & \text{if } \xi < x \text{ and } \zeta \to x \\ \frac{1}{4ik_0\left(1-i\eta/2\right)}\frac{|\xi-x|}{\xi-x} e^{-k_0\eta|\tilde{\xi}-\tilde{x}|} e^{k_0^2\eta^2\left(\frac{\sigma_\xi^2+\sigma_x^2}{2}\right)} & \text{else} \end{cases} \tag{5.64}$$

First order moments solution

Considering equations (5.43) and (5.44) for rod 1, equations (5.50) and (5.51) for rod 2, an coupling relations (5.54) and (5.55), it's possible to solve the linear system obtaining all the first order moment.

Linear system solution:

$$\begin{aligned} 0 &= \frac{F_0}{E_1S_1}\Big\langle G_1(\tilde{x}_1-\tilde{x}_f)\Big\rangle + \Big\langle \frac{\partial w(\tilde{x}_1)}{\partial x}\Big\rangle G_1(\tilde{x}_1-\tilde{x}_1) \\ &\quad -\Big\langle \frac{\partial w^{(1)}(\tilde{x}_0)}{\partial x}\Big\rangle\Big\langle G_1(\tilde{x}_1-\tilde{x}_0)\Big\rangle + \Big\langle w^{(1)}(\tilde{x}_0)\Big\rangle\Big\langle \frac{\partial G_1(\tilde{x}_1-\tilde{x}_0)}{\partial x}\Big\rangle, \qquad (5.65) \\ 0 &= \frac{F_0}{E_1S_1}\Big\langle G_1(\tilde{x}_0-\tilde{x}_f)\Big\rangle + \Big\langle \frac{\partial w(\tilde{x}_1)}{\partial x}\Big\rangle\Big\langle G_1(\tilde{x}_0-\tilde{x}_1)\Big\rangle \\ &\quad -\Big\langle \frac{\partial w^{(1)}(\tilde{x}_0)}{\partial x}\Big\rangle G_1(\tilde{x}_0-\tilde{x}_0) + \Big\langle w^{(1)}(\tilde{x}_0)\Big\rangle\Big(\frac{\partial G_1(\tilde{x}_0-\tilde{x}_0)}{\partial x}-1\Big), \qquad (5.66) \\ 0 &= \Big\langle \frac{\partial w(\tilde{x}_2)}{\partial x}\Big\rangle G_2(\tilde{x}_2-\tilde{x}_2) - \Big\langle \frac{\partial w^{(2)}(\tilde{x}_0)}{\partial x}\Big\rangle\Big\langle G_2(\tilde{x}_2-\tilde{x}_0)\Big\rangle \\ &\quad +\Big\langle w^{(2)}(\tilde{x}_0)\Big\rangle\Big\langle \frac{\partial G_2(\tilde{x}_2-\tilde{x}_0)}{\partial x}\Big\rangle, \qquad (5.67) \\ 0 &= \Big\langle \frac{\partial w(\tilde{x}_2)}{\partial x}\Big\rangle\Big\langle G_2(\tilde{x}_0-\tilde{x}_2)\Big\rangle - \Big\langle \frac{\partial w^{(2)}(\tilde{x}_0)}{\partial x}\Big\rangle G_2(\tilde{x}_0-\tilde{x}_0) \end{aligned}$$

$$+\Big\langle w^{(2)}(\tilde{x}_0)\Big\rangle\Big(\frac{\partial G_2(\tilde{x}_0-\tilde{x}_0)}{\partial x}-1\Big), \tag{5.68}$$

$$0 = \Big\langle w^{(1)}(\tilde{x}_0)\Big\rangle+\Big\langle w^{(2)}(\tilde{x}_0)\Big\rangle, \tag{5.69}$$

$$0 = Y_1S_1\Big\langle\frac{\partial w^{(1)}(\tilde{x}_0)}{\partial x}\Big\rangle-Y_2S_2\Big\langle\frac{\partial w^{(2)}(\tilde{x}_0)}{\partial x}\Big\rangle. \tag{5.70}$$

Second order moments solution

Using the previous results of the first order moment, is possible to obtain the solution for two other unknowns of the first rod.
Using equation (5.45) is possible to evaluate $\langle\partial w^*(\tilde{x}_1)/\partial x\cdot G_1(\tilde{x}_1-\tilde{x}_f)\rangle$, then using equation (5.40), is possible to evaluate $\langle|\partial w(\tilde{x}_1)/\partial x|^2\rangle$:

$$\begin{aligned}\Big\langle\frac{\partial w^*(\tilde{x}_1)}{\partial x}G_1(\tilde{x}_1-\tilde{x}_f)\Big\rangle &= \frac{-\Big(\frac{F_0}{E_1S_1}\Big)^*\Big\langle\Big|G_1(\tilde{x}_1-\tilde{x}_f)\Big|^2\Big\rangle}{G_1^*(\tilde{x}_1-\tilde{x}_1)}\\ &\quad+\frac{\Big\langle\frac{\partial w^{(1)*}(\tilde{x}_0)}{\partial x}\Big\rangle\Big\langle G_1(\tilde{x}_1-\tilde{x}_f)\Big\rangle\Big\langle G_1^*(\tilde{x}_1-\tilde{x}_0)\Big\rangle}{G_1^*(\tilde{x}_1-\tilde{x}_1)}\\ &\quad-\frac{\Big\langle w^{(1)*}(\tilde{x}_0)\Big\rangle\Big\langle G_1(\tilde{x}_1-\tilde{x}_f)\Big\rangle\Big\langle\frac{\partial G_1^*(\tilde{x}_1-\tilde{x}_0)}{\partial x}\Big\rangle}{G_1^*(\tilde{x}_1-\tilde{x}_1)}.\\ \Big\langle\Big|\frac{\partial w(\tilde{x}_1)}{\partial x}\Big|^2\Big\rangle &= -\frac{\frac{F_0}{E_1S_1}\Big\langle\frac{\partial w^*(\tilde{x}_1)}{\partial x}G_1(\tilde{x}_1-\tilde{x}_f)\Big\rangle}{G_1(\tilde{x}_1-\tilde{x}_1)}\\ &\quad+\frac{\Big\langle\frac{\partial w^{(1)}(\tilde{x}_0)}{\partial x}\Big\rangle\Big\langle\frac{\partial w^*(\tilde{x}_1)}{\partial x}\Big\rangle\Big\langle G_1(\tilde{x}_1-\tilde{x}_0)\Big\rangle}{G_1(\tilde{x}_1-\tilde{x}_1)}\\ &\quad-\frac{\Big\langle w^{(1)}(\tilde{x}_0)\Big\rangle\Big\langle\frac{\partial w^*(\tilde{x}_1)}{\partial x}\Big\rangle\Big\langle\frac{\partial G_1(\tilde{x}_1-\tilde{x}_0)}{\partial x}\Big\rangle}{G_1(\tilde{x}_1-\tilde{x}_1)}.\end{aligned}$$

Getting the conjugate of equation (5.49), one can get the equation for the conjugate unknowns $\Big\langle w^{(2)}(\tilde{x}_0)\cdot\partial w^{(2)*}(\tilde{x}_0)/\partial x\Big\rangle$ and $\Big\langle w^{(2)*}(\tilde{x}_0)\cdot\partial w^{(2)}(\tilde{x}_0)/\partial x\Big\rangle$:

$$\begin{aligned}0 &= \Big\langle\frac{\partial w^*(\tilde{x}_2)}{\partial x}\Big\rangle\Big\langle w^{(2)}(\tilde{x}_0)\Big\rangle\Big\langle G_2^*(\tilde{x}_0-\tilde{x}_2)\Big\rangle-\Big\langle\frac{\partial w^{(2)*}(\tilde{x}_0)}{\partial x}w^{(2)}(\tilde{x}_0)\Big\rangle G_2^*(\tilde{x}_0-\tilde{x}_0)\\ &\quad+\Big\langle\Big|w^{(2)}(\tilde{x}_0)\Big|^2\Big\rangle\Big(\frac{\partial G_2^*(\tilde{x}_0-\tilde{x}_0)}{\partial x}-1\Big)\end{aligned} \tag{5.71}$$

Then using the coupling equations (5.56)-(5.59) is possible to reduce the number of unknowns and solve the linear system for second order unknowns.

5.3.5 SIF two coupled rods: results

- Configuration n.1
  Two similar rod are considered in this configuration, with similar geometrical and physical properties. The same randomness is applied to the boundary points. The physical properties of configuration n.1 are reported in table 5.12 and results of FOM

in figures 5.31 and 5.32, SOM in figures 5.33 and 5.34.
$\sigma_1 = \sigma_2 = \sigma_0 = \sigma_f = 0.03$.

	length [m]	x_f [m]	E [N/m^2]	S [m^2]	η [%]	ρ [kg/m^3]
Rod 1	2.45	1.50	$2.1 \cdot 10^{11}$	10^{-4}	2	7800
Rod 2	3.20		$2.1 \cdot 10^{11}$	10^{-4}	2	7800

Table 5.12: SIF application. Parameters of the two rods, configuration n.1

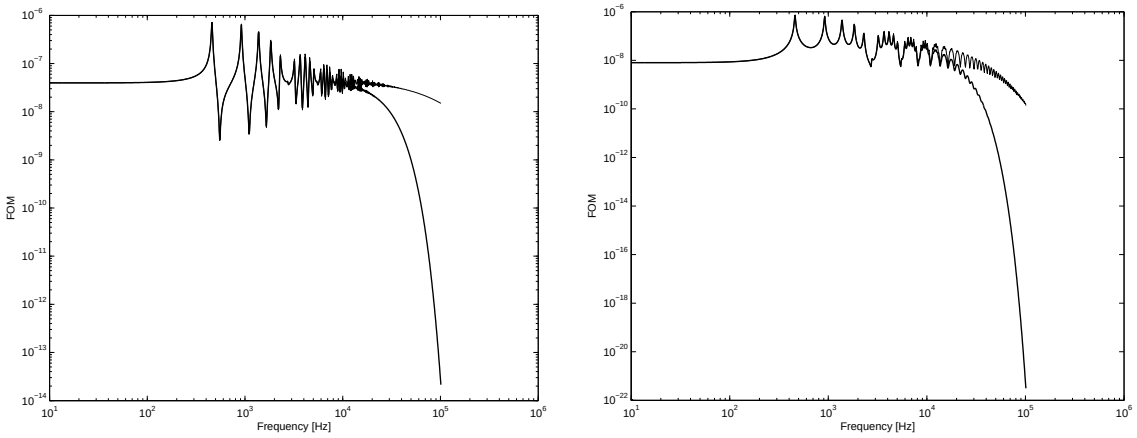

(a) (b)

Figure 5.31: SIF two coupled rods. Frequency evolution of the modulus of the first order moment $\langle \partial w/\partial x \rangle$ at $\tilde{x}_1$ (a) and $\tilde{x}_2$ (b). Configuration n.1. —— SIF —— BEM.

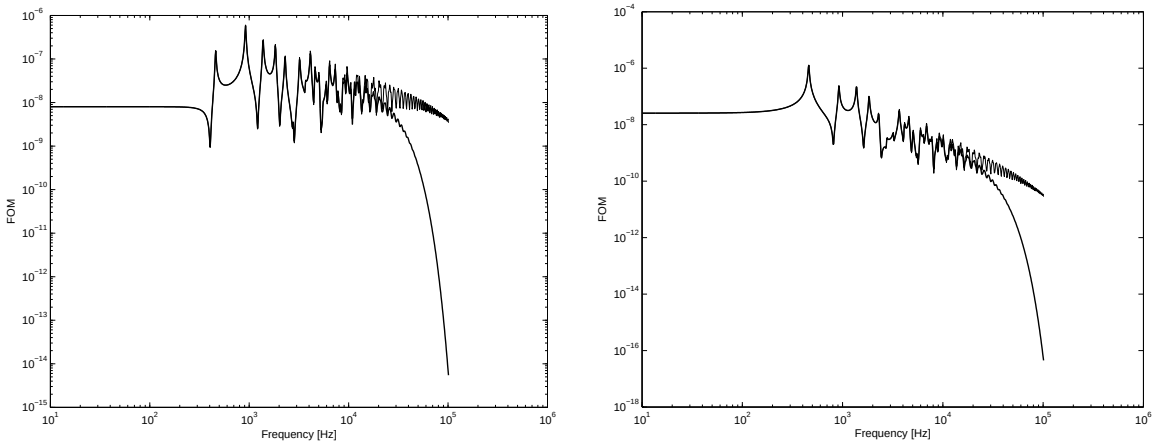

(a) (b)

Figure 5.32: SIF two coupled rods. Frequency evolution of the modulus of the first order moment $\langle \partial w/\partial x \rangle$ (a) and $\langle w \rangle$ (b) at $\tilde{x}_0$. Configuration n.1. —— SIF —— BEM.

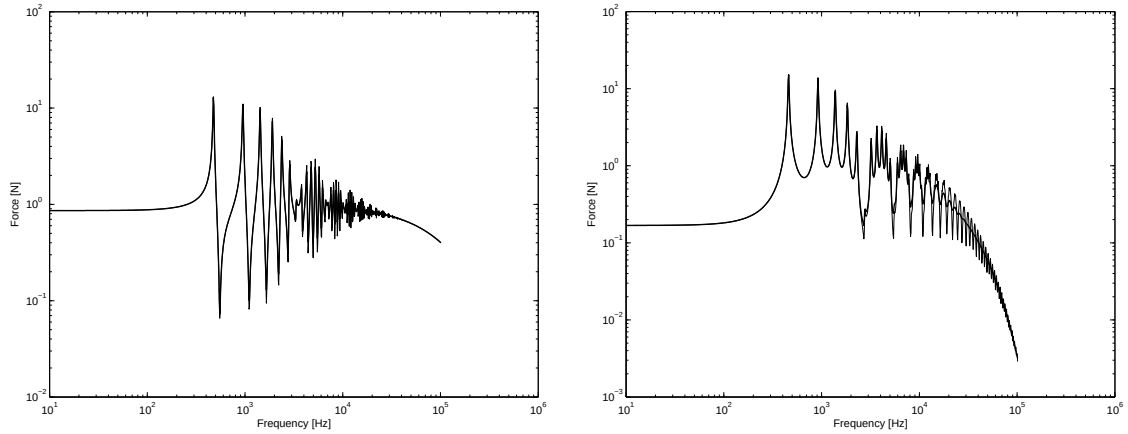

(a) (b)

Figure 5.33: SIF two coupled rods. Frequency evolution of the modulus of the second order moment, traction at $\tilde{x}_1$ (a) and $\tilde{x}_2$ (b). Configuration n.1. —— SIF BEM.

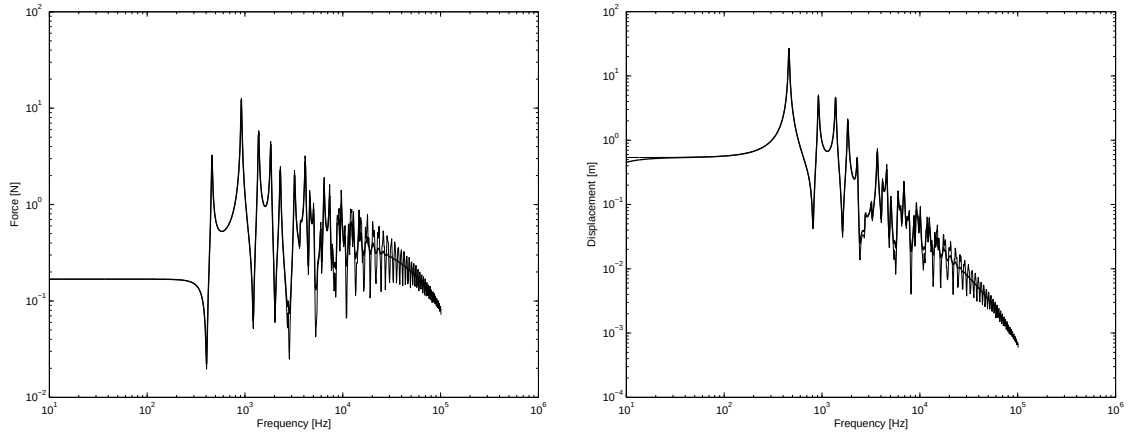

(a) (b)

Figure 5.34: SIF two coupled rods. Frequency evolution of the modulus of the second order moment, traction (a) and displacement (b) at $\tilde{x}_0$. Configuration n.1. —— SIF BEM.

- Configuration n.2
  Two different behavior rods are considered, rod 1, the excited one, is typically low frequency because is stiff and short, while rod 2 is typically high frequency because is thin,long and flexible. Also different physical properties characterize the two rods in terms of flexibility and damping. The physical properties of configuration n.2 are reported in table 5.13 and results of FOM in figures 5.35 and 5.36, SOM in figures 5.37 and 5.38.
  $\sigma_1 = \sigma_2 = \sigma_0 = \sigma_f = 0.03$.

	length [m]	x_f [m]	E [N/m^2]	S [m^2]	η [%]	ρ [kg/m^3]
Rod 1	1.67	0.48	$2.1 \cdot 10^{11}$	10^{-3}	2	7800
Rod 2	8.92		$2.1 \cdot 10^{10}$	10^{-5}	3	7800

Table 5.13: SIF application. Parameters of the two rods, configuration n.2

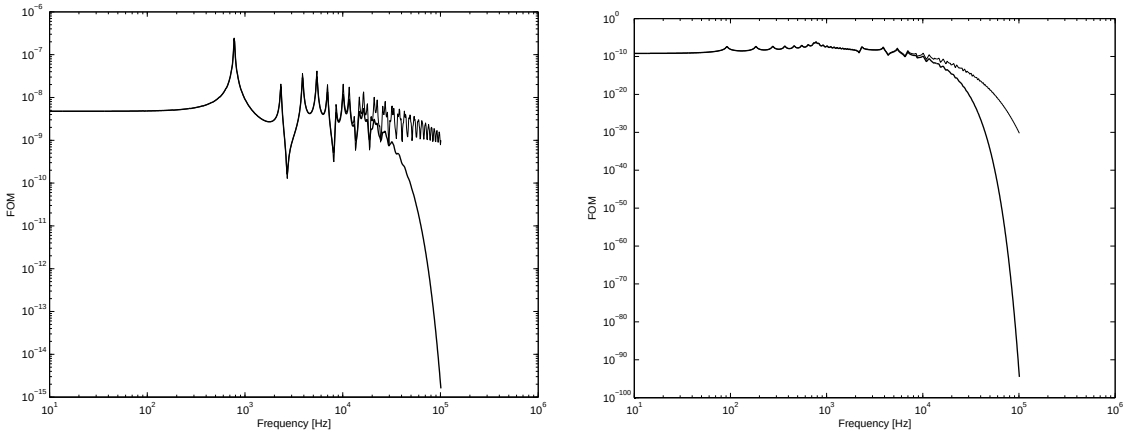

(a) (b)

Figure 5.35: SIF two coupled rods. Frequency evolution of the modulus of the first order moment $\langle \partial w/\partial x \rangle$ at $\tilde{x}_1$ (a) and $\tilde{x}_2$ (b). Configuration n.2. —— SIF —— BEM.

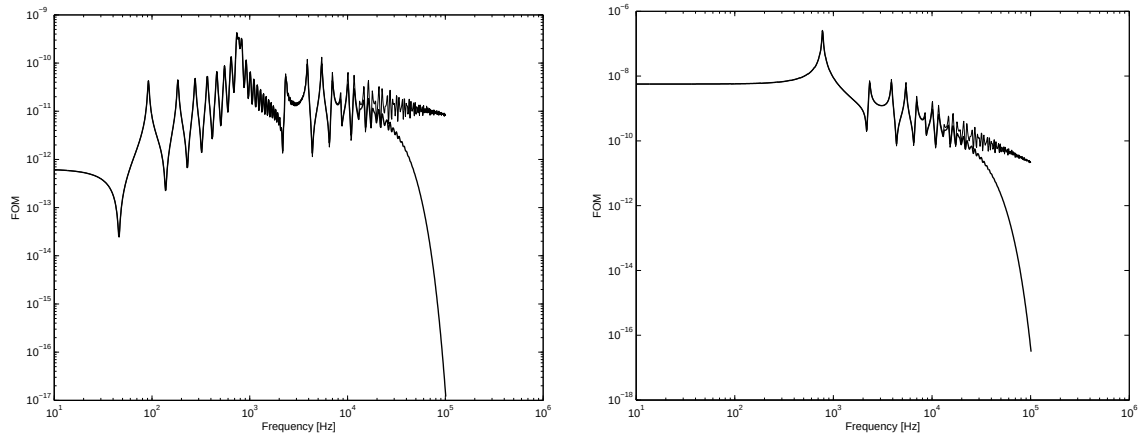

(a) (b)

Figure 5.36: SIF two coupled rods. Frequency evolution of the modulus of the first order moment $\langle \partial w/\partial x \rangle$ (a) and $\langle w \rangle$ (b) at $\tilde{x}_0$. Configuration n.2. —— SIF —— BEM.

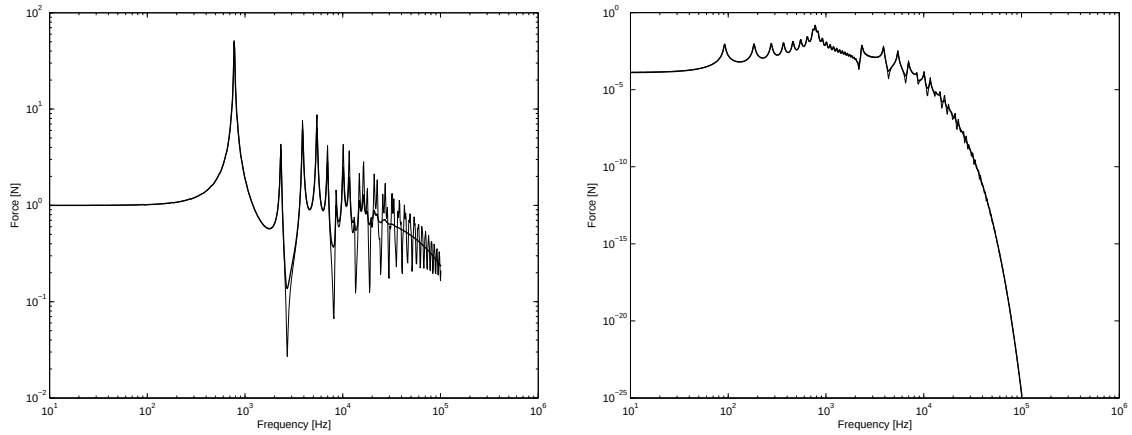

(a) (b)

Figure 5.37: SIF two coupled rods. Frequency evolution of the modulus of the second order moment, traction at $\tilde{x}_1$ (a) and $\tilde{x}_2$ (b). Configuration n.2. —— SIF —— BEM.

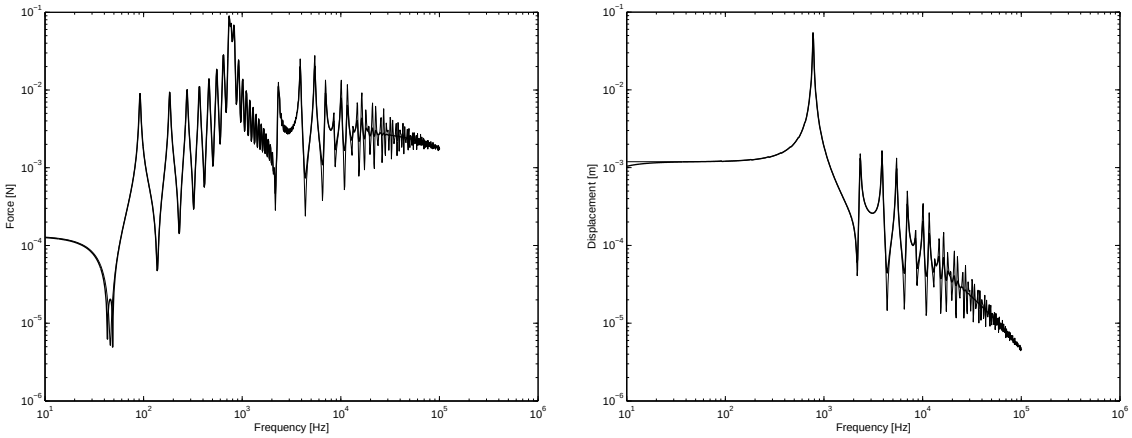

(a) (b)

Figure 5.38: SIF two coupled rods. Frequency evolution of the modulus of the second order moment, traction (a) and displacement (b) at $\tilde{x}_0$. Configuration n.2. —— SIF —— BEM.

- Configuration n.3
  Two different behavior rods are considered, rod 1, the excited one, is typically high frequency because is thin, long and flexible, while rod 2 is typically low frequency because is short and stiff. Also different physical properties characterize the two rods in terms of flexibility and damping. The physical properties of configuration n.3 are reported in table 5.14 and results of FOM in figures 5.39 and 5.40, SOM in figures 5.41 and 5.42.
  $\sigma_1 = \sigma_2 = \sigma_0 = \sigma_f = 0.03$.

	length [m]	x_f [m]	E [N/m^2]	S [m^2]	η [%]	ρ [kg/m^3]
Rod 1	8.12	2.50	$2.1 \cdot 10^{10}$	10^{-4}	3	7800
Rod 2	2.33		$2.1 \cdot 10^{11}$	10^{-3}	2	7800

Table 5.14: SIF application. Parameters of the two rods, configuration n.3

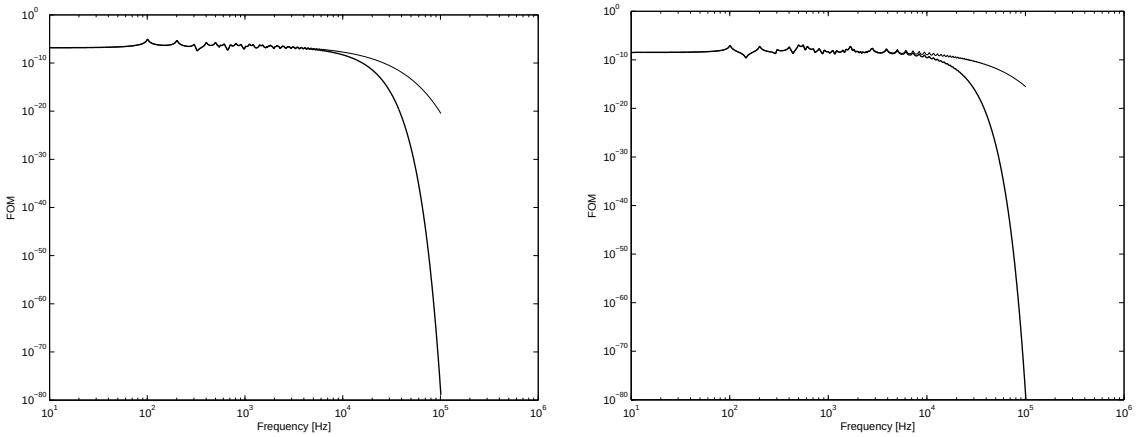

(a) (b)

Figure 5.39: SIF two coupled rods. Frequency evolution of the modulus of the first order moment $\langle \partial w/\partial x \rangle$ at $\tilde{x}_1$ (a) and $\tilde{x}_2$ (b). Configuration n.3. —— SIF —— BEM.

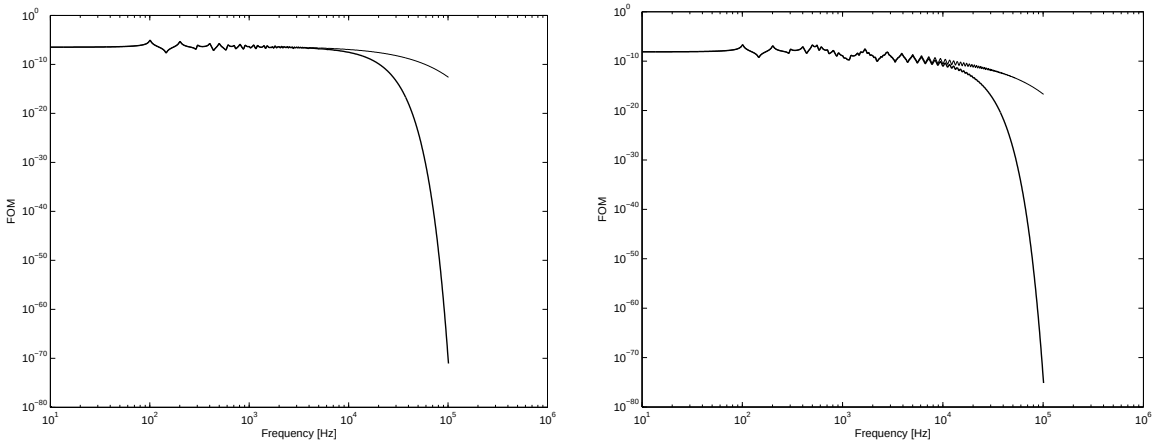

(a) (b)

Figure 5.40: SIF two coupled rods. Frequency evolution of the modulus of the first order moment $\langle \partial w/\partial x \rangle$ and $\langle w \rangle$ at $\tilde{x}_0$ (b). Configuration n.3. —— SIF —— BEM.

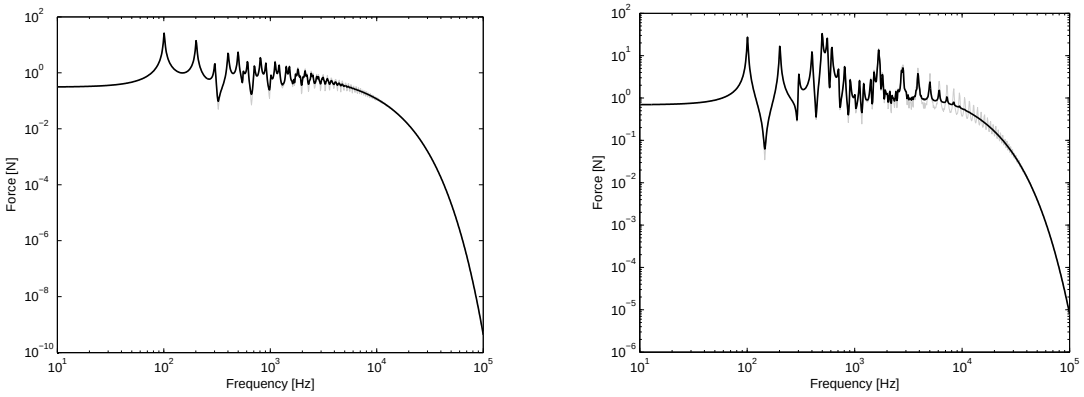

(a) (b)

Figure 5.41: SIF two coupled rods. Frequency evolution of the modulus of the second order moment, traction at $\tilde{x}_1$ (a) and $\tilde{x}_2$ (b). Configuration n.3. —— SIF —— BEM.

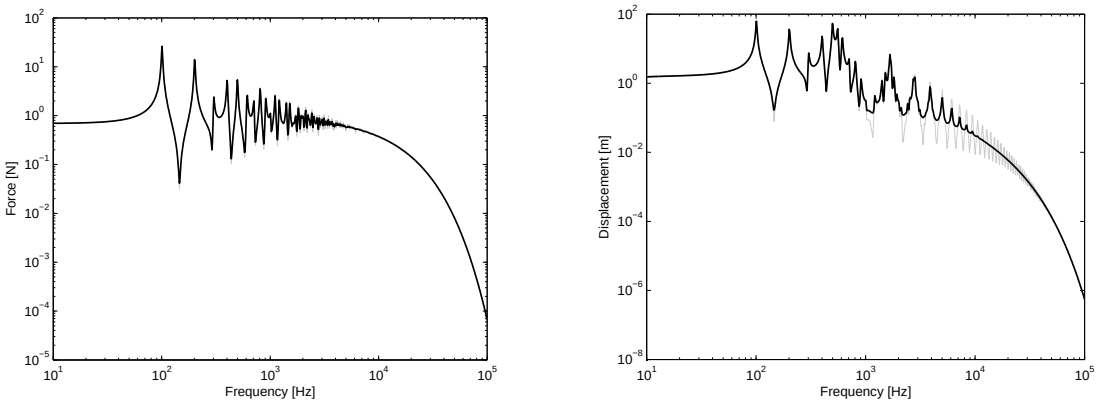

(a) (b)

Figure 5.42: SIF two coupled rods. Frequency evolution of the modulus of the second order moment, traction (a) and displacement (b) at $\tilde{x}_0$. Configuration n.3. —— SIF —— BEM.

- Configuration n.4
  The rod properties is equal to the configuration n.3. Randomness is introduced only on $\tilde{x}_1$ and $\tilde{x}_f$, while the other boundary points are deterministic. The physical properties of configuration n.4 are reported in table 5.15 and results of FOM in figures 5.43 and 5.44, SOM in figures 5.45 and 5.46.
  $\sigma_1 = \sigma_f = 0.05$, $\sigma_2 = \sigma_0 = 0.00$.

	length [m]	x_f [m]	E [N/m^2]	S [m^2]	η [%]	ρ [kg/m^3]
Rod 1	8.12	2.50	$2.1 \cdot 10^9$	10^{-5}	1	7800
Rod 2	2.33		$2.1 \cdot 10^{11}$	10^{-3}	1	7800

Table 5.15: SIF application. Parameters of the two rods, configuration n.4

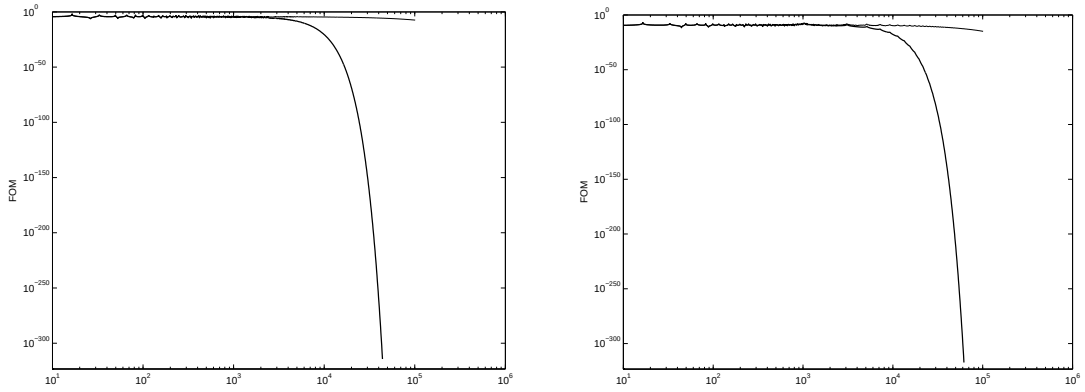

(a) (b)

Figure 5.43: SIF two coupled rods. Frequency evolution of the modulus of the first order moment $\langle \partial w/\partial x \rangle$ at $\tilde{x}_1$ (a) and $\tilde{x}_2$ (b). Configuration n.4. —— SIF BEM.

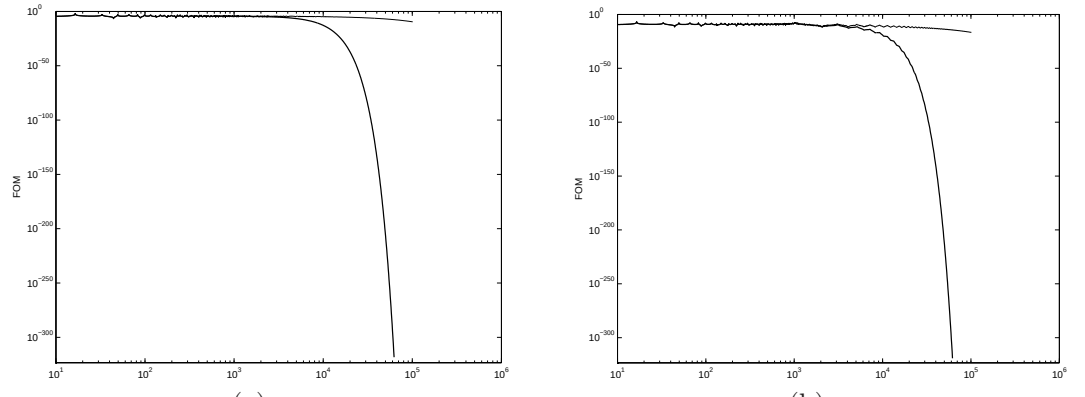

(a) (b)

Figure 5.44: SIF two coupled rods. Frequency evolution of the modulus of the first order moment $\langle \partial w/\partial x \rangle$ (a) and $\langle w \rangle$ (b) at $\tilde{x}_0$. Configuration n.4. —— SIF BEM.

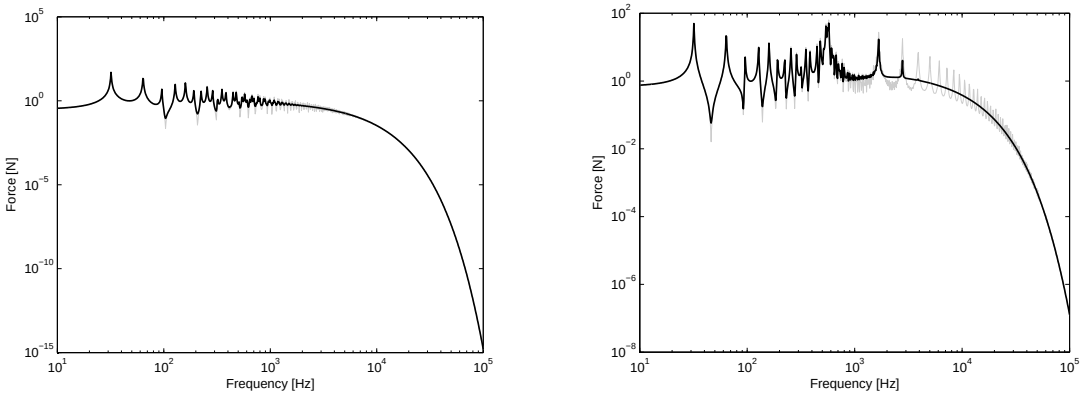

(a) (b)

Figure 5.45: SIF two coupled rods. Frequency evolution of the modulus of the second order moment, traction at $\tilde{x}_1$ (a) and $\tilde{x}_2$ (b). Configuration n.4. —— SIF —— BEM.

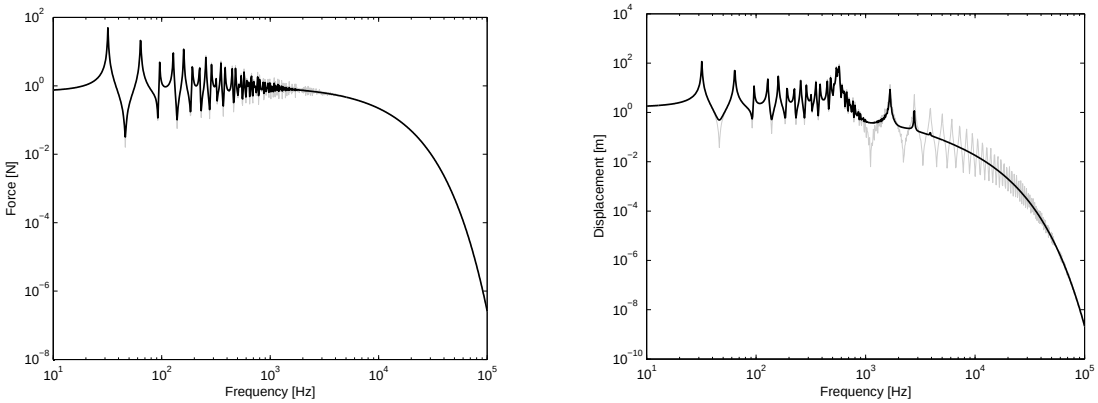

(a) (b)

Figure 5.46: SIF two coupled rods. Frequency evolution of the modulus of the second order moment, traction (a) and displacement (b) at $\tilde{x}_0$. Configuration n.4. —— SIF —— BEM.

5.3.6 Discussion

It's important to notice that the SIF formulation is able to correctly predict the behavior of two coupled rods in different configurations. The low frequency response is accurately described whilst the high frequency evolution of the stochastic response gives a smooth trend of the deterministic results, as we can see from configuration n.1. When the rods presents different frequency behaviors, and the excitation is applied on the short member, like in case n.2, the SIF formulation works perfectly. We can notice from pictures 5.37 that the response at $\tilde{x}_1$ is characterized by the modes od rod 1, the rigid and excited rod, which is the driving structure for the response. The response at $\tilde{x}_2$ is affected by the modes of both the rods. In configuration n.3 the rod 1, the excited one, is high-frequency behaving. The physical properties are not so different between the two rods, and they are both randomized. The SIF formulation is able to model this configuration as one's can see

from figures 5.41, 5.42.

Some problems appear when configuration n.4 is solved. SIF gives a sooth response for all the boundaries, but there's no influence of the deterministic rod; all the peaks of the deterministic rods, except the first one, are smoothed. This is not exactly what we want to obtain, because we want to correctly predict the response of a deterministic system and to obtain a smooth contribution for the high-frequency part.
This discussion leads to some reflections about the use of a complete SIF formulation to model a mid-frequency range, and they are reported in the next chapters, together with a a feasible solution

5.4 The Smooth Integral Formulation for High-frequency applications

For practical use, the SIF is not meant for low-frequency simulations due to the introduction of uncertainties which is useless in the low-frequency range. When restricting the investigations to the high-frequency domain, the number of unknowns can be reduced. Indeed, in the high-frequency field, the expectations of the kinematic variables converge to zero. This is due to the fact that these unknowns rapidly oscillate around zero when the frequency is high. Therefore, it is not necessary to calculate these first order moments, which may be fixed to zero when high-frequency investigations are performed. This enables to decrease the number of unknowns. As an example, when considering isolated systems, it can be deduced from equations (4.6) and (4.7), that getting rid of the first order moments leads to writing a set of equations containing $2(N_u + N_T)$ unknowns instead of $3(N_u + N_T)$.

The simplified SIF is now verified for the two coupled rod structure, fig. 5.30. Two similar rod are considered in this configuration, with similar geometrical and physical properties. The same randomness is applied to the boundary points. The physical properties of configuration n.1 are reported in table 5.16 and results of FOM in figures 5.47 and 5.48, SOM in figures 5.49 and 5.50.
$\sigma_1 = \sigma_2 = \sigma_0 = \sigma_f = 0.03$.

	length [m]	x_f [m]	E [N/m^2]	S [m^2]	η [%]	ρ [kg/m^3]
Rod 1	5.64	3.96	$2.1 \cdot 10^{11}$	10^{-4}	2	7800
Rod 2	4.83		$2.1 \cdot 10^{11}$	10^{-4}	2	7800

Table 5.16: SIF application for the high-frequency domain. Parameters of the two rods.

As expected, the SIF response is smooth and effectively gives the correct trend of the response in the high-frequency field. On the other hand, not taking into account the first order moments leads to removing the peaks which were predicted before by the SIF in the low-frequency field, and the results become inaccurate in this domain.

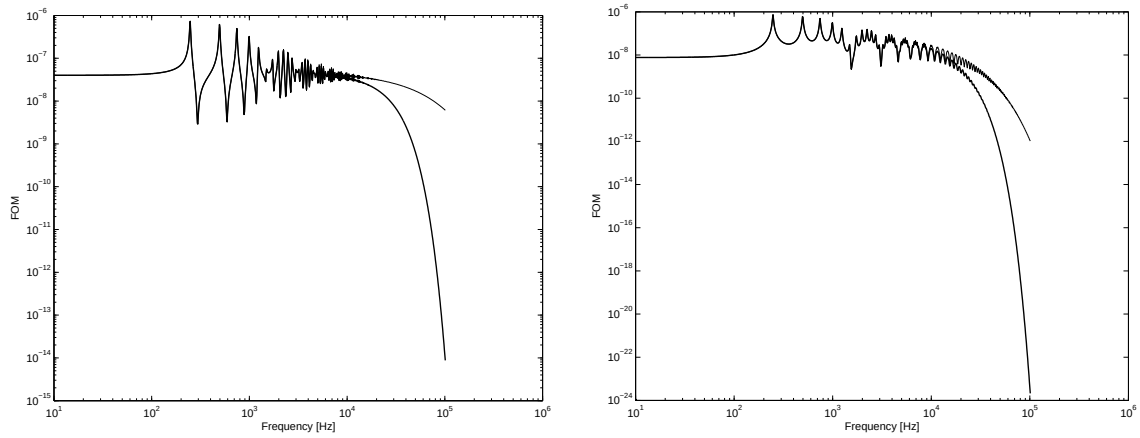

(a) (b)

Figure 5.47: SIF application for the high-frequency domain, two coupled rods. Frequency evolution of the modulus of the first order moment $\langle \partial w/\partial x \rangle$ at $\tilde{x}_1$ and $\tilde{x}_2$ (b). —— SIF —— BEM

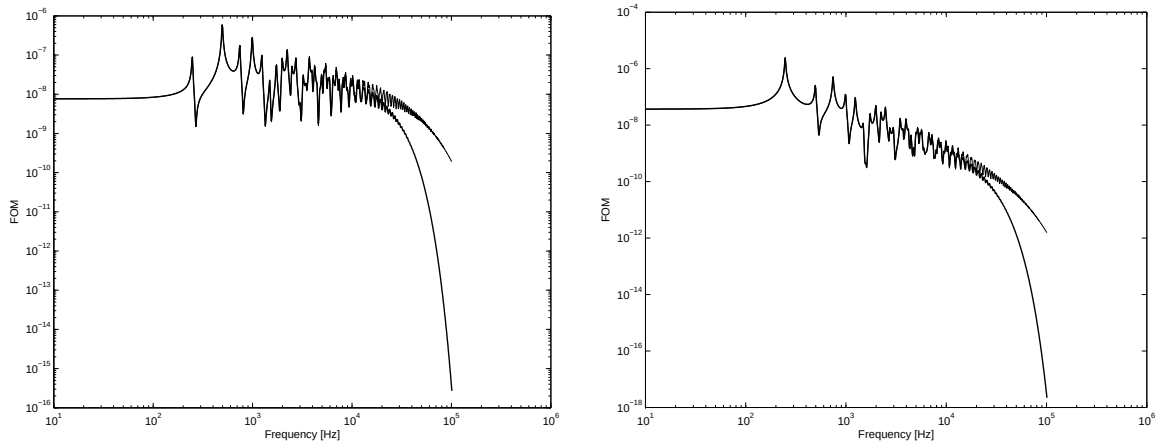

(a) (b)

Figure 5.48: SIF application for the high-frequency domain, two coupled rods. Frequency evolution of the modulus of the first order moment $\langle \partial w/\partial x \rangle$ (a) and $\langle w \rangle$ (b) at $\tilde{x}_0$. —— SIF —— BEM

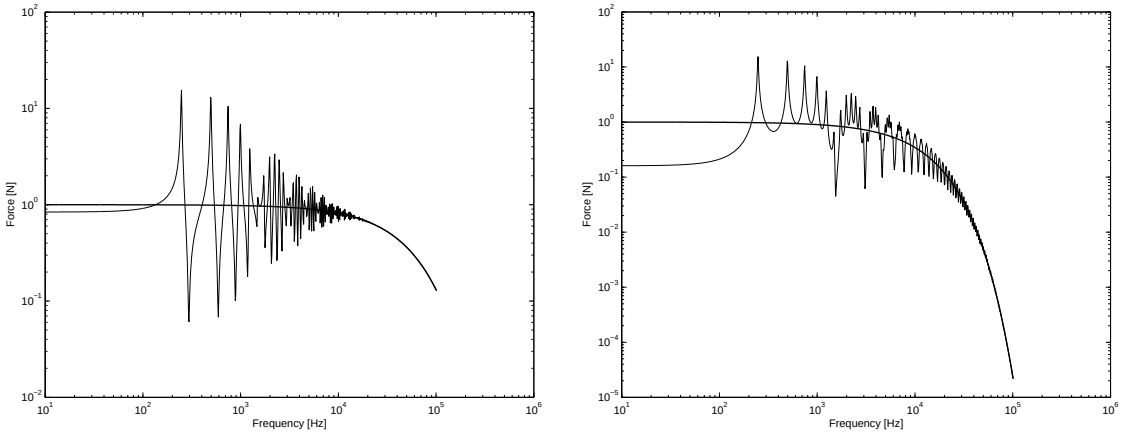

(a) (b)

Figure 5.49: SIF application for the high-frequency domain, two coupled rods. Frequency evolution of the modulus of the second order moment, traction at $\tilde{x}_1$ (a) and $\tilde{x}_2$ (b). —— SIF BEM

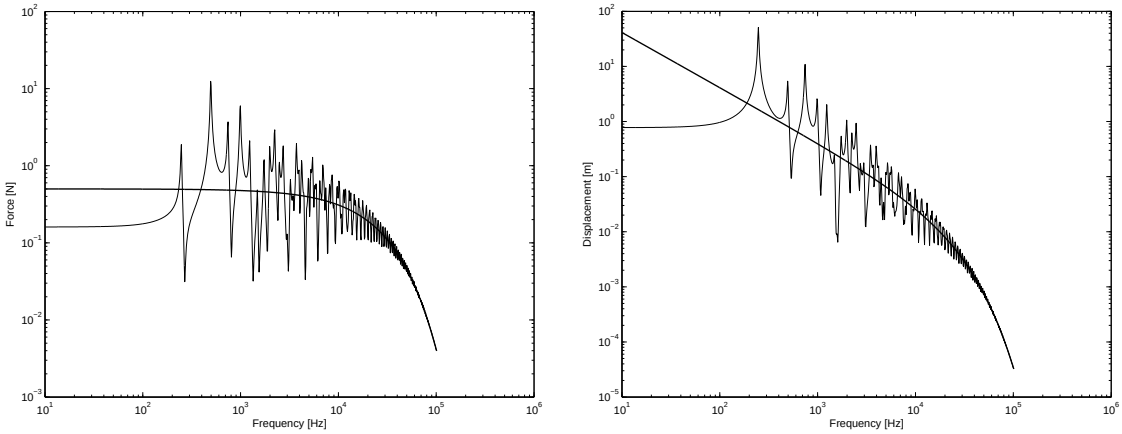

(a) (b)

Figure 5.50: SIF application for the high-frequency domain, two coupled rods. Frequency evolution of the modulus of the second order moment, traction (a) and displacement (b) at $\tilde{x}_0$. —— SIF BEM

5.5 SIF and MonteCarlo comparison

In this section we want to compare the results given by the SIF formulation and those obtained using a Monte Carlo method. We have chosen the Monte Carlo method because it is suited for uncertain problems.

Monte Carlo (MC) methods are stochastic techniques, meaning they are based on the use of random numbers and probability statistics to investigate problems [60]. The method is useful for obtaining numerical solutions to problems which are too complicated to solve analytically, and applies to problems with no probabilistic content as well as to those with inherent probabilistic structure. Monte Carlo methods are a widely used class of computational algorithms for simulating the behavior of various physical and mathematical systems. They are distinguished from other simulation methods (such as molecular dynamics) by being stochastic, that is nondeterministic in some manner - normally by using random numbers (or, more often, pseudo-random numbers) - as opposed to deterministic algorithms. Because of the repetition of algorithms and the large number of calculations involved, Monte Carlo is a method which requires cluster calculation when dealing with complex structures.

We want to apply the SIF and the MC method to the structure made of two couple rods, fig. 5.23. The rods behavior is described using a BEM formulation, and a Monte Carlo simulation is performed introducing a randomness on x_1, x_2 and x_f, with a gaussian distribution. Then all the curves belonging to the different simulations are superposed in a plot and a mean is carried out for each boundary unknown (black line curves). Those results are compared with the SIF results (red line curves).

We can see from figures 5.51-5.54 that the results obtained with SIF are in good agreement with those obtained with MC as the frequency increases. We can conclude that the SIF formulation is a useful and powerful tool for the analysis of uncertain systems.

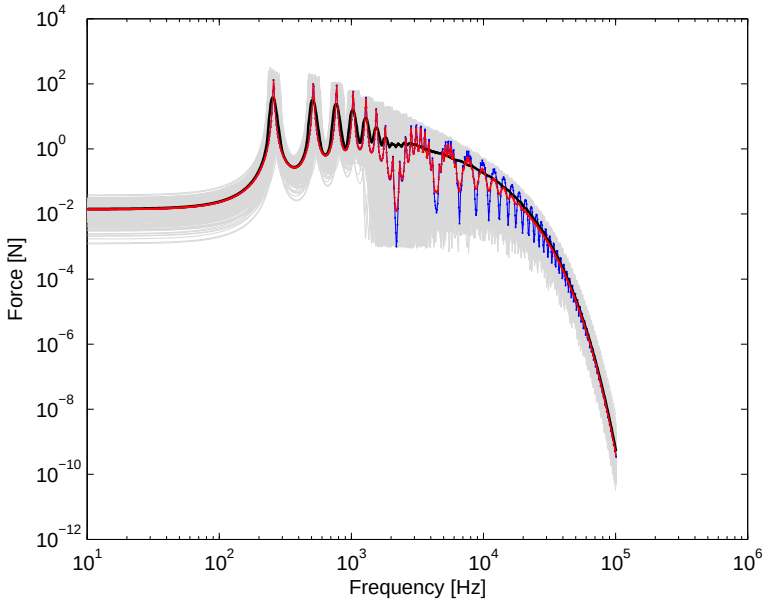

Figure 5.51: SIF and MonteCarlo. Frequency evolution of the modulus of the second order moment, traction at $\tilde{x}_1$. —— MC spread of results, —— BEM nominal structure, —— MonteCarlo mean, —— SIF

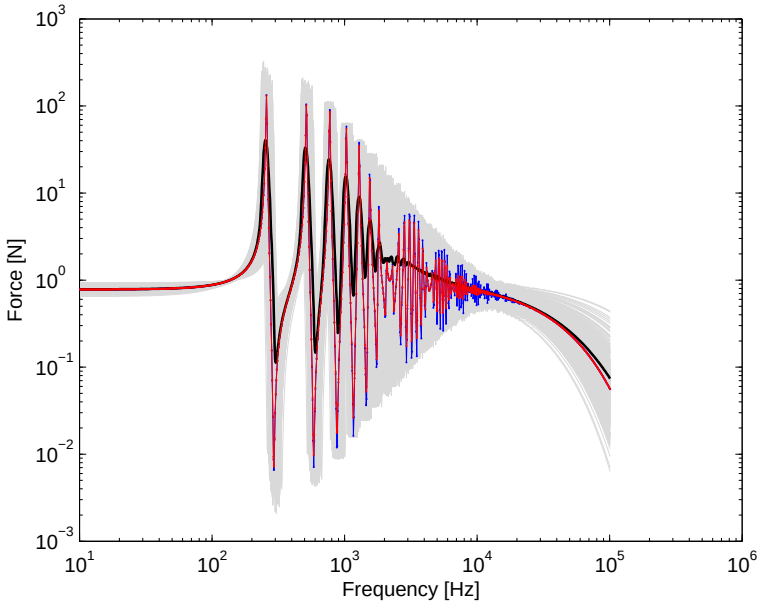

Figure 5.52: SIF and MonteCarlo. Frequency evolution of the modulus of the second order moment, traction at $\tilde{x}_2$. —— MC spread of results, —— BEM nominal structure, —— MonteCarlo mean, —— SIF

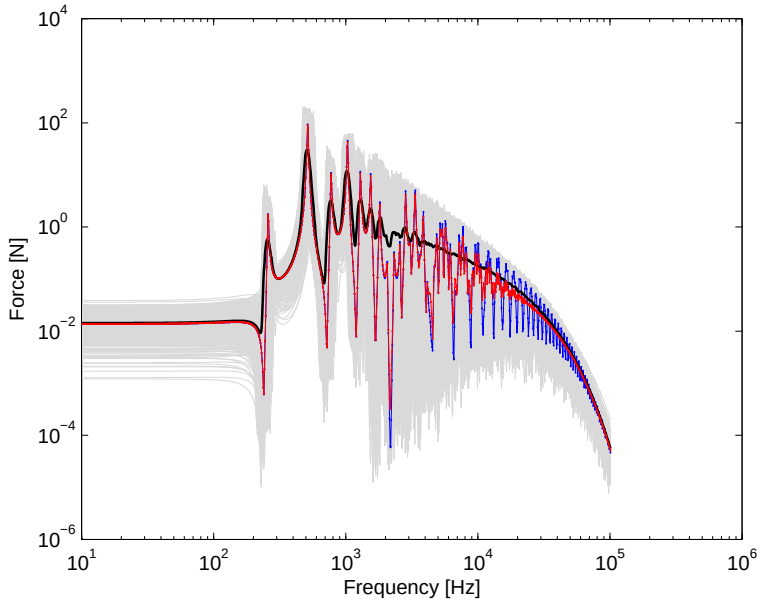

Figure 5.53: SIF and MonteCarlo. Frequency evolution of the modulus of the second order moment, traction at $\tilde{x}_0$. —— MC spread of results, —— BEM nominal structure, —— MonteCarlo mean, —— SIF

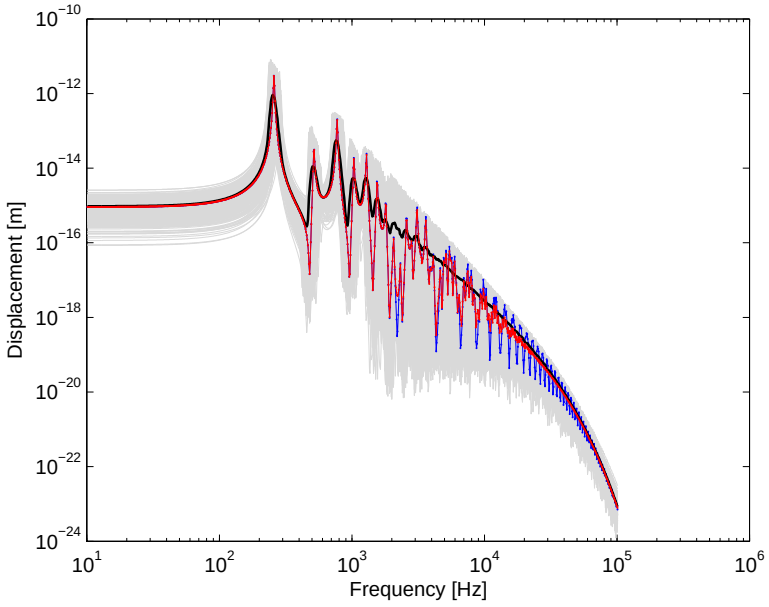

Figure 5.54: SIF and MonteCarlo. Frequency evolution of the modulus of the second order moment, displacement at $\tilde{x}_0$. —— MC spread of results, —— BEM nominal structure, —— MonteCarlo mean, —— SIF

Chapter 6

Application of the SIF to the mid-frequency range

In this chapter we want to investigate the capabilities of SIF to model the mid-frequency structures. Referring to section 5.3.5, we have seen that SIF formulation can correctly predict the response of a structure made of two random subsystems, with similar vibro-acoustical behavior. It also gives correct results for a mid-frequency structure, when the excitation is applied on the short member. But it fails to give the exact deterministic contribution of the low-frequency part when the excitation is applied on the long member. So we want to understand the reason for those results and to improve the formulation.

6.1 Deterministic-SIF formulations

The objective of this work is to develop a formulation which is able to model a complex structure made up of subsystems which have different vibroacoustic behavior, high frequency and low frequency. SIF formulation is able to model structures of this kind, but it presents the drawback of mathematical complexity. Moreover the SIF formulation presents some problems when dealing with mid-frequency structure if the excitation is located on the random subsystems. In this section the mid-frequency problem will be investigated deeply by means of SIF and developing some mid-frequency applications of SIF formulation. The problem noticed in section 5.3.4 is fully analyzed and solved in section 6.5 of this chapter.
What we want to do is to develop a formulation in which low frequency systems are treated as deterministic without the introduction of statistic (this produces a reduction of the number of equations and their complexity), the high frequency systems are treated with SIF formulation.
No randomness is introduced into the description of the low-frequency behaving subsystems, since the response of a low-frequency behaving system is not influenced by the randomness present on its boundaries. Nonetheless the unknowns of the deterministic part are still random variables even if their boundary location is deterministic. This is due to the fact that the response of the deterministic part is directly influenced by the contribution coming from the statistical part of the structure, which is a random contribution. So we cannot treat the unknowns of the deterministic part as deterministic variables, and we also have to consider their reciprocal correlation.
Two different approaches are presented in this work:

1. an approach characterized by the assumption of deterministic boundaries for the low frequency rod, but the formulation based on SIF is still used, considering all the first and second order moments for both the two rods, sec. 6.2,

2. the second one, introducing mid-frequency assumptions, the low frequency rod is described using the first order moment, supposing a low frequency behavior in all the frequency range, while the statistical rod is modelled using only the second order moments. For the second approach two different rod configurations are presented, to investigate all the possible different cases and as well as the capacity of the formulation to simulate the physical behavior.

A simple structure, two coupled rods, has been chosen to develop the deterministic-SIF formulation, secs. 6.3, 6.4, 6.5.

6.2 SIF application in the mid-frequency range: two coupled rods

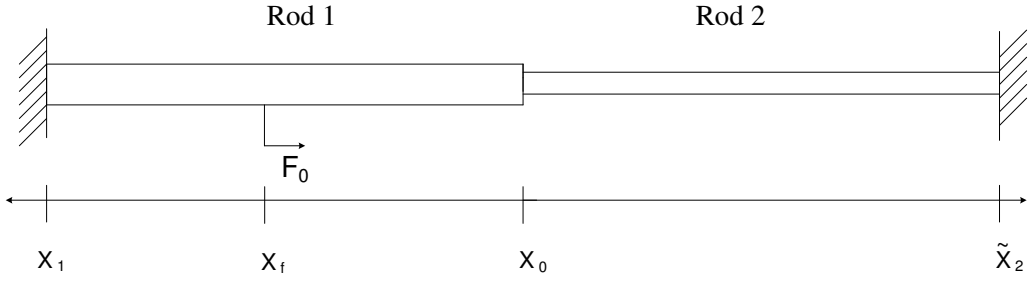

Figure 6.1: SIF application in the mid-frequency range. Two coupled rod structure, rod 1 is low-frequency, rod 2 is high frequency behaving.

Rod 1 is considered to be deterministic, so it's boundaries are x_1 and x_0, while rod 2 is statistic because high-frequency behaving, so boundary $\tilde{x}_2$ is characterized by a deterministic value x_2 plus a gaussian zero mean random part ε_2, fig. 6.1.
Rod 2 is analyzed with SIF formulation, getting the expectation of the BEM equations.
The boundary conditions are clamped- clamped, $w(x_1) = w(x_2) = 0$. The physical properties of the structure are reported in table 6.1
The influence of randomness of $\tilde{x}_2$ on boundary unknowns in x_0 and x_1 has to be evaluated in this work. In the following picture is showed the influence of σ_2 on first order moments. In the three simulations σ is equal to 0.00 gray line, 0.05 green line and 0.10 black line.

	length [m]	x_f [m]	E [N/m^2]	S [m^2]	η [%]	ρ [kg/m^3]
Rod 1	1.72	0.98	$2.1 \cdot 10^{11}$	10^{-3}	2	7800
Rod 2	8.12		$2.1 \cdot 10^{10}$	10^{-5}	1	7800

Table 6.1: SIF application in the mid-frequency range. Parameters of the two rods.

The first order moments are evaluated using SIF theory, introducing two different values for randomness on $\tilde{x}_2$. As we can see from the figures 6.2 and 6.3, only the boundary unknowns at $\tilde{x}_2$ and the traction at x_0 are influenced from the change of value of σ_2, the other unknowns are the same in the two configuration.

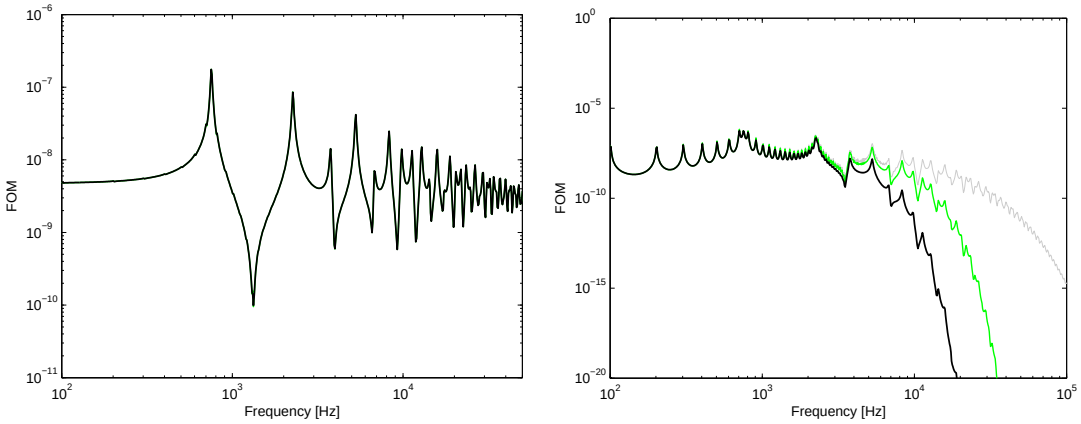

(a) (b)

Figure 6.2: SIF application in the mid-frequency range. First order moment comparison at boundaries x_1 (a) and $\tilde{x}_2$ (b).

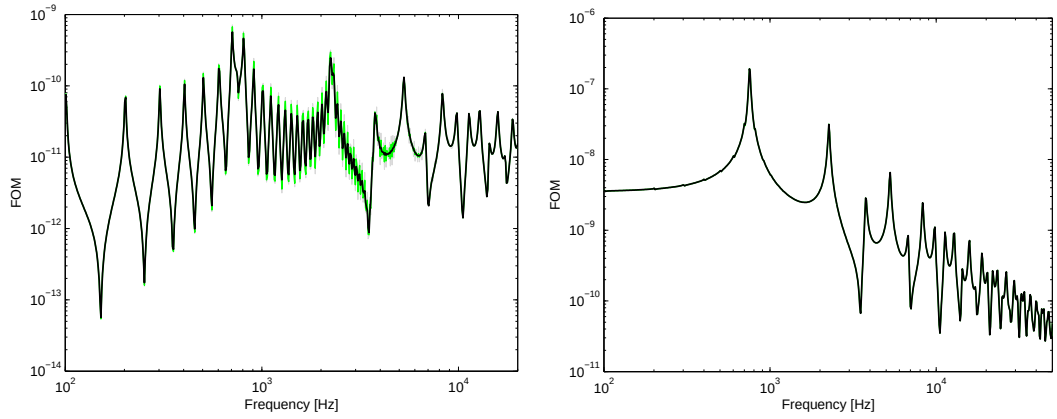

(a) (b)

Figure 6.3: SIF application in the mid-frequency range. First order moment comparison at boundaries x_0, force (a) and displacement (b).

As expected, figures 6.4 and 6.5 we have the same influence of σ_2 to the second order moment at $\tilde{x}_2$, and to the square traction at x_0, but not on the displacement which is driven by rod 1 fig.6.6, the stiffer one. As the value of randomness increases, the smoothing effect starts at lower frequencies in the response of structures, because, from a physical point of view, the amount of uncertainty becomes comparable with the wavelength at lower frequencies.

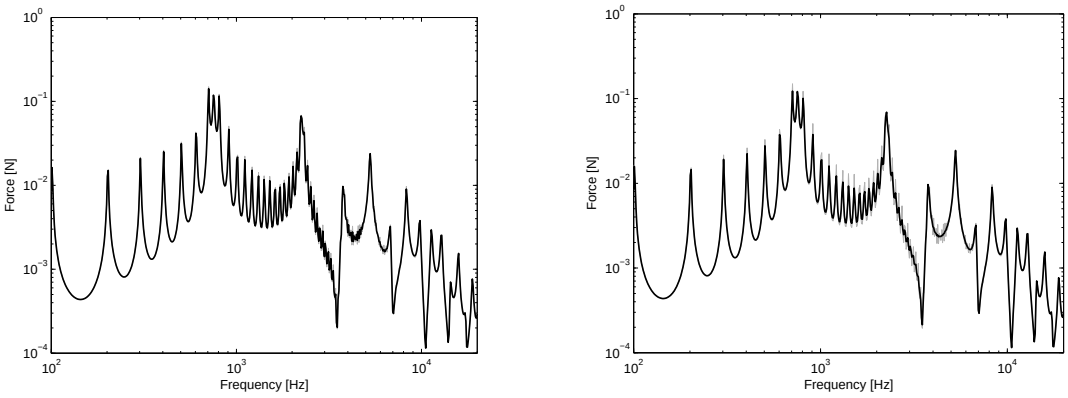

(a) (b)

Figure 6.4: SIF application in the mid-frequency range. Second order moment comparison at boundaries x_2 with different values of σ_2, 0.03 (a) and 0.10 (b) respectively. —– BEM solution, —- SIF solution.

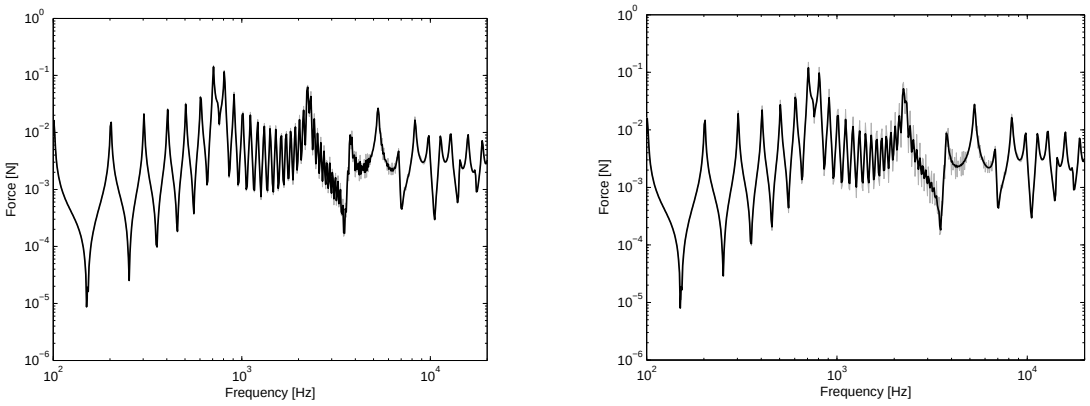

(a) (b)

Figure 6.5: SIF application in the mid-frequency range. Second order moment (traction) comparison at boundaries x_0 with different values of σ_2, 0.03 (a) and 0.10 (b) respectively. —— SIF —– BEM

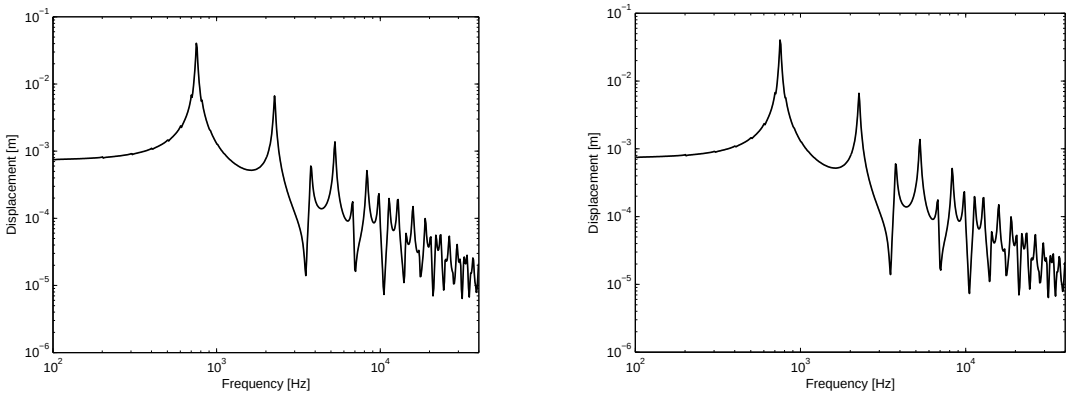

(a) (b)

Figure 6.6: SIF application in the mid-frequency range. Second order moment (displacement) comparison at boundaries x_0 with different values of σ_2, 0.03 (a) and 0.10 (b) respectively. —— SIF —— BEM

6.2.1 SIF application in the mid-frequency range: deriving the equations

In this first BEM-SIF coupling formulation, even if rod 1 has deterministic locations for its boundaries, both the first and second order moments are used to describe the high frequency behavior of rod 1.

BEM equations with random boundaries:
Rod 1:

$$\begin{aligned} 0 &= \frac{F_0}{E_1 S_1} G_1(x_1 - x_f) + \frac{\partial w(x_1)}{\partial x} G_1(x_1 - x_1) \\ &\quad - \frac{\partial w^{(1)}(x_0)}{\partial x} G_1(x_1 - x_0) + w^{(1)}(x_0) \frac{\partial G_1(x_1 - x_0)}{\partial x} \end{aligned} \tag{6.1}$$

$$\begin{aligned} 0 &= \frac{F_0}{E_1 S_1} G_1(x_0 - x_f) + \frac{\partial w(x_1)}{\partial x} G_1(x_0 - x_1) \\ &\quad - \frac{\partial w^{(1)}(x_0)}{\partial x} G_1(x_0 - x_0) + w^{(1)}(x_0) \Big(\frac{\partial G_1(x_0 - x_0)}{\partial x} - 1 \Big) \end{aligned} \tag{6.2}$$

Rod 2:

$$\begin{aligned} 0 &= \frac{\partial w(\tilde{x}_2)}{\partial x} G_2(\tilde{x}_2 - \tilde{x}_2) - \frac{\partial w^{(2)}(x_0)}{\partial x} G_2(\tilde{x}_2 - x_0) \\ &\quad + w^{(2)}(x_0) \frac{\partial G_2(\tilde{x}_2 - x_0)}{\partial x} \end{aligned} \tag{6.3}$$

$$\begin{aligned} 0 &= \frac{\partial w(\tilde{x}_2)}{\partial x} G_2(x_0 - \tilde{x}_2) - \frac{\partial w^{(2)}(x_0)}{\partial x} G_2(x_0 - x_0) \\ &\quad + w^{(2)}(x_0) \Big(\frac{\partial G_2(x_0 - x_0)}{\partial x} - 1 \Big) \end{aligned} \tag{6.4}$$

Coupling equations:

$$w^{(1)}(x_0) = -w^{(2)}(x_0) \tag{6.5}$$

$$E_1 S_1 \frac{\partial w^{(1)}(x_0)}{\partial x} = E_2 S_2 \frac{\partial w^{(2)}(x_0)}{\partial x} \tag{6.6}$$

List of the unknowns:

Rod 1 (7 unknowns)

$$\Big\langle \frac{\partial w(x_1)}{\partial x} \Big\rangle, \Big\langle \frac{\partial w^{(1)}(x_0)}{\partial x} \Big\rangle, \Big\langle w^{(1)}(x_0) \Big\rangle,$$
$$\Big\langle \Big| \frac{\partial w(x_1)}{\partial x} \Big|^2 \Big\rangle, \Big\langle \Big| \frac{\partial w^{(2)}(x_0)}{\partial x} \Big|^2 \Big\rangle, \Big\langle \Big| w^{(1)}(x_0) \Big|^2 \Big\rangle,$$
$$\Big\langle w^{(1)}(x_0) \cdot \frac{\partial w^{(1)*}(x_0)}{\partial x} \Big\rangle, \Big\langle w^{(1)*}(x_0) \cdot \frac{\partial w^{(1)}(x_0)}{\partial x} \Big\rangle.$$

Rod 2 (9 unknowns)

$$\Big\langle \frac{\partial w(\tilde{x}_2)}{\partial x} \Big\rangle, \Big\langle \frac{\partial w^{(2)}(x_0)}{\partial x} \Big\rangle, \Big\langle w^{(2)}(x_0) \Big\rangle,$$
$$\Big\langle \Big| \frac{\partial w(\tilde{x}_2)}{\partial x} \Big|^2 \Big\rangle, \Big\langle \Big| \frac{\partial w^{(2)}(x_0)}{\partial x} \Big|^2 \Big\rangle, \Big\langle \Big| w^{(2)}(x_0) \Big|^2 \Big\rangle,$$
$$\Big\langle w^{(2)}(x_0) \cdot \frac{\partial w^{(2)*}(x_0)}{\partial x} \Big\rangle, \Big\langle w^{(2)*}(x_0) \cdot \frac{\partial w^{(2)}(x_0)}{\partial x} \Big\rangle,$$
$$\Big\langle \frac{\partial w^{(2)}(x_0)}{\partial x} \cdot G_2(\tilde{x}_2 - x_0) \cdot \frac{\partial w^*(\tilde{x}_2)}{\partial x} \Big\rangle, \Big\langle w^{(2)}(x_0) \cdot \frac{\partial G_2(\tilde{x}_2 - x_0)}{\partial x} \cdot \frac{\partial w^*(\tilde{x}_2)}{\partial x} \Big\rangle.$$

Equations of rod 1:

The first equation is obtained by multiplying the first basic equation, (6.1), by the conjugate of $\partial w(x_1)/\partial x$ and getting the expectation with respect to x_1, x_0 and x_f; while the second and the third equations are obtained from the multiplication of the second equation, (6.2) respectively by the conjugate of $\partial w^{(1)}(x_0)/\partial x$ and $w^{(1)}(x_0)$ and then applying the expectation operator.
The fourth and fifth equations are obtained as the expectations of the basic equations, (6.1) and (6.2).

$$\begin{aligned}
0 &= \frac{F_0}{E_1 S_1} \Big\langle \frac{\partial w^*(x_1)}{\partial x} \Big\rangle G_1(x_1 - x_f) + \Big\langle \Big| \frac{\partial w(x_1)}{\partial x} \Big|^2 \Big\rangle G_1(x_1 - x_1) \\
&\quad - \Big\langle \frac{\partial w^{(1)}(x_0)}{\partial x} \Big\rangle \Big\langle \frac{\partial w^*(x_1)}{\partial x} \Big\rangle G_1(x_1 - x_0) \\
&\quad + \Big\langle w^{(1)}(x_0) \Big\rangle \Big\langle \frac{\partial w^*(x_1)}{\partial x} \Big\rangle \frac{\partial G_1(x_1 - x_0)}{\partial x}, \qquad (6.7) \\
0 &= \frac{F_0}{E_1 S_1} \Big\langle \frac{\partial w^{(1)*}(x_0)}{\partial x} \Big\rangle G_1(x_0 - x_f) + \Big\langle \frac{\partial w(x_1)}{\partial x} \Big\rangle \Big\langle \frac{\partial w^{(1)*}(x_0)}{\partial x} \Big\rangle G_1(x_0 - x_1) \\
&\quad - \Big\langle \Big| \frac{\partial w^{(1)}(x_0)}{\partial x} \Big|^2 \Big\rangle G_1(x_0 - x_0)
\end{aligned}$$

$$+\Big\langle w^{(1)}(x_0)\frac{\partial w^{(1)*}(x_0)}{\partial x}\Big\rangle\Big(\frac{\partial G_1(x_0-x_0)}{\partial x}-1\Big), \tag{6.8}$$

$$\begin{aligned}0 &= \frac{F_0}{E_1S_1}\Big\langle w^{(1)*}(x_0)\Big\rangle G_1(x_0-x_f)+\Big\langle\frac{\partial w(x_1)}{\partial x}\Big\rangle\Big\langle w^{(1)*}(x_0)\Big\rangle G_1(x_0-x_1)\\ &\quad -\Big\langle\frac{\partial w^{(1)}(x_0)}{\partial x}w^{(1)*}(x_0)\Big\rangle G_1(x_0-x_0)\\ &\quad +\Big\langle\Big|w^{(1)}(x_0)\Big|^2\Big\rangle\Big(\frac{\partial G_1(x_0-x_0)}{\partial x}-1\Big),\end{aligned} \tag{6.9}$$

$$\begin{aligned}0 &= \frac{F_0}{E_1S_1}G_1(x_1-x_f)+\Big\langle\frac{\partial w(x_1)}{\partial x}\Big\rangle G_1(x_1-x_1)\\ &\quad -\Big\langle\frac{\partial w^{(1)}(x_0)}{\partial x}\Big\rangle G_1(x_1-x_0)+\Big\langle w^{(1)}(x_0)\Big\rangle\frac{\partial G_1(x_1-x_0)}{\partial x},\end{aligned} \tag{6.10}$$

$$\begin{aligned}0 &= \frac{F_0}{E_1S_1}G_1(x_0-x_f)+\Big\langle\frac{\partial w(x_1)}{\partial x}\Big\rangle G_1(x_0-x_1)\\ &\quad -\Big\langle\frac{\partial w^{(1)}(x_0)}{\partial x}\Big\rangle G_1(x_0-x_0)+\Big\langle w^{(1)}(x_0)\Big\rangle\Big(\frac{\partial G_1(x_0-x_0)}{\partial x}-1\Big),\end{aligned} \tag{6.11}$$

Equations of rod 2:

The first equation is obtained from the multiplication of the first basic equation, (6.3), by the conjugate of $\partial w(\tilde{x}_2)/\partial x$ and applying the expectation operator with respect to $\tilde{x}_2$ and 0; while the second and the third equations are obtained from the multiplication of the second equation, (6.4) respectively by the conjugate of $\partial w^{(2)}(x_0)/\partial x$ and $w^{(2)}(x_0)$ then calculating the expectation.
The fourth and fifth equations are obtained as the expectations of the basic equations, (6.3) and (6.4).
The sixth equation is obtained multiplying the conjugate of the first basic equation, (6.3), by $\partial w^{(2)}(x_0)/\partial x G_2(\tilde{x}_2-x_0)$; while the seventh multiplying by $w^{(2)}(x_0)\partial G_2(\tilde{x}_2-x_0)/\partial x$ and then calculating the expectation.

$$\begin{aligned}0 &= \Big\langle\Big|\frac{\partial w(\tilde{x}_2)}{\partial x}\Big|^2\Big\rangle G_2(\tilde{x}_2-\tilde{x}_2)-\Big\langle\frac{\partial w^{(2)}(x_0)}{\partial x}\frac{\partial w^*(\tilde{x}_2)}{\partial x}\ G_2(\tilde{x}_2-x_0)\Big\rangle\\ &\quad +\Big\langle w^{(2)}(x_0)\frac{\partial w^*(\tilde{x}_2)}{\partial x}\frac{\partial G_2(\tilde{x}_2-x_0)}{\partial x}\Big\rangle,\end{aligned} \tag{6.12}$$

$$\begin{aligned}0 &= \Big\langle\frac{\partial w(\tilde{x}_2)}{\partial x}\Big\rangle\Big\langle\frac{\partial w^{(2)*}(x_0)}{\partial x}\Big\rangle\Big\langle G_2(x_0-\tilde{x}_2)\Big\rangle-\Big\langle\Big|\frac{\partial w^{(2)}(x_0)}{\partial x}\Big|^2\Big\rangle G_2(x_0-x_0)\\ &\quad +\Big\langle w^{(2)}(x_0)\frac{\partial w^{(2)*}(x_0)}{\partial x}\Big\rangle\Big(\frac{\partial G_2(x_0-x_0)}{\partial x}-1\Big),\end{aligned} \tag{6.13}$$

$$\begin{aligned}0 &= \Big\langle\frac{\partial w(\tilde{x}_2)}{\partial x}\Big\rangle\Big\langle w^{(2)*}(x_0)\Big\rangle\Big\langle G_2(x_0-\tilde{x}_2)\Big\rangle-\Big\langle\frac{\partial w^{(2)}(x_0)}{\partial x}w^{(2)*}(x_0)\Big\rangle G_2(x_0-x_0)\\ &\quad +\Big\langle\Big|w^{(2)}(x_0)\Big|^2\Big\rangle\Big(\frac{\partial G_2(x_0-x_0)}{\partial x}-1\Big),\end{aligned} \tag{6.14}$$

$$\begin{aligned}0 &= \Big\langle\frac{\partial w(\tilde{x}_2)}{\partial x}\Big\rangle G_2(\tilde{x}_2-\tilde{x}_2)-\Big\langle\frac{\partial w^{(2)}(x_0)}{\partial x}\Big\rangle\Big\langle G_2(\tilde{x}_2-x_0)\Big\rangle\\ &\quad +\Big\langle w^{(2)}(x_0)\Big\rangle\Big\langle\frac{\partial G_2(\tilde{x}_2-x_0)}{\partial x}\Big\rangle,\end{aligned} \tag{6.15}$$

$$0 = \Big\langle\frac{\partial w(\tilde{x}_2)}{\partial x}\Big\rangle\Big\langle G_2(x_0-\tilde{x}_2)\Big\rangle-\Big\langle\frac{\partial w^{(2)}(x_0)}{\partial x}\Big\rangle G_2(x_0-x_0)$$

$$+\Big\langle w^{(2)}(x_0)\Big\rangle\Big(\frac{\partial G_2(x_0-x_0)}{\partial x}-1\Big), \tag{6.16}$$

$$\begin{aligned}0 \;=\; &\Big\langle \frac{\partial w^*(\tilde{x}_2)}{\partial x} w^{(2)}(x_0)\frac{\partial G_2(\tilde{x}_2-x_0)}{\partial x}\Big\rangle\, G_2^*(\tilde{x}_2-\tilde{x}_2)\\ &-\Big\langle \frac{\partial w^{(2)*}(x_0)}{\partial x} w^{(2)}(x_0)\Big\rangle\Big\langle \frac{\partial G_2(\tilde{x}_2-x_0)}{\partial x} G_2^*(\tilde{x}_2-x_0)\Big\rangle\\ &+\Big\langle \Big|w^{(2)}(x_0)\Big|^2\Big\rangle\Big\langle \Big|\frac{\partial G_2(\tilde{x}_2-x_0)}{\partial x}\Big|^2\Big\rangle,\end{aligned} \tag{6.17}$$

$$\begin{aligned}0 \;=\; &\Big\langle \frac{\partial w^*(\tilde{x}_2)}{\partial x}\frac{\partial w^{(2)}(x_0)}{\partial x} G_2(\tilde{x}_2-x_0)\Big\rangle G_2(\tilde{x}_2-\tilde{x}_2) -\\ &\Big\langle \Big|\frac{\partial w^{(2)}(x_0)}{\partial x}\Big|^2\Big\rangle\Big\langle \Big|G_2(\tilde{x}_2-x_0)\Big|^2\Big\rangle\\ &+\Big\langle w^{(2)*}(x_0)\frac{\partial w^{(2)}(x_0)}{\partial x}\Big\rangle\Big\langle G_2(\tilde{x}_2-x_0)\frac{\partial G_2^*(\tilde{x}_2-x_0)}{\partial x}\Big\rangle.\end{aligned} \tag{6.18}$$

Coupling equations:

$$\Big\langle w^{(1)}(x_0)\Big\rangle = -\Big\langle w^{(2)}(x_0)\Big\rangle \tag{6.19}$$

$$Y_1S_1\Big\langle \frac{\partial w^{(1)}(x_0)}{\partial x}\Big\rangle = Y_2S_2\Big\langle \frac{\partial w^{(2)}(x_0)}{\partial x}\Big\rangle \tag{6.20}$$

$$\Big(Y_1S_1\Big)^*\Big\langle w^{(1)}(x_0)\frac{\partial w^{(1)*}(x_0)}{\partial x}\Big\rangle = -\Big(Y_2S_2\Big)^*\Big\langle w^{(2)}(x_0)\frac{\partial w^{(2)*}(x_0)}{\partial x}\Big\rangle \tag{6.21}$$

$$\Big\langle \Big|w^{(1)}(x_0)\Big|^2\Big\rangle = \Big\langle \Big|w^{(1)}(x_0)\Big|^2\Big\rangle \tag{6.22}$$

$$\Big|Y_1S_1\Big|^2\Big\langle \Big|\frac{\partial w^{(1)}(x_0)}{\partial x}\Big|^2\Big\rangle = \Big|Y_2S_2\Big|^2\Big\langle \Big|\frac{\partial w^{(2)}(x_0)}{\partial x}\Big|^2\Big\rangle \tag{6.23}$$

$$Y_1S_1\Big\langle w^{(1)*}(x_0)\frac{\partial w^{(1)}(x_0)}{\partial x}\Big\rangle = -Y_2S_2\Big\langle w^{(2)*}(x_0)\frac{\partial w^{(2)}(x_0)}{\partial x}\Big\rangle \tag{6.24}$$

Solving the problem

Green Kernel expectation
Rod green kernel definition:

$$G(\tilde{\xi}-x) = \frac{1}{2ik_0\big(1-i\eta/2\big)} e^{-ik_0\big(1-i\eta/2\big)|\tilde{\xi}-x|} \tag{6.25}$$

Calculations od the expectations:

$$\Big\langle G(\tilde{\xi}-x)\Big\rangle \;=\; \begin{cases} \frac{1}{2ik_0\big(1-i\eta/2\big)} & \text{if } \xi = x\\ \frac{1}{2ik_0\big(1-i\eta/2\big)} e^{-ik_0\big(1-i\eta/2\big)|\xi-x|} e^{k_0^2\frac{\eta^2}{4}\left(\frac{\sigma_\xi^2}{2}\right)} & \\ \qquad \cdot e^{-k_0^2\left(\frac{\sigma_\xi^2}{2}\right)} e^{ik_0^2\frac{\eta}{2}\left(\sigma_\xi^2\right)} & \text{else}\end{cases} \tag{6.26}$$

$$\Big\langle \frac{\partial G(\tilde{\xi}-x)}{\partial x}\Big\rangle \;=\; \begin{cases} \frac{1}{2} & \text{if } \xi > x \text{ and } \xi \to x\\ -\frac{1}{2} & \text{if } \xi < x \text{ and } \xi \to x\\ \frac{1}{2}\frac{|\xi-x|}{\xi-x} e^{-ik_0\big(1-i\eta/2\big)|\xi-x|} e^{k_0^2\frac{\eta^2}{4}\left(\frac{\sigma_\xi^2}{2}\right)} & \\ \qquad \cdot e^{-k_0^2\left(\frac{\sigma_\xi^2}{2}\right)} e^{ik_0^2\frac{\eta}{2}\left(\sigma_\xi^2\right)} & \text{else}\end{cases} \tag{6.27}$$

$$\left\langle \left| \frac{\partial G(\tilde{\xi}-x)}{\partial x} \right|^2 \right\rangle = \begin{cases} \frac{1}{4} & \text{if } \xi = x \\ \frac{1}{4} e^{-k_0\eta|\xi-x|} e^{k_0^2\eta^2\left(\frac{\sigma_\xi^2}{2}\right)} & \text{else} \end{cases} \tag{6.28}$$

$$\left\langle \left| G(\tilde{\xi}-x) \right|^2 \right\rangle = \begin{cases} \frac{1}{k_0^2\left(\eta^2-4\right)} & \text{if } \xi = x \\ \frac{1}{k_0^2\left(\eta^2-4\right)} e^{-k_0\eta|\xi-x|} e^{k_0^2\eta^2\left(\frac{\sigma_\xi^2}{2}\right)} & \text{else} \end{cases} \tag{6.29}$$

$$\left\langle G(\tilde{\xi}-x) \frac{\partial G^*(\tilde{\xi}-x)}{\partial x} \right\rangle = \begin{cases} \frac{1}{4ik_0\left(1-i\eta/2\right)} & \text{if } \xi > x \text{ and } \zeta \to x \\ -\frac{1}{4ik_0\left(1-i\eta/2\right)} & \text{if } \xi < x \text{ and } \zeta \to x \\ \frac{1}{4ik_0\left(1-i\eta/2\right)} \frac{|\xi-x|}{\xi-x} e^{-k_0\eta|\xi-x|} e^{k_0^2\eta^2\left(\frac{\sigma_\xi^2}{2}\right)} & \text{else} \end{cases} \tag{6.30}$$

System solution:

The system of equations made up by the equation of rod 1, rod 2 and the coupling equations is solved in the same way as explained in SIF 2 rods paragraph.
Initially the first order moment system is solved using equations (6.10), (6.11), (6.15), (6.16), (6.20) and (6.21). Then it is possible to evaluate $\langle |\partial w(x_1)/\partial x|^2 \rangle$ solving equation (6.7). The remaining unknowns are calculated with the other equations.

6.2.2 SIF application in the mid-frequency range: results

- Configuration n.1
  Two different behavior rods are considered, rod 1, the excited one, is typically low frequency because is stiff and short, while rod 2 is typically high frequency because is thin, long and flexible. Also different physical properties characterize the two rods in terms of flexibility and damping. Randomness on x_2 is the only random parameter, $\sigma_2 = 0.05$.
  The physical properties of configuration n.1 are reported in table 6.2 and the results of SOM in figures 6.7 and 6.8.

	length [m]	x_f [m]	E [N/m^2]	S [m^2]	η [%]	ρ [kg/m^3]
Rod 1	1.00	0.47	$2.1 \cdot 10^{11}$	10^{-4}	2	7800
Rod 2	9.50		$2.1 \cdot 10^{10}$	10^{-5}	0.2	7800

Table 6.2: SIF application in the mid-frequency range. Parameters of the two rods. Configuration n.1

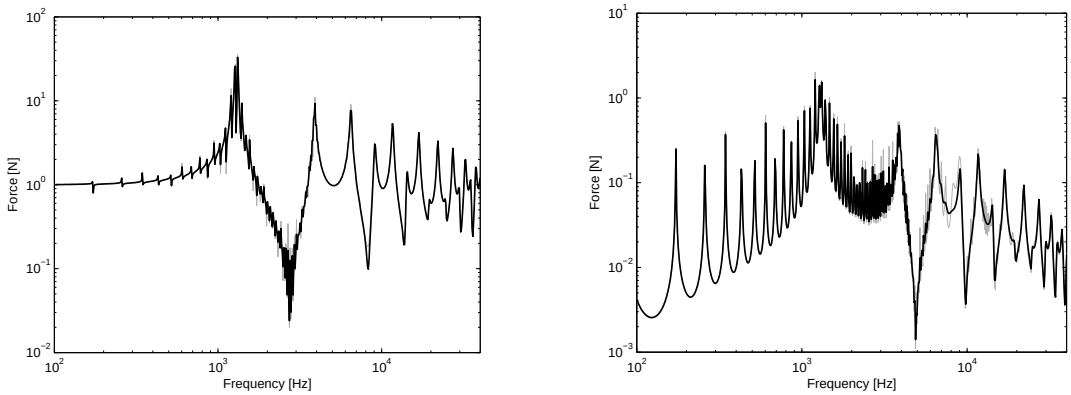

(a) (b)

Figure 6.7: SIF application in the mid-frequency range. Frequency evolution of the modulus of the second order moment, traction at x_1 (a) and $\tilde{x}_2$ (b). Configuration n.1. —— SIF —— BEM

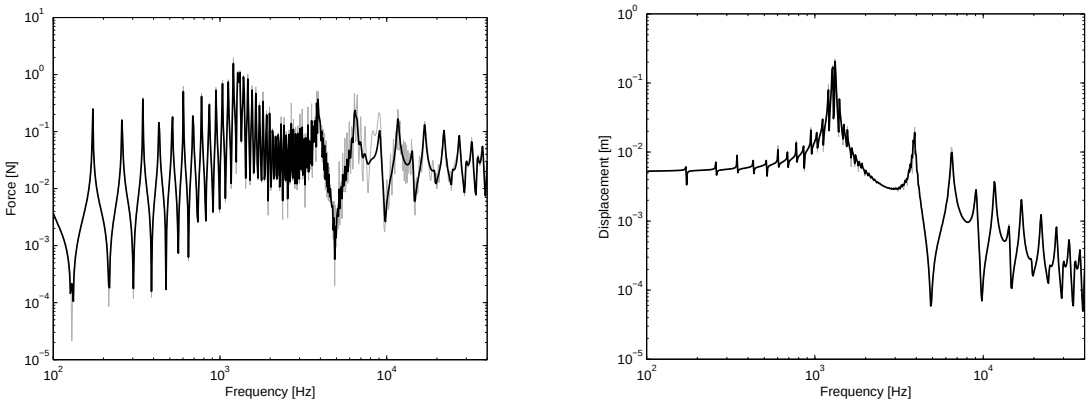

(a) (b)

Figure 6.8: SIF application in the mid-frequency range. Frequency evolution of the modulus of the second order moment, traction (a) and displacement (b) at x_0. Configuration n.1. —— SIF —— BEM

- Configuration n.2
  In this configuration the difference in the vibrational behavior of the two rods is much more evident, in terms of flexibility and randomness, than configuration n.1. Randomness on x_2 is the only random parameter, $\sigma_2 = 0.15$.
  The physical properties of configuration n.2 are reported in table 6.3 and results SOM in figures 6.9 and 6.10.

	length [m]	x_f [m]	E [N/m^2]	S [m^2]	η [%]	ρ [kg/m^3]
Rod 1	1.83	0.77	$2.1 \cdot 10^{11}$	10^{-3}	2	7800
Rod 2	11.65		$2.1 \cdot 10^{9}$	10^{-5}	0.2	7800

Table 6.3: SIF application in the mid-frequency range. Parameters of the two rods. Configuration n.2

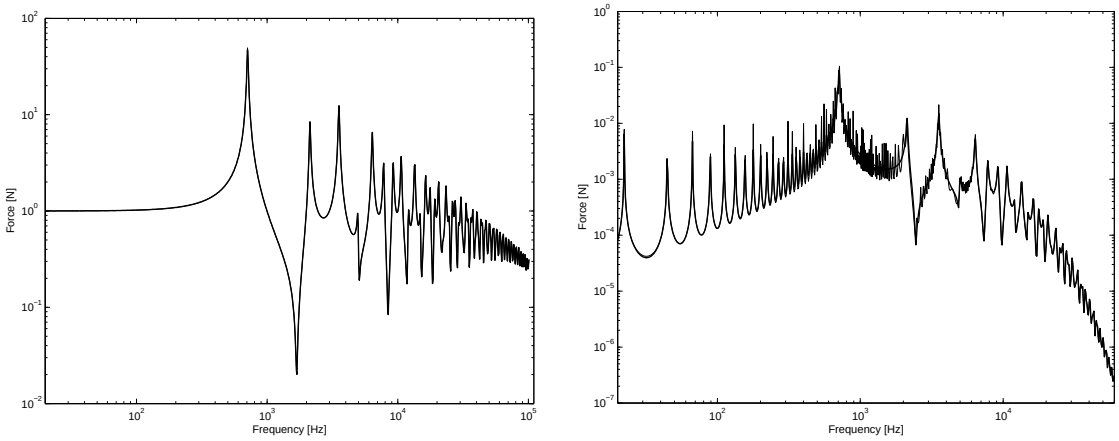

(a) (b)

Figure 6.9: SIF application in the mid-frequency range. Frequency evolution of the modulus of the second order moment, traction at x_1 (a) and $\tilde{x}_2$ (b). Configuration n.2. —— SIF —— BEM

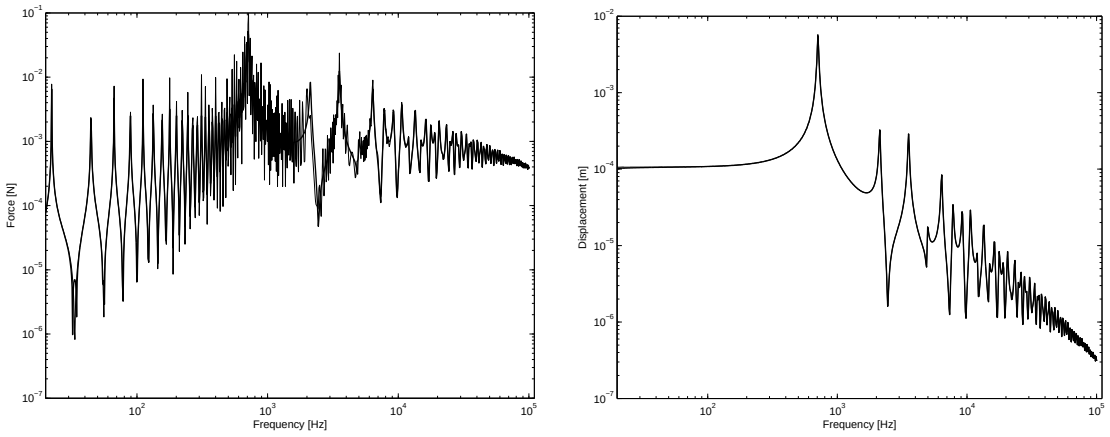

(a) (b)

Figure 6.10: SIF application in the mid-frequency range. Frequency evolution of the modulus of the second order moment, traction (a) and displacement (b) at x_0. Configuration n.2. —— SIF —— BEM

6.2.3 Discussion

The results obtained with this formulation, using the SIF for a system made up by two rods with different physical behavior, are good. Rod 1 is treated as deterministic and this causes a reduction in complexity and in the number of equations. This formulation is able to model the transition from low frequency and high frequency behavior of the complex system.

Traction in x_1 and displacement in x_0 are not influenced from randomness in x_2, while traction in x_0 and traction in x_2 are influenced from the presence of a random boundaries. The number of variables for the SIF application in the mid-frequency range is equal to 16, so we have a reduction of only 3 unknowns respect to complete SIF thanks to the deterministic description of rod 1. The unknowns of complete SIF, sec. 5.3.4, like $\langle \partial w^*(\tilde{x}_1)/\partial x \cdot G_1(\tilde{x}_1 - \tilde{x}_f)\rangle$ due to the correlation among the primary force F_0 and the boundary locations become FOMs $\langle \partial w^*(\tilde{x}_1)/\partial x\rangle$. The formulation is simpler but we still need to account for the SOMs also for the rod 1.

6.3 BEM-SIF application: two coupled rods with mid-frequency assumptions

In this section we want to treat the same application, a mid-frequency structure, but utilizing a proper mid-frequency formulation. The deterministic part is modeled deterministically, and the other part by means of SIF. Thus rod 2 is analyzed with SIF formulation. Some assumptions are introduced:

- Rod 1 is considered to be a low frequency behavior rod, so it's behavior is correctly described by first order moment even in high frequency range. So $\langle \partial w(x_1)/\partial x\rangle$, $\langle \partial w^{(1)}(x_0)/\partial x\rangle$ and $\langle w^{(1)}(x_0)\rangle$ are used to describe the model.

- Rod 2 is considered to be a high frequency behavior rod, so it's behavior is described by second order moments, while first order moments vanish to zero very rapidly as the frequency increase. So $\langle \partial w(\tilde{x}_2)/\partial x\rangle$ is not influent for the solution of rod 2, while $\langle \partial w^{(2)}(x_0)/\partial x\rangle$ and $\langle w^{(2)}(x_0)\rangle$ are important for the solution because they come from rod 1 which is deterministic.

6.3.1 BEM-SIF two coupled rods with mid-frequency assumptions: deriving the equations

BEM equations with random boundaries:
Rod 1:

$$\begin{aligned} 0 &= \frac{F_0}{E_1 S_1} G_1(x_1 - x_f) + \frac{\partial w(x_1)}{\partial x} G_1(x_1 - x_1) \\ &\quad - \frac{\partial w^{(1)}(x_0)}{\partial x} G_1(x_1 - x_0) + w^{(1)}(x_0) \frac{\partial G_1(x_1 - x_0)}{\partial x} \\ 0 &= \frac{F_0}{E_1 S_1} G_1(x_0 - x_f) + \frac{\partial w(x_1)}{\partial x} G_1(x_0 - x_1) \end{aligned} \tag{6.31}$$

$$-\frac{\partial w^{(1)}(x_0)}{\partial x}G_1(x_0-x_0)+w^{(1)}(x_0)\Big(\frac{\partial G_1(x_0-x_0)}{\partial x}-1\Big) \tag{6.32}$$

Rod 2:

$$\begin{aligned} 0 &= \frac{\partial w(\tilde{x}_2)}{\partial x}G_2(\tilde{x}_2-\tilde{x}_2)-\frac{\partial w^{(2)}(x_0)}{\partial x}G_2(\tilde{x}_2-x_0) \\ &\quad +w^{(2)}(x_0)\frac{\partial G_2(\tilde{x}_2-x_0)}{\partial x} \end{aligned} \tag{6.33}$$

$$\begin{aligned} 0 &= \frac{\partial w(\tilde{x}_2)}{\partial x}G_2(x_0-\tilde{x}_2)-\frac{\partial w^{(2)}(x_0)}{\partial x}G_2(x_0-x_0) \\ &\quad +w^{(2)}(x_0)\Big(\frac{\partial G_2(x_0-x_0)}{\partial x}-1\Big) \end{aligned} \tag{6.34}$$

Coupling equations:

$$w^{(1)}(x_0)=-w^{(2)}(x_0) \tag{6.35}$$

$$E_1S_1\frac{\partial w^{(1)}(x_0)}{\partial x}=E_2S_2\frac{\partial w^{(2)}(x_0)}{\partial x} \tag{6.36}$$

List of the unknowns:

Rod 1 (3 unknowns)

$$\Big\langle\frac{\partial w(x_1)}{\partial x}\Big\rangle,\Big\langle\frac{\partial w^{(1)}(x_0)}{\partial x}\Big\rangle,\Big\langle w^{(1)}(x_0)\Big\rangle.$$

Rod 2 (9 unknowns)

$$\Big\langle\frac{\partial w^{(2)}(x_0)}{\partial x}\Big\rangle,\Big\langle w^{(2)}(x_0)\Big\rangle,$$
$$\Big\langle\Big|\frac{\partial w(\tilde{x}_2)}{\partial x}\Big|^2\Big\rangle,\Big\langle\Big|\frac{\partial w^{(2)}(x_0)}{\partial x}\Big|^2\Big\rangle,\Big\langle\Big|w^{(2)}(x_0)\Big|^2\Big\rangle,$$
$$\Big\langle w^{(2)}(x_0)\cdot\frac{\partial w^{(2)*}(x_0)}{\partial x}\Big\rangle,\Big\langle w^{(2)*}(x_0)\cdot\frac{\partial w^{(2)}(x_0)}{\partial x}\Big\rangle,$$
$$\Big\langle\frac{\partial w^{(2)}(x_0)}{\partial x}\cdot G_2(\tilde{x}_2-x_0)\cdot\frac{\partial w^*(\tilde{x}_2)}{\partial x}\Big\rangle,\Big\langle w^{(2)}(x_0)\cdot\frac{\partial G_2(\tilde{x}_2-x_0)}{\partial x}\cdot\frac{\partial w^*(\tilde{x}_2)}{\partial x}\Big\rangle.$$

The number of unknowns of rod 2 reduces to five using the previous assumptions and the coupling equations between rod 1 and rod 2:

$$\Big\langle\Big|\frac{\partial w^{(1)}(x_0)}{\partial x}\Big|^2\Big\rangle=\Big\langle\frac{\partial w^{(1)}(x_0)}{\partial x}\Big\rangle\Big\langle\frac{\partial w^{(1)*}(x_0)}{\partial x}\Big\rangle=\Big\langle\Big|\frac{\partial w^{(2)}(x_0)}{\partial x}\Big|^2\Big\rangle,$$
$$\Big\langle\Big|w^{(1)}(x_0)\Big|^2\Big\rangle=\Big\langle w^{(1)}(x_0)\Big\rangle\Big\langle w^{(1)*}(x_0)\Big\rangle=\Big\langle\Big|w^{(1)}(x_0)\Big|^2\Big\rangle,$$
$$\Big\langle w^{(1)}(x_0)\frac{\partial w^{(1)*}(x_0)}{\partial x}\Big\rangle=\Big\langle w^{(1)}(x_0)\Big\rangle\Big\langle\frac{\partial w^{(1)*}(x_0)}{\partial x}\Big\rangle=-\Big(\frac{Y_2S_2}{Y_1S_1}\Big)^*\Big\langle w^{(2)}(x_0)\Big\rangle\Big\langle\frac{\partial w^{(2)*}(x_0)}{\partial x}\Big\rangle;$$

only five unknowns remains:

$$\Big\langle \frac{\partial w^{(2)}(x_0)}{\partial x} \Big\rangle, \Big\langle w^{(2)}(x_0) \Big\rangle,$$
$$\Big\langle \Big| \frac{\partial w(\tilde{x}_2)}{\partial x} \Big|^2 \Big\rangle,$$
$$\Big\langle \frac{\partial w^{(2)}(x_0)}{\partial x} \cdot G_2(\tilde{x}_2 - x_0) \cdot \frac{\partial w^*(\tilde{x}_2)}{\partial x} \Big\rangle, \Big\langle w^{(2)}(x_0) \cdot \frac{\partial G_2(\tilde{x}_2 - x_0)}{\partial x} \cdot \frac{\partial w^*(\tilde{x}_2)}{\partial x} \Big\rangle.$$

Equations of rod 1:

The two equations, (6.37) and (6.38), are obtained getting the expectation of the basic equations, (6.31) and (6.32).

$$\begin{aligned} 0 &= \frac{F_0}{E_1 S_1} G_1(x_1 - x_f) + \Big\langle \frac{\partial w(x_1)}{\partial x} \Big\rangle G_1(x_1 - x_1) \\ &\quad - \Big\langle \frac{\partial w^{(1)}(x_0)}{\partial x} \Big\rangle G_1(x_1 - x_0) + \Big\langle w^{(1)}(x_0) \Big\rangle \frac{\partial G_1(x_1 - x_0)}{\partial x}, \qquad (6.37) \\ 0 &= \frac{F_0}{E_1 S_1} G_1(x_0 - x_f) + \Big\langle \frac{\partial w(x_1)}{\partial x} \Big\rangle G_1(x_0 - x_1) \\ &\quad - \Big\langle \frac{\partial w^{(1)}(x_0)}{\partial x} \Big\rangle G_1(x_0 - x_0) + \Big\langle w^{(1)}(x_0) \Big\rangle \Big(\frac{\partial G_1(x_0 - x_0)}{\partial x} - 1 \Big), \qquad (6.38) \end{aligned}$$

Equations of rod 2:

The first equation (6.39), is obtained by multiplying the first basic equation, (6.33), by the conjugate of $\partial w(\tilde{x}_2)/\partial x$ and getting the expectation with respect to $\tilde{x}_2$ and x_0; while the second and the third equations (6.40) and (6.41) are obtained getting the expectation of the basic equations, (6.33) and (6.34).
The fourth equation (6.42) is obtained by multiplying the conjugate of the first basic equation (6.33) by $\partial w^{(2)}(x_0)/\partial x \cdot G_2(\tilde{x}_2 - x_0)$; while the fifth (6.43) multiplying by $w^{(2)}(x_0) \cdot \partial G_2(\tilde{x}_2 - x_0)/\partial x$ then getting the expectation.

$$\begin{aligned} 0 &= \Big\langle \Big| \frac{\partial w(\tilde{x}_2)}{\partial x} \Big|^2 \Big\rangle G_2(\tilde{x}_2 - \tilde{x}_2) - \Big\langle \frac{\partial w^{(2)}(x_0)}{\partial x} \frac{\partial w^*(\tilde{x}_2)}{\partial x} \, G_2(\tilde{x}_2 - x_0) \Big\rangle \\ &\quad + \Big\langle w^{(2)}(x_0) \frac{\partial w^*(\tilde{x}_2)}{\partial x} \frac{\partial G_2(\tilde{x}_2 - x_0)}{\partial x} \Big\rangle, \qquad (6.39) \\ 0 &= - \Big\langle \frac{\partial w^{(2)}(x_0)}{\partial x} \Big\rangle \Big\langle G_2(\tilde{x}_2 - x_0) \Big\rangle + \Big\langle w^{(2)}(x_0) \Big\rangle \Big\langle \frac{\partial G_2(\tilde{x}_2 - x_0)}{\partial x} \Big\rangle, \qquad (6.40) \\ 0 &= - \Big\langle \frac{\partial w^{(2)}(x_0)}{\partial x} \Big\rangle G_2(x_0 - x_0) + \Big\langle w^{(2)}(x_0) \Big\rangle \Big(\frac{\partial G_2(x_0 - x_0)}{\partial x} - 1 \Big), \qquad (6.41) \\ 0 &= \Big\langle \frac{\partial w^*(\tilde{x}_2)}{\partial x} w^{(2)}(x_0) \frac{\partial G_2(\tilde{x}_2 - x_0)}{\partial x} \Big\rangle \, G_2^*(\tilde{x}_2 - \tilde{x}_2) \\ &\quad - \Big\langle \frac{\partial w^{(2)*}(x_0)}{\partial x} w^{(2)}(x_0) \Big\rangle \Big\langle \frac{\partial G_2(\tilde{x}_2 - x_0)}{\partial x} G_2^*(\tilde{x}_2 - x_0) \Big\rangle \\ &\quad + \Big\langle \Big| w^{(2)}(x_0) \Big|^2 \Big\rangle \Big\langle \Big| \frac{\partial G_2(\tilde{x}_2 - x_0)}{\partial x} \Big|^2 \Big\rangle, \qquad (6.42) \\ 0 &= \Big\langle \frac{\partial w^*(\tilde{x}_2)}{\partial x} \frac{\partial w^{(2)}(x_0)}{\partial x} G_2(\tilde{x}_2 - x_0) \Big\rangle G_2(\tilde{x}_2 - \tilde{x}_2) - \end{aligned}$$

$$\Big\langle \Big| \frac{\partial w^{(2)}(x_0)}{\partial x} \Big|^2 \Big\rangle \Big\langle \Big| G_2(\tilde{x}_2 - x_0) \Big|^2 \Big\rangle + \Big\langle w^{(2)*}(x_0) \frac{\partial w^{(2)}(x_0)}{\partial x} \Big\rangle \Big\langle G_2(\tilde{x}_2 - x_0) \frac{\partial G_2^*(\tilde{x}_2 - x_0)}{\partial x} \Big\rangle. \tag{6.43}$$

Coupling equations:

$$\Big\langle w^{(1)}(x_0) \Big\rangle = -\Big\langle w^{(2)}(x_0) \Big\rangle \tag{6.44}$$

$$Y_1 S_1 \Big\langle \frac{\partial w^{(1)}(x_0)}{\partial x} \Big\rangle = Y_2 S_2 \Big\langle \frac{\partial w^{(2)}(x_0)}{\partial x} \Big\rangle \tag{6.45}$$

$$\Big(Y_1 S_1 \Big)^* \Big\langle w^{(1)}(x_0) \frac{\partial w^{(1)*}(x_0)}{\partial x} \Big\rangle = -\Big(Y_2 S_2 \Big)^* \Big\langle w^{(2)}(x_0) \frac{\partial w^{(2)*}(x_0)}{\partial x} \Big\rangle \tag{6.46}$$

$$\Big\langle \Big| w^{(1)}(x_0) \Big|^2 \Big\rangle = \Big\langle \Big| w^{(1)}(x_0) \Big|^2 \Big\rangle \tag{6.47}$$

$$\Big| Y_1 S_1 \Big|^2 \Big\langle \Big| \frac{\partial w^{(1)}(x_0)}{\partial x} \Big|^2 \Big\rangle = \Big| Y_2 S_2 \Big|^2 \Big\langle \Big| \frac{\partial w^{(2)}(x_0)}{\partial x} \Big|^2 \Big\rangle \tag{6.48}$$

$$Y_1 S_1 \Big\langle w^{(1)*}(x_0) \frac{\partial w^{(1)}(x_0)}{\partial x} \Big\rangle = -Y_2 S_2 \Big\langle w^{(2)*}(x_0) \frac{\partial w^{(2)}(x_0)}{\partial x} \Big\rangle \tag{6.49}$$

Solving the problem

System solution:

The system of equations made up by the equation of rod 1, rod 2 and the coupling equations is solved the same way as explained in SIF 2 rods paragraph.
First is solved the first order moments system using equations (6.37), (6.38), (6.41), (6.44) and (6.45); for the first order solution the third and not the second equation of rod 2 is used, because it's necessary to use the equation which refers to the point in which we want to evaluate the unknowns, x_0 in this configuration.
Then is possible to solve the second order equation of rod 2, equations (6.39), (6.42), (6.43).

6.3.2 BEM-SIF two coupled rods with mid-frequency assumptions: results

- Configuration n.1
  Two different behavior rods are considered, rod 1, the excited one, is typically low frequency because is stiff and short, while rod 2 is typically high frequency because is thin, long and flexible. Also different physical properties characterize the two rods in terms of flexibility and damping. Randomness on x_2 is the only random parameter, $\sigma_2 = 0.05$.
  The physical properties of configuration n.1 are reported in table 6.4 and results SOM in figures 6.11 and 6.12.

	length [m]	x_f [m]	E [N/m^2]	S [m^2]	η [%]	ρ [kg/m^3]
Rod 1	1.80	0.65	$2.1 \cdot 10^{11}$	10^{-4}	1	7800
Rod 2	6.50		$2.1 \cdot 10^{10}$	10^{-5}	1	7800

Table 6.4: BEM-SIF two coupled rods with mid-frequency assumptions. Parameters of the two rods. Configuration n.1

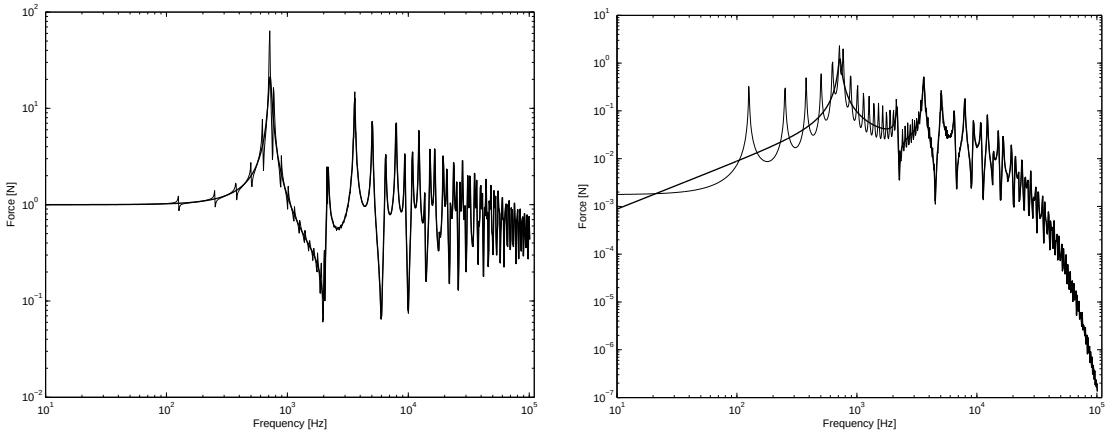

(a) (b)

Figure 6.11: BEM-SIF two coupled rods with mid-frequency assumptions. Frequency evolution of the modulus of the second order moment, traction at x_1 (a) and $\tilde{x}_2$ (b). Configuration n.1. —— BEM-SIF —— BEM

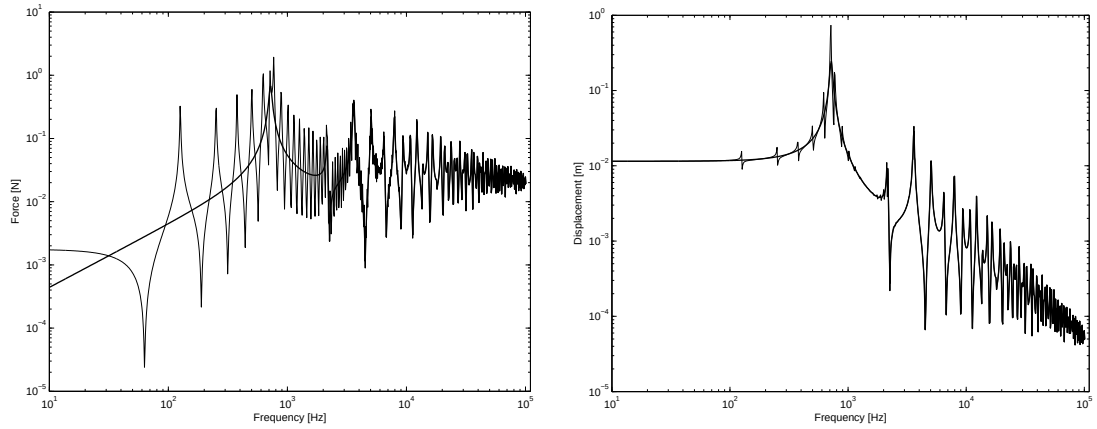

(a) (b)

Figure 6.12: BEM-SIF two coupled rods with mid-frequency assumptions. Frequency evolution of the modulus of the second order moment, traction (a) and displacement (b) at x_0. Configuration n.1. —— BEM-SIF —— BEM

- Configuration n.2
  In this configuration the difference in the vibrational behavior of the two rods is much more evident, in terms of flexibility and randomness, than configuration n.1. Randomness on x_2 is the only random parameter, $\sigma_2 = 0.2$.
  The physical properties of configuration n.2 are reported in table 6.5 and results SOM in figures 6.13 and 6.14.

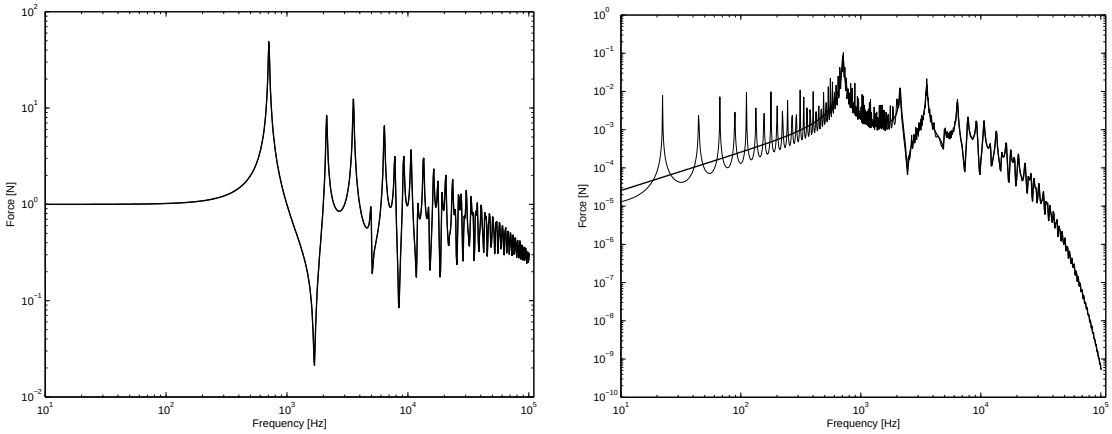

(a) (b)

Figure 6.13: BEM-SIF two coupled rods with mid-frequency assumptions. Frequency evolution of the modulus of the second order moment, traction at x_1 (a) and $\tilde{x}_2$ (b). Configuration n.2. —— BEM-SIF BEM

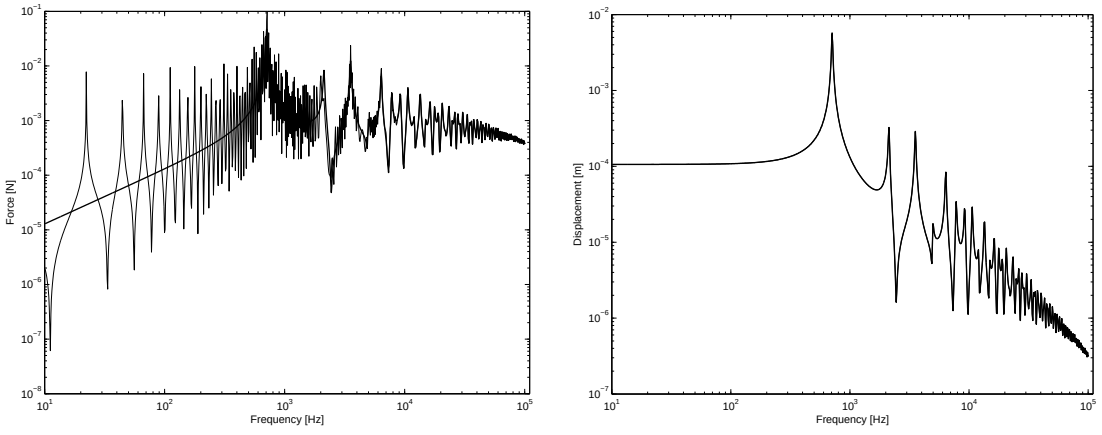

(a) (b)

Figure 6.14: BEM-SIF two coupled rods with mid-frequency assumptions. Frequency evolution of the modulus of the second order moment, traction (a) and displacement (b) at x_0. Configuration n.2. —— BEM-SIF BEM

	length [m]	x_f [m]	E [N/m^2]	S [m^2]	η [%]	ρ [kg/m^3]
Rod 1	1.83	0.77	$2.1 \cdot 10^{11}$	10^{-3}	2	7800
Rod 2	11.65		$2.1 \cdot 10^{9}$	10^{-5}	0.2	7800

Table 6.5: BEM-SIF two coupled rods with mid-frequency assumptions. Parameters of the two rods. Configuration n.2

- Configuration n.3
  This configuration is not a mid-frequency configuration, the rods have more or less the same vibro-acoustical behavior, and it is presented only to show that the simplifications of the formulation are licit only for a mid-frequency structure. The modified SIF formulation for the mid-frequency range is no more flexible as before. The physical properties of configuration n.3 are reported in table 6.6 and results SOM in figures 6.15 and 6.16.

	length [m]	x_f [m]	E [N/m^2]	S [m^2]	η [%]	ρ [kg/m^3]
Rod 1	9.53	6.78	$2.1 \cdot 10^{11}$	10^{-5}	2	7800
Rod 2	7.66		$2.1 \cdot 10^{11}$	10^{-5}	2	7800

Table 6.6: BEM-SIF two coupled rods with mid-frequency assumptions. Parameters of the two rods. Configuration n.3

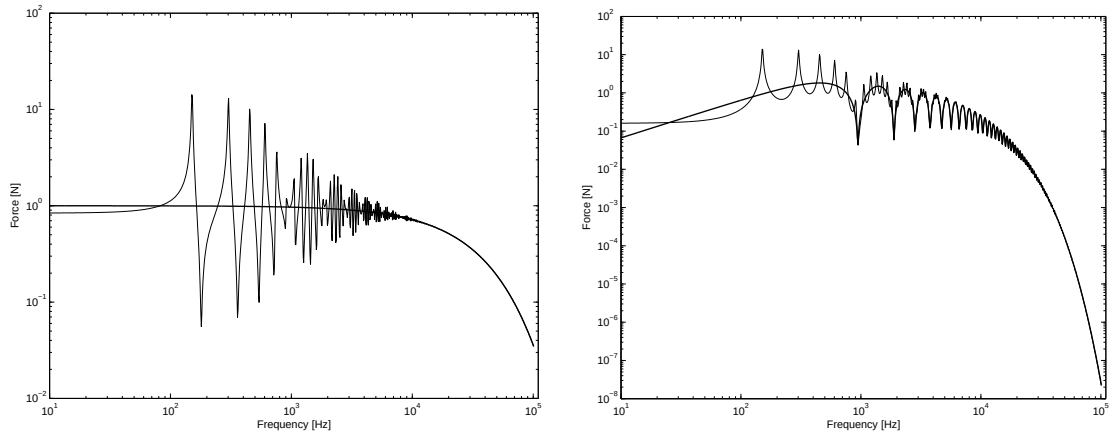

(a) (b)

Figure 6.15: BEM-SIF two coupled rods with mid-frequency assumptions. Frequency evolution of the modulus of the second order moment, traction at x_1 (a) and $\tilde{x}_2$ (b). Configuration n.3. —— BEM-SIF —— BEM

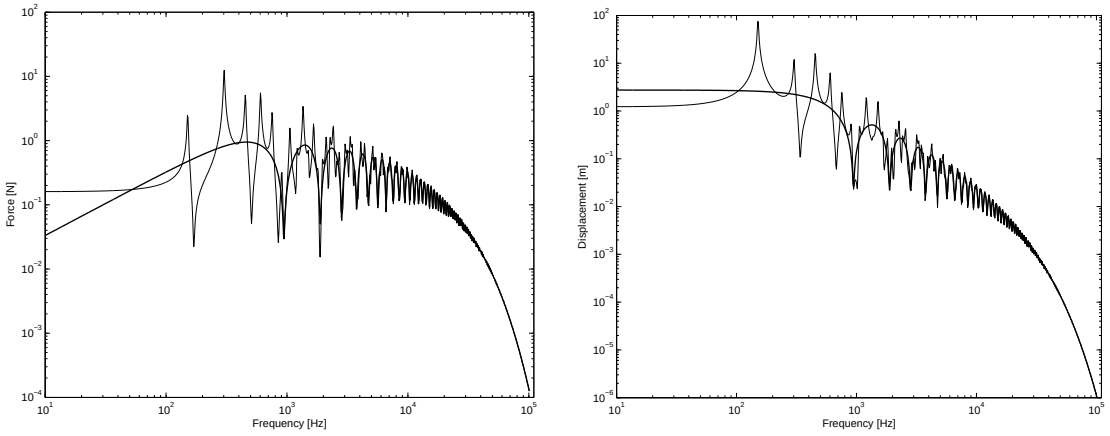

(a) (b)

Figure 6.16: BEM-SIF two coupled rods with mid-frequency assumptions. Frequency evolution of the modulus of the second order moment, traction (a) and displacement (b) at x_0. Configuration n.3. —— BEM-SIF —— BEM

6.3.3 Discussion

The results obtained with this BEM-SIF formulation with mid-frequency assumptions are very good. The formulation works perfectly with configurations corresponding to the requirements introduced with the assumption, but, as it is reported in configuration n.3 results, it doesn't work in configurations different from the required one, so it is no more general as complete SIF formulation.
The curves follows the deterministic behavior of rod 1 in the low frequency range, then there is a transition behavior in the mid-frequency range with a smoothing effect of the modes of rod 2, forward there is the high frequency range behavior which is ruled by the deterministic behavior of rod 1 because that rod is supposed to be low frequency behavior in the whole frequency range.
The number of variables for the BEM-SIF application is equal to 12, so we have a reduction of 7 unknowns respect to complete SIF thanks to the deterministic description of rod 1. The reduction of unknowns is relevant compared to the complete SIF formulation, because we do not need a SOM description of rod 1. We will see in next section, 6.4 that the FOM description is effective for rod 1 if the excitation is located on rod 1 itself, so when the excitation is on the short member, otherwise some difficulties arise and a new approach for the deterministic parts is required, sec. 6.5.

6.4 BEM-SIF application: two coupled rods with mid-frequency assumptions with different rod properties

The classical structure made of two coupled ords is used in this section, but differently from previous cases the excitation is now applied on the long member, on the high frequency rod, rod 2, fig. 6.17.

Rod 1 is considered to be deterministic, so it's boundaries are x_1 and x_0, while Rod 2 is considered to be statistic, so boundary $\tilde{x}_2$ is characterized by a deterministic value x_2 plus a gaussian zero mean random part ε_2. Rod 2 is the excited one, so $\tilde{x}_f$, the excitation

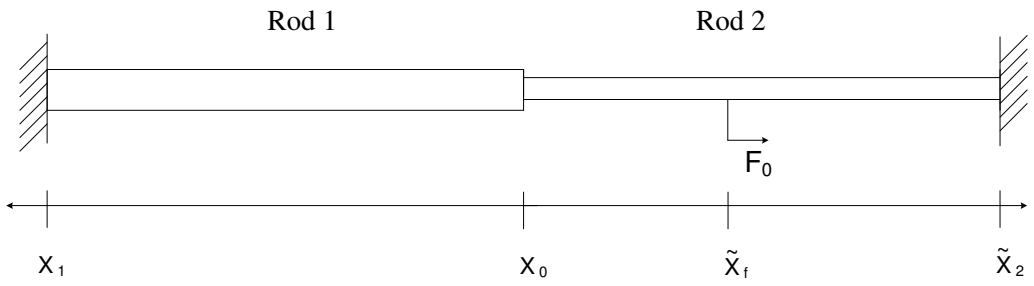

Figure 6.17: BEM-SIF formulation. Two coupled rods structure, rod 1 is low-frequency, rod 2 is high frequency behaving. The excitation F_0 is applied on rod 2.

point, is affected from randomness.
The BEM-SIF formulation used in this section is obtained the same way than the one in the previous section: rod 1 is modelled using first order moments, while rod 2 is modelled using only second order moments.

6.4.1 BEM-SIF application with mid-frequency assumptions and different rod properties: results

- Configuration n.1
  Two different behaving rods are considered: rod 1, the excited one, is typically low frequency because it is stiff and short, while rod 2 is typically high frequency because it is thin, long and flexible. Also different physical properties characterize the two rods in terms of flexibility and damping. x_2 and x_f are random parameter, $\sigma_2 = \sigma_f = 0.05$.
  The physical properties of configuration n.1 are reported in table 6.7 and the results of SOM in figures 6.18 and 6.19.

	length [m]	x_f [m]	E [N/m^2]	S [m^2]	η [%]	ρ [kg/m^3]
Rod 1	1.13		$2.1 \cdot 10^{11}$	10^{-4}	1	7800
Rod 2	8.64	4.96	$2.1 \cdot 10^{10}$	10^{-5}	1	7800

Table 6.7: BEM-SIF two coupled rods with mid-frequency assumptions with different rod properties. Parameters of the two rods. Configuration n.1

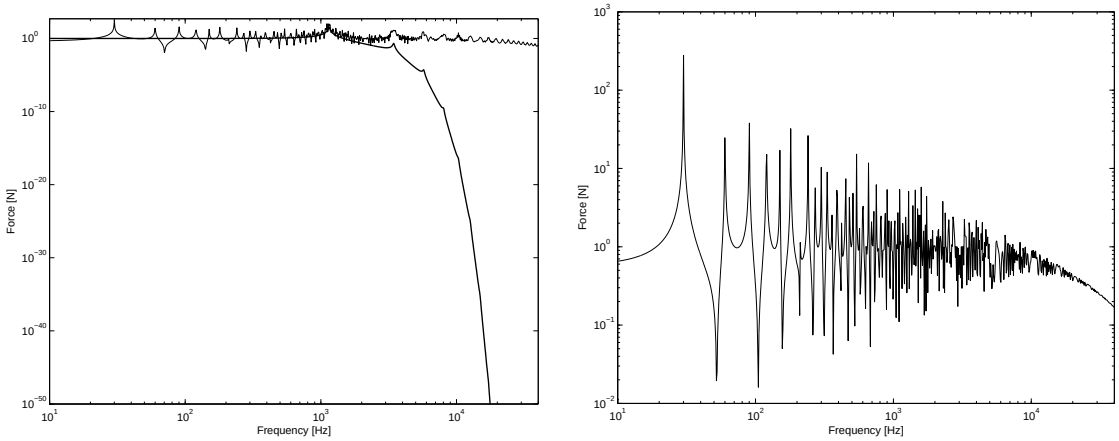

(a) (b)

Figure 6.18: BEM-SIF two coupled rods with mid-frequency assumptions with different rod properties. Frequency evolution of the traction at x_1 (a) and $\tilde{x}_2$ (b). Configuration n.1. —— BEM-SIF —— BEM

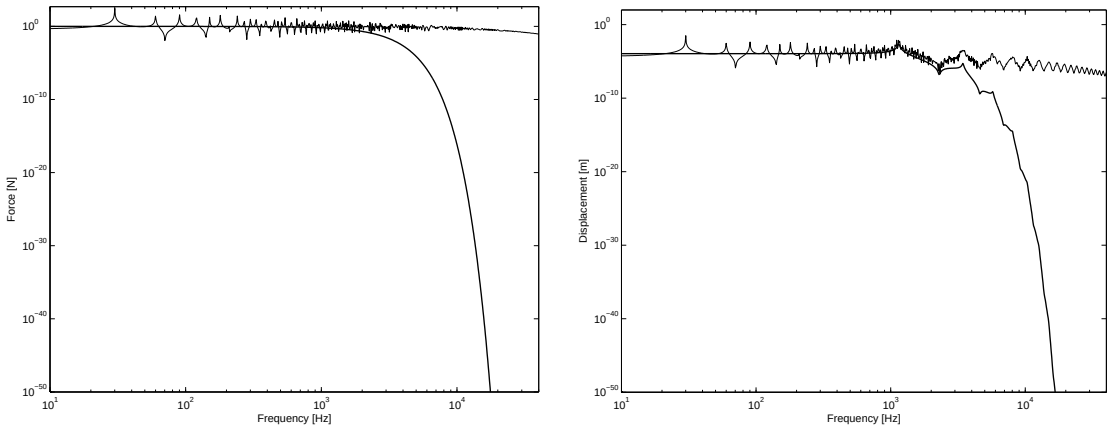

(a) (b)

Figure 6.19: BEM-SIF two coupled rods with mid-frequency assumptions with different rod properties. Frequency evolution of the traction (a) and displacement (b) at $\tilde{x}_0$. Configuration n.1. —— BEM-SIF —— BEM

- Configuration n.2
  The configuration of the rods is exactly the same than configuration n.1, but randomness is actually applied only at the location of the external force, $\sigma_f = 0.05$, $\sigma_2 = 0.00$. The physical properties of configuration n.2 are reported in table 6.8 and results SOM in figures 6.20 and 6.21.

	length [m]	x_f [m]	E [N/m^2]	S [m^2]	η [%]	ρ [kg/m^3]
Rod 1	1.83		$2.1 \cdot 10^{11}$	10^{-3}	2	7800
Rod 2	11.65	6.77	$2.1 \cdot 10^{9}$	10^{-5}	0.2	7800

Table 6.8: BEM-SIF two coupled rods with mid-frequency assumptions with different rod properties. Parameters of the two rods. Configuration n.2

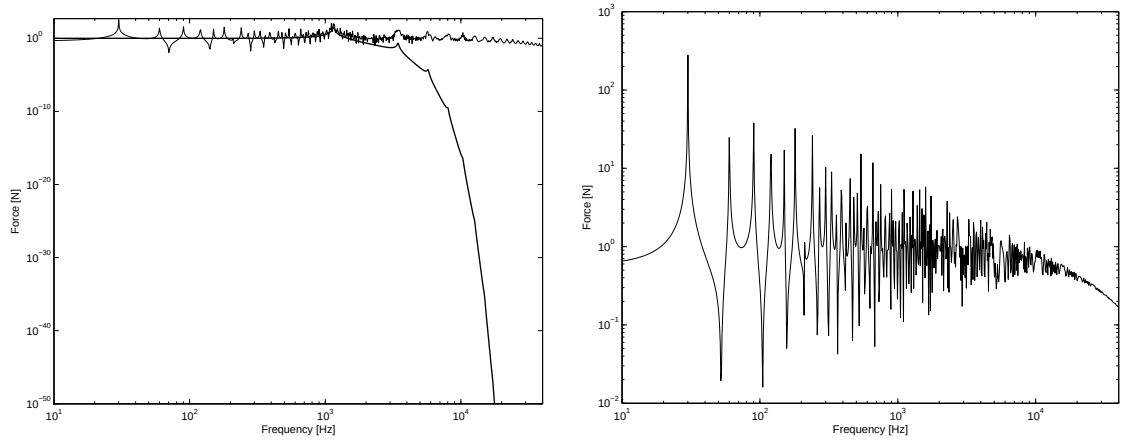

(a) (b)

Figure 6.20: BEM-SIF two coupled rods with mid-frequency assumptions with different rod properties. Frequency evolution of the traction at x_1 (a) and $\tilde{x}_2$ (b). Configuration n.2. —— BEM-SIF —— BEM

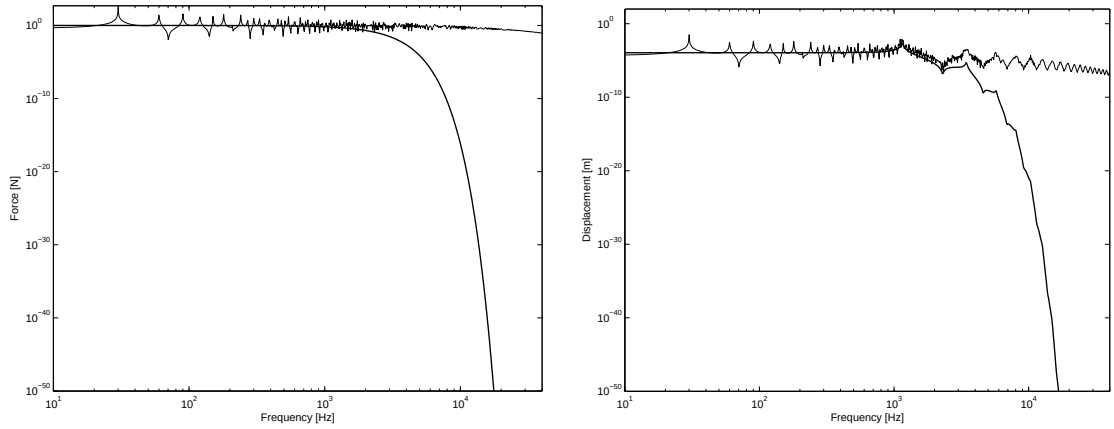

(a) (b)

Figure 6.21: BEM-SIF two coupled rods with mid-frequency assumptions with different rod properties. Frequency evolution of the traction (a) and displacement (b) at $\tilde{x}_0$. Configuration n.2. —— BEM-SIF —— BEM

- Configuration n.3
  The configuration of the rods is exactly the same than configuration n.1 and n.2,

but randomness is actually applied only at boundary x_2, $\sigma_f = 0.00$, $\sigma_2 = 0.05$. The physical properties of configuration n.3 are reported in table 6.9 and the results of SOM in figures 6.22 and 6.23.

	length [m]	x_f [m]	E [N/m^2]	S [m^2]	η [%]	ρ [kg/m^3]
Rod 1	1.83		$2.1 \cdot 10^{11}$	10^{-3}	2	7800
Rod 2	11.65	6.77	$2.1 \cdot 10^{9}$	10^{-5}	0.2	7800

Table 6.9: BEM-SIF two coupled rods with mid-frequency assumptions with different rod properties. Parameters of the two rods. Configuration n.3

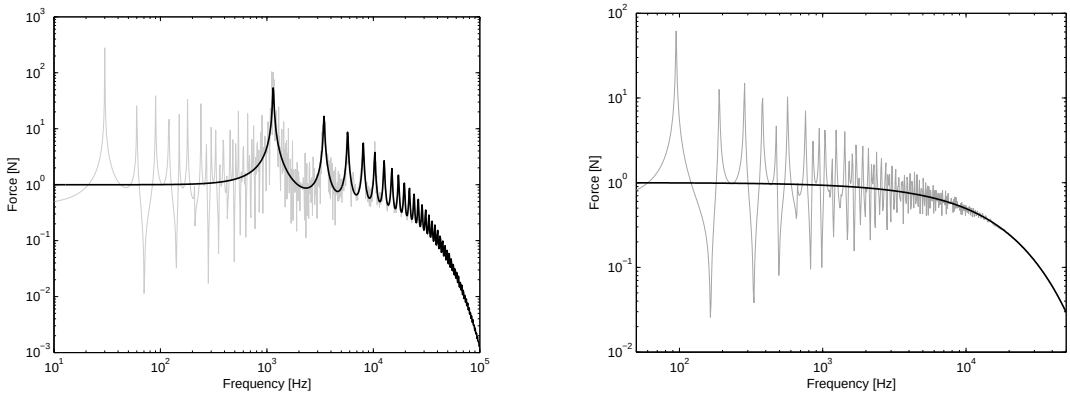

(a) (b)

Figure 6.22: BEM-SIF two coupled rods with mid-frequency assumptions with different rod properties. Frequency evolution of the traction at x_1 (a) and $\tilde{x}_2$ (b). Configuration n.3. —— BEM-SIF —— BEM

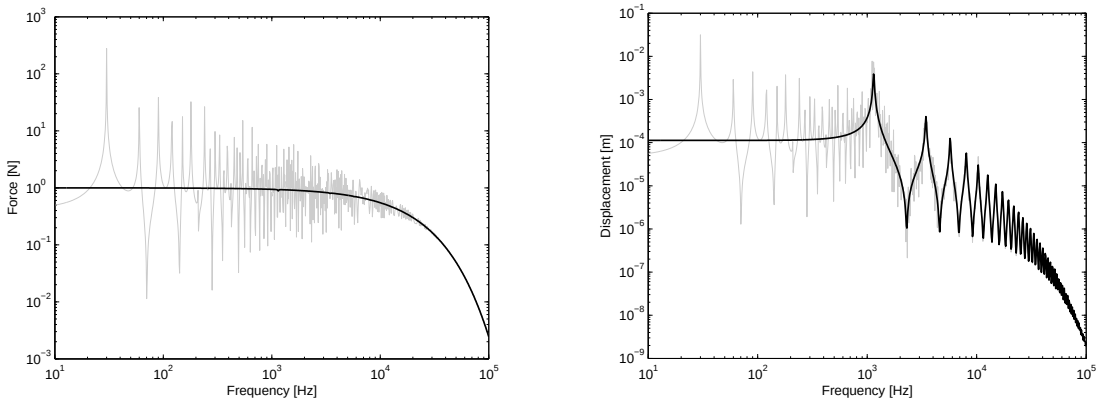

(a) (b)

Figure 6.23: BEM-SIF two coupled rods with mid-frequency assumptions with different rod properties. Frequency evolution of the traction (a) and displacement (b) at $\tilde{x}_0$. Configuration n.3. —— BEM-SIF —— BEM

6.4.2 Discussion

These numerical applications were performed in order to investigate the capability of BEM-SIF and SIF formulations to simulate the behavior of complex structure in different configurations from the general one reported in section 5.3.4. As we can see from the previous results, in the configuration in which rod 2, the random one, is excited, BEM-SIF and complete SIF are able to correctly model the response of the system only in configuration n.3, in which there is an unique random boundary $\tilde{x}_2$, the farthest one from the deterministic rod. While in configuration n.1 and n.2, in which there is a randomness at $\tilde{x}_f$, the curves presents an "irregular" smoothing effect in the mid-high frequency range even for the peaks belonging to the deterministic rod.
As a consequence of that in configurations n.1 and 2, where the deterministic description of rod 1 it is not correct and effective, it is no possible to evaluate the response at $\tilde{x}_2$, which instead can be calculated in configuration n.3.

We can conclude that when dealing with a mid-frequency system we need to account very carefully for the excitation contributions. When the excitation is located on a deterministic subsystem, the primary source contributions are deterministic terms and can be easily treated as FOM, thus a BEM-SIF formulation is suitable for this purpose. Instead, when dealing with a structure which is excited on long members, we can't account for the deterministic contributions only with FOM. We need to model differently the deterministic parts of the structure in terms of correlation among unknowns, otherwise we lose the deterministic modal contributions.

6.5 Deterministic-SIF theory and correct formulation

In this section, a deterministic-SIF formulation will be developed. We want to obtain a formulation which is consistent in the case of excitation on the short member but also if the excitation is applied on the long member. The deterministic system needs to be properly described by means of correlation relationships among its unknowns. Let's consider the two rod system with the force applied on the random rod, fig. 6.24:

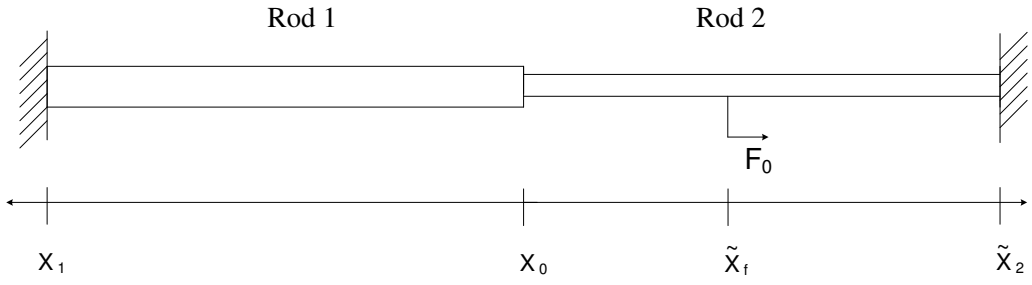

Figure 6.24: BEM-SIF formulation. Two coupled rods structure, rod 1 is low-frequency, rod 2 is high frequency behaving. The excitation F_0 is applied on rod 2.

With an image source approximation, considering only the direct field term, we can write that:

$$w(x_0) = \frac{F_0}{Y_2 S_2} G_2(x_0 - \tilde{x}_f) \tag{6.50}$$

In x_1 we have:

$$w(x_1) = \frac{F_0}{Y_2 S_2} G_2(x_0 - \tilde{x}_f) G_1(x_0 - x_1) = w(x_0) G_1(x_0 - x_1), \tag{6.51}$$

so, getting the expectations:

$$\langle w(x_1) \rangle = \langle w(x_0) G_1(x_0 - x_1) \rangle = \langle w(x_0) \rangle G_1(x_0 - x_1). \tag{6.52}$$

$G_1(x_0 - x_1)$ is a deterministic term so we can say that $w(x_1)$ and $w(x_0)$ are correlated, therefore it is not possible to write:

$$\langle w^*(x_0) w(x_1) \rangle = \langle w^*(x_0) \rangle \langle w(x_1) \rangle, \tag{6.53}$$

so in the second order equations of a deterministic rod it's necessary to keep all the cross correlations.

The assumptions of SIF theory remain valid also in a deterministic-random configuration for the random rod; for the deterministic rod, the deterministic boundaries are correlated each other. The amplitude term of a secondary source is correlated with the other amplitude terms of the deterministic rod, while it is not correlated with the propagative terms because they are deterministic.

The results with the random rod excited and the randomness applied at the excitation point are very important. As we have seen in the previous results, figures 6.20 and 6.21, all the first order moments go to zero so it is no more possible to characterize the deterministic rod behavior with only the first order moments, it is necessary to write the second order equations with all the cross correlations.

6.5.1 Deterministic-SIF theory and correct formulation: deriving the equations

BEM random equations:
Rod 1:

$$\begin{aligned} 0 &= \frac{\partial w(x_1)}{\partial x} G_1(x_1 - x_1) - \frac{\partial w^{(1)}(x_0)}{\partial x} G_1(x_1 - x_0) \\ &\quad + w^{(1)}(x_0) \frac{\partial G_1(x_1 - x_0)}{\partial x} \end{aligned} \tag{6.54}$$

$$\begin{aligned} 0 &= \frac{\partial w(x_1)}{\partial x} G_1(x_0 - x_1) - \frac{\partial w^{(1)}(x_0)}{\partial x} G_1(x_0 - x_0) \\ &\quad + w^{(1)}(x_0) \Big(\frac{\partial G_1(x_0 - x_0)}{\partial x} - 1 \Big) \end{aligned} \tag{6.55}$$

Rod 2:

$$0 = \frac{F_0}{Y_2 S_2} G_2(\tilde{x}_2 - \tilde{x}_f) + \frac{\partial w(\tilde{x}_2)}{\partial x} G_2(\tilde{x}_2 - \tilde{x}_2)$$

$$-\frac{\partial w^{(2)}(x_0)}{\partial x}G_2(\tilde{x}_2-x_0)+w^{(2)}(x_0)\frac{\partial G_2(\tilde{x}_2-x_0)}{\partial x} \tag{6.56}$$

$$\begin{aligned}0 &= \frac{F_0}{Y_2S_2}G_2(x_0-\tilde{x}_f)+\frac{\partial w(\tilde{x}_2)}{\partial x}G_2(x_0-\tilde{x}_2)\\ &\quad -\frac{\partial w^{(2)}(x_0)}{\partial x}G_2(x_0-x_0)+w^{(2)}(x_0)\Big(\frac{\partial G_2(x_0-x_0)}{\partial x}-1\Big)\end{aligned} \tag{6.57}$$

First order equations:
Rod 1:

$$\begin{aligned}0 &= \Big\langle\frac{\partial w(x_1)}{\partial x}\Big\rangle G_1(x_1-x_1)-\Big\langle\frac{\partial w^{(1)}(x_0)}{\partial x}\Big\rangle G_1(x_1-x_0)\\ &\quad +\Big\langle w^{(1)}(x_0)\Big\rangle\frac{\partial G_1(x_1-x_0)}{\partial x}\end{aligned} \tag{6.58}$$

$$\begin{aligned}0 &= \Big\langle\frac{\partial w(x_1)}{\partial x}\Big\rangle G_1(x_0-x_1)-\Big\langle\frac{\partial w^{(1)}(x_0)}{\partial x}\Big\rangle G_1(x_0-x_0)\\ &\quad +\Big\langle w^{(1)}(x_0)\Big\rangle\Big(\frac{\partial G_1(x_0-x_0)}{\partial x}-1\Big)\end{aligned} \tag{6.59}$$

Rod 2:

$$\begin{aligned}0 &= \frac{F_0}{Y_2S_2}\Big\langle G_2(\tilde{x}_2-\tilde{x}_f)\Big\rangle+\Big\langle\frac{\partial w(\tilde{x}_2)}{\partial x}\Big\rangle G_2(\tilde{x}_2-\tilde{x}_2)\\ &\quad -\Big\langle\frac{\partial w^{(2)}(x_0)}{\partial x}\Big\rangle\Big\langle G_2(\tilde{x}_2-x_0)\Big\rangle+\Big\langle w^{(2)}(x_0)\Big\rangle\Big\langle\frac{\partial G_2(\tilde{x}_2-x_0)}{\partial x}\Big\rangle\end{aligned} \tag{6.60}$$

$$\begin{aligned}0 &= \frac{F_0}{Y_2S_2}\Big\langle G_2(x_0-\tilde{x}_f)\Big\rangle+\Big\langle\frac{\partial w(\tilde{x}_2)}{\partial x}\Big\rangle\Big\langle G_2(x_0-\tilde{x}_2)\Big\rangle\\ &\quad -\Big\langle\frac{\partial w^{(2)}(x_0)}{\partial x}\Big\rangle G_2(x_0-x_0)+\Big\langle w^{(2)}(x_0)\Big\rangle\Big(\frac{\partial G_2(x_0-x_0)}{\partial x}-1\Big)\end{aligned} \tag{6.61}$$

As we can see from the results, when a randomness is applied on the excitation point on the random rod, $\tilde{x}_f$, all the first order moments of both rods go to zero very rapidly, so in the second order moment equations they can be neglected.

List of the unknowns

Rod 1 (12 unknowns)

$$\Big\langle\Big|\frac{\partial w(x_1)}{\partial x}\Big|^2\Big\rangle,\Big\langle\Big|\frac{\partial w^{(1)}(x_0)}{\partial x}\Big|^2\Big\rangle,\Big\langle\Big|w^{(1)}(x_0)\Big|^2\Big\rangle,$$
$$\Big\langle w^{(1)}(x_0)\cdot\frac{\partial w^{(1)*}(x_0)}{\partial x}\Big\rangle,\Big\langle w^{(1)*}(x_0)\cdot\frac{\partial w^{(1)}(x_0)}{\partial x}\Big\rangle,$$
$$\Big\langle w^{(1)}(x_0)\cdot\frac{\partial w^{*}(x_1)}{\partial x}\Big\rangle,\Big\langle w^{(1)*}(x_0)\cdot\frac{\partial w(x_1)}{\partial x}\Big\rangle,$$
$$\Big\langle\frac{\partial w^{(1)}(x_0)}{\partial x}\cdot\frac{\partial w^{*}(x_1)}{\partial x}\Big\rangle,\Big\langle\frac{\partial w^{(1)*}(x_0)}{\partial x}\cdot\frac{\partial w(x_1)}{\partial x}\Big\rangle.$$

Rod 2 (11 unknowns)

$$\Big\langle\Big|\frac{\partial w(\tilde{x}_2)}{\partial x}\Big|^2\Big\rangle, \Big\langle\Big|\frac{\partial w^{(2)}(x_0)}{\partial x}\Big|^2\Big\rangle, \Big\langle\Big|w^{(2)}(x_0)\Big|^2\Big\rangle,$$
$$\Big\langle w^{(2)}(x_0)\cdot\frac{\partial w^{(2)*}(x_0)}{\partial x}\Big\rangle, \Big\langle w^{(2)*}(x_0)\cdot\frac{\partial w^{(2)}(x_0)}{\partial x}\Big\rangle,$$
$$\Big\langle\frac{\partial w^*(\tilde{x}_2)}{\partial x}\cdot G_2(\tilde{x}_2-\tilde{x}_f)\Big\rangle, \Big\langle\frac{\partial w^{(2)*}(x_0)}{\partial x}\cdot G_2(x_0-\tilde{x}_f)\Big\rangle, \Big\langle w^{(2)*}(x_0)\cdot G_2(x_0-\tilde{x}_f)\Big\rangle$$

Second order equations of Rod 1:

$$\begin{aligned}
0 &= \Big\langle\Big|\frac{\partial w(x_1)}{\partial x}\Big|^2\Big\rangle G_1(x_1-x_1) - \Big\langle\frac{\partial w^{(1)}(x_0)}{\partial x}\cdot\frac{\partial w^*(x_1)}{\partial x}\Big\rangle G_1(x_1-x_0) \\
&\quad + \Big\langle w^{(1)}(x_0)\cdot\frac{\partial w^*(x_1)}{\partial x}\Big\rangle\frac{\partial G_1(x_1-x_0)}{\partial x}, \qquad (6.62)\\
0 &= \Big\langle\frac{\partial w(x_1)}{\partial x}\cdot\frac{\partial w^{(1)*}(x_0)}{\partial x}\Big\rangle G_1(x_0-x_1) - \Big\langle\Big|\frac{\partial w^{(1)}(x_0)}{\partial x}\Big|^2\Big\rangle G_1(x_0-x_0) \\
&\quad + \Big\langle w^{(1)}(x_0)\cdot\frac{\partial w^{(1)*}(x_0)}{\partial x}\Big\rangle\Big(\frac{\partial G_1(x_0-x_0)}{\partial x}-1\Big), \qquad (6.63)\\
0 &= \Big\langle\frac{\partial w(x_1)}{\partial x}\cdot w^{(1)*}(x_0)\Big\rangle G_1(x_0-x_1) - \Big\langle\frac{\partial w^{(1)}(x_0)}{\partial x}\cdot w^{(1)*}(x_0)\Big\rangle G_1(x_0-x_0) \\
&\quad + \Big\langle\Big|w^{(1)}(x_0)\Big|^2\Big\rangle\Big(\frac{\partial G_1(x_0-x_0)}{\partial x}-1\Big), \qquad (6.64)\\
0 &= \Big\langle\frac{\partial w^*(x_1)}{\partial x}\cdot\frac{\partial w^{(1)}(x_0)}{\partial x}\Big\rangle G_1(x_1-x_0)G_1^*(x_1-x_1) \\
&\quad - \Big\langle\Big|\frac{\partial w^{(1)}(x_0)}{\partial x}\Big|^2\Big\rangle\Big|G_1(x_1-x_0)\Big|^2 \\
&\quad + \Big\langle w^{(1)*}(x_0)\cdot\frac{\partial w^{(1)}(x_0)}{\partial x}\Big\rangle G_1(x_1-x_0)\frac{\partial G_1^*(x_1-x_0)}{\partial x}, \qquad (6.65)\\
0 &= \Big\langle\frac{\partial w^*(x_1)}{\partial x}\cdot w^{(1)}(x_0)\Big\rangle\frac{\partial G_1(x_1-x_0)}{\partial x}G_1^*(x_1-x_1) \\
&\quad - \Big\langle\frac{\partial w^{(1)*}(x_0)}{\partial x}\cdot w^{(1)}(x_0)\Big\rangle\frac{\partial G_1(x_1-x_0)}{\partial x}G_1^*(x_1-x_0) \\
&\quad + \Big\langle\Big|w^{(1)}(x_0)\Big|^2\Big\rangle\Big|\frac{\partial G_1(x_1-x_0)}{\partial x}\Big|^2. \qquad (6.66)
\end{aligned}$$

Second order equations of Rod 2:

$$\begin{aligned}
0 &= \frac{F_0}{Y_2S_2}\Big\langle\frac{\partial w^*(\tilde{x}_2)}{\partial x}G_2(\tilde{x}_2-\tilde{x}_f)\Big\rangle + \Big\langle\Big|\frac{\partial w(\tilde{x}_2)}{\partial x}\Big|^2\Big\rangle G_2(\tilde{x}_2-\tilde{x}_2), \qquad (6.67)\\
0 &= \frac{F_0}{Y_2S_2}\Big\langle\frac{\partial w^{(2)*}(x_0)}{\partial x}G_2(x_0-\tilde{x}_f)\Big\rangle - \Big\langle\Big|\frac{\partial w^{(2)}(x_0)}{\partial x}\Big|^2\Big\rangle G_2(x_0-x_0) \\
&\quad + \Big\langle w^{(2)}(x_0)\frac{\partial w^{(2)*}(x_0)}{\partial x}\Big\rangle\Big(\frac{\partial G_2(x_0-x_0)}{\partial x}-1\Big), \qquad (6.68)\\
0 &= \frac{F_0}{Y_2S_2}\Big\langle w^{(2)*}(x_0)G_2(x_0-\tilde{x}_f)\Big\rangle - \Big\langle\frac{\partial w^{(2)}(x_0)}{\partial x}w^{(2)*}(x_0)\Big\rangle G_2(x_0-x_0) \\
&\quad + \Big\langle\Big|w^{(2)}(x_0)\Big|^2\Big\rangle\Big(\frac{\partial G_2(x_0-x_0)}{\partial x}-1\Big), \qquad (6.69)\\
0 &= \Big(\frac{F_0}{Y_2S_2}\Big)^*\Big\langle\Big|G_2(\tilde{x}_2-\tilde{x}_f)\Big|^2\Big\rangle
\end{aligned}$$

$$+\Big\langle \frac{\partial w^*(\tilde{x}_2)}{\partial x} G_2(\tilde{x}_2 - \tilde{x}_f)\Big\rangle G_2^*(\tilde{x}_2 - \tilde{x}_2), \tag{6.70}$$

$$0 = \Big(\frac{F_0}{Y_2 S_2}\Big)^* \Big\langle \Big| G_2(x_0 - \tilde{x}_f)\Big|^2 \Big\rangle - \Big\langle \frac{\partial w^{(2)*}(x_0)}{\partial x} G_2(x_0 - \tilde{x}_f)\Big\rangle G_2^*(x_0 - x_0)$$
$$+\Big\langle w^{(2)*}(x_0) G_2(x_0 - \tilde{x}_f)\Big\rangle \Big(\frac{\partial G_2^*(x_0 - x_0)}{\partial x} - 1\Big). \tag{6.71}$$

Conjugate equations of Rod 1:

$$0 = \Big\langle \Big|\frac{\partial w(x_1)}{\partial x}\Big|^2 \Big\rangle G_1^*(x_1 - x_1) - \Big\langle \frac{\partial w^{(1)*}(x_0)}{\partial x} \cdot \frac{\partial w(x_1)}{\partial x}\Big\rangle G_1^*(x_1 - x_0)$$
$$+\Big\langle w^{(1)*}(x_0) \cdot \frac{\partial w(x_1)}{\partial x}\Big\rangle \frac{\partial G_1^*(x_1 - x_0)}{\partial x}, \tag{6.72}$$

$$0 = \Big\langle \frac{\partial w^*(x_1)}{\partial x} \cdot \frac{\partial w^{(1)}(x_0)}{\partial x}\Big\rangle G_1^*(x_0 - x_1) - \Big\langle \Big|\frac{\partial w^{(1)}(x_0)}{\partial x}\Big|^2 \Big\rangle G_1^*(x_0 - x_0)$$
$$+\Big\langle w^{(1)*}(x_0) \cdot \frac{\partial w^{(1)}(x_0)}{\partial x}\Big\rangle \Big(\frac{\partial G_1(x_0 - x_0)}{\partial x} - 1\Big)^*, \tag{6.73}$$

$$0 = \Big\langle \frac{\partial w^*(x_1)}{\partial x} \cdot w^{(1)}(x_0)\Big\rangle G_1^*(x_0 - x_1) - \Big\langle \frac{\partial w^{(1)*}(x_0)}{\partial x} \cdot w^{(1)}(x_0)\Big\rangle G_1^*(x_0 - x_0)$$
$$+\Big\langle \Big|w^{(1)}(x_0)\Big|^2 \Big\rangle \Big(\frac{\partial G_1(x_0 - x_0)}{\partial x} - 1\Big)^*. \tag{6.74}$$

6.5.2 Deterministic-SIF theory and correct formulation: results

Rod 1 is considered to be deterministic, so its boundaries are x_1 and x_0, while rod 2 is considered to be statistic, so boundary $\tilde{x}_2$ is characterized by a deterministic value x_2 plus a gaussian zero mean random part ε_2. Rod 2 is the excited one, so $\tilde{x}_f$, the excitation point, is affected by randomness.
x_2 and x_f are random parameter, $\sigma_2 = \sigma_f = 0.05$.
The physical properties of the structure are reported in table 6.10 and the results of SOM in figures 6.25 and 6.26.

	length [m]	x_f [m]	E [N/m^2]	S [m^2]	η [%]	ρ [kg/m^3]
Rod 1	1.13		$2.1 \cdot 10^{11}$	10^{-4}	1	7800
Rod 2	8.64	4.96	$2.1 \cdot 10^{10}$	10^{-5}	1	7800

Table 6.10: BEM-SIF two coupled rods with mid-frequency assumptions with different rod properties. Correct formulation. Parameters of the two rods.

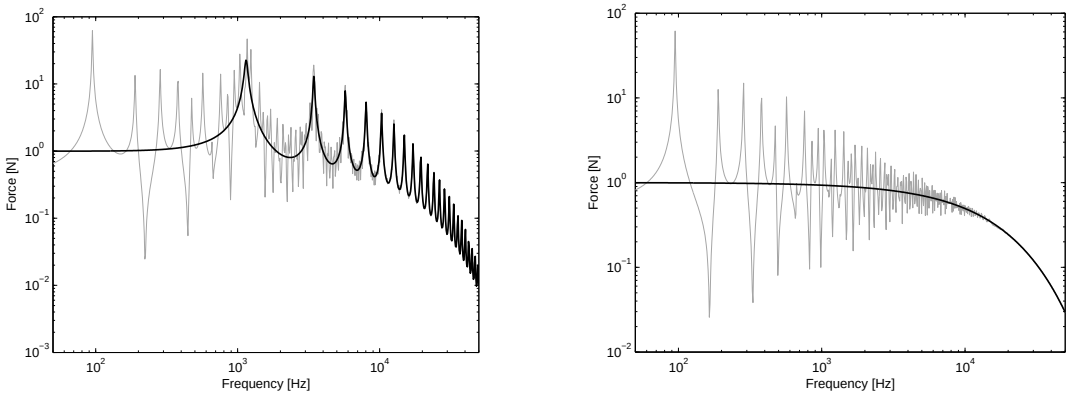

(a) (b)

Figure 6.25: BEM-SIF two coupled rods with mid-frequency assumptions with different rod properties. Correct formulation. Frequency evolution of the modulus of the second order moment, traction at x_1 (a) and $\tilde{x}_2$ (b). —— BEM-SIF —— BEM

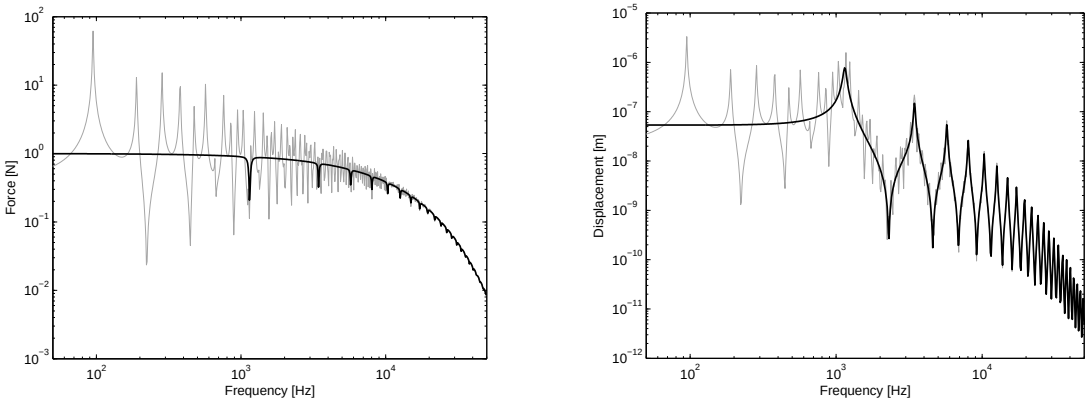

(a) (b)

Figure 6.26: BEM-SIF two coupled rods with mid-frequency assumptions with different rod properties. Correct formulation. Frequency evolution of the modulus of the second order moment, traction (a) and displacement (b) at x_0. —— BEM-SIF —— BEM

In figures 6.25-6.26 we can have the verification of the effectiveness of the formulation for the structures vibrating in the mid-frequency range with excitation located on the long member. The modal contributions belonging to the rod 1 is perfectly described, while the rod 2 add a mean contribution. The displacement in x_0, fig. 6.26, is governed by rod 1 which is stiffer, while the traction is governed by the resistance given by rod 2 which is softer. We can see that the mean contribution of traction at x_0 presents some antiresonance in correspondence of the resonance peaks of the traction and displacement of rod 1. Those antiresonance peaks also appears in the BEM results and perfectly fit in terms of value and position.

6.5.3 Discussion

It's important to notice that the SIF formulation, in the deterministic-random form, is able to correctly predict the behavior of two coupled rods in different configurations, even if the two rods are characterized by different physical behavior, one deterministic rod and one statistical rod. The Deterministic-SIF formulation is obtained directly from the SIF theory, applying the previous considerations on deterministic boundaries assumptions.
This is a very important result which gives us a very clear indication about the way to proceed to the development of the hybrid formulation for the mid-frequency range. The deterministic subsystem requires a second order modelling when the excitation is located on the random subsystem.
The number of unknowns of the Deterministic-SIF formulation is equal to 23, so it is bigger than the complete SIF which was 19. This has bad consequence in terms of complexity of the formulation and in terms of computational efficiency. This is a crucial topic that we will investigate an it importance will increase for more complex systems like 2D, sec. 9.5; however we should not forget to notice that the formulation is more complex than SIF because the capability of modelling mid-frequency structures with excitation on the long members has been added to the basic random formulation. The basic SIF was not adequate to this kind of problems as we have seen in section 6.4. The formulation is now robust and effective for the mid.frequency problem.

Chapter 7

Summary on SIF formulation

SIF theory has been proved to be a consistent theory for the analysis of the vibro-acoustic behavior of a complex system, in the previous chapters for the case of two coupled rod systems. The assumptions used to simplify the formulation are consistent for all the rod configurations. Particular attention should be payed to the analysis of the system behavior, it means that if for instance a rod exhibits a typically LF behavior, it should be treated with the deterministic assumptions.

In this chapter is reported a graph, figure 7.1, illustrating the application of the SIF formulation for the analysis of various systems. Starting from the classification of the systems in terms of deterministic or statistical behavior, the steps of the application moves from the FOM solution to the SOM equations. The central part is dedicated to the assumptions which rules the correlations among statistical variables and which constitute the real core of the formulation. At the bottom there are the SOM and the results.

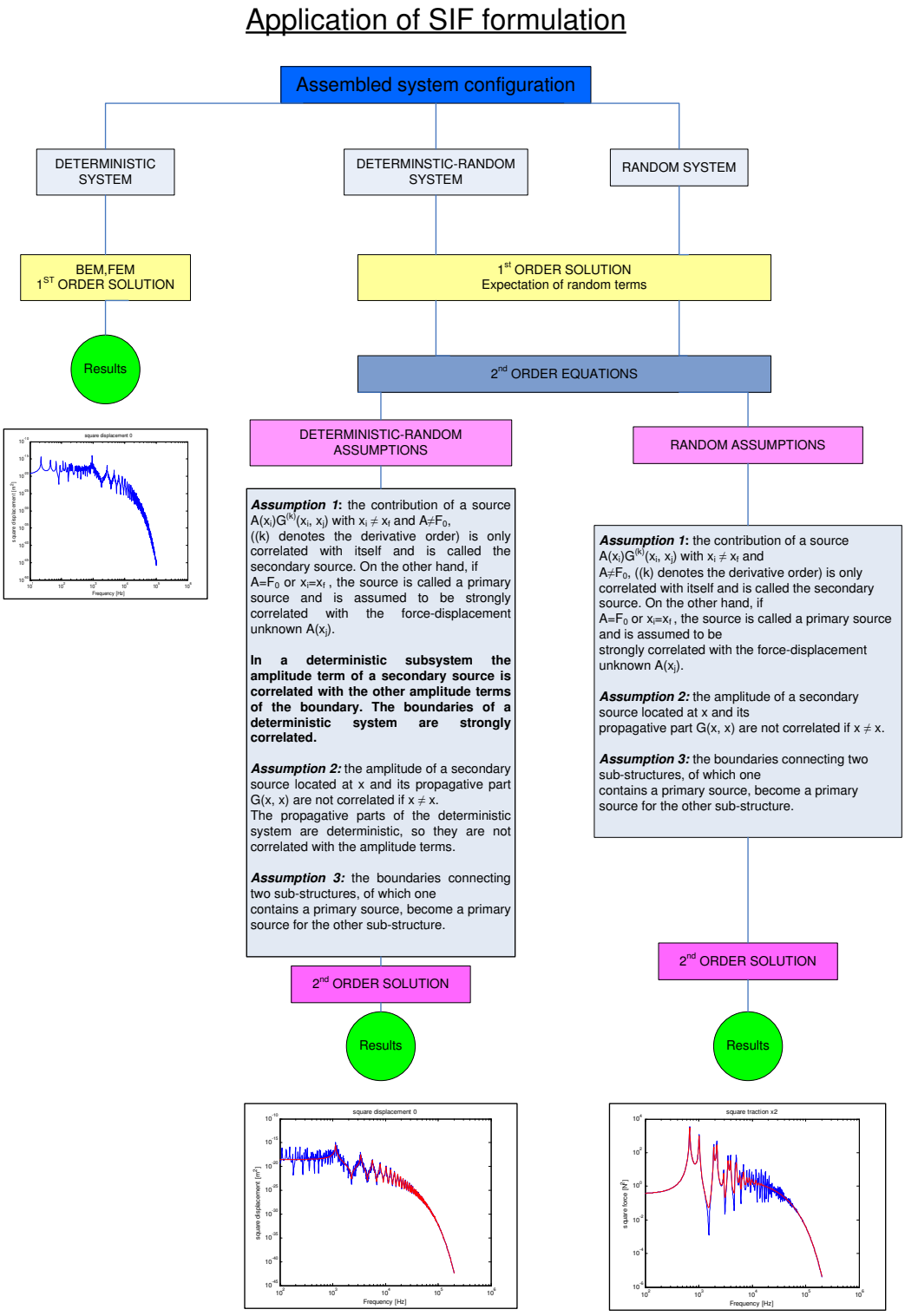

Figure 7.1: SIF table of application

Chapter 8

A new approach for mid-frequency modelling: coupling FEM and SIF

The approach chosen to analyse the mid-frequency problem is based on a hybrid formulation. This choice has the advantage of using the proper formulation for each different contribution in the response of the structure, a high frequency method for the HF parts, and FEM for the others. There is no loss of information for the FEM subsystems: the response still retains local and frequency (not averaged) information. On the other hand using the SIF formulation we should be able to account properly for the contributions of the HF parts of the structure, including also the effects of uncertainties.

8.1 Introducing the FEM-SIF theory

As an extension of the previous mid-frequency formulation, reported in section 6.5, the SIF is now coupled to an FE description. More precisely, the low-frequency behaving subsystems are modelled with the FEM while the high-frequency behaving subsystems are modelled with the SIF. The coupling allows to account for both deterministic and statistical contributions in the response of the structure. The objective was to obtain a consistent formulation for the mid-frequency range in terms of results, complexity and computational resources.
An advantage of this method is that both FEM and SIF variables are expressed, for instance, in terms of force and displacement, therefore they are homogeneous and can be easily coupled. The method does not present the difficulty to couple force and displacement with power and energy quantities of FEM-SEA hybrid methods. Moreover, thanks to use of the SIF formulation for the HF part of the structure, there is no need for a refined discretization of the long subsystem because of the slow spatial variations of the responses. A gain in terms of computational resources is consequently achieved.

In this section the formulation is explicitly derived for a simple structure made of two subsystems. It can be extended to any kind of two- and three-dimensional structures.
The external loading is applied to the random high-frequency behaving subsystem and the first order moments are suppressed from the formulation, assuming that these unknowns rapidly vanish to zero. The FOM are not include in the formulation to proceed with the methodology used in chapter 6, in order to simplify the formulation. The FOM can be included in the formulation without losing generality and effectiveness.

The deterministic subsystem is described by means of a FEM formulation. Considering the contribution of all the elements in terms of mass and stiffness matrices (damping is introduced in the Young modulus), and using a harmonic external excitation, it is possible to obtain the general FEM formulation for the whole subsystem, as follows:

$$\mathbf{A}_{\mathrm{FEM}} \cdot \mathbf{u}_{\mathrm{FEM}} = \mathbf{F} \qquad \text{and} \qquad \mathbf{A}_{\mathrm{FEM}} = [\mathbf{K} - \omega^2 \cdot \mathbf{M}], \tag{8.1}$$

$\mathbf{u}_{\mathrm{FEM}}$ is the vector of unknowns at nodes, $\mathbf{A}_{\mathrm{FEM}}$ is the dynamic matrix, and $\mathbf{F}$ is the vector of external forces, which are applied on nodes. The external excitations on the boundaries of the deterministic subsystem can be expressed as functions of the boundary unknowns. For instance, if we consider a clamped boundary element, at the clamped node j we will have:

$$w(j) = 0, \qquad ES \cdot \frac{\partial w(j)}{\partial x} = F(j) \tag{8.2}$$

where $F(j)$ is the external force applied by the clamp to the element j, and x is the direction of longitudinal displacement.

For each node of the FEM model it is possible to write the equilibrium equations as classical nodal equations. If we use a second order differential formulation for FE description of rod elements, and consider a node connecting two linear elements, node i in fig. 8.1, we can write the equilibrium equation for that node:

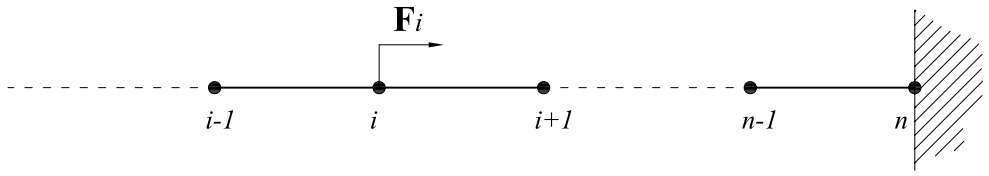

Figure 8.1: FEM elements scheme.

$$a_{ii-1} \cdot u(i-1) + a_{ii} \cdot u(i) + a_{ii+1} \cdot u(i+1) = F(i) \tag{8.3}$$

and

$$a_{ii} = k_{ii} - \omega^2 \cdot m_{ii},$$

where k_{ii} is the concentrated stiffness at node i, while m_{ii} is the concentrated mass.

In other respect, the SIF model is employed for describing the vibrational behaviour of the random subsystem, and the classical kinematic junction conditions are expressed at the boundaries between high-frequency and low-frequency subsystems.
The aim is now to rewrite eq. (8.1) in order to obtain a Finite Element formulation (FE) which can be coupled with SIF.
An advantage of FE formulation is that the coupling conditions are explicitly expressed in terms of kinematic variables, eq. (8.2). Thus, coupling a FEM subsystem with a SIF one

requires to write displacement and force continuity relationship (also slope and moment, depending from the differential order of the problem), and does not present the difficulty to couple force and energy quantities for instance of FEM-SEA hybrid methods.
As explained in the previous section, even for the low-frequency subsystem, the first order moments vanish to zero in the mid-, and high-frequency range. Among other reasons, this is due to the fact that the unknowns of the low-frequency behaving subsystems are random even if the subsystem is geometrically deterministic. This randomness is intrinsically brought by the high-frequency subsystems which are geometrically randomised.
The SIF formulation of the HF subsystem is a second order formulation. It means that the unknowns are the square modulus of the boundary unknowns. To couple SIF with FE, we need to rewrite the FEM obtaining a SIF-consistent formulation. A procedure analogous to the one introduced in section 4.4, to derive SIF equations from random BEM, is used. For each node the corresponding equilibrium equation, eq. (8.3), is multiplied by the conjugate of the nodal unknown at the same spatial position. n second order equations are obtained. For node i, we can write eq. (8.3) an then multiplying by $u^*(i)$ and getting the expectation, we obtain:

$$\begin{aligned} &a_{ii-1} \cdot \langle u(i-1) \cdot u^*(i) \rangle + a_{ii} \cdot \langle |u(i)|^2 \rangle + a_{ii+1} \cdot \langle u(i+1) \cdot u^*(i) \rangle \\ &= F(i) \cdot \langle u^*(i) \rangle. \end{aligned} \tag{8.4}$$

We should also consider that the FEM subsystem is deterministic, so its unknowns are not uncorrelated to each other (sec. 6.5). The unknowns that we want to evaluate are the second order unknown like $\langle |u(i)|^2 \rangle$, but to do that we need to account also of $\langle u(i-1) \cdot u^*(i) \rangle$ and $\langle u(i+1) \cdot u^*(i) \rangle$ in eq. (8.4). This leads to a great number of second order unknowns and so other equations have to be added to obtain a consistent set of equations. These equations are obtained multiplying the nodal equations, eq. (8.3) by the conjugate of the unknowns of nodes which are close to the considered one in terms of spatial locations:

$$\begin{aligned} &a_{ii-1} \cdot \langle |u(i-1)|^2 \rangle + a_{ii} \cdot \langle u(i) \cdot u^*(i-1) \rangle + a_{ii+1} \cdot \langle u(i+1) \cdot u^*(i-1) \rangle \\ &= F(i) \cdot \langle u^*(i-1) \rangle. \end{aligned} \tag{8.5}$$

and

$$\begin{aligned} &a_{ii-1} \cdot \langle u(i-1) \cdot u^*(i+1) \rangle + a_{ii} \cdot \langle u(i) \cdot u^*(i+1) \rangle + a_{ii+1} \cdot \langle |u(i+1)|^2 \rangle \\ &= F(i) \cdot \langle u^*(i+1) \rangle. \end{aligned} \tag{8.6}$$

Finally, from each nodal equilibrium equation, we obtain one second order unknown, in the form $\langle |u(i)|^2 \rangle$, and four other cross-product unknowns: $\langle u(i-1) \cdot u^*(i) \rangle$, $\langle u(i+1) \cdot u^*(i) \rangle$, $\langle u(i-1) \cdot u^*(i+1) \rangle$ and $\langle u(i+1) \cdot u^*(i-1) \rangle$. The unknowns $\langle u^*(i-1) \cdot u(i) \rangle$ and $\langle u^*(i+1) \cdot u(i) \rangle$ are accounted in the unknowns coming from the second order equations of node $i-1$ and $i+1$. Each node has five second order unknowns, so if we want to calculate the n second order unknowns (the expectation of the square modulus of the displacement at n nodes), we need to solve a linear system in $5n$ unknowns.
This implies that we need to account also for the $2n$ conjugates of the auxiliary equations, eqs. (8.5) and (8.6).
At last a SIF consistent set of equations is obtained. The number of equations depends from the differential order of the problem. Equations (8.4)-(8.6) can be written for each node of the FE subsystem and, getting rid of the first order moments, they can be collected into a unique matrix equation:

$$\mathbf{B}_{\mathrm{FEM}} \cdot \langle \mathbf{u}^2_{\mathrm{FEM}} \rangle = 0. \tag{8.7}$$

where $\mathbf{B}_{\text{FEM}}$ is the matrix of coefficient of the first order moments, and $\mathbf{u}^2_{\text{FEM}}$ is the vector of the second order unknowns which contains both square modulus $\langle |u(i)|^2 \rangle$ and cross product terms $\langle u^*(i) \cdot u(j) \rangle$.

To solve more effectively the numerical system, a condensation technique is introduced. This technique enabled the authors to reduce the overall number of unknowns of the formulation. A classical reduction method is used on eq. (8.7):

$$\mathbf{B}_{\text{FEM}} = \left[\begin{array}{c|c} \mathbf{B}_{bb} & \mathbf{B}_{bi} \\ \hline \mathbf{B}_{ib} & \mathbf{B}_{ii} \end{array}\right] \text{ and } \left[\begin{array}{c|c} \mathbf{B}_{bb} & \mathbf{B}_{bi} \\ \hline \mathbf{B}_{ib} & \mathbf{B}_{ii} \end{array}\right] \cdot \left\{ \begin{array}{c} \langle \mathbf{u}^2_{\text{FEM}} \rangle_{\text{boundaries}} \\ \hline \langle \mathbf{u}^2_{\text{FEM}} \rangle_{\text{internal}} \end{array} \right\} = 0 \tag{8.8}$$

Evaluating $\langle \mathbf{u}^2_{\text{FEM}} \rangle_{\text{internal}}$ from the lower part of eq. (8.8) and substituting in the upper part:

$$\left\{ \begin{array}{l} \langle \mathbf{u}^2_{\text{FEM}} \rangle_{\text{internal}} = \mathbf{B}_{ii}^{-1} \cdot \mathbf{B}_{ib} \cdot \langle \mathbf{u}^2_{\text{FEM}} \rangle_{\text{boundaries}} \\ \left\{ \mathbf{B}_{bb} - \mathbf{B}_{bi} \cdot \mathbf{B}_{ii}^{-1} \cdot \mathbf{B}_{ib} \right\} \cdot \langle \mathbf{u}^2_{\text{FEM}} \rangle_{\text{boundaries}} = 0 \end{array} \right. ,$$

$$\mathbf{B}_{\text{reduced}} = \left\{ \mathbf{B}_{bb} - \mathbf{B}_{bi} \cdot \mathbf{B}_{ii}^{-1} \cdot \mathbf{B}_{ib} \right\}$$

and

$$\mathbf{B}_{\text{reduced}} \cdot \langle \mathbf{u}^2_{\text{FEM}} \rangle_{\text{boundaries}} = 0. \tag{8.9}$$

$\mathbf{B}_{\text{reduced}}$ is the matrix obtained applying the reduction technique, and contains the formulation of the whole structure condensed at boundary nodes.
When observing the developments above, the interesting point to notice is that even if the unknowns that must be solved are not the usual first order kinematic variable, the matrices involved, $\mathbf{B}_{\text{FEM}}$ and $\mathbf{B}_{\text{reduced}}$, are comprised of elements of the classical FEM matrices $\mathbf{A}_{\text{FEM}}$, which can be obtained from a commercial FEM solver. Once the reduced matrix has been calculated, the second order system can be solved.
At last eqs. (8.9) for FEM, and classical equations without first order moments for SIF, are considered for the hybrid formulation. Coupling relationships are added to obtain a consistent set of equations.

8.2 Numerical application of FEM-SIF theory

The entire formulation will be developed for the structure made of two coupled rods.

8.2.1 FEM-SIF two coupled rods: deriving the equations

The formulation defined above is applied to two coupled rods, fig. 8.2. Rod 1 is stiff and short and thus modelled deterministically, while rod 2 is flexible and long and it is considered random. The loading is applied on the high-frequency rod, and a clamped-clamped configuration is considered. The randomness is introduced to the boundaries of rod 2 and force location. External excitation on nodes 0 and n (corresponding to point x_0 and x_1) can be expressed as:

$$F(0) = E_1 S_1 \cdot \frac{\partial w(0)}{\partial x}, \qquad F(n) = E_1 S_1 \cdot \frac{\partial w(n)}{\partial x}.$$

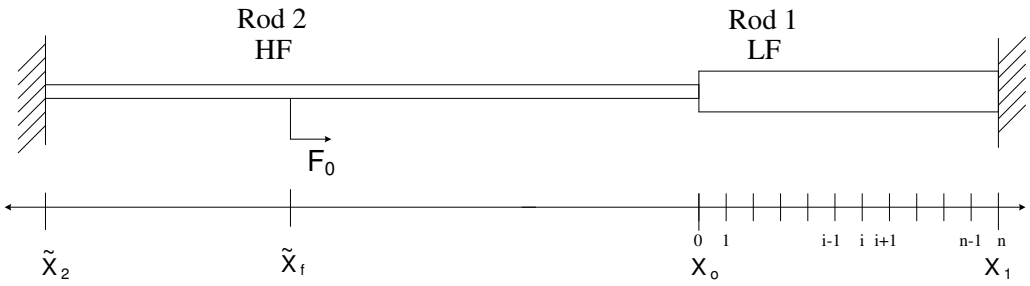

Figure 8.2: Structure made of two coupled rods. Clamped-clamped boundary conditions. FEM discretization of the deterministic rod.

We consider the finite element basic equilibrium equation for each node of rod 1, they are $n+1$ equations:

$$\begin{cases} a_{00} \cdot w(0) + a_{01} \cdot w(1) = E_1 S_1 \cdot \dfrac{\partial w(0)}{\partial x} \\ a_{10} \cdot w(0) + a_{11} \cdot w(1) + a_{12} \cdot w(2) = 0 \\ \vdots \\ a_{n-1n-2} \cdot w(n-2) + a_{n-1n-1} \cdot w(n-1) + a_{n-1n} \cdot w(n) = 0 \\ a_{nn-1} \cdot w(n-1) + a_{nn} \cdot w(n) = E_1 S_1 \cdot \dfrac{\partial w(n)}{\partial x} \end{cases} \tag{8.10}$$

The aim is to obtain the second order formulation also for the FEM rod to couple its formulation with SIF. To obtain the second order equations, each one of the equilibrium equations of rod 1, eq. (8.10), is respectively multiplied by the conjugate of one of the unknowns present in the equations (then, to obtain a different equation, by a different unknown of the same equation), and then the expectation is considered.
If we consider a clamped configuration, eq. (8.2), we obtain $3n+1$ equations and $5n+1$ unknowns. At node, i, we have:

$$a_{ii-1} \cdot \langle w(i-1) \cdot w^*(i) \rangle + a_{ii} \cdot \langle |w(i)|^2 \rangle + a_{ii+1} \cdot \langle w(i+1) \cdot w^*(i) \rangle = 0 \tag{8.11}$$

$$a_{ii-1} \cdot \langle |w(i-1)|^2 \rangle + a_{ii} \cdot \langle w(i) \cdot w^*(i-1) \rangle + a_{ii+1} \cdot \langle w(i+1) \cdot w^*(i-1) \rangle = 0 \tag{8.12}$$

$$a_{ii-1} \cdot \langle w(i-1) \cdot w^*(i+1) \rangle + a_{ii} \cdot \langle w(i) \cdot w^*(i+1) \rangle + a_{ii+1} \cdot \langle |w(i+1)|^2 \rangle = 0, \tag{8.13}$$

and the corresponding unknowns related to that node, i:

$$\langle |w(i)|^2 \rangle \quad , \quad \langle w(i-1) \cdot w^*(i) \rangle \quad , \quad \langle w(i+1) \cdot w^*(i) \rangle,$$
$$\langle w(i-1) \cdot w^*(i+1) \rangle \quad , \quad \langle w^*(i-1) \cdot w(i+1) \rangle.$$

SIF theory is used for the high-frequency behaving rod. We finally obtain five equations and eight unknowns for rod 2:

- ◇ Expectation of square modulus of boundary unknowns

$$\left\langle \left| \frac{\partial w^{(2)}(x_0)}{\partial x} \right|^2 \right\rangle, \left\langle \left| w^{(2)}(x_0) \right|^2 \right\rangle, \left\langle \left| \frac{\partial w(\tilde{x_2})}{\partial x} \right|^2 \right\rangle,$$

◇ Expectations of cross-product of unknowns at coupling point

$$\left\langle w^{(2)}(x_0)\cdot\frac{\partial w^{(2)*}(x_0)}{\partial x}\right\rangle,\left\langle w^{(2)*}(x_0)\cdot\frac{\partial w^{(2)}(x_0)}{\partial x}\right\rangle,$$

◇ Expectations of boundary unknowns multiplied for the external force contribution

$$\left\langle\frac{\partial w^{(2)*}(x_0)}{\partial x}\cdot G_2(x_0,\tilde{x_f})\right\rangle,\left\langle w^{(2)*}(x_0)\cdot G_2(x_0,\tilde{x_f})\right\rangle,$$
$$\left\langle\frac{\partial w^{*}(\tilde{x_2})}{\partial x}\cdot G_2(\tilde{x_2},\tilde{x_f})\right\rangle.$$

We should also consider the four coupling equations, written at the coupling point x_0: the continuity of displacement (written in terms of square displacement modulus), of traction, cross product of displacement and traction and the conjugate one. Evaluating the number of equations and unknowns obtained up to now, to solve the system we need $2n$ more equations, which can be obtained as the conjugate of the second order FEM equations, eqs. (8.11)-(8.13). The consistent set of equations for the entire structure is constituted of $5n+10$ equations. The condensation technique introduced previously is now applied to the second order linear system of equations of the subsystem modelled with FEM. The dimension of the deterministic matrix, $\mathbf{B}_{\text{FEM}}$, is reduced from $[(5n+1)\times(5n+2)]$ to $[4\times 5]$. All the formulation of rod 1 is condensed into five unknowns:

$$\langle\mathbf{u}^2_{\text{FEM}}\rangle_{\text{boundaries}}=\begin{bmatrix}\left\langle\left|w^{(1)}(0)\right|^2\right\rangle\\ \left\langle w^{(1)}(0)\cdot\frac{\partial w^{(1)*}(0)}{\partial x}\right\rangle\\ \left\langle w^{(1)*}(0)\cdot\frac{\partial w^{(1)}(0)}{\partial x}\right\rangle\\ \left\langle\left|\frac{\partial w^{(1)}(0)}{\partial x}\right|^2\right\rangle\\ \left\langle\left|\frac{\partial w(n)}{\partial x}\right|^2\right\rangle\end{bmatrix},$$

and four equations:

$$\begin{aligned}&\mathbf{B}(1,1)_{\text{reduced}}\cdot\left\langle\left|w^{(1)}(0)\right|^2\right\rangle+\mathbf{B}(1,2)_{\text{reduced}}\cdot\left\langle w^{(1)}(0)\cdot\frac{\partial w^{(1)*}(0)}{\partial x}\right\rangle\\ &\quad+\mathbf{B}(1,3)_{\text{reduced}}\cdot\left\langle w^{(1)*}(0)\cdot\frac{\partial w^{(1)}(0)}{\partial x}\right\rangle\\ &\quad+\mathbf{B}(1,5)_{\text{reduced}}\cdot\left\langle\left|\frac{\partial w(n)}{\partial x}\right|^2\right\rangle=0 \qquad (8.14)\\ &\mathbf{B}(2,1)_{\text{reduced}}\cdot\left\langle\left|w^{(1)}(0)\right|^2\right\rangle+\mathbf{B}(2,2)_{\text{reduced}}\cdot\left\langle w^{(1)}(0)\cdot\frac{\partial w^{(1)*}(0)}{\partial x}\right\rangle\\ &\quad+\mathbf{B}(2,3)_{\text{reduced}}\cdot\left\langle w^{(1)*}(0)\cdot\frac{\partial w^{(1)}(0)}{\partial x}\right\rangle\\ &\quad+\mathbf{B}(2,4)_{\text{reduced}}\cdot\left\langle\left|\frac{\partial w^{(1)}(0)}{\partial x}\right|^2\right\rangle=0 \qquad (8.15)\\ &\mathbf{B}(3,1)_{\text{reduced}}\cdot\left\langle\left|w^{(1)}(0)\right|^2\right\rangle+\mathbf{B}(3,2)_{\text{reduced}}\cdot\left\langle w^{(1)}(0)\cdot\frac{\partial w^{(1)*}(0)}{\partial x}\right\rangle\\ &\quad+\mathbf{B}(3,3)_{\text{reduced}}\cdot\left\langle w^{(1)*}(0)\cdot\frac{\partial w^{(1)}(0)}{\partial x}\right\rangle=0 \qquad (8.16)\end{aligned}$$

	length [m]	x_f [m]	E [N/m^2]	S [m^2]	η [%]	ρ [kg/m^3]
Rod 1	1.13		$2.1 \cdot 10^{11}$	10^{-3}	2	7800
Rod 2	8.64	4.96	$2.1 \cdot 10^{10}$	10^{-5}	0.2	7800

Table 8.1: FEM-SIF numerical application. Parameters of the coupled rod system.

$$\mathbf{B}(4,1)_{\text{reduced}} \cdot \left\langle \left| w^{(1)}(0) \right|^2 \right\rangle + \mathbf{B}(4,2)_{\text{reduced}} \cdot \left\langle w^{(1)}(0) \cdot \frac{\partial w^{(1)*}(0)}{\partial x} \right\rangle$$
$$+\mathbf{B}(4,3)_{\text{reduced}} \cdot \left\langle w^{(1)*}(0) \cdot \frac{\partial w^{(1)}(0)}{\partial x} \right\rangle = 0 \tag{8.17}$$

Finally, using the four equations above, five equations for rod 2 and four coupling relations, one obtains a consistent linear $[13 \times 13]$ system.

8.2.2 FEM-SIF Two rods: results

The geometrical and physical properties of the structure made of two coupled rods, are reported in table 8.1. The frequency variations of the second order moments, the traction at the boundary of rod 1 and the displacement at the junction between the two rods, are illustrated in figures 8.3-8.6. Like in section 6.5, we obtain a smooth response for the unknowns of the random rod, and a detailed description of the response of the deterministic rod. The upper value of the frequency range has been limited to 20000 Hz even if this formulation produces exact results above this frequency limit. The reason is that when frequency increases, rod 1 finally reaches the domain where his contribution to the global response of the structure can be identified as a high-frequency contribution. Thus, the global structure has moved from the mid-frequency domain to the high-frequency field.

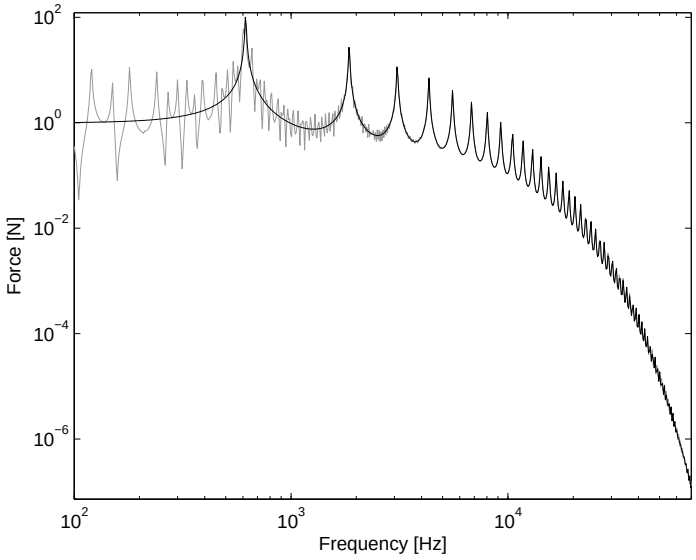

Figure 8.3: FEM-SIF formulation. Frequency evolution of the modulus of traction at x_1 for the structure made of two coupled rods. —— FEM-SIF. —— BEM.

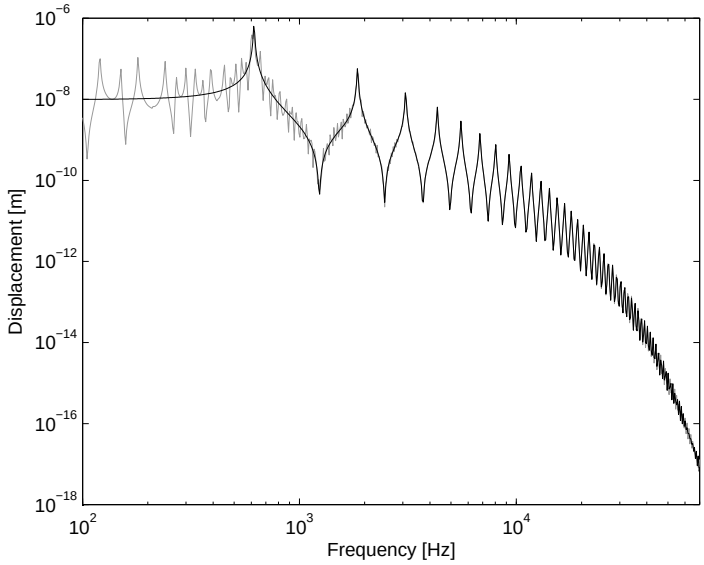

Figure 8.4: FEM-SIF formulation. Frequency evolution of the modulus of displacement at x_0 for the structure made of two coupled rods. —— FEM-SIF. —— BEM.

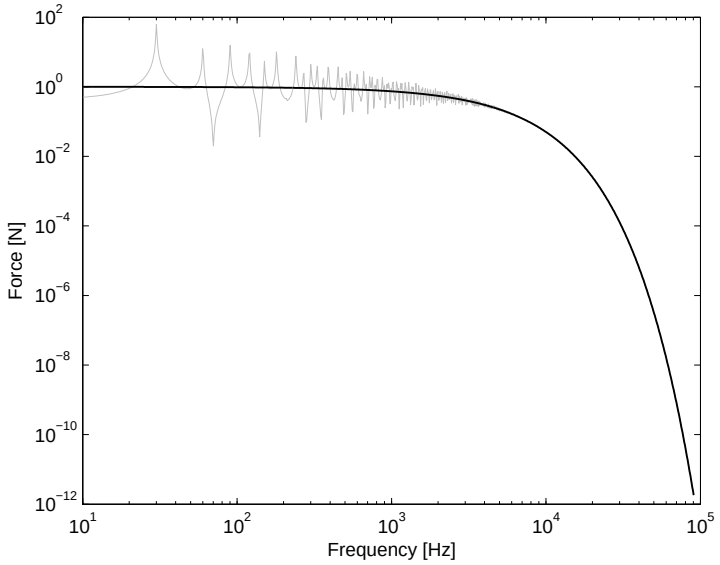

Figure 8.5: FEM-SIF formulation. Frequency evolution of the modulus of traction at x_2 for the structure made of two coupled rods. —— FEM-SIF. —— BEM.

8.2.3 Discussion

Figures 8.3-8.6 illustrate that coupling FEM and SIF theory to model a mid-frequency behaving structure leads to relevant results. The contribution of the deterministic part is correctly modelled with the FEM formulation, modified to be SIF consistent.

Another important aspect of the application of FEM-SIF is that the final formulation

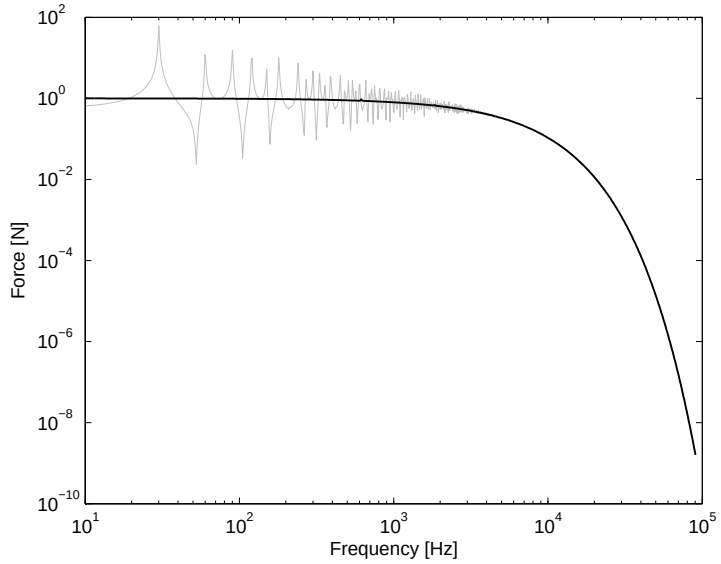

Figure 8.6: FEM-SIF formulation. Frequency evolution of the modulus of traction at x_0 for the structure made of two coupled rods. —— FEM-SIF. —— BEM.

for 1D system, has a number of unknowns which is proportional to the number of elements of the FEM subsystem, n. In the next chapter the hybrid formulation will be extended to 2D systems and it will be interesting to compare the number of unknowns for the 1D and 2D formulations to judge the computational efficiency and the complexity of the formulation

In this section it has been proved that coupling of SIF formulation with a deterministic technique, FEM, is possible and it is a feasible solution and a big step towards the development of a mid-frequency formulation for the analysis of complex systems.

Chapter 9

Extension of the hybrid formulation to 2D structures

In this section the SIF formulation is extended to the 2D structures. The first step to apply the SIF, is to develop a consinstent BEM representation of the structure that we want to analyze. Then introducing the random parameters to the description of the boundary, we will develop the SIF formulation.
The 2D structures, as expected, are more complicated to model using the BEM with respect to the 1D structures. This is due to the fact that the boundary are no more points, but are linear boundaries, which are discretized through the collocation method into finite length elements. The Green kernel functions needs to be integrated over a linear domain. This integration requires to manage singularities. Moreover, an analytical solution, as in the case of rods and beams, is often not available, thus a numerical integration is required.
In the following sections a general overview on the application of BEM to 2D structures will be given, and also the method used for the calculation of the Green Kernels contributions, (in BEM and SIF), will be presented.
An acoustic application of BEM has been chosen, in order to deal with interactions between vibrating structures and acoustic systems. We want to test the SIF formulation for this kind of applications to be able to couple it with a deterministic formulation, and to obtain a hybrid formulation for 2D structure as we have done for the 1D FEM-SIF.
The 2D domain also presents some interesting aspects in terms of computational resources and dependency of the solution from the quality of the discretization that has been chosen. By means of a 2D application we will be able to test the SIF and the Hybrid-SIF also in terms of computational requirements, test which was not representative and significant for 1D systems.

9.1 2D BEM theory for acoustics

For steady state, constant frequency motion, the acoustic wave equation reduces to the Helmholtz equation

$$\nabla^2 p(\vec{r}) + kp(\vec{r}) = 0 \tag{9.1}$$

where p is the acoustic pressure and $k = \omega/c$ is the wavenumber, c is the sound speed. $\vec{r}$ is the generic vector which define the field point.

The right hand side of the equation (9.1) can be modified to include the source function of any incident waves. The problem domain V is completely enclosed by a surface S. The boundary condition on S can take several forms:

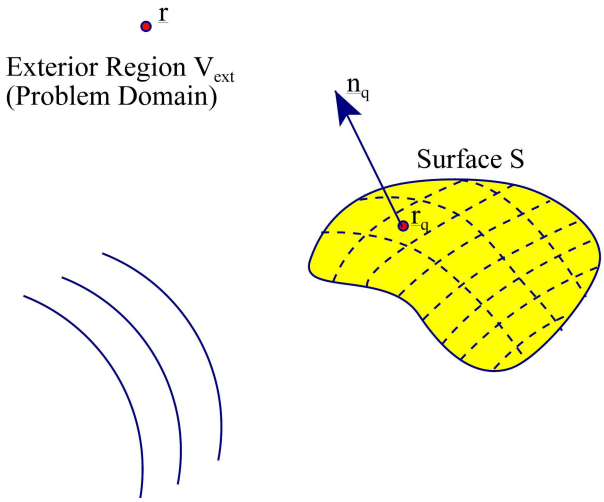

Figure 9.1: Acoustic boundary domain.

- rigid: $\dfrac{\partial \vec{r}_q}{\partial \vec{n}_q} = 0, \qquad \vec{r}_q \in S,$
- pressure release: $p(\vec{r}_q) = 0, \qquad \vec{r}_q \in S,$
- impedance surface: $\dfrac{\partial \vec{r}_q}{\partial \vec{n}_q} = -jk\beta p(\vec{r}_q) \quad \text{where} \quad \beta = \rho c/Z, \qquad \vec{r}_q \in S,$
- structure coupling: $\dfrac{\partial \vec{r}_q}{\partial \vec{n}_q} = \rho\omega^2 u_n, \qquad \vec{r}_q \in S$

where u_n is the displacement in the direction of the surface normal $\vec{n}_q$.

9.2 2D BEM theory: interior problem

Green's first and second theorem provide the basis for transforming the differential equations (9.1) in the problem domain V and the boundary conditions on the surface S, into an integral equation over the surface S, eq.(9.2). In an interior problem, figure 9.2, the problem domain V is the region V_{int} inside the enclosing surface S.

$$\int_S \left[p(\vec{r}_q) \frac{\partial G(\vec{r}, \vec{r}_q)}{\partial \vec{n}_q} - \frac{\partial p(\vec{r}_q)}{\partial \vec{n}_q} G(\vec{r}, \vec{r}_q) \right] dS = \begin{cases} -p(\vec{r}), & \vec{r} \in V_{int} \\ -\frac{1}{2} p(\vec{r}), & \vec{r} \in S \\ 0, & \vec{r} \in V_{ext} \end{cases} \tag{9.2}$$

$G(\vec{r}, \vec{r}_q)$ is called the Green's function - a kernel function that is given by the fundamental solution of an acoustic point source. The corresponding Green's function for the 2-dimensional problem is:

$$G(\vec{r}, \vec{r}_q) = -\frac{i}{4} H_0^{(1)}(k|\vec{r} - \vec{r}_q|) \tag{9.3}$$

$H_0^{(1)}$ denotes the Hankel function of the first kind of order zero. More generally $H_n^{(1)}$ denotes the Hankel function of the first kind of order n. The Hankel functions are a type of Bessel function; indeed $H_n^{(1)}$ is a solution of Bessel's equation of order n. $H_n^{(1)}$ is defined in

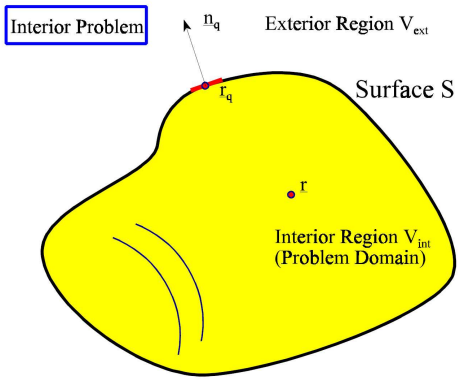

Figure 9.2: Acoustic boundary domain: interior problem.

terms of the more standard Bessel functions J_n and Y_n by $H_n^{(1)}(z) = J_n(z) + iY_0(z)$ [61]. We term the function $G(\vec{r}, \vec{r}_q)$ that we have just written down a fundamental solution of the Helmholtz equation, which just means that it is a solution of the Helmholtz equation appropriate to a point source excitation. We also call $G(\vec{r}, \vec{r}_q)$ the free-field Green's function, meaning that it is the (unique) solution to the problem of a point source in free space.

9.3 BEM application: 2D acoustical domain

In this section the general formulation of BEM is derived for a 2D acoustical domain Ω with boundary S. S_f is the internal boundary where the external force is applied, S_p is the boundary with pressure conditions assigned, $\hat{p}(\vec{r})$, and $S_{\partial p}$ is the boundary with derivative of pressure conditions assigned, $\partial\hat{p}(\vec{r})/\partial\vec{n}_r$. In our formulation we suppose to divide the domain S into pressure and derivative of pressure boundary conditions, so we have $S = S_p + S_{\partial p}$, fig. 9.3. $\vec{r}_i$ is the vector which indicates the boundary i, and $\vec{n}_i$ is the outward normal at boundary i. We also assume that the value of a generic boundary unknown is constant along the element.
The collocation method is employed which enables the transformation of the integral equations, eqs. (9.2), into a discrete set of equations. The boundary S_p ($S_{\partial p}$ respectively) is discretized into N_p elements ($N_{\partial p}$).

As an illustration, the equation (9.2) evaluated at point $\vec{r}_i$, $\vec{r}_i \in S_{\partial p}$ is reported.

$$\begin{aligned}\frac{1}{2}p(\vec{r}_i) &= \sum_{j=1}^{N_p}\int_{S_j}\hat{p}(\vec{r})\frac{\partial G(\vec{r}_i,\vec{r})}{\partial\vec{n}_j}dS - \sum_{i=j}^{N_{\partial p}}p(\vec{r}_j)\int_{S_j}\frac{\partial G(\vec{r}_i,\vec{r})}{\partial\vec{n}_j}dS \\ &+ \sum_{k=1}^{N_p}\frac{\partial p(\vec{r}_k)}{\partial\vec{n}_k}\int_{S_k}G(\vec{r}_i,\vec{r}) - \sum_{k=1}^{N_{\partial p}}\int_{S_k}\frac{\partial\hat{p}(\vec{r})}{\partial\vec{n}_k}G(\vec{r}_i,\vec{r})dS \\ &+ \int_{S_f}f(\vec{y})G(\vec{r}_i,\vec{y})dS \end{aligned} \tag{9.4}$$

In equation (9.4) $\vec{r}$ is the generic vector which define the point of integration which moves along the boundary S_j or S_k, and $\vec{y}$ is the vector of coordinates of the force location

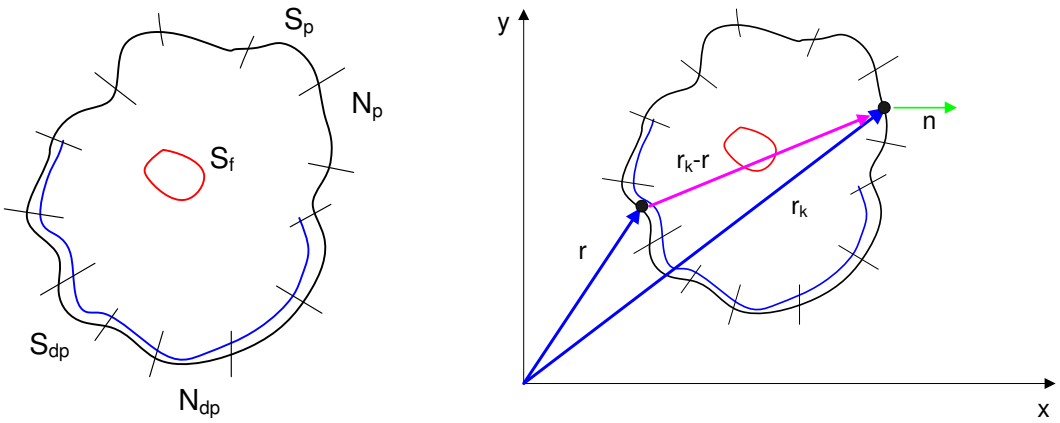

Figure 9.3: Acoustic boundary domain: interior problem, Qualitative representation of a 2D domain.

on boundary S_f, fig. 9.3.
$G(\vec{r}_i, \vec{r})$ is the Green Kernel for the acoustic domain, eq. (9.3), and it represent the propagative part of the source located on boundary S_k towards $\vec{r}_i$. $\partial G(\vec{r}_i, \vec{r})/\partial \vec{n}_k$ is the first order derivative of the Green Kernel with respect to the outward normal at boundary S_k. Let $\vec{z} = \vec{r}_i - \vec{r}$, we have:

$$G(k\vec{z}) = -\frac{i}{4} H_0^{(1)}(k|\vec{r} - \vec{r}_q|) = -\frac{i}{4}(J_0(k\vec{z}) + iY_0(k\vec{z})) \tag{9.5}$$

$$\begin{aligned} \frac{\partial G(k\vec{z})}{\partial \vec{n}} &= \frac{\partial G(k\vec{z})}{\partial \vec{z}} \cdot \frac{-\vec{r}\cdot\vec{n}}{r} = (-\frac{i}{4} H_1^{(1)}(k|z|)) \cdot \frac{-\vec{r}\cdot\vec{n}}{r} \\ &= (-\frac{i}{4}(J_1(k\vec{z}) + iY_1(k\vec{z}))) \cdot \frac{-\vec{r}\cdot\vec{n}}{r} \end{aligned} \tag{9.6}$$

9.3.1 Evaluation of the singularities

The singularities of fundamental solutions requires careful analysis when the load point is accommodated on the boundary. In our case, when $z \longrightarrow 0$ ($\vec{r} \longrightarrow \vec{r}_i$), the source and the field point belongs to the same boundary element, we need to calculate $\int_{S_k} G(\vec{r}_i, \vec{r})$ and $\int_{S_j} (\partial G(\vec{r}_i, \vec{r})/\partial \vec{n}_j) dS$ which presents singularities.
In details, for $z \longrightarrow 0$

$$\begin{aligned} \frac{\partial G(\vec{z})}{\partial \vec{n}} &\longrightarrow \frac{1}{z} \quad \text{strong singularity} \\ G(\vec{z}) &\longrightarrow \ln(z) \quad \text{weak singularity} \end{aligned}$$

For a weak singularity, the integral exists and is smooth at the singularity, it can be calculated using some integration rules. The strong singularity requires an interpretation as Cauchy Principal Value for the integration [7, 9].
The Cauchy Principal Value of a divergent integral is the limit as the radius goes to zero of the integral of the function outside a circular neighborhood of the singularity.

If we locate the load point on the boundary, we need to manage the singularities in boundary integrals. To calculate for instance $\int_\Gamma (\partial G(\vec{r}_i, \vec{r})/\partial \vec{n}) d\Gamma$, we first adjust the boundary such that it contains the point inside a circle of radius ϵ according to fig. 9.4.

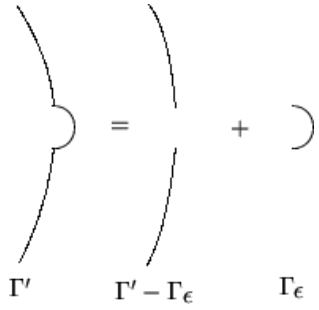

Figure 9.4: Evaluation of singularities: boundary extension by a circle.

$$\Gamma' = (\Gamma' - \Gamma_\varepsilon) \cup \Gamma_\varepsilon \tag{9.7}$$

Thus the point ξ is inside the domain and eq. (9.4) is still valid.
The integral $\int_\Gamma (\partial G(\vec{r}_i, \vec{r})/\partial \vec{n}) d\Gamma$ can be rewritten as:

$$\lim_{\varepsilon \longrightarrow 0} \int_{\Gamma'} \frac{\partial G(\vec{r}_i, \vec{r})}{\partial \vec{n}} d\Gamma = \lim_{\varepsilon \longrightarrow 0} \int_{\Gamma' - \Gamma_\varepsilon} \frac{\partial G(\vec{r}_i, \vec{r})}{\partial \vec{n}} d\Gamma + \lim_{\varepsilon \longrightarrow 0} \int_{\Gamma_\varepsilon} \frac{\partial G(\vec{r}_i, \vec{r})}{\partial \vec{n}} d\Gamma \tag{9.8}$$

The second integral, assuming that $\Gamma_\varepsilon = \varepsilon d\varphi$, fig. 9.5, we have $z = \varepsilon$ and

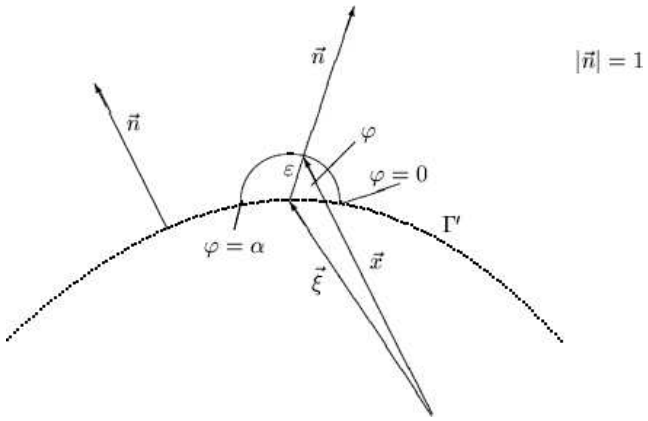

Figure 9.5: Evaluation of singularities: Geometry for accommodating the load point on the boundary.

$$\lim_{\varepsilon \longrightarrow 0} \int_{\Gamma_\varepsilon} \frac{\partial G(\vec{r}_i, \vec{r})}{\partial \vec{n}} d\Gamma = \lim_{\varepsilon \longrightarrow 0} \int_{\Gamma_\varepsilon} \frac{1}{z} d\Gamma = \lim_{\varepsilon \longrightarrow 0} \int_{\varphi=0}^{\alpha} \frac{1}{\varepsilon} \varepsilon d\varphi = \alpha \tag{9.9}$$

The first integral on the right side of eq. (9.8) is a strongly singular integral calculated by Cauchy's Principal Value:

$$\lim_{\varepsilon \longrightarrow 0} \int_{\Gamma' - \Gamma_\varepsilon} \frac{\partial G(\vec{r}_i, \vec{r})}{\partial \vec{n}} d\Gamma = CPV \int_{\Gamma' - \Gamma_\varepsilon} \frac{\partial G(\vec{r}_i, \vec{r})}{\partial \vec{n}} d\Gamma \tag{9.10}$$

Supposing to have Γ of boundary $[a, b]$ and G is singular in $c \in [a, b]$:

$$CPV \quad = \quad \lim_{\varepsilon \longrightarrow 0} \Big(\int_a^{c-\varepsilon} \frac{1}{z} dz + \int_{c+\varepsilon}^{b} \frac{1}{z} dz \Big) =$$

$$
\begin{aligned}
&= \lim_{\varepsilon \longrightarrow 0} \left(\Big[\ln z \Big]_a^{c-\varepsilon} + \Big[\ln z \Big]_{c+\varepsilon}^{b} \right) \\
&= \lim_{\varepsilon \longrightarrow 0} \Big(\ln a - lnc - \varepsilon + lnc + \varepsilon - lnb \Big) \\
&= \lim_{\varepsilon \longrightarrow 0} \Big(\ln \frac{a}{b} + \ln \frac{c+\varepsilon}{c-\varepsilon} \Big) = \ln \frac{a}{b}
\end{aligned} \tag{9.11}
$$

9.3.2 Numerical integration

The integration over S_i of the Kernel functions is done by mean of a numerical integration scheme, the Gaussian quadrature. The simplest form of Gaussian Integration is based on the use of an optimally chosen polynomial to approximate the integrand $f(t)$ over the interval $[-1, +1]$. The simplest form uses a uniform weighting over the interval, and the particular points at which to evaluate $f(t)$ are the roots of a particular class of polynomials, the Legendre polynomials, over the interval. It can be shown that the best estimate of the integral is then:

$$\int_{-1}^{1} f(t)dt = \sum_{1=1}^{n} w_i f(t_i) \tag{9.12}$$

where t_i is a designated evaluation point, and w_i is the weight of that point in the sum. If the number of points at which the function $f(t)$ is evaluated is n, the resulting value of the integral is of the same accuracy as a simple polynomial method (such as Simpson's Rule) of about twice the degree (ie. of degree $2n$). Thus the carefully designed choice of function evaluation points in the Gauss-Legendre form results in the same accuracy for about half the number of function evaluations, and thus at about half the computing effort.
In most cases we will want to evaluate the integral on a more general interval, say (a, b). We will use the variable x on this more general interval, and linearly map the (a,b) interval for x onto the $[-1, +1]$ interval for t using the linear transformation:

$$x = c + mt, \qquad \text{where} \qquad c = (b+a)/2 \qquad \text{and} \qquad m = (b-a)/2 \tag{9.13}$$

It is easily verified that substituting $t = -1$ gives $x = a$ and $t = 1$ gives $x = b$. We can now write the integral as:

$$I = \int_a^b f(x)dx = m \int_{-1}^{1} f(c + mt)dt \tag{9.14}$$

The factor of m in the second integral arises from the change of the variable of integration from x to t, which introduces the factor $\partial x/\partial t$. Finally, we can write the Gauss-Legendre estimate of the integral as:

$$I = \int_a^b f(x)dx = m \sum_{1=1}^{n} w_i f(c + mt_i) \tag{9.15}$$

The Gaussian integration scheme is used to calculate the integral of the fundamental solutions on the boundary elements, but also to calculate the integrals on the probability distribution of the random parameters, ε_i and ε_k, due to the expectation operation.

9.3.3 BEM 2D domain: equations and results

As an example, the BEM is applied in this paper to a square 2D domain, figure 9.6 characterized by Helmholtz equation. The boundaries of the domain are divided into N

elements. p_0 is the external punctual excitation acting on the structure which is supposed to pressure release boundary conditions:

$$p(\vec{r}_i) = 0 \qquad \text{for} \qquad i = 1 : N_p$$

The general BEM equation (9.4) reduces to:

$$0 = \sum_{k=1}^{N_p} \frac{\partial p(\vec{r}_k)}{\partial \vec{n}_k} \int_{S_k} G(\vec{r}_i, \vec{r}) dS + \int_{S_f} p_0 G(\vec{r}_i, \vec{y}) dS \tag{9.16}$$

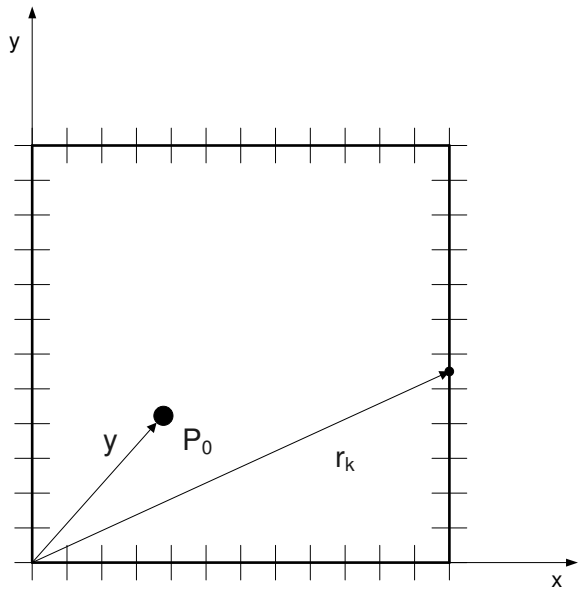

Figure 9.6: Acoustic 2D domain.

The geometrical and physical properties of the domain are reported in table 9.1. The solution in terms of $\partial p(\vec{r}_i)/\partial \vec{n}$ is reported in figures 9.7-9.8 at different boundary locations.

	Side Length [m]	Sound speed [m/s]	ρ [kg/m^3]	η (%)
Acoustic Domain	1	50.5	10.5	0.03

Table 9.1: BEM application. Acoustic 2D domain: geometrical and physical properties of the acoustic domain.

BEM is able to model properly the vibrational behavior of an acoustical domain, as we can see from the comparison between the results obtained using BEM (evaluating the response of the domain at different nodes along the boundary and then superposing all the curves), and the results obtained with an analytical calculation, fig. 9.9.

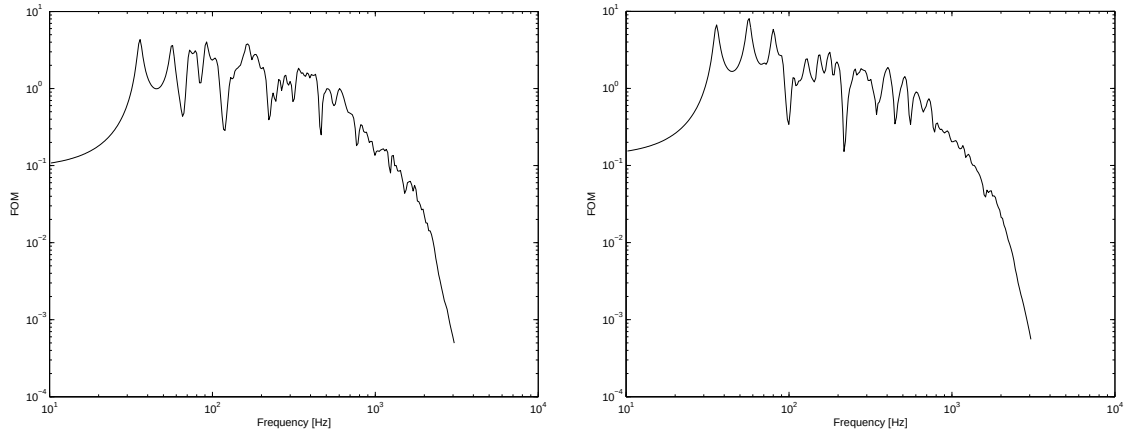

(a) (b)

Figure 9.7: BEM acoustical domain. Frequency evolution of the modulus of the first order moment, $\partial p(\vec{r}_i)/\partial \vec{n}$ at nodes 25 (a) and 31 (b).

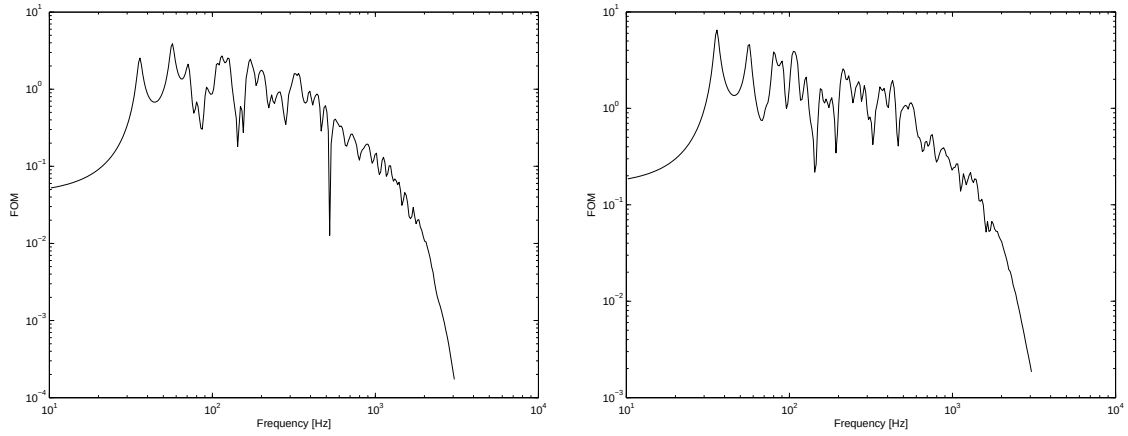

(a) (b)

Figure 9.8: BEM acoustical domain. Frequency evolution of the modulus of the first order moment, $\partial p(\vec{r}_i)/\partial \vec{n}$ at nodes 43 (a) and 49 (b).

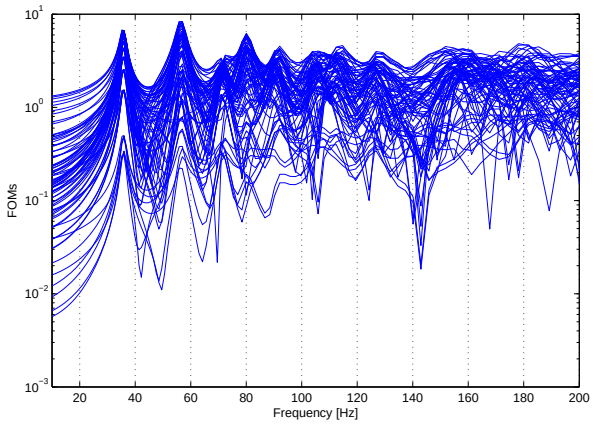

(a)

n	m	Nat.Freq. [Hz]
1	1	**36**
2	1	**56**
1	2	**56**
2	2	**71**
1	3	**80**
3	1	**80**
2	3	**91**
3	2	**91**
1	4	**104**
4	1	**104**
3	3	**107**
2	4	**113**
4	2	**113**
3	4	**126**
4	3	**126**

(b)

Figure 9.9: BEM acoustical domain. Comparison of the value of the natural frequencies for a BEM calculation (a) and analytical calculation (b). Response of BEM calculated at different nodes along the boundary.

9.4 SIF application: 2D acoustical domain

As an example, the SIF is applied in this paper to a square 2D domain characterized by Helmholtz equation.

9.4.1 SIF 2D acoustical domain: deriving the equations

The BEM boundary equations for an acoustical domain with pressure release boundary condition $p(\vec{r}_k) = 0$ is recalled in this section:

$$0 = \sum_{k=1}^{N_p} \frac{\partial p(\vec{r}_k)}{\partial \vec{n}_k} \int_{S_k} G(\vec{r}_i, \vec{r}) dS + p_0 G(\vec{r}_i, \vec{y}) \tag{9.17}$$

Randomness is introduced in the boundary description, section 9.4.2, and it is indicated by $\tilde{\vec{r}}$.

$$0 = \sum_{k=1}^{N_p} \frac{\partial p(\tilde{\vec{r}}_k)}{\partial \vec{n}_k} \int_{\tilde{S}_k} G(\tilde{\vec{r}}_i, \tilde{\vec{r}}) dS + p_0 G(\tilde{\vec{r}}_i, \tilde{\vec{y}}) \tag{9.18}$$

The SIF equations for the acoustical domain

The SIF equations, according to procedure in section 4.4 are obtained multiplying each side of the basic equations (9.18) for the conjugate of the boundary unknowns, $\partial p(\vec{r}_i)/\partial \vec{n}$, and getting the expectation.
For $i = 1, 2, ...N_p$, $\tilde{\vec{r}}_i \in \tilde{S}_p$:

$$\begin{aligned} 0 \;=\; & \Big\langle \Big| \frac{\partial p(\tilde{\vec{r}}_i)}{\partial \vec{n}} \Big|^2 \Big\rangle \Big\langle \int_{\tilde{S}_i} G(\tilde{\vec{r}}_i, \tilde{\vec{r}}) dS \Big\rangle + \Big\langle \frac{\partial p^*(\tilde{\vec{r}}_i)}{\partial \vec{n}} \Big\rangle \sum_{\substack{k=1 \\ k \neq i}}^{N_p} \Big\langle \frac{\partial p(\tilde{\vec{r}}_k)}{\partial \vec{n}} \Big\rangle \Big\langle \int_{\tilde{S}_k} G(\tilde{\vec{r}}_i, \tilde{\vec{r}}) dS \Big\rangle \\ & + p_0 \Big\langle \frac{\partial p^*(\tilde{\vec{r}}_i)}{\partial \vec{n}} G(\tilde{\vec{r}}_i, \tilde{\vec{y}}) \Big\rangle \end{aligned} \tag{9.19}$$

The unknowns of the formulation are clearly the expectation of the square modulus of the boundary unknowns, $\langle |\partial p(\tilde{\vec{r}}_i)/\partial \vec{n}|^2 \rangle$ for $i = 1, 2, ...N_p$.
The auxiliary equation are the expectation of the basic equations (9.17), to evaluate the first order moments, and the conjugate of the basic equations multiplied by the contribution of the primary source $p_0 G(\tilde{\vec{r}}_i, \tilde{\vec{y}})$. The total number of unknowns is $3N_p$.

FOM equations

For $i = 1, 2, ...N_p$, $\tilde{\vec{r}}_i \in \tilde{S}_p$:

$$0 = \sum_{k=1}^{N_p} \Big\langle \frac{\partial p(\tilde{\vec{r}}_k)}{\partial \vec{n}_i} \Big\rangle \Big\langle \int_{\tilde{S}_k} G(\tilde{\vec{r}}_i, \tilde{\vec{r}}) dS \Big\rangle + p_0 \Big\langle G(\tilde{\vec{r}}_i, \tilde{\vec{y}}) \Big\rangle \tag{9.20}$$

Auxiliary equations

For $i = 1, 2, ...N_p$, $\tilde{\vec{r}}_i \in \tilde{S}_p$:

$$\begin{aligned} 0 \;=\; & \Big\langle \frac{\partial p^*(\tilde{\vec{r}}_i)}{\partial \vec{n}} \frac{\partial G(\tilde{\vec{r}}_i, \tilde{\vec{y}})}{\partial \vec{n}} \Big\rangle \Big\langle \int_{\tilde{S}_i} G^*(\tilde{\vec{r}}_i, \tilde{\vec{r}}) dS \Big\rangle \\ & + \sum_{\substack{k=1 \\ k \neq i}}^{N_p} \Big\langle G(\tilde{\vec{r}}_i, \tilde{\vec{y}}) \Big\rangle \Big\langle \frac{\partial p^*(\tilde{\vec{r}}_i)}{\partial \vec{n}} \Big\rangle \Big\langle \int_{\tilde{S}_k} G^*(\tilde{\vec{r}}_i, \tilde{\vec{r}}) dS \Big\rangle + p_0 \Big\langle \Big| G(\tilde{\vec{r}}_i, \tilde{\vec{y}}) \Big|^2 \Big\rangle \end{aligned} \tag{9.21}$$

9.4.2 Analytical representation of the random boundaries

In order to solve the SIF set of equations, the numerical evaluation of the expectations of boundary and domain integrals must be carried out. The integration paths are random, therefore it is not possible to commutate the expectation and the integral operators (as for rods and beams). To simplify this evaluation, it will be shown that the random variable can be judiciously chosen in order to get rid of the randomness in the integration path by means of a change of variable. The way to proceed is illustrated for two different types of boundaries: an arc of a circle and a straight segment, [54].

The random circular boundary

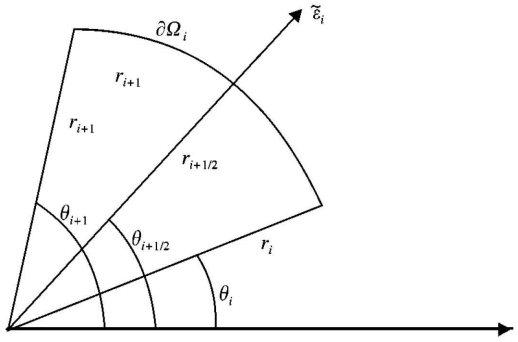

Figure 9.10: SIF acoustical domain. Notation for the circular boundary element

A circle $\partial\Omega$, is divided into n elements. One of these elements $\partial\Omega_i$ is defined by the radius of the circle r, the current angle θ and the two bounds of the element, respectively, defined by their co-ordinates (θ_i, r) and (θ_{i+1}, r). Figure 9.10 illustrates this notation. Then, a random variable is introduced in the definition of the radius r, such as $\partial\tilde{\Omega}(\theta) = \tilde{r}$. More precisely, the random boundary element is defined using the three conditions:

$$\partial\tilde{\Omega}_i(\theta_i) = r, \qquad \partial\tilde{\Omega}_i(\theta_{i+1}) = r, \qquad \partial\tilde{\Omega}_i(\theta_{i+1/2}) = r + \tilde{\varepsilon}_i$$

with $\theta_{i+1/2} = (\theta_i + \theta_{i+1})/2$ and $\tilde{\varepsilon}_i$ is a zero mean random variable. Finally, $\partial\tilde{\Omega}_i$ is defined as a parabolic function of θ

$$\partial\tilde{\Omega}_i(\theta) = \frac{\tilde{\varepsilon}_i\theta^2 - (\theta_i + \theta_{i+1})\tilde{\varepsilon}_i\theta + \theta_i\theta_{i+1}\tilde{\varepsilon}_i - r(\theta_i\theta_{i+1/2} - \theta_i\theta_{i+1} - \theta_{i+1/2}^2 + \theta_{i+1/2}\theta_{i+1})}{-\theta_i\theta_{i+1/2} + \theta_i\theta_{i+1} + \theta_{i+1/2}^2 - \theta_{i+1/2}\theta_{i+1}} \tag{9.22}$$

In order to evaluate the integral of any function $F(\theta)$ over the integration path $\partial\tilde{\Omega}_i$, one may write

$$\int_{\partial\tilde{\Omega}_i} F(\vec{r})d\partial\tilde{\Omega}_i = \int_{\theta_i}^{\theta_{i+1}} F(\theta)\sqrt{\frac{\partial\partial\tilde{\Omega}_i^2}{\partial\theta} + \partial\tilde{\Omega}_i^2}d\theta \tag{9.23}$$

Observation of the right-hand term of the above expression allows one to say that the random variable has disappeared from the integration path. One can finally interchange the integration and the statistical operators. This way of introducing the random parameter in

the definition of the boundary is particularly well suited for circular boundaries; however, this random definition could easily be extended to any other types of boundaries which can be defined in terms of polar co-ordinates.

The random straight boundary

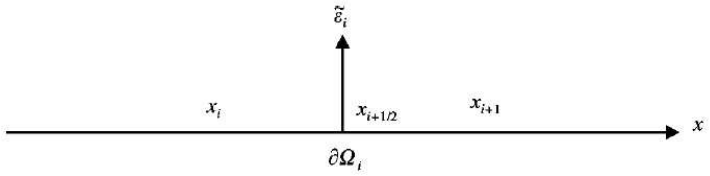

Figure 9.11: SIF acoustical domain. Notation for straight boundary element

Usual mechanical systems are made of assembled rectangular panels with straight boundaries. For this type of geometry, the random variable is introduced using a similar process as for the circular boundaries. Indeed, one may consider a straight boundary element $\partial\tilde{\Omega}_i$, bounded by two points (x_i, y_i) and (x_{i+1}, y_{i+1}). The local frame of reference is chosen so that $y_i = y_{i+1} = y$. The boundary element is represented by figure 9.11.
The random variable is introduced in the definition of the boundary element. Finally, the random element $\partial\tilde{\Omega}_i$ is a parabolic function of the coordinate x, defined by three points:

$$\partial\tilde{\Omega}_i(x_i) = y, \qquad \partial\tilde{\Omega}_i(x_{i+1}) = y, \qquad \partial\tilde{\Omega}_i(x_{i+1/2}) = y + \tilde{y}_{\varepsilon_i}$$

$\tilde{y}_{\varepsilon_i}$ is a zero mean random variable and $x_{i+1/2} = (x_i + x_{i+1})/2$. The analytical expression of $\partial\tilde{\Omega}_i$ may be written as

$$\partial\tilde{\Omega}_i(x) = \frac{\tilde{y}_{\varepsilon_i}x^2 - (x_i + x_{i+1})\tilde{y}_{\varepsilon_i}x + x_i x_{i+1}\tilde{y}_{\varepsilon_i} - y(x_i x_{i+1/2} - x_i x_{i+1} - x_{i+1/2}^2 + x_{i+1}x_{i+1/2})}{-x_i x_{i+1/2} + x_i x_{i+1} + x_{i+1/2}^2 - x_{i+1}x_{i+1/2}} \tag{9.24}$$

The integrals may be evaluated over $\partial\tilde{\Omega}_i$ using a change of variables:

$$\int_{\partial\tilde{\Omega}_i} F(\tilde{x}) d\partial\tilde{\Omega}_i = \int_{x_i}^{x_{i+1}} F(x)\sqrt{1 + \Big(\frac{\partial\partial\tilde{\Omega}_i}{\partial x}\Big)^2}\, dx \tag{9.25}$$

The integration path does not depend on the random variable anymore. Therefore, it is possible to switch the integration and the expectation operators.

9.4.3 SIF 2D acoustical domain: results

As an example, the SIF is applied in this paper to a square 2D domain characterized by Helmholtz equation, figure 9.12. The boundaries of the domain are divided into N elements. F_0 is the external excitation acting on the structure which is supposed to have pressure release boundary conditions:

$$p(\tilde{\vec{r}}_i) = 0 \qquad \text{for} \qquad i = 1 : N_p, N_p = N$$

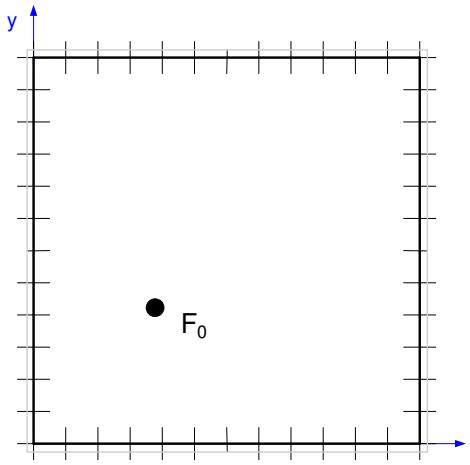

Figure 9.12: SIF acoustical domain. Acoustic 2D domain with random boundaries.

Randomness is introduced in the description of boundary locations and also in the external source location description. The mechanical and geometrical properties of the structure are given in table 9.2, properties which have been selected in such a manner that the membrane presents a mid- high-frequency behaviour in the frequency range of interest. $\sigma_i = 0.05$ for $i = 1 : N_p$.

	Side Length [m]	Sound speed [m/s]	ρ [kg/m^3]	η (%)
Acoustic Domain	1	50.5	10.5	0.03

Table 9.2: SIF application. Acoustic 2D domain: geometrical and physical properties of the acoustic domain.

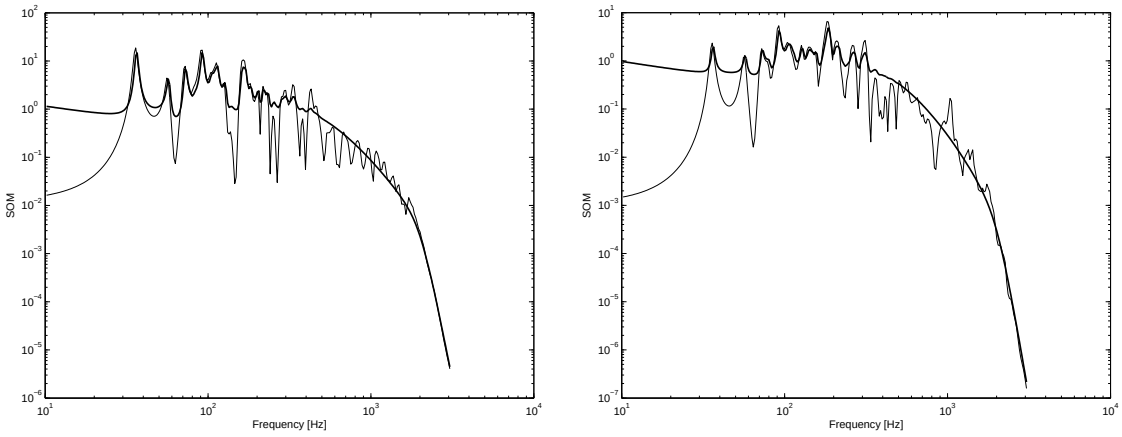

(a) (b)

Figure 9.13: SIF acoustical domain. Frequency evolution of the modulus of the second order moment, $\langle|\partial p(\vec{r}_i)/\partial\vec{n}|^2\rangle$ at nodes 16 (a) and 19 (b). —— SIF. —— BEM.

Figures 9.13-9.16 represent the frequency variations of the expectation of the square

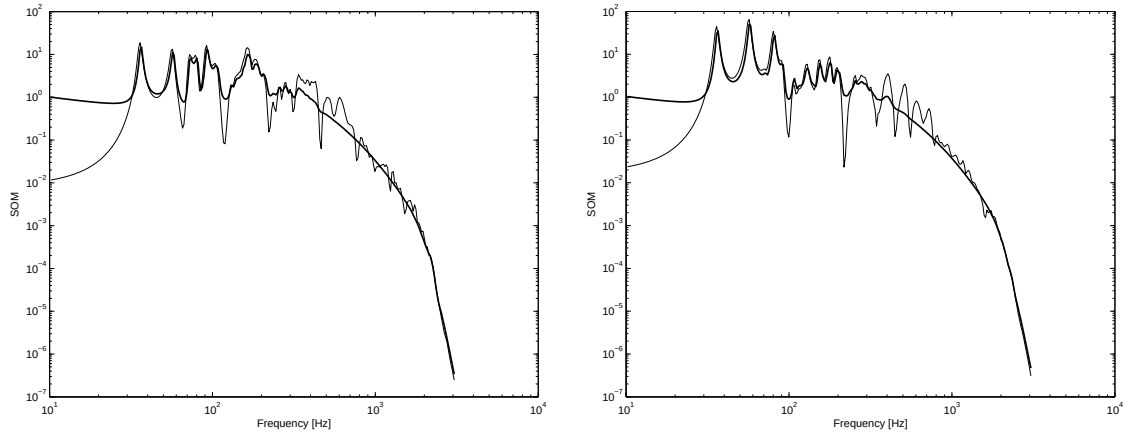

(a) (b)

Figure 9.14: SIF acoustical domain. Frequency evolution of the modulus of the second order moment, $\langle |\partial p(\vec{r}_i)/\partial \vec{n}|^2 \rangle$ at nodes 25 (a) and 31 (b). —— SIF. —— BEM.

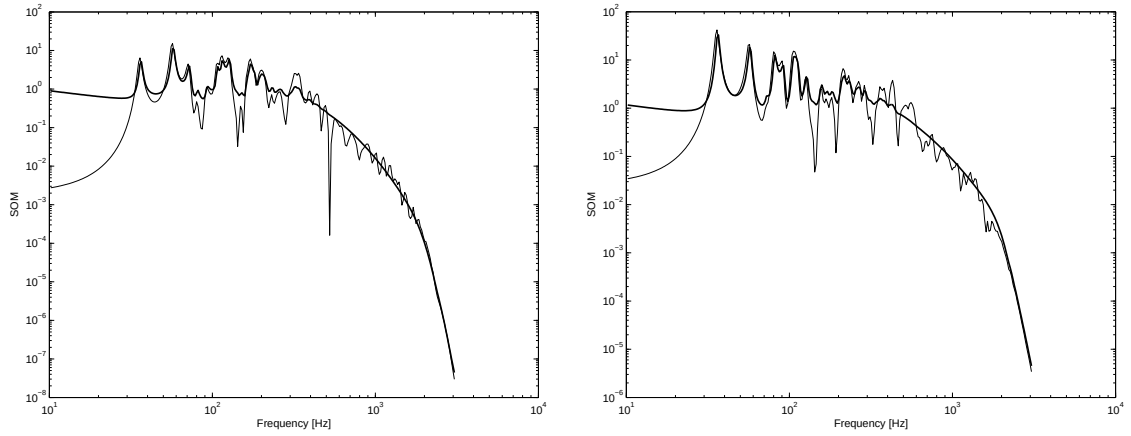

(a) (b)

Figure 9.15: SIF acoustical domain. Frequency evolution of the modulus of the second order moment, $\langle |\partial p(\vec{r}_i)/\partial \vec{n}|^2 \rangle$ at nodes 43 (a) and 49 (b). —— SIF. —— BEM.

modulus of the pressure at two distinct boundary locations. The observation of the curves highlights some important elements concerning the effectiveness of the random formulation. At first, one can globally state that the influence of the randomness increases with frequency. The SIF curves give a precise representation of the modal behaviour in the low-frequency range. On the other hand, the high-frequency behaviour of the random formulation simulation is smooth and only delivers information on the general trend of the frequency variation of the boundary unknowns.

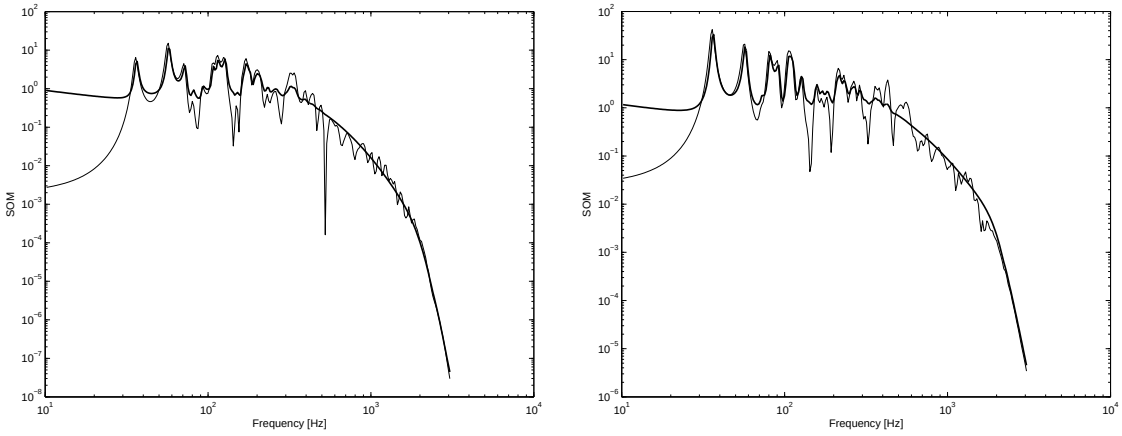

(a) (b)

Figure 9.16: SIF acoustical domain. Frequency evolution of the modulus of the second order moment, $\langle|\partial p(\vec{r}_i)/\partial\vec{n}|^2\rangle$ at nodes 43 (a) and 49 (b). —— SIF. —— BEM.

9.5 BEM-SIF: two acoustical domains

Now we want to extend the hybrid formulation developer for the case of two rods, chapter 8, to a more complex structure. The system chosen is comprised of two 2D acoustic domains, with different sound speed and density, coupled on one side, fig. 9.17.

We want to model the domain 1 with SIF formulation, introducing randomness on the

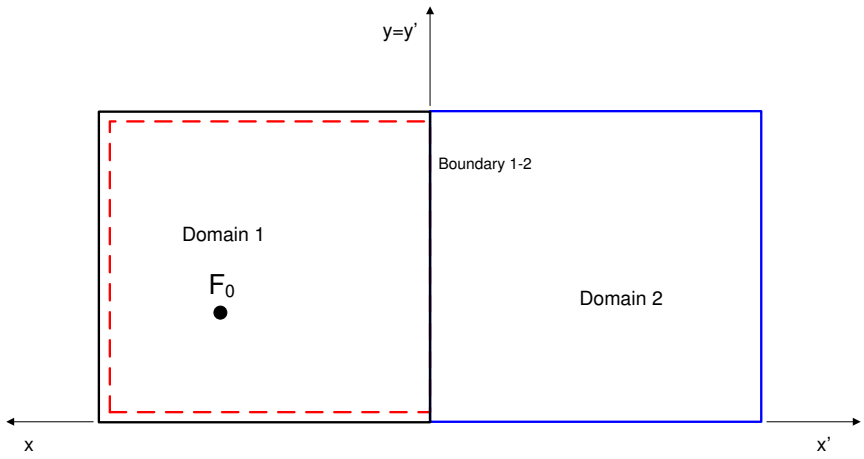

Figure 9.17: BEM-SIF 2acoustical domains. Structure made of two coupled acoustical domain.

uncoupled boundaries. The domain 2, which is low frequency will be modeled with BEM (instead of FEM).

The external excitation F_0 is applied on domain 1, which is the high frequency domain. Thus according to the formulation developed in section 6.5, we should treat the unknowns of domain 2, as correlated each other. As a consequence of this, the number of unknowns of the hybrid formulation will increase dramatically, and consequently the complexity of

the formulation and the calculation resources. The unknowns located on boundary 1-2, which are primary sources for domain number 2 according to the methodology developed in section 6.5, are correlated each other. Indeed they are secondary sources for domain 1 but they are determinictically described. This cause an additional increase of unknowns for the SIF formulation of domain 1.

9.5.1 BEM-SIF two acoustical domains: deriving the equations

The starting point to develop the BEM-SIF formulation is the general BEM equation for an acoustical boundary, eq. (9.4):

$$\begin{aligned}\frac{1}{2}p(\vec{r}_i) &= \sum_{j=1}^{N_p}\int_{S_j}\hat{p}(\vec{r})\frac{\partial G(\vec{r}_i,\vec{r})}{\partial\vec{n}_i}dS - \sum_{j=1}^{N_{\partial p}}p(\vec{r}_j)\int_{S_j}\frac{\partial G(\vec{r}_i,\vec{r})}{\partial\vec{n}_i}dS \\ &+\sum_{j=1}^{N_p}\frac{\partial p(\vec{r}_j i)}{\partial\vec{n}_i}\int_{S_j}G(\vec{r}_i,\vec{r})dS - \sum_{j=1}^{N_{\partial p}}\int_{S_j}\frac{\partial\hat{p}(\vec{r}_j)}{\partial\vec{n}_i}G(\vec{r}_i,\vec{r})dS \\ &+\int_{S_f}f(\vec{y})G(\vec{r}_i,\vec{y})dS \end{aligned} \tag{9.26}$$

To simplify the formulation, without losing generality, we suppose to simplify the formulation to have an equal number of elements on the coupled boundary 1-2, equal to n. While on the other boundary we suppose to have n_1 elements for domain 1, and n_2 elements for domain 2. According to this convention the randomness is applied on the n_1 elements of domain 1.
The structure is supposed to have rigid boundary:

$$\frac{\partial p(\vec{r}_i)}{\partial\vec{n}} = 0 \qquad \text{for} \qquad i = 1:n_1, \text{ and } i = 1:n_2$$

In the equations, we also simplify the notation, writing only the $G(\vec{r}_i,\vec{r})$, instead of $\int_{S_j}G(\vec{r}_i,\vec{r})dS$.
Introducing the random description on boundaries n_1 we can write the first order random equations:

Domain 1

- for $i = 1:n_1$

$$\begin{aligned}-\frac{1}{2}p(\tilde{\vec{r}}_i) &= \sum_{j=1}^{n_1}p(\tilde{\vec{r}}_j)\frac{\partial G_1(\tilde{\vec{r}}_i,\tilde{\vec{r}}_j)}{\partial\vec{n}} + \sum_{j=n_1+1}^{n_1+n}p(\vec{r}_j)\frac{\partial G_1(\tilde{\vec{r}}_i,\vec{r}_j)}{\partial\vec{n}} \\ &-\sum_{k=n_1+1}^{n_1+n}\frac{\partial p(\tilde{\vec{r}}_k)}{\partial\vec{n}}G_1(\tilde{\vec{r}}_i,\vec{r}_k) + F_0G_1(\tilde{\vec{r}}_i,\tilde{\vec{r}}_f)\end{aligned} \tag{9.27}$$

- for $i = n_1+1:n_1+n$

$$\begin{aligned}-\frac{1}{2}p(\vec{r}_i) &= \sum_{j=1}^{n_1}p(\vec{r}_j)\frac{\partial G_1(\vec{r}_i,\tilde{\vec{r}}_j)}{\partial\vec{n}} + \sum_{j=n_1+1}^{n_1+n}p(\vec{r}_j)\frac{\partial G_1(\vec{r}_i,\vec{r}_j)}{\partial\vec{n}} \\ &-\sum_{k=n_1+1}^{n_1+n}\frac{\partial p(\tilde{\vec{r}}_k)}{\partial\vec{n}}G_1(\vec{r}_i,\vec{r}_k) + F_0G_1(\vec{r}_i,\tilde{\vec{r}}_f)\end{aligned} \tag{9.28}$$

Domain 2

- for $i = 1 : n_2 + n$

$$-\frac{1}{2}p(\vec{r}_i) = \sum_{j=1}^{n_2+n} p(\vec{r}_j)\frac{\partial G_2(\vec{r}_i,\vec{r}_j)}{\partial \vec{n}} - \sum_{k=n_2+1}^{n_2+n} \frac{\partial p(\vec{r}_k)}{\partial \vec{n}} G_2(\vec{r}_i,\vec{r}_k) \tag{9.29}$$

Coupling conditions (continuity of force and displacement)

- for $i = 1 : n$

$$p^{(1)}(\vec{r}_i) = p^{(2)}(\vec{r}_i) \tag{9.30}$$

$$\frac{1}{\rho_1}\frac{\partial p^{(1)}(\vec{r}_i)}{\partial \vec{n}} = -\frac{1}{\rho_2}\frac{\partial p^{(2)}(\vec{r}_i)}{\partial \vec{n}} \tag{9.31}$$

The SIF equations for domain 1 are obtained using the classical method reported in section 4.4, while for the second order equations of domain 2, the procedure developed for the FEM-SIF is used, sec. 8.2.

SIF equations domain 1

- for $i = 1 : n_1$

$$\begin{aligned}
-\frac{1}{2}\Big\langle\Big|p(\tilde{\vec{r}}_i)\Big|^2\Big\rangle &= \sum_{\substack{j=1\\ j\neq i}}^{n_1} \Big\langle p^*(\tilde{\vec{r}}_i)\Big\rangle\Big\langle p(\tilde{\vec{r}}_j)\Big\rangle\Big\langle\frac{\partial G_1(\tilde{\vec{r}}_i,\tilde{\vec{r}}_j)}{\partial \vec{n}}\Big\rangle \\
&+ \sum_{j=n_1+1}^{n_1+n} \Big\langle p^*(\tilde{\vec{r}}_i)\Big\rangle\Big\langle p(\vec{r}_j)\Big\rangle\Big\langle\frac{\partial G_1(\tilde{\vec{r}}_i,\vec{r}_j)}{\partial \vec{n}}\Big\rangle \\
&- \sum_{k=n_1+1}^{n_1+n} \Big\langle p^*(\tilde{\vec{r}}_i)\Big\rangle\Big\langle\frac{\partial p(\tilde{\vec{r}}_k)}{\partial \vec{n}}\Big\rangle\Big\langle G_1(\tilde{\vec{r}}_i,\vec{r}_k)\Big\rangle \\
&+ F_0\Big\langle p^*(\tilde{\vec{r}}_i)G_1(\tilde{\vec{r}}_i,\tilde{\vec{r}}_f)\Big\rangle + \Big\langle\Big|p(\tilde{\vec{r}}_i)\Big|^2\Big\rangle\frac{\partial G(\tilde{\vec{r}}_i,\tilde{\vec{r}}_i)}{\partial \vec{n}}
\end{aligned} \tag{9.32}$$

- $i = n_1 + 1 : n_1 + n$

$$\begin{aligned}
-\frac{1}{2}\Big\langle\Big|p(\vec{r}_i)\Big|^2\Big\rangle &= \sum_{j=1}^{n_1} \Big\langle p^*(\vec{r}_i)\Big\rangle\Big\langle p(\vec{r}_j)\Big\rangle\Big\langle\frac{\partial G_1(\vec{r}_i,\tilde{\vec{r}}_j)}{\partial \vec{n}}\Big\rangle \\
&+ \sum_{\substack{j=n_1+1\\ j\neq i}}^{n_1+n} \Big\langle p^*(\vec{r}_i)p(\vec{r}_j)\Big\rangle\frac{\partial G_1(\vec{r}_i,\vec{r}_j)}{\partial \vec{n}} \\
&- \sum_{\substack{k=n_1+1\\ k\neq i}}^{n_1+n} \Big\langle p^*(\vec{r}_i)\frac{\partial p(\tilde{\vec{r}}_k)}{\partial \vec{n}}\Big\rangle G_1(\vec{r}_i,\vec{r}_k) \\
&+ F_0\Big\langle p^*(\vec{r}_i)G_1(\vec{r}_i,\tilde{\vec{r}}_f)\Big\rangle + \Big\langle\Big|p(\vec{r}_i)\Big|^2\Big\rangle\frac{\partial G(\vec{r}_i,\vec{r}_i)}{\partial \vec{n}} \\
&- \Big\langle p^*(\vec{r}_i)\frac{\partial p(\vec{r}_i)}{\partial \vec{n}}\Big\rangle G(\vec{r}_i,\vec{r}_i)
\end{aligned} \tag{9.33}$$

$$
\begin{aligned}
-\frac{1}{2}\Big\langle p(\vec{r}_i)\frac{\partial p^*(\vec{r}_i)}{\partial \vec{n}}\Big\rangle &= \sum_{j=1}^{n_1}\Big\langle \frac{\partial p^*(\vec{r}_i)}{\partial \vec{n}}\Big\rangle\Big\langle p(\vec{r}_j)\Big\rangle\Big\langle \frac{\partial G_1(\vec{r}_i,\tilde{\vec{r}}_j)}{\partial \vec{n}}\Big\rangle \\
&+ \sum_{\substack{j=n_1+1\\ j\neq i}}^{n_1+n}\Big\langle \frac{\partial p^*(\vec{r}_i)}{\partial \vec{n}} p(\vec{r}_j)\Big\rangle \frac{\partial G_1(\vec{r}_i,\vec{r}_j)}{\partial \vec{n}} \\
&- \sum_{\substack{k=n_1+1\\ k\neq i}}^{n_1+n}\Big\langle \frac{\partial p^*(\vec{r}_i)}{\partial \vec{n}}\frac{\partial p(\tilde{\vec{r}}_k)}{\partial \vec{n}}\Big\rangle G_1(\vec{r}_i,\vec{r}_k) \\
&+ F_0\Big\langle \frac{\partial p^*(\vec{r}_i)}{\partial \vec{n}} G_1(\vec{r}_i,\tilde{\vec{r}}_f)\Big\rangle - \Big\langle \Big|\frac{\partial p^*(\vec{r}_i)}{\partial \vec{n}}\Big|^2\Big\rangle G(\vec{r}_i,\vec{r}_i) \\
&- \Big\langle p(\vec{r}_i)\frac{\partial p^*(\vec{r}_i)}{\partial \vec{n}}\Big\rangle \frac{\partial G(\vec{r}_i,\vec{r}_i)}{\partial \vec{n}} \qquad (9.34)
\end{aligned}
$$

SIF equations domain 2

- for $i = 1 : n_2$

$$
\begin{aligned}
-\frac{1}{2}\Big\langle \Big|p(\vec{r}_i)\Big|^2\Big\rangle &= \sum_{\substack{j=1\\ j\neq i}}^{n_2+n}\Big\langle p^*(\vec{r}_i)p(\vec{r}_j)\Big\rangle \frac{\partial G_2(\vec{r}_i,\vec{r}_j)}{\partial \vec{n}} \\
&- \sum_{k=n_2+1}^{n_2+n}\Big\langle p^*(\vec{r}_i)\frac{\partial p(\vec{r}_k)}{\partial \vec{n}}\Big\rangle G_2(\vec{r}_i,\vec{r}_k) \\
&+ \Big\langle \Big|p(\vec{r}_i)\Big|^2\Big\rangle \frac{\partial G(\vec{r}_i,\vec{r}_i)}{\partial \vec{n}} \qquad (9.35)
\end{aligned}
$$

- for $i = n_2 + 1 : n_2 + n$

$$
\begin{aligned}
-\frac{1}{2}\Big\langle \Big|p(\vec{r}_i)\Big|^2\Big\rangle &= \sum_{\substack{j=1\\ j\neq i}}^{n_2+n}\Big\langle p^*(\vec{r}_i)p(\vec{r}_j)\Big\rangle \frac{\partial G_2(\vec{r}_i,\vec{r}_j)}{\partial \vec{n}} \\
&- \sum_{\substack{k=n_2+1\\ k\neq i}}^{n_2+n}\Big\langle p^*(\vec{r}_i)\frac{\partial p(\vec{r}_k)}{\partial \vec{n}}\Big\rangle G_2(\vec{r}_i,\vec{r}_k) \\
&+ \Big\langle \Big|p(\vec{r}_i)\Big|^2\Big\rangle \frac{\partial G(\vec{r}_i,\vec{r}_i)}{\partial \vec{n}} - \Big\langle p^*(\vec{r}_i)\frac{\partial p(\vec{r}_i)}{\partial \vec{n}}\Big\rangle G(\vec{r}_i,\vec{r}_i) \qquad (9.36)
\end{aligned}
$$

$$
\begin{aligned}
-\frac{1}{2}\Big\langle p(\vec{r}_i)\frac{\partial p^*(\vec{r}_i)}{\partial \vec{n}}\Big\rangle &= \sum_{\substack{j=1\\ j\neq i}}^{n_2+n}\Big\langle \frac{\partial p^*(\vec{r}_i)}{\partial \vec{n}} p(\vec{r}_j)\Big\rangle \frac{\partial G_2(\vec{r}_i,\vec{r}_j)}{\partial \vec{n}} \\
&- \sum_{\substack{k=n_2+1\\ k\neq i}}^{n_2+n}\Big\langle \frac{\partial p^*(\vec{r}_i)}{\partial \vec{n}}\frac{\partial p(\vec{r}_k)}{\partial \vec{n}}\Big\rangle G_2(\vec{r}_i,\vec{r}_k) \\
&- \Big\langle \Big|\frac{\partial p^*(\vec{r}_i)}{\partial \vec{n}}\Big|^2\Big\rangle G(\vec{r}_i,\vec{r}_i) \\
&+ \Big\langle p(\vec{r}_i)\frac{\partial p^*(\vec{r}_i)}{\partial \vec{n}}\Big\rangle \frac{\partial G((\vec{r}_i,\vec{r}_i))}{\partial \vec{n}} \qquad (9.37)
\end{aligned}
$$

$n_{elements}$	$\mathrm{n}_{unknowns}$ domain1	$\mathrm{n}_{unknowns}$ domain 2	$\mathrm{n}_{unknowns}$ total
8	32	100	132
16	96	400	496
40	480	2500	2980

Table 9.3: BEM-SIF numerical application. Unknowns of the formulation as a function of the number of boundary elements.

As we can understand from the equations (9.32)-(9.37) the number of unknowns has increased of one order with respect to the classical formulation for 1D systems. In particular it is a function of $n^2_{elements}$ as we can understand from table 9.3, where $n_{elements}$ is the total number of elements on each acoustical domain. Thus the formulation is heavy from the computational point of view.

The missing equations, can be found as usual, getting the expectation of the basic random equations, eqs. (9.27)-(9.29), for first order moment solution (if required). Moreover, multiplying the basic equations of both domain 1 (and 2), for the contribution of the primary source, F_0 (the unknowns on the boundary 1-2 which is an extended primary source for domain 2).

9.5.2 BEM-SIF two acoustical domains: results

The hybrid formulation has been used to evaluate the response of a structure made of two coupled 2D acoustic domains, fig. 9.17. Domain 1 exhibits a HF behaviour in the frequency range of interest. Randomness is introduced to its boundaries and to the force location. Domain 2 is LF behaving and is deterministically described. The coupling boundary between domain 1 and 2 is deterministic. The physical properties of the structure, which have been tuned to satisfy the mid-frequency condition, are reported in table 9.4. External excitation is located at point $x_f = 0.41$m, $y_f = 0.23$m. Domain 1 is modelled with SIF, and randomness ($\sigma = 0.05$) is introduced on boundaries which are not coupled with domain 2, which is deterministic and modelled with FEM. First order moments are included into the formulation to have a more accurate response even at low frequencies.

The frequency variations of the pressure at distinct locations, on domain 1 and 2, are depicted on figs. 9.18-9.23. The frequency variation of the response is gradually getting smoother when the frequency increases for the domain 1, and simultaneously, an accurate description of the response of the deterministic domain is obtained.

	side length [m]	sound speed [m/s]	ρ [kg/m^3]	η [%]
Domain 1	1.0	25	10	0.02
Domain 2	1.0	600	250	0.02

Table 9.4: BEM-SIF numerical application: two acoustic domains. Parameters of the coupled acoustical domains

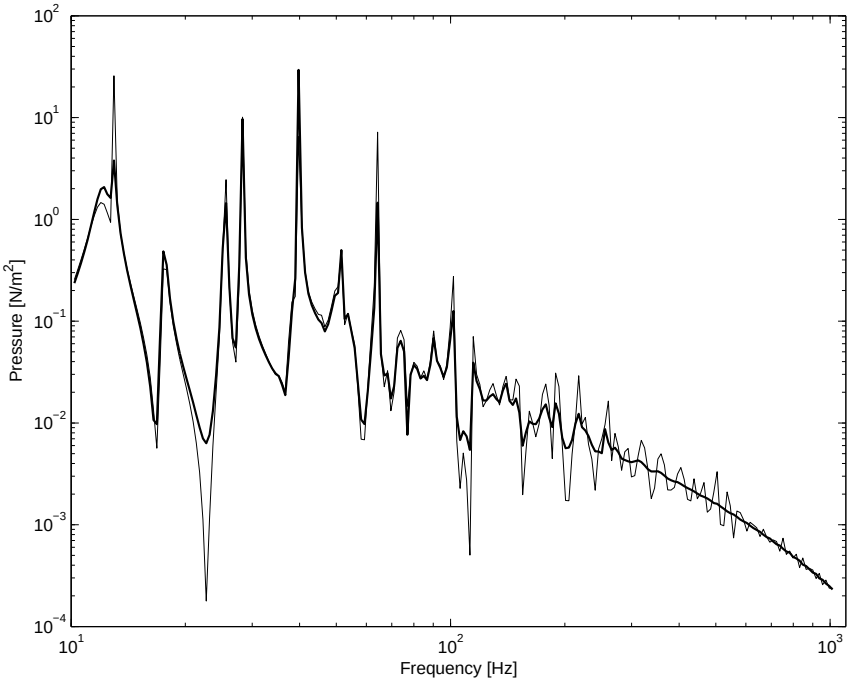

Figure 9.18: Application of hybrid BEM-SIF formulation: two acoustical domains. Frequency evolution of the pressure value at a boundary node of domain 1. —— BEM-SIF. —— BEM.

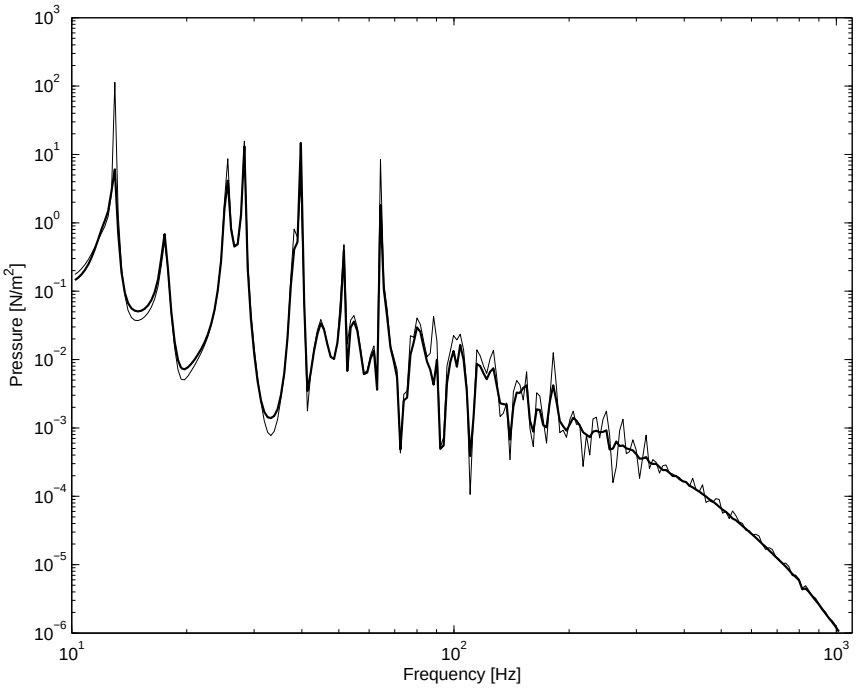

Figure 9.19: Application of hybrid BEM-SIF formulation: two acoustic domains. Frequency evolution of the pressure value at a boundary node of domain 1. —— BEM-SIF. —— BEM.

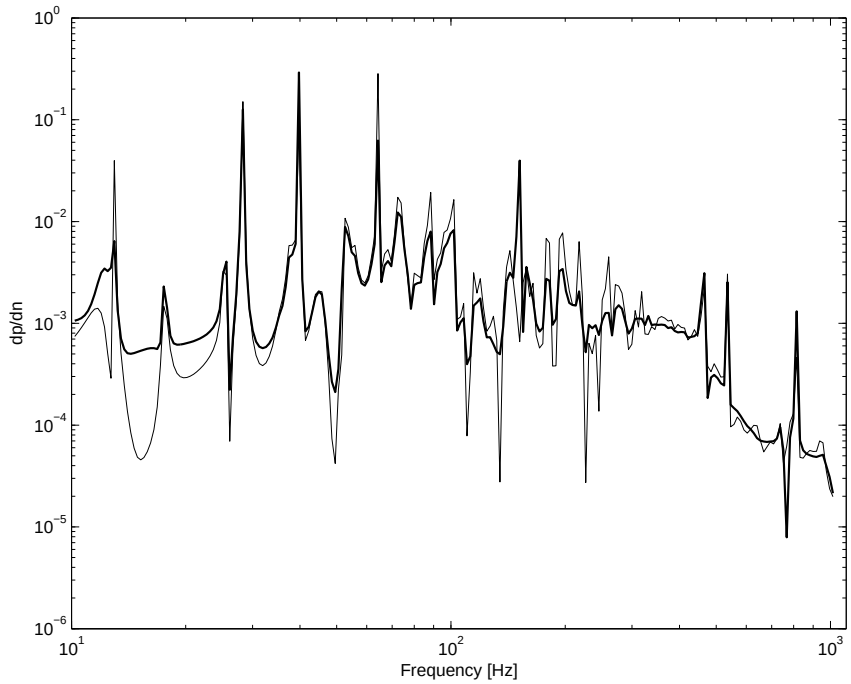

Figure 9.20: Application of hybrid FEM-SIF formulation: two acoustic domains. Frequency evolution of the $\partial p/\partial n$ value at a boundary node of domain 1. —— BEM-SIF. —— BEM.

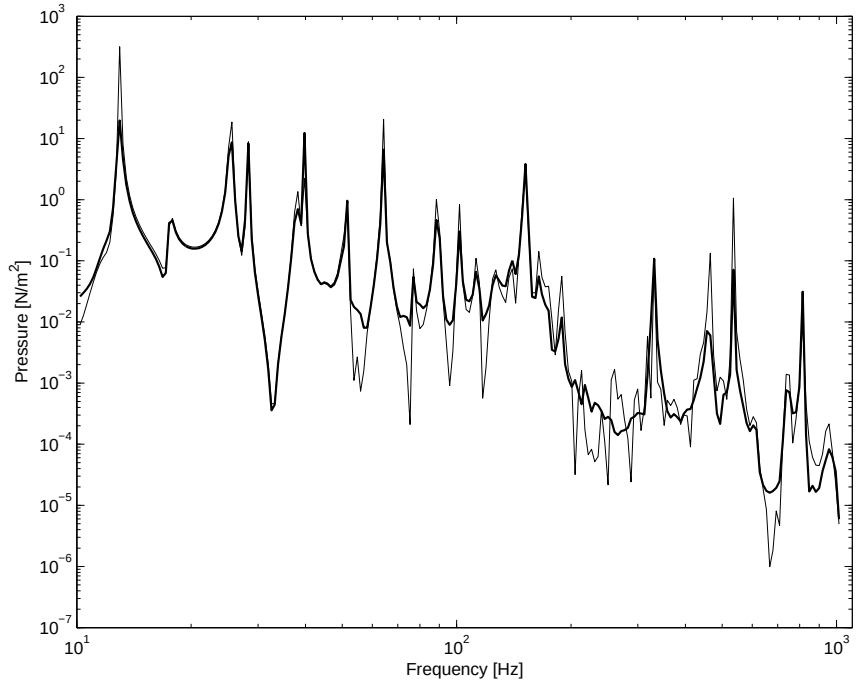

Figure 9.21: Application of hybrid FEM-SIF formulation: two acoustic domains. Frequency evolution of the pressure value at a boundary node of domain 2. —— BEM-SIF. —— BEM.

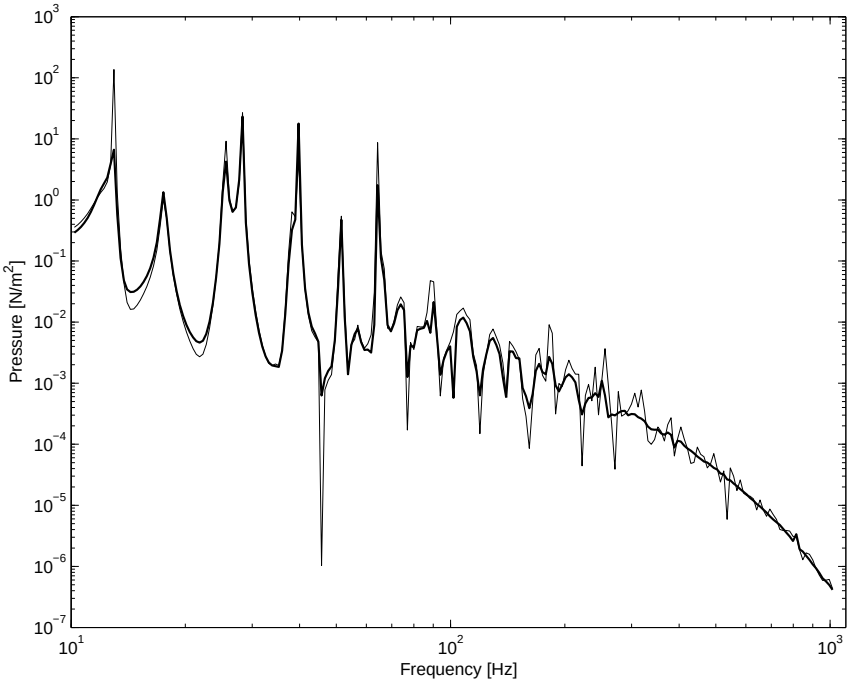

Figure 9.22: Application of hybrid FEM-SIF formulation: two acoustic domains. Frequency evolution of the pressure value at a boundary node of domain 2. —— BEM-SIF. —— BEM.

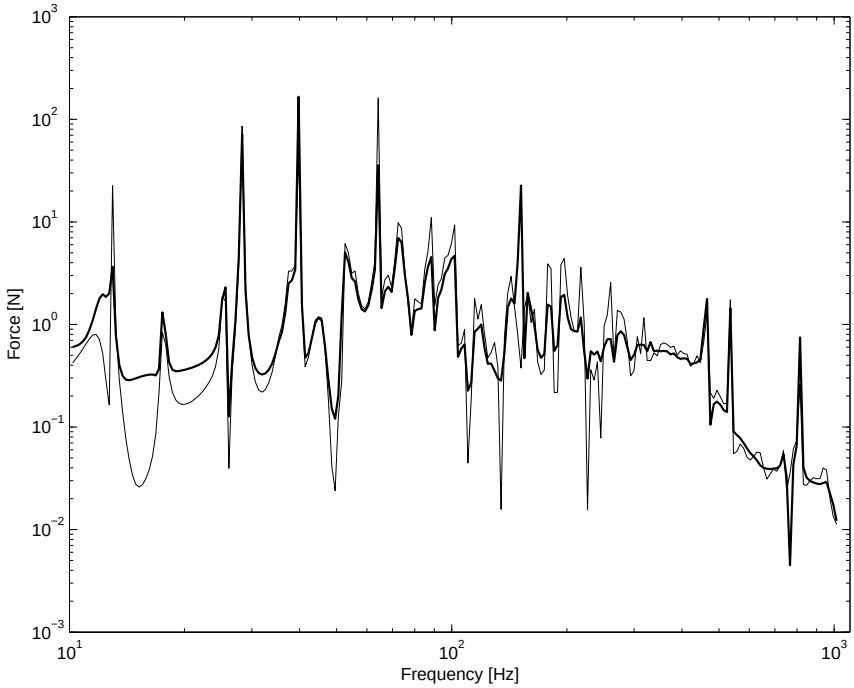

Figure 9.23: Application of hybrid FEM-SIF formulation: two acoustic domains. Frequency evolution of the $\partial p/\partial n$ value at a boundary node of domain 2. —— BEM-SIF. —— BEM.

9.6 Discussion

The hybrid formulation which has been developed for the two rods, is a consinstent formulation for the mid-frequency problem. The results obtained for a 2D structure are good and consinstent to those obtained for the two rods. The frequency variation of the response is gradually getting smoother when the frequency increases for the domain 1, and simultaneously, an accurate description of the response of the deterministic domain is obtained. Moreover The SIF formulation has been proved to be consistent to deal with the high-frequency part of a mid-frequency structure.
The major drawback of this formulation is the increased complexity of the method when dealing with more complex structure than 1D. This could be a limitation when dealing with complex structure made of several components.

It will be the topic of the next chapter the simplification and the improvement of the formulation to deal with 2D structure made of a greater number of subsystems than 2.

Chapter 10

Simplification and improvement of the formulation for mid-frequency applications

The hybrid formulation which have been presented in the previous chapter, has been proved to be consistent for dealing with mid-frequency structures, but it presents a complexity drawback if we think to an application on a very complex structure, made of several subsystems.
Now we want to improve the formulation to simplify it, and also to make it more "mid-frequency". This is done in the optic to make the formulation usable for more complex structures, because already for a a simple structure made of two coupled domains we obtain a model which is complex to make it easy to use, even if it works perfectly and accounts properly to all the different contributions which are present in the structure response.

To do this an approach which is very similar to those used by Vlahopoulos [52], Langley [47] and Soize [42] is developed. The external force is supposed to be applied on a short member (but an analogous method can be used if the excitation is applied on short members), so a subsystem which present a LF behavior. The underlying idea of the approach is that when dealing with a structure made of several subsystems with both LF and HF behavior in the frequency range of interest, we can split the contribution into the primary and predominant direct contributions belonging to the excited deterministic subsystems, the contributions of the other deterministic subsystems, and the reverberant contributions of the attached HF subsystems. In this view, we can first solve the deterministic subsystems accounting only for the HF parts treated as semi-infinite because supposed to vibrate in their HF field. Then solve the HF parts in terms of statistical variables.

We use an approach in which first are solved the deterministic structure, accounting only for the reverberant contribution in terms of damping of the statistical subsystems. Then, once the deterministic contributions are solved, thanks to SIF we can model also the response of the high frequency part of the structure.

The formulation is developed and illustrated for a structure made of three subsystems, three acoustical domains. Domain number 1 is a LF domain and it is directly excited. Some HF and LF subsystems are coupled to this subsystems.

The method to can be summarized into 3 steps:

1. The subsystem 1, the one directly excited is solved as coupled only with the bound-

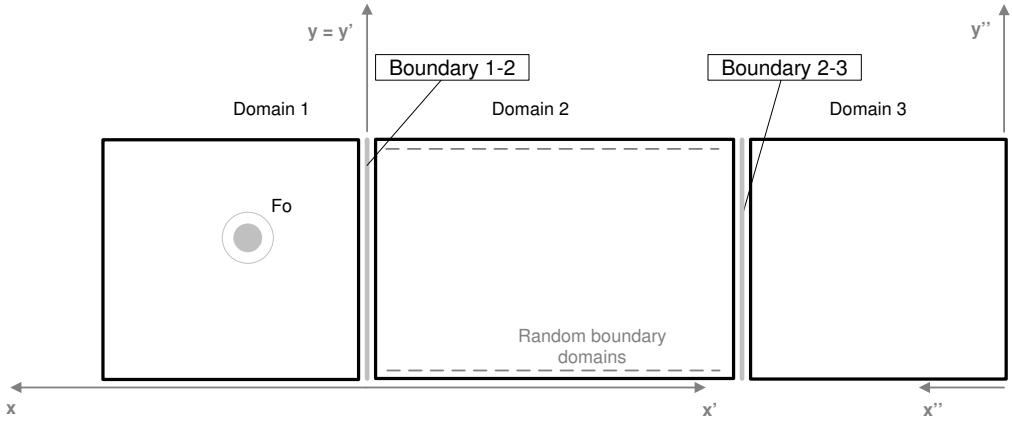

Figure 10.1: Three coupled acoustical domains

ary 1-2, figure 10.2. The domain 2, the HF domain, is supposed to be completely reverberant. In terms of direct field contribution stemming from the domain 1, it can be considered as a semi-infinite domain, without reflection contributions coming from the other side of the domain except for the one coupled with domain 1. The solution which we evaluate is a FOM solution, because domain 1 is the driving domain in terms of importance of contributions, and it can be completely characterized using the FOM.

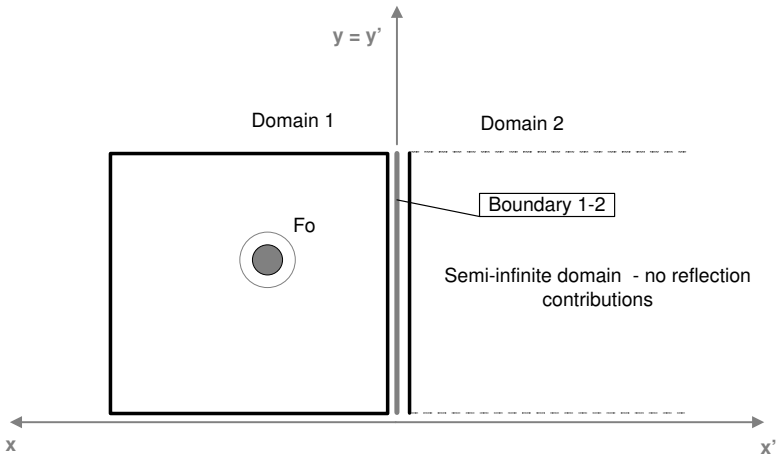

Figure 10.2: Step 1 of the mid-frequency method

2. Then domain 3 it is solved coupled to boundary 2-3, figure 10.3. The contribution coming from boundary 1-2 (solved at step 1) are the exciting sources. Those contributions are direct contributions and are sufficiently to characterize the response of domain 3.

3. Finally, the boundaries of domain 2 which are not coupled with the other LF domains are solved, figure 10.4. The SIF formulation is used and randomness is introduced in the description of uncoupled sides geometry. The solution is obtained in terms of

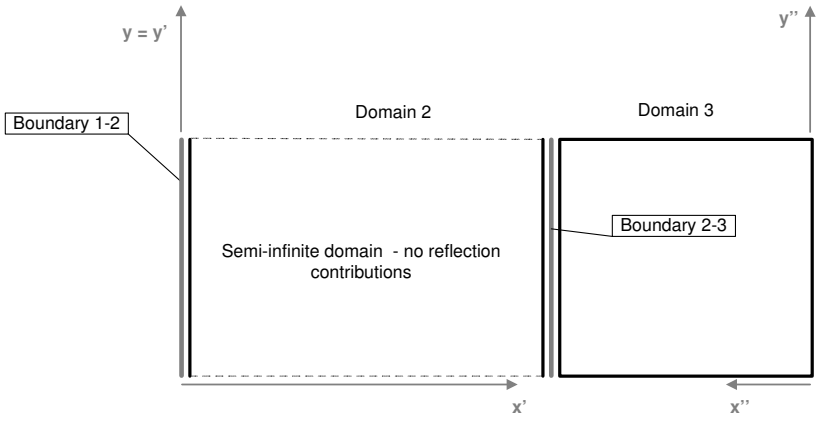

Figure 10.3: Step 2 of the mid-frequency method

SOM moments.

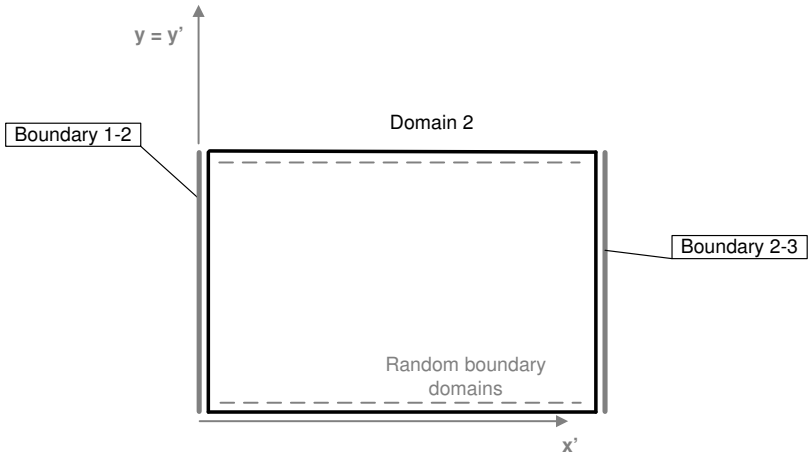

Figure 10.4: Step 3 of the mid-frequency method

The main advantage of a formulation built this way is that the features the mid-frequency range are used to simplify the formulation previously developed. The refinement of the discretization used in this method it is ruled by the LF subsystems, because for the HF subsystems a statistical formulation is used and this produces no need of a refined mesh.
This method also allows to couple efficiently, in principle, as many subsystems as we want without increasing the complexity of the formulation itself. This is a great advantage compared to the complexity required for instance to solve the structure made of two coupled acoustical domains of section 9.5.
The efficiency of this methodology will be proved in the following sections with some numerical examples.

10.1 Application FEM-SIF to a fluid-structure system

A numerical application of the FEM-SIF formulation to a structure made of an acoustic domain coupled with a beam, figure 10.5, is presented section. Before presenting the results obtained with the hybrid method, we need to have a brief review of the FEM-BEM method to deal with fluid-structure coupling problems.

10.1.1 The FEM-BEM for fluid-structure interaction

The hybrid FEM-BEM formulation is used in structural acoustics for the numerical prediction of the dynamic response of coupled fluid-structure systems [62, 63].
The fluid is treated as a compressible, inviscid, non-flowing medium whose pressure satisfies the wave equation

$$\nabla^2 p = \frac{\ddot{p}}{c^2} \tag{10.1}$$

where ∇^2 is the Laplacian operator, p is the dynamic fluid pressure (the excess above ambient), c is the wave speed in the fluid, and dots denote partial differentiation with respect to time. Boundary conditions include the rigid wall condition,

$$\frac{\partial p}{\partial \vec{n}} = 0 \tag{10.2}$$

(where n is the normal), and the pressure-release condition, $p = 0$.
At an accelerating boundary (a fluid-structure interface), momentum and continuity considerations require that

$$\frac{\partial p}{\partial \vec{n}} = -\rho \ddot{u}_n \tag{10.3}$$

where ρ is the fluid density, and $\ddot{u}_n$, is the normal component of fluid particle acceleration. This condition expresses the effect of structural motion on the fluid. The effect of fluid pressure on the structure is imposed as a load, proportional to pressure, applied to the wet surface of the structure.
For time-harmonic excitation, for which the time dependence is $e^{i\omega t}$, the wave equation (10.1) becomes the Helmholtz equation

$$\nabla^2 p(\vec{r}) + kp(\vec{r}) = 0 \tag{10.4}$$

where ω is the circular frequency, p now represents the complex amplitude of pressure, and $k = \omega/c$ is the acoustic wavenumber.
The structure, if it can be assumed to remain elastic, behaves according to the theory of elasticity and the various approximate engineering theories for beams, plates, and shells. The structure is supposed to be modelled using a classical finite element method formulation, which for time-harmonic excitation can be written as:

$$[-\omega^2 M + K]u = [F] \tag{10.5}$$

where $[u]$ is the vector of unknowns, K is the stiffness matrix which accounts also for the damping effects, M is the mass matrix, $[F]$ is the vector of forces acting on the structure. The two method can be easily coupled, supposing to have fluids heavy enough to influence structural response, so that a two-way coupling is required.

Structure FEM equations

$$[-\omega^2 M + K]u = [F_e] - [N][A]p, \tag{10.6}$$

where $[A]$ is the "wet" surface area matrix, $[N]$ is the matrix of rectangular transformation which converts the globa coordinates to the normal coordinates, and $[F_e]$ is the vector of external forces acting on the structure (no fluid interactions).

Fluid BEM equations

$$-\frac{1}{2}p(\vec{r}) = \int_S \Big[p(\vec{r}_q)\frac{\partial G(\vec{r},\vec{r}_q)}{\partial \vec{n}_q} - \frac{\partial p(\vec{r}_q)}{\partial \vec{n}_q}G(\vec{r},\vec{r}_q)\Big]dS + \int_{S_f} F(\vec{r}_f)G(\vec{r},\vec{r}_f)dS_f \tag{10.7}$$

where $F(\vec{r}_f)$ is the external force acting in the fluid at location $\vec{r}_f$.

Coupling equations at the wet surface

$$\frac{\partial p(\vec{r})}{\partial \vec{n}} = -\rho\omega^2[u_n], \tag{10.8}$$

where $[u_n] = [N][u]$ is the vector of normal displacement respect the wet surface.

10.1.2 FEM-SIF for a fluid-structure system

The hybrid FEM-SIF formulation is developed according to the steps presented at the beginning of this chapter. The SIF is used to model the HF fluid subsystem and replaces the BEM formulation in fluid-structure coupling.
A numerical application of the FEM-SIF formulation to a mid-frequency structure made of an acoustic domain coupled with a beam, figure 10.5, is presented. The beam is supposed to be LF behaving. It is a clamped-clamped beam, coupled with one side of the membrane, and it is excited by a bending moment, M_0, and shear, T_0. The acoustical domain is supposed to be HF and its boundary locations which are not coupled with the beam, are affected from randomness. The physical properties of the structure, which have been tuned to have an effective mid-frequency behaviour, are reported in tables 10.1 and 10.2.

	Side Length [m]	Sound speed [m/s]	ρ [kg/m^3]	η (%)
Acoustic Domain	1	100.5	10.5	0.02

Table 10.1: Mid-frequency structure: geometrical and physical properties of the Acoustic domain.

The frequency variations of the second order moment at point P_0 and P_2 which are inside

	Length [m]	E [N/m^2]	S [m^2]	ρ [kg/m^3]	I$_z$ [m^4]	η (%)
Beam	1	$2.1\cdot 10^{-11}$	$2.5\cdot 10^{-2}$	7800	$3.25\cdot 10^{-6}$	0.02

Table 10.2: Mid-frequency structure: Geometrical and physical properties of the beam.

the acoustical domain are illustrated by figures 10.6 and 10.7. We obtain a smooth contribution for the unknowns of the random acoustical domain, and a detailed description of the contribution of the deterministic beam. Figures 10.6 and 10.7 illustrates that coupling FEM and SIF theory to model a mid-frequency behaving structure leads to relevant results.
From the legend in figures 10.6 and 10.7 we can also notice that the FEM-SIF formulation requires a less refined mesh than classical FEM-BEM method. Thus the formulation of the

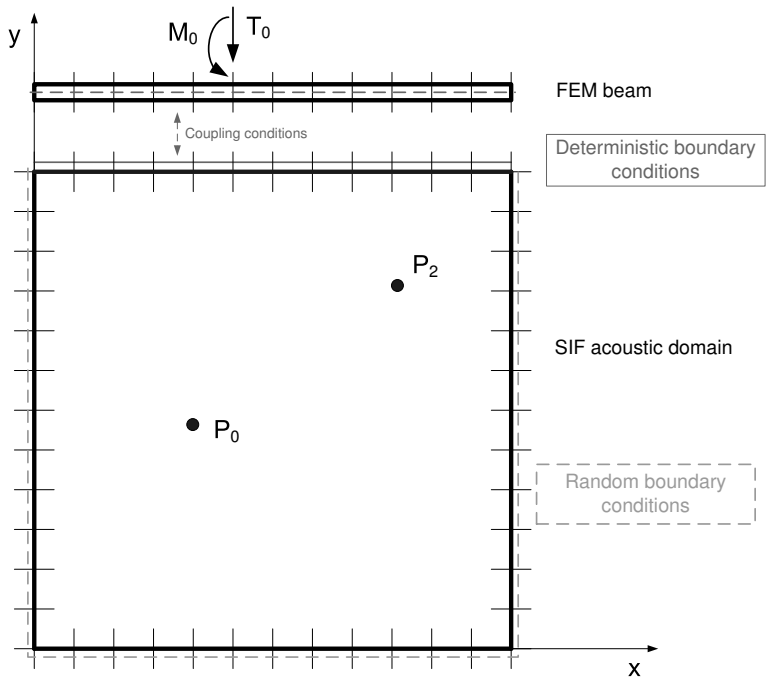

Figure 10.5: Mid-frequency structure: acoustic random domain coupled with a deterministic beam.

hybrid method can be regarded as more complex than classical techniques, but it presents a benefit in terms of number of elements required to obtain significative results.
Other relevant results evaluated at boundary points, for different properties of the structure, configuration n.2 tables 10.3 and 10.4, are reported in figure 10.8.

	Side Length [m]	Sound speed [m/s]	ρ [kg/m^3]	η (%)
Acoustic Domain	1	57.0	76.5	0.02

Table 10.3: Mid-frequency structure: geometrical and physical properties of the Acoustic domain. Configuration n.2.

	Length [m]	E [N/m^2]	S [m^2]	ρ [kg/m^3]	I$_z$ [m^4]	η (%)
Beam	1	$2.1\cdot 10^{-11}$	$2.5\cdot 10^{-3}$	7800	$3.8\cdot 10^{-6}$	0.02

Table 10.4: Mid-frequency structure: Geometrical and physical properties of the beam. Configuration n.2.

These results are very important because they prove that SIF theory can be coupled to a deterministic technique to predict the dynamic behaviour of a mid-frequency structure. This hybrid technique appears like an efficient approach to treat structure-borne mid-frequency problem.

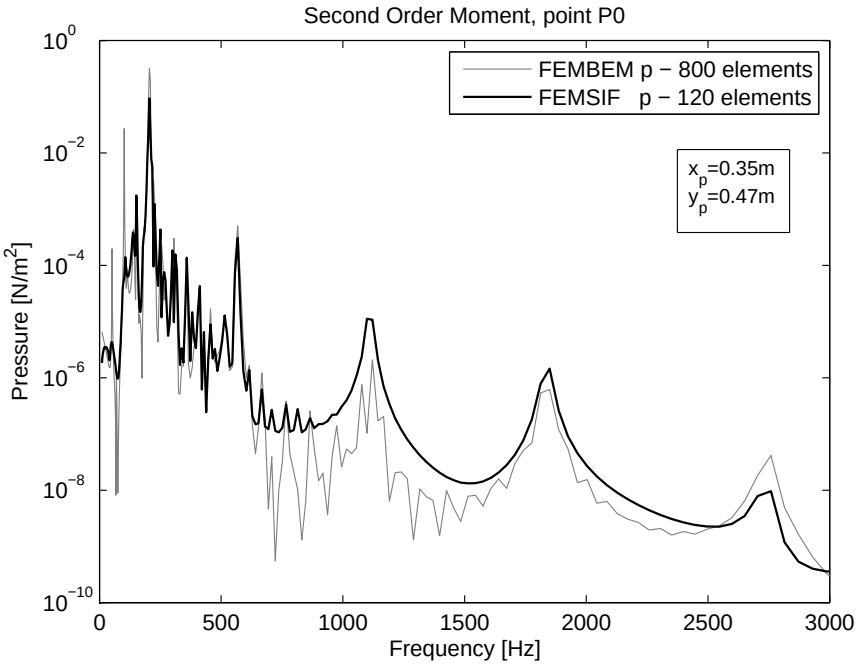

Figure 10.6: FEM-SIF formulation for mid-frequency application: Frequency variation of the second order moments at point P_0 and inside the domain, comparison of the deterministic result with the SIF predictions. —— FEM-SIF. —— FEM-BEM.

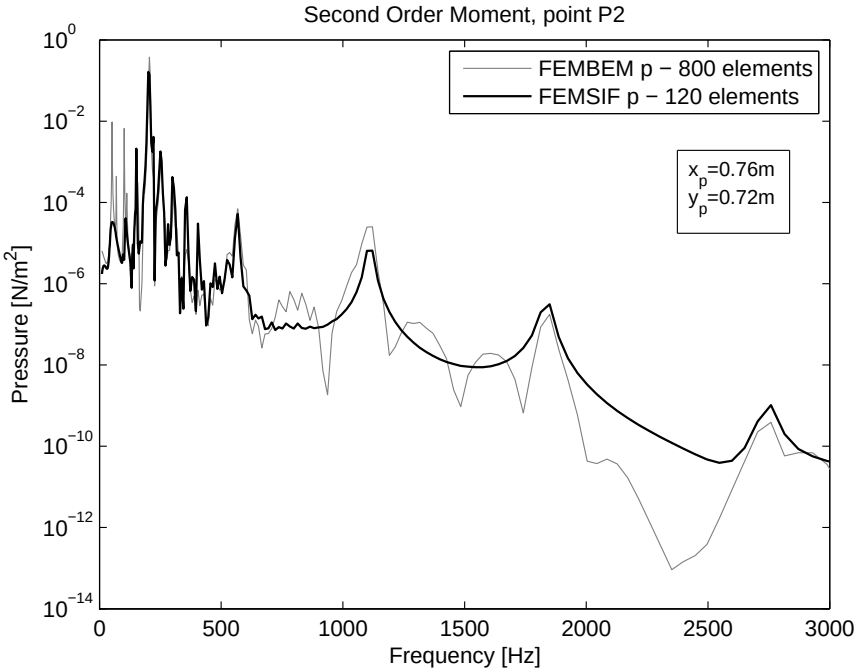

Figure 10.7: FEM-SIF formulation for mid-frequency application: Frequency variation of the second order moments at point P_2 and inside the domain, comparison of the deterministic result with the SIF predictions. —— FEM-SIF. —— FEM-BEM.

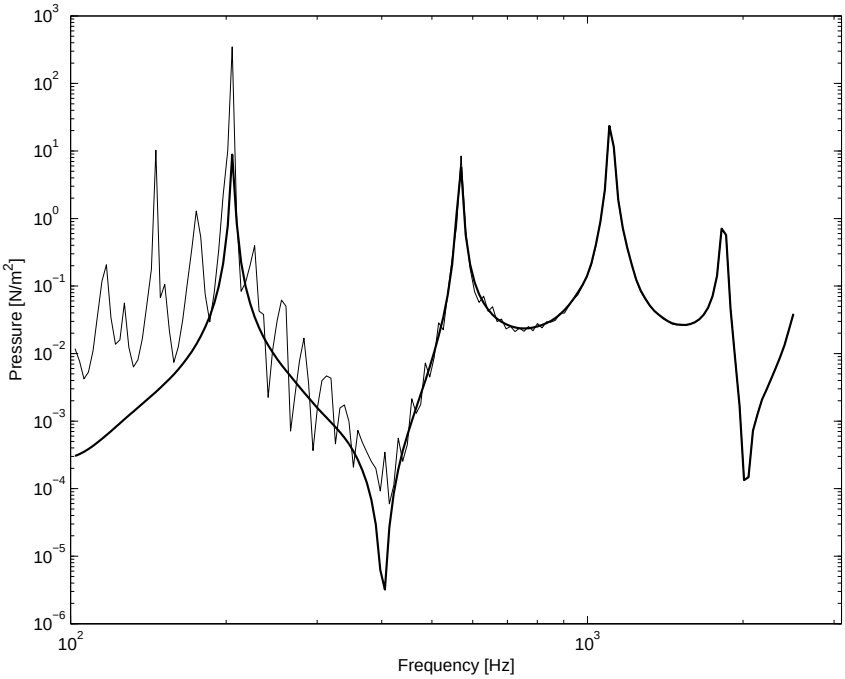

(a)

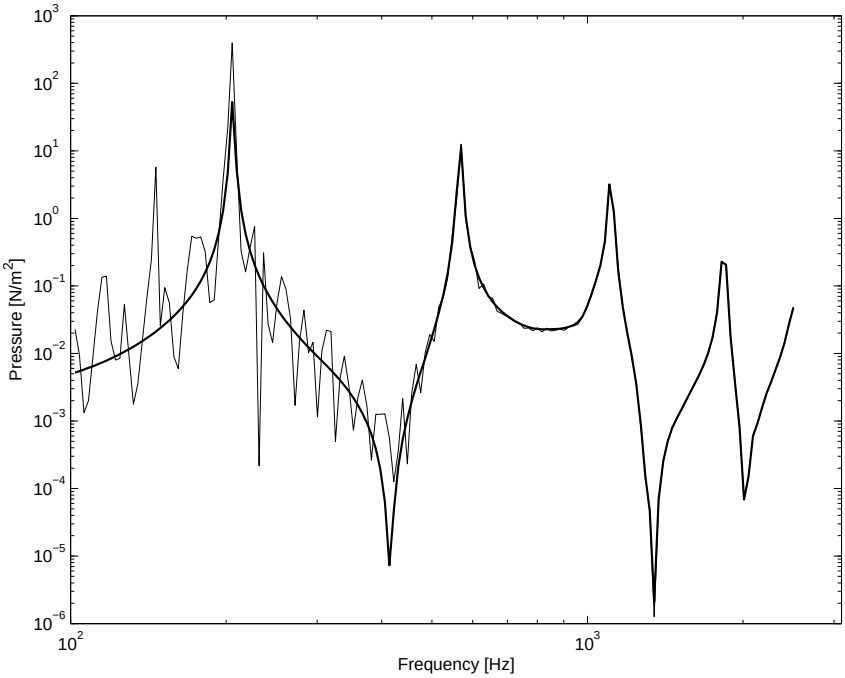

(b)

Figure 10.8: FEM-SIF formulation for mid-frequency application: Frequency variation of the second order moments at boundary points on the wet surface, comparison of the deterministic result with the SIF predictions node 64 (a) and 67 (b). —— FEM-SIF. —— FEM-BEM.

10.2 Application FEM-SIF: two beams coupled with an acoustic domain

As an extension of the formulation introduced in the previous section, we want now to apply the FEM-SIF formulation to a structure made of three subsystems. Two beam which are coupled with a 2D acoustic domain, like a "sandwich" structure, figure 10.9. The application of the methodology to a three dimensional structure allows us to test entirely the formulation.

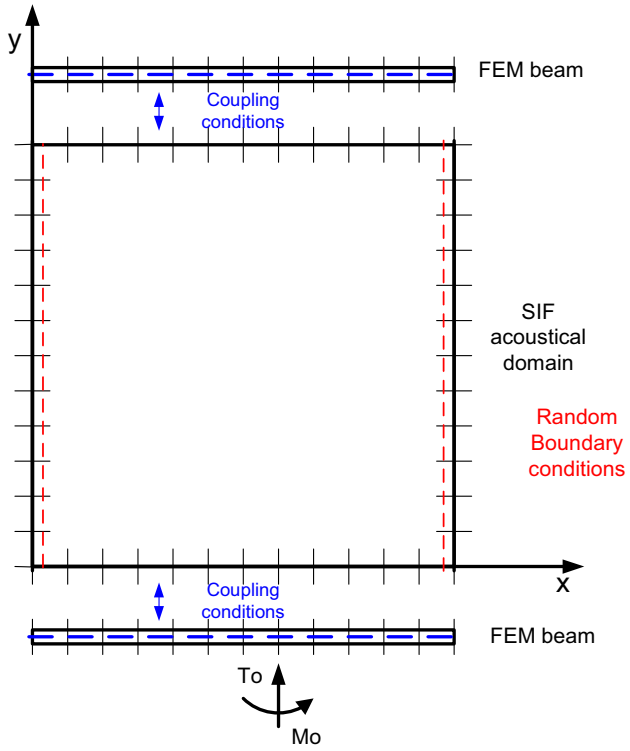

Figure 10.9: Mid-frequency structure, two beams-acoustic domain: acoustic random domain coupled with two deterministic beams.

The geometrical and physical properties of the structure are reported in tables 10.5 and 10.6.

	Side Length [m]	Sound speed [m/s]	ρ [kg/m^3]	η (%)
Acoustic Domain	1	79.5	76.5	0.02

Table 10.5: Mid-frequency structure, two beams-acoustic domain: geometrical and physical properties of the Acoustic domain.

We obtain a smooth contribution for the unknowns of the random acoustical domain, and a detailed description of the contribution of the deterministic beam. Figures 10.10-10.11 illustrates that coupling FEM and SIF theory to model a mid-frequency behaving structure leads to relevant results.

	Length [m]	E [N/m^2]	S [m^2]	ρ [kg/m^3]	I$_z$ [m^4]	η (%)
Beam 1	1	$2.1\cdot 10^{-11}$	$2.5\cdot 10^{-3}$	7800	$3.25\cdot 10^{-6}$	0.01
Beam 2	1	$1.9\cdot 10^{-11}$	$3.1\cdot 10^{-3}$	7700	$3.98\cdot 10^{-6}$	0.01

Table 10.6: Mid-frequency structure, two beams-acoustic domain: Geometrical and physical properties of the beams.

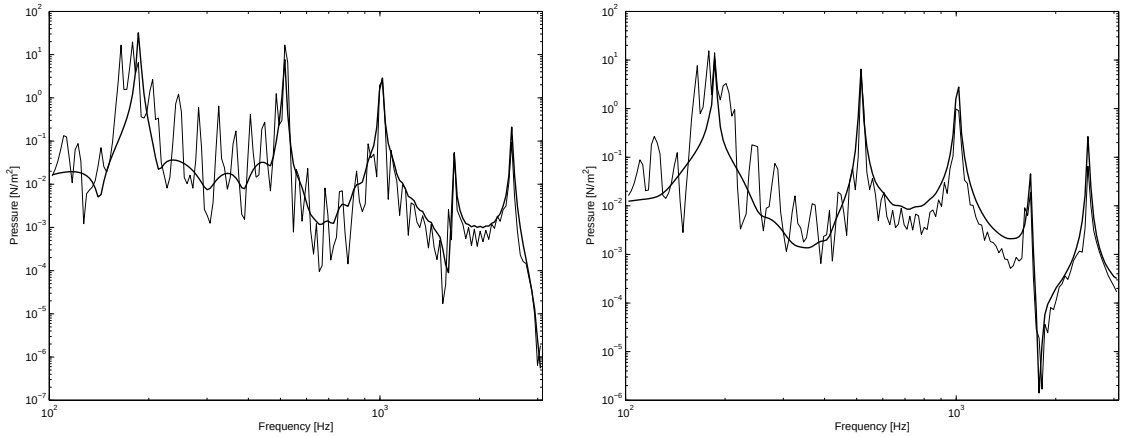

(a) (b)

Figure 10.10: FEM-SIF formulation for mid-frequency application, two beams-acoustic domain: Frequency variation of the second order moments at boundary point on the uncoupled side of the domain, comparison of the deterministic result with the SIF predictions nodes 11 (a) and 51 (b). —— FEM-SIF. —— FEM-BEM.

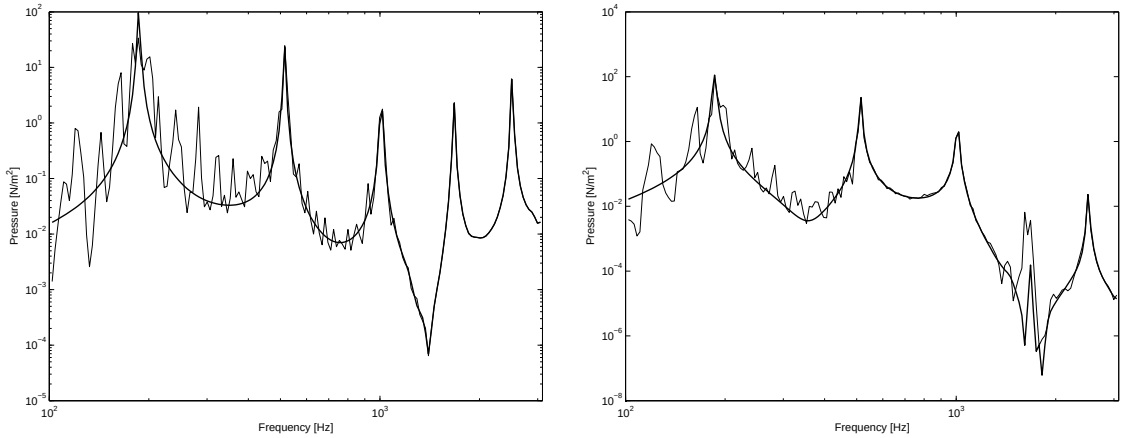

(a) (b)

Figure 10.11: FEM-SIF formulation for mid-frequency application, two beams-acoustic domain: Frequency variation of the second order moments at boundary points on the wet surface between the domain and the excited beam (a) node 73 and the opposite beam (b) node 35, comparison of the deterministic result with the SIF predictions. —— FEM-SIF. —— FEM-BEM.

10.3 Application BEM-SIF: three acoustic domains

A second application for a structure made of three subsystems is here reported. This kind of application has been chosen to prove the efficiency of the formulation to model

complex structures. The structure chosen is made of three 2D acoustical domains, figure 10.12. Domain 1 is a LF domain and is directly excited with a punctual pressure source F_0 on point $x_f = 0.41$m, $y_f = 0.23$m. Domain 2 is a HF domain, and randomness is applied on the boundaries which are uncoupled with domains 1 and 3. Domain 3 is a LF domain. For the LF domain a BEM formulation is used, even if boundary variables are random parameters because affected from randomness of domain 2, section 6.1. The HF subsystem is modelled with SIF formulation.
The external boundaries of the domains are supposed to be rigid, so the boundary condition $\partial p/\partial \vec{n} = 0$ is applied. The properties of the structure are reported in table 10.7, and an analytical calculation of the natural frequencies of the domains as a function of sound speed are reported in figure 10.13, just to show the differencies in vibro-acoustic behavior between the HF and the LF parts.

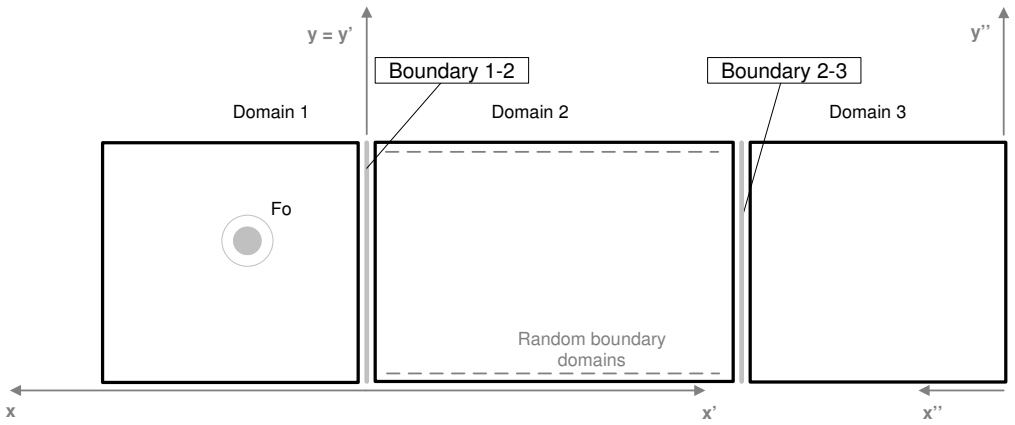

Figure 10.12: 3 Acoustical domains

	Side Length [m]	Sound speed [m/s]	ρ [kg/m^3]	η (%)
Acoustic Domain 1	1	550.0	234.5	0.01
Acoustic Domain 2	1	97.5	55.5	0.02
Acoustic Domain 3	1	400.5	200.5	0.01

Table 10.7: Application BEM-SIF: three acoustic domains. Geometrical and physical properties of the acoustic domains.

The frequency evolution of the responses at different boundary location over the three domains are reported in figures 10.14-10.22. The numerical results obtained with the hybrid formulation for the mid-frequency structures are compared to those obtained using a classical BEM formulation.
The initial four pictures are FOM solution on boundaries of domain 1 and 3, obtained in steps 1 and 2 of the formulation, to prove the effectiveness of the FOM modelling of the LF domains in the frequency range of interest. The following pictures are SOM solutions on the boundaries of the three domains. Those belonging to domains 1 and 3 are simply obtained multiplying the FOM solutions for their conjugates. The second order solutions for boundary nodes 9 and 53 are obtained through step 3 by the SIF second order formulation Those node belong to the two sides of domain 2 which are not coupled with the

Domain 3

n	m	Freq. Nat [Hz]
1	1	**283**
2	1	**448**
1	2	**448**
2	2	**566**
1	3	**633**
3	1	**633**
2	3	**722**
3	2	**722**
1	4	**826**
4	1	**826**
3	3	**850**
2	4	**896**
4	2	**896**
3	4	**1001**

Domain 2

n	m	Freq. Nat [Hz]
1	1	**69**
2	1	**109**
1	2	**109**
2	2	**138**
1	3	**154**
3	1	**154**
2	3	**176**
3	2	**176**
1	4	**201**
4	1	**201**
3	3	**207**
2	4	**218**
4	2	**218**
3	4	**244**

Figure 10.13: Application BEM-SIF: three acoustic domains. Analytical calculation of natural frequencies of the acoustical domain 3, $c = 400.5$ m/s, and domain 2, $c = 97.5$ m/s respectively.

deterministic domains, and their locations are affected from randomness, $\sigma = 0.05$.
We obtain a smooth contribution for the unknowns of the random acoustical domain, and a detailed description of the contributions of the deterministic domains. Figures 10.14-10.22 illustrates that coupling a deterministic formulation and SIF theory to model a mid-frequency behaving structure leads to relevant results.

For the deterministic-SIF solution a discretization of 80 elements for each domain has been used, 20 elements each side. For the BEM deterministic calculation, according to the wavelength of domain 2 at the upper value of the frequency range of interests, 2500 Hz, we have to use at least 500 elements each side. This is due to the fact that the mesh size is ruled by the frequency behavior of the HF domain; using a statistical formulation for the HF parts allows us to reduce the mesh size and consequently to gain in terms of complexity and calculation time. Those time comparisons are reported in table 10.8, they are qualitative results because they are obtained on a desktop pc.

We can easily understand that the det-SIF formulation is more complex than a classical deterministic formulation but it is a statistical formulation so it provides a solution which is representative of a population of structure in the HF range, and this is fundamental in the mid-frequency range, section 3.3. Moreover both the mesh dimension and the frequency step can be reduced for a calculation in the frequency domain where the structure can be regarded as mid-frequency, thanks to the use of a statistical formulation for the HF parts.

	BEM deterministic formulation	BEM-SIF mid-frequency formulation
Number of elements	120	120
Computational time [s]	1.27	20.9
Number of elements	3000	240
Computational time [s]	587	83.5

Table 10.8: Application BEM-SIF: three acoustic domains. Computational details, single frequency confrontation.

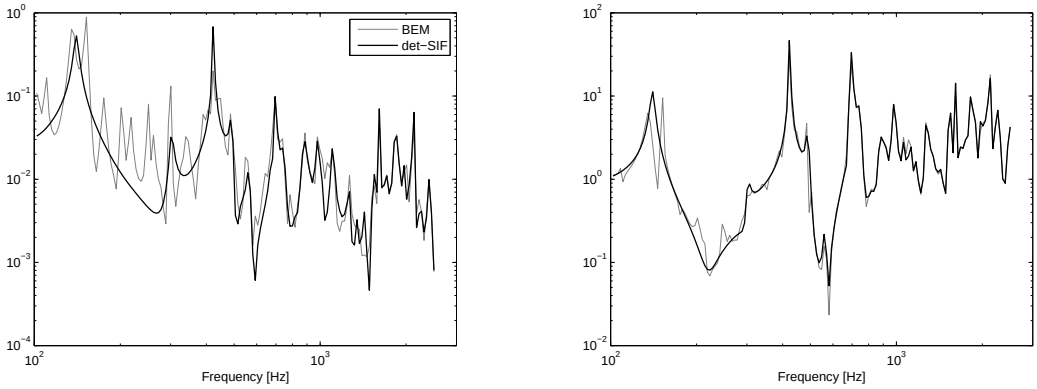

(a) (b)

Figure 10.14: Application BEM-SIF: three acoustic domains. FOM solution Domain 1, pressure at node 63 (a), and $\partial p/\partial \vec{n}$ at node 65 (b), on the coupled side. —— BEM-SIF. —— BEM.

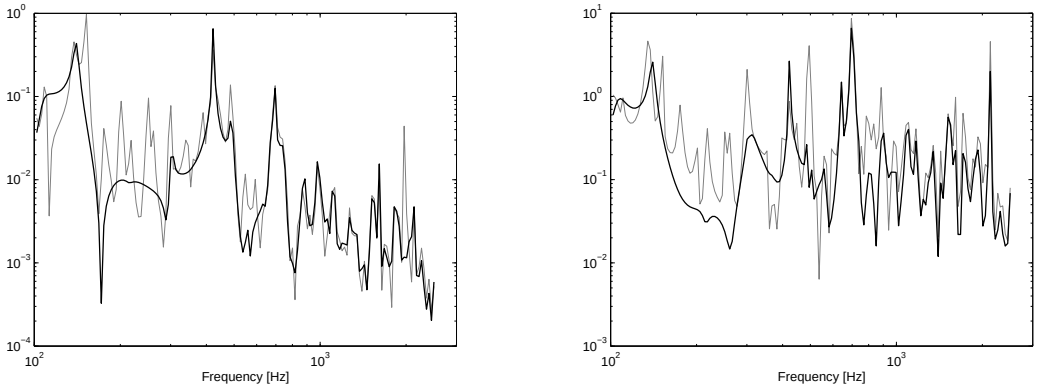

(a) (b)

Figure 10.15: Application BEM-SIF: three acoustic domains. FOM solution Domain 3, pressure at node 37 (a), and $\partial p/\partial \vec{n}$ at node 31 (b), on the coupled side. —— BEM-SIF. —— BEM.

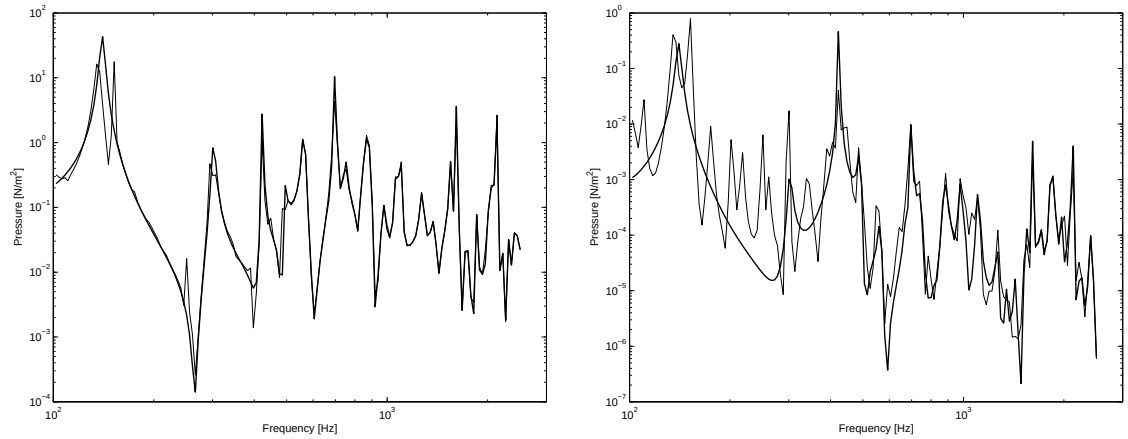

(a) (b)

Figure 10.16: Application BEM-SIF: three acoustic domains. SOM solution Domain 1, pressure at node 13 uncoupled (a), and pressure at node 63 coupled with domain 2 (b). —— BEM-SIF. —— BEM.

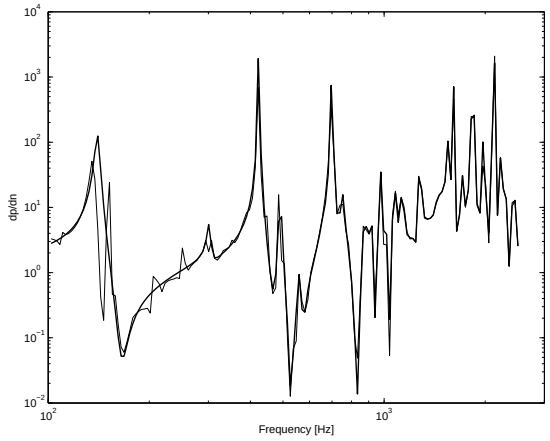

Figure 10.17: Application BEM-SIF: three acoustic domains. SOM solution Domain 1, $\partial p/\partial \vec{n}$ at node 75 on the coupled side. —— BEM-SIF. —— BEM.

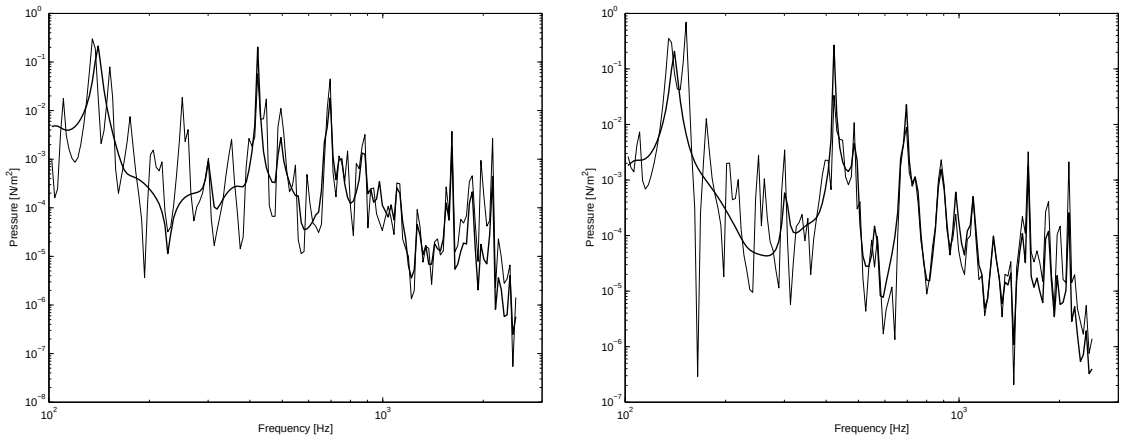

(a) (b)

Figure 10.18: Application BEM-SIF: three acoustic domains. SOM solution Domain 2, pressure at nodes 9 (a) and 53 (b) on the uncoupled sides. —— BEM-SIF. —— BEM.

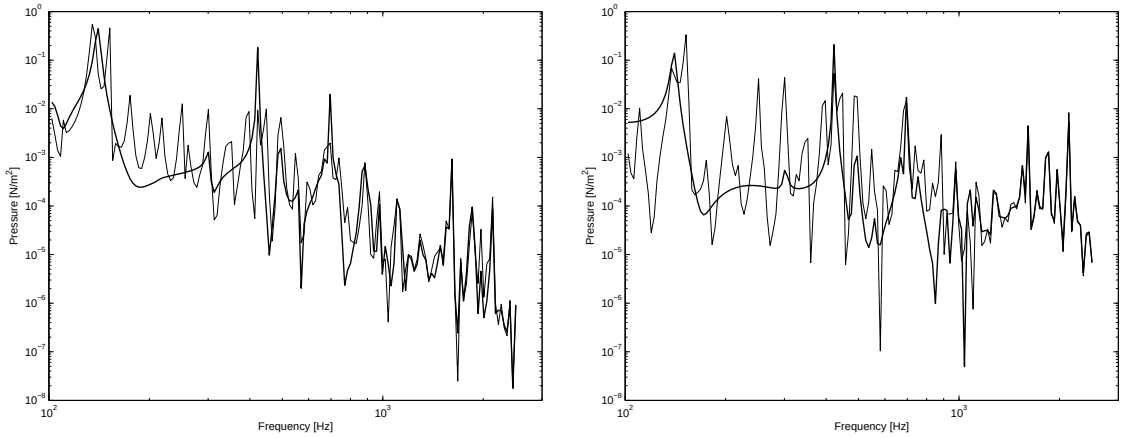

(a) (b)

Figure 10.19: Application BEM-SIF: three acoustic domains. SOM solution Domain 2, pressure at nodes 29 (a) and 75 (b) on coupled sides, respectively with domain 3 and domain 1. —— BEM-SIF. —— BEM.

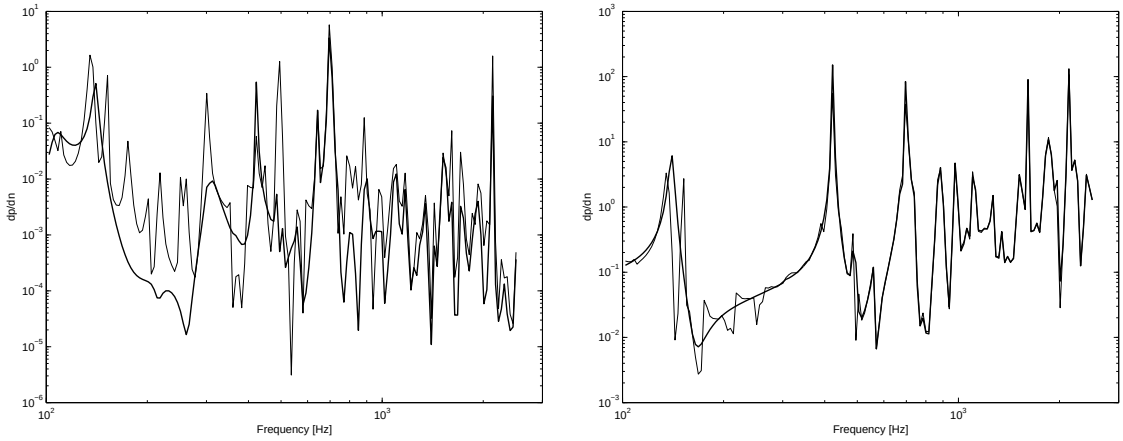

(a) (b)

Figure 10.20: Application BEM-SIF: three acoustic domains. SOM solution Domain 2 $\partial p/\partial \vec{n}$ at nodes 31 (a) and 69 (b) on the coupled sides, respectively with domain 3 and domain 1. —— BEM-SIF. —— BEM.

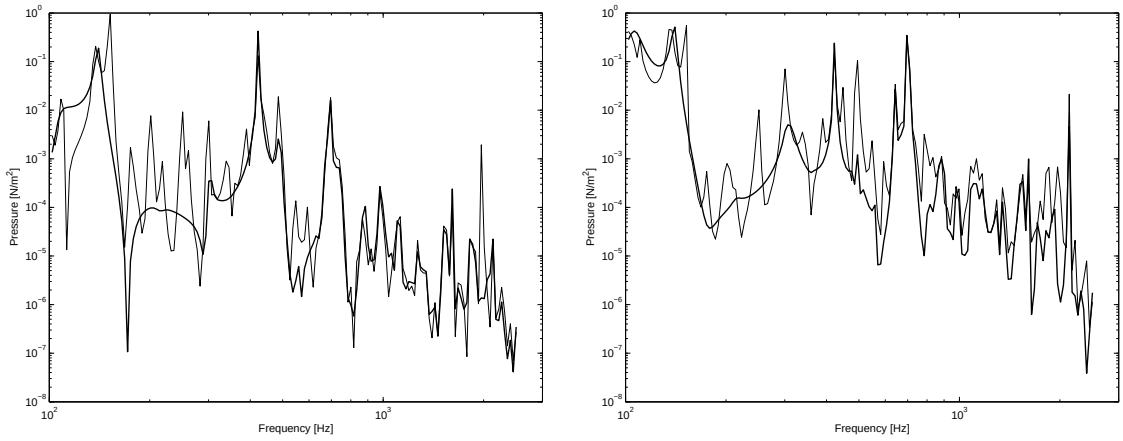

(a) (b)

Figure 10.21: Application BEM-SIF: three acoustic domains. SOM solution Domain 3 pressure at nodes 37 (a), on the coupled side with domain 2, and at node 71 (b) on the uncoupled side. —— BEM-SIF. —— BEM.

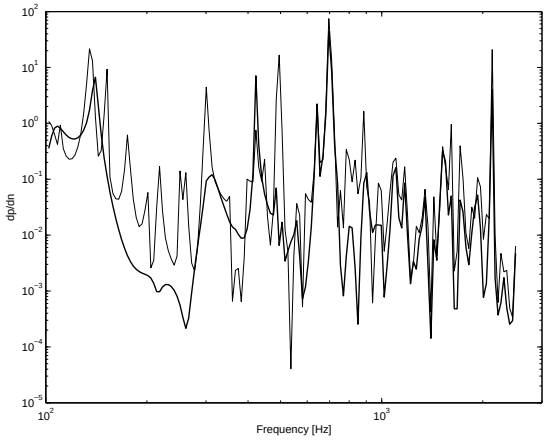

Figure 10.22: Application BEM-SIF: three acoustic domains. SOM solution Domain 3 $\partial p/\partial \vec{n}$ at node 31, coupled with domain. —— BEM-SIF. —— BEM.

10.4 Discussion

In this chapter the hybrid method, initially developed by the authors in chapter 6, has been improved and simplified in order to be able to correctly model complex structures. Different test structures have been analyzed obtaining good results: we obtain a smooth contribution for the unknowns of the random parts, and a detailed description of the contributions of the deterministic parts. The limitations in terms of heaviness and complexity which have been found in section 9.5, have been reduced by means of a first order modelling of the deterministic parts of the structure, which allows to reduce the number of unknowns.
The results obtained are consinstent for the mid-frequency range, because they provide a detailed and precise description of the response of the deterministic parts, accounting for the damping contribution of the high frequency parts; moreover they gives a statistical description of the high-frequency parts which accounts for all the possible effects of uncertainties in the geometric description of the structure.

Chapter 11

Conclusions and perspectives

The work reported in this thesis is about the development of a formulation for the analysis of structures in the mid-frequency range. In that perspective two main aspects of the frequency analysis of the structures have been considered: the correct prediction of the contribution of the LF structural parts, and the effect of uncertainties in geometrical dimensions for the HF parts. The method has been validated numerically with many different applications in terms of structural behavior and complexity.

11.1 Summary

The study of the peculiarities of the mid-frequency range and the state of the art of mid-frequency formulations, are the initial part of this Ph.D. work in order to understand the mid-frequency problem and to evaluate and choose the adequate way to manage the mid-frequency analysis.
The starting point is a statistical formulation, the SIF. It is based on a boundary integral formulation coupled with a statistical approach to account for uncertainties in the structural parameters. In order to solve the problem, some fundamental assumptions dealing with the correlation among the unknowns of the formulation are introduced. Those assumptions allows to obtain a close system solution of the SIF which does not require a recursive method. The SIF allows to describe the low-frequency modal behaviour of the structure with a precision close to the deterministic results, without being affected by the random description. In the high-frequency domain, the increasing complexity of the deterministic response is erased and the SIF only delivers the relevant information which is the global behaviour of the response of the structure. The middle frequency field corresponds to a transition zone between the precise low-frequency results and the smooth and global high-frequency response.

In this thesis, the fundamentals of the SIF were summarized. Some numerical applications of the SIF were proposed for different 1D and 2D structures, in order to illustrate the effectiveness of this approach on a wide frequency range. It was shown that in the low frequencies the SIF is able to precisely describe the successive modes and when the frequency increases the SIF prediction is able to give the trend of the strongly oscillating deterministic response. The SIF was then applied to the high-frequency domain. In this domain, the number of unknowns can be reduced, because it is not necessary to calculate the first order moments, which converge to zero. This enables to decrease the number of unknowns. The high-frequency SIF response is smooth and effectively gives the correct

trend of the response.

Then the SIF formulation was applied to structures which have a mid-frequency behavior in the frequency range of interest for the analysis. Different configuration of a simple structure, two coupled rods, were analyzed in order to understand the capabilities of SIF and the problem dealing with the mid frequency modelling of a structure. In details two different approaches were used:

1. an approach characterized by the assumption of deterministic boundaries for the low frequency rod, but the formulation based on SIF is still used, considering all the first and second order moments for both the two rods,

2. the second one introducing mid-frequency assumptions, the low frequency rod is described using the first order moment, supposing a low frequency behavior in all he frequency range, while the statistical rod is modelled using only the second order moments. For the second approach two different rods configuration are presented, to investigate all the possible different cases and to investigate the capacity of the formulation to simulate the physical behavior.

The use of these different approaches succeeded in understanding the modelling strategies: the deterministic system requires a model which accounts for the correlation among unknowns in order to capture the contributions of the LF parts.

Then, in order to develop a proper mid-frequency method, some hybrid formulations were developed, coupling the SIF formulation with different deterministic techniques, FEM and BEM. For this purpose, it was assumed that the mid-frequency range is the domain where a structure is constituted of two group of subsystems: one of stiff members exhibiting a low-frequency behaviour, and one of flexible members with a high-frequency behaviour. The HF parts of the structure have to be modelled using a statistical formulation to account for the fact that the properties of a structure are intrinsically uncertain. This global uncertainty plays no role in the low-frequency field, on the other hand it has a large influence on the high-frequency responses. The LF parts of the structure requires a LF modelling to account for the modal contributions. Starting from the previous assumptions a hybrid formulation was developed and tested. The entire formulation was derived for a structure made of two subsystems, the LF part is modeled with FE whereas the flexible part is modeled with SIF. This novel formulation was applied to two coupled rods. The results show that the hybrid formulation is able to accurately predict the modal behaviour of the LF subsystems and give the smooth trend of the fast varying response, contribution of the HF subsystems.
An advantage of the hybrid formulation based on SIF, arises from the fact that the equations of SIF are based on the classical governing equations, which allows to write the usual boundary and assembly conditions in terms of displacements and forces. The derivation of coupling factors (such as for the SEA) is not required for the random formulation. Both FEM (or BEM) and SIF variables are expressed, for instance, in terms of force and displacement, therefore they are homogeneous and can be easily coupled. The method does not present the difficulty to couple force and displacement with power and energy quantities of FEM-SEA hybrid methods.

The method is then extended to some 2D structures, in particular acoustic domains based on Helmholtz law. The 2D applications allows to better understand and to evidence

the problematic relative to the complexity of the formulation and the calculation efforts. A SIF application to a random isolated domain highlighted the effectiveness of SIF also for the 2D structures. SIF was then coupled to BEM to investigate the response of a structure made of 2D acoustical domains, with mid-frequency properties. This application of BEM-SIF gave really good results and confirmed the right choices for mid-frequency modelling. As before, the frequency variation of the response gradually gets smoother when the frequency increases and simultaneously an accurate description of the response of the deterministic domain is obtained. The only drawback was the excessive complexity of the formulation, which can limit the easy of use of the formulation for more complex systems.

In the last chapter, the final version of the hybrid method was presented. Even if it is based on the same assumptions that ruled the development of the method and its previous application, the formulation was simplified and made it more easy to use. In details, the deterministic parts of the structure are solved first, in terms of first order moments, accounting for the contributions of the HF members as reverberant contributions, to add the damping effect. Then, once the first order solution of the LF parts is obtained, the HF part is solved in terms of second order moments. Thanks to the use of SIF, the formulation results lighter but equally effective and easy to use for more complex systems.
This final formulation gave very good results and demonstrated the effectiveness of the hybrid method for treating mid-frequency structures. Thanks to the simplification it was possible to solve more complex structures like three coupled domains and a "sandwich 2D structure" made of beams and an acoustic cavity.
The advantages of this hybrid method, FEM-SIF or BEM-SIF are:

- the frequency step that is used for the calculations may be sensitively coarsen when employing the FEM-SIF formulation. The "non-modal" output obtained for the HF subsystems, which leads to a smooth frequency response enables to link the frequency step to the wavelength of the LF frequency subsystems, which are characterized by a low modal density. This allows us to reduce the number of frequency calculation steps for the hybrid method, and thus sensitively reduce the calculation times.

- the use of the SIF formulation for the HF part of the structure. There is no need for a refined discretization of the long subsystem because of the slow spatial variations of the responses. A gain in terms of computational resources is consequently achieved.

In conclusion we can say that with the development of the hybrid formulation based on SIF, a possible solution to the mid-frequency problem is given.

11.2 Future perspectives

The hybrid method is actually in its initial stage and it has been developed for classical and simple structures. The formulation has to be extended and improved to be suitable for practical applications. At present the hybrid method needs an experimental validation, and a subsequent development to treat a simple and practical case. Two possible and interesting applications of the method can be envisaged:

- the SIF formulation should be extended to the 3D case, in particular to treat the acoustic cavities, which usually presents a high frequency behavior with respect to the structural parts of a vehicle. The 3D SIF formulation could be then coupled to the

FEM of some structural parts. The use of SIF instead of SEA to model the acoustic cavity, like the passenger compartment, has the advantage to give a statistical result, but also not spatially averaged. Having the punctual response is useful for all the applications dedicated to the improvement of NVH performances as well as to the sound quality and sound perception (e.g speech intelligibility index) in a car;

- the hybrid FEM-SIF formulation can be used to model the effect of the damping on the structure applied to the acoustic components. The structural components are modelled using a deterministic formulation, while the damping and statistical contributions of the acoustic foams and layers can be modelled using a statistic method. The effect and the contributions evaluated could then be used in the FEM model of a vehicle structure.

The application of the hybrid method to those cases could lead to relevant results because of the flexibility and consistency of the hybrid formulation. And those application could be relevant for the automotive industry in order to provide a tool to effectively simulate the mid-frequency behavior of vehicle structures.

Appendix A

Calculation of the expectation of a complex exponential function

In this appendix we want to evaluate the analytical expression of the expectation of a generic complex exponential term like $e^{ik(x+\varepsilon)}$. ε is an uncertain variable, $k = k_0(1 - i\eta/2)$ is a complex constant, and x is a deterministic variable. The evaluation of the expectation is carried out on the term $e^{ik(x+\varepsilon)}$, ε is a zero mean gaussian variable, with standard deviation σ. The probability density function is:

$$f(y) = \frac{1}{\sqrt{2\pi}\sigma} e^{-\frac{y^2}{2\sigma^2}} \tag{A.1}$$

The analytical calculation of expectation of $e^{ik(x+\varepsilon)}$ can be carried out:

$$\langle e^{ik\varepsilon} \rangle_\varepsilon = \frac{1}{\sqrt{2\pi}\sigma} \int_{-\infty}^{\infty} e^{-\frac{y^2}{2\sigma^2}} e^{iky} dy \tag{A.2}$$

We can change the integration variable: $X = \dfrac{y}{\sqrt{2}\sigma}$ and rewrite eq.(A.2):

$$\begin{aligned} \langle e^{ik\varepsilon} \rangle_\varepsilon &= \frac{1}{\sqrt{\pi}} \int_{-\infty}^{\infty} e^{-X^2 + ik\sqrt{2}\sigma X} dX \\ &= \frac{1}{\sqrt{\pi}} \int_{-\infty}^{\infty} e^{-X^2 + \eta k_0 \frac{\sqrt{2}}{2}\sigma X + ik_0\sqrt{2}\sigma X} dX \\ &= \frac{e^{\eta^2 k_0^2 \sigma^2/8}}{\sqrt{\pi}} \int_{-\infty}^{\infty} e^{-(X^2 - \eta k_0 \frac{\sqrt{2}}{4}\sigma)^2} e^{ik_0\sqrt{2}\sigma X} dX \end{aligned} \tag{A.3}$$

Another change of variable is required: $Y = X - \eta k_0 \dfrac{\sqrt{2}}{4}\sigma$.
Thanks to the odd property of the integral function, we finally obtain:

$$\begin{aligned} \langle e^{ik\varepsilon} \rangle_\varepsilon &= \frac{e^{\eta^2 k_0^2 \sigma^2/8} e^{i\eta k_0^2 \sigma^2/2}}{\sqrt{\pi}} \int_{-\infty}^{\infty} e^{-Y^2} e^{ik_0\sqrt{2}\sigma Y} dY \\ &= \frac{e^{\eta^2 k_0^2 \sigma^2/8} e^{i\eta k_0^2 \sigma^2/2}}{\sqrt{\pi}} \int_{-\infty}^{\infty} e^{-Y^2} \cos(k_0\sqrt{2}\sigma Y) dY \end{aligned} \tag{A.4}$$

The last integral in a known definite integral, which can be found on specialized mathematical books [64], and we obtain:

$$\langle e^{ik\varepsilon} \rangle_\varepsilon = \frac{e^{\eta^2 k_0^2 \sigma^2/8} e^{i\eta k_0^2 \sigma^2/2}}{\sqrt{\pi}} \sqrt{\pi} e^{-k_0^2 \sigma^2/2}$$

$$= \quad e^{\eta^2 k_0^2 \sigma^2/8} e^{i\eta k_0^2 \sigma^2/2} e^{-k_0^2 \sigma^2/2} \tag{A.5}$$

Bibliography

[1] W.Desmet, Mid-frequency vibro-acoustic modelling: challenges and potential solutions, *ISMA International Conference on Noise & Vibration Engineering*, 16-18 September 2002, Leuven (Belgium).

[2] R.Ohayon and C.Soize, *Structural Acoustics and Vibration: Mechanical models, Variational Formulations and Discretization*, Academic Press, San Diego, CA.

[3] N.Baldanzini, Progettazione meccanica per la riduzione del rumore e delle vibrazioni: lo strumento della Statistical Energy Anlysis, *XXX Convegno Nazionale AIAS*, Alghero, 12-15 Settembre 2001.

[4] P.J.Shorter, B.K.Gardner, P.G.Bremner, *A Review of Mid-Frequency Methods for Automotive Structure-Borne Noise*, Vibro-Acoustic Sciences, 2001.

[5] M.P.Castanier and C.Pierre, *Mid-Frequency Vibrational Analysis of Complex Structures: State of the Art and Future Directions*, Report of the Department of Mechanical Engineering, 2003, The University of Michigan, Ann Arbor, MI.

[6] O.C.Zienkiewicz and R.L.Taylor, *The finite Element Method*, 2000.

[7] R.Butterfield and K.Bannerjee, *Boundary Element Methods in Engineering Science*. NewYork, 1981.

[8] C.A.Brebbia, *The Boundary Element Method for Engineers*, Pentech. London, 1984.

[9] R.D.Ciskowski and C.A.Brebbia, *Boundary Element Methods in Acoustics*,WIT Press, Southampton, 1991..

[10] L.Cremer, M.Henckl, E.E.Ungar, *Structure Borne Sound*, New York Springler- Verlag, 1973.

[11] J.Guyader, C.Boisson, C.Lesueur, Energy transmission in finite coupled plates, Part.1 Theory, *Journal of Sound and Vibrations*, 81(1), 81-92, 1982.

[12] B.Mace, P.Shorter, Energy Flow models from finite element analysis, *Journal of Sound and Vibrations*, 233(3), 369-389, 2000.

[13] *M.S.C. Nastran, 2001 Quick Reference Guide*, The MacNeal-Schwendler Corporation, CA, 2001.

[14] R.H.Lyon and R.DeJong, *Theory and application of Statistical Energy Analysis*. Butterworth-Heinemann, 1995.

[15] A.Le Bot, A vibro-acoustic model for high-frequency analysis. *Journal of Sound and Vibration*, 211(4), 537-554, 1998.

[16] M.N.Ichchou, A.Le Bot and L.Jezequel, Energy Models of One-Dimensional, Multi-Propagative Systems, *Journal of Sound and Vibration*, 201, pp. 535-554, 1997.

[17] J.A.Steel and R.J.M. Craik, *Sound Transmission through Buildings using Statistical Energy Analysis*. Gower, England, 1996.

[18] K. De Langhe, *High-frequency Vibrations: Contributions to Experimental and Computational SEA Parameter Identification Techniques*, PhD Thesis, Katholieke Universiteit Leuven, Belgium, February 1996.

[19] R.Langley, A general derivation of the statistical energy analysis equations for coupled dynamic systems, *Journal of Sound and Vibrations*, 135(3), 499-508, 1989.

[20] B.Mace, Wave coherence, coupling power and statistical energy analysis, *Journal of Sound and Vibrations*, 199(3), 369-380, 1997.

[21] R.Langley, K.Heron, Elastic wave transmission through plate/beam junctions, *Journal of Sound and Vibrations* , 143(2), 241-253, 1990.

[22] R.Langley, P.Shorter, The wave transmission coefficients and coupling loss factors of point connected structures, *Journal of Acoustic Society of America*, 113 (4), 1947-1964, 2003.

[23] J.C. Wohlever, R.J. Bernhard, Mechanical energy flow models of rods and beams. *Journal of Sound and Vibration*, vol.153(1), 1-19, 1992.

[24] O.M. Bouthier, R.J. Bernhard, Simple models of the energetics of transversely vibrating plates. *Journal of Sound and Vibration*, vol. 182(1), 149-166, 1995.

[25] Y. Lase, M.N. Ichchou, L. Jezequel, Energy flow analysis of bars and beams: theoretical formulations. *Journal of Sound and Vibration*, vol.192(1), 281-305, 1996.

[26] R.S. Langley, On the vibrational conductivity approach to high frequency dynamics for two-dimensional structural components. *Journal of Sound and Vibration*, vol. 182(4), 637-657, 1995.

[27] A. Carcaterra, A. Sestieri, Energy density equations and power flow in structures. *Journal of Sound and Vibration*, vol. 188(2), 269-282, 1995.

[28] A.Pierce, *Acoustics*, McGraw-Hill 1991.

[29] R.Waterhouse, Interference patterns in reverberant sound fields, *The Journal of Acoustic Society of America*, 27(2), 247-258, 1995.

[30] N. Vlahopoulos and X. Zhao, An investigation of power flow in the mid-frequency range for systems of co-linear beams based on a hybrid finite element formulation. *Journal of Sound and Vibration*, 242(3), 445-473, 2001.

[31] P.J.Shorter, B.K.Gardner, A.V.Parrett, Q.Zhang, Full-spectrum structural-acoustic response predictions using the RESOUND approach to the mid-frequency problem, *Proceedings of INTER-NOISE 2002 Conference*, 19-21 August, Dearborn, USA.

[32] L. Gagliardini, L. Houillon, L. Petrinelli, and G. Borello, Virtual SEA: mid-frequency structure-borne noise modeling based on finite element analysis, *Proceedings of the SAE Noise and Vibration Conference*, Traverse City, Michigan USA, May 2003.

[33] R.S.Langley, P.Bremner, A hybrid method for the vibration analysis of complex structural-acoustic systems, *Journal of Acoustic Society of America* , 105 (3), 1657-1671, 1999.

[34] R.R.Craig and M.C.C.Bampton, Coupling of substructures for dynamic analysis, *AIAA Journal*, 6, 1313-1319.

[35] R.S.Langley, A wave intensity technique for the analysis of high-frequency vibrations, *Journal of Sound and Vibration* , 159(3), 483-502, 1992.

[36] C.Simmons, Structure-Borne Sound Transmission Through Plate Junctions and Estimates of SEA Coupling Loss Factors Using the Finite Element Method, *Journal of Sound and Vibration*, 144, pp. 215-227, 1991.

[37] L.Maxit and J.L.Guyader, Estimation of SEA Coupling Loss Factors Using a Dual Formulation and FEM Modal Information, Part I: Theory, *Journal of Sound and Vibration*, 239, pp. 907-930, 2001.

[38] L.Maxit and J.L.Guyader, Estimation of SEA Coupling Loss Factors Using a Dual Formulation and FEM Modal Information, Part 11: Numerical Applications, *Journal of Sound and Vibration*, 239, pp. 931-948, 2001.

[39] N.Baldanzini, M.Pierini and A.Scippa, On the integration of finite elements and statistical energy analysis to improve the calculation of coupling loss factors, *ISMA International Conference on Noise & Vibration Engineering*, 20-22 September 2004, Leuven (Belgium).

[40] H.Yan, A.Parrett and W.Nack, Statistical Energy Analysis by Finite Elements for Middle Frequency Vibration, *Finite Elements in Analysis and Design*, 35, pp. 297-304, 2000.

[41] C.Soize, P.M.Hutin, A.Desanti, J.M.David and F.Chabas, Linear Dynamic Analysis of Mechanical Systems in the Medium Frequency Range, *Computers and Structures*, 23, pp. 605-637, 1986.

[42] C.Soize, A model and numerical method in the medium frequency range for vibro-acoustic predictions using the theory of structural fuzzy, *Journal of the Acoustical Society of America*, 94, 849-865, 1993.

[43] C.Soize and K.Bjaoui, Estimation of Fuzzy Structure Parameters for Continuous Junctions, *Journal of the Acoustical Society of America*, 107, pp. 201 1-2020, 2000.

[44] A.K.Belyaev, Dynamic Simulation of High-Frequency Vibration of Extended Complex Structures, *Mechanics of Structures and Machines*, 20, pp. 155-168, 1992.

[45] A.K.Belyaev, High-Frequency Vibration of Extended Complex Structures, *Probabilistic Engineering Mechanics*, 8, pp. 15-24, 1993.

[46] P.J. Shorter, R.S. Langley, On the reciprocity relationship between direct field radiation and diffuse reverberant loading. *Journal of Acoustical Society of America*, 288(3), 669-699, 2005.

[47] P.J. Shorter, R.S. Langley, Vibro-acoustic analysis of complex systems. *Journal of Sound and Vibration*, 117(1), 85-95, 2005.

[48] N.Vlahopoulos and X.Zhao, Basic Development of Hybrid Finite Element Method for Midfrequency Structural Vibrations, *AIAA Journal*, 37, pp. 1495-1505, 1999.

[49] X.Zhao and N.Vlahopoulos, Coupling the Finite Element and the Energy Finite Element Solutions for Calculating the Vibration of Co-linear Beams in the Mid-Frequency Range, *Noise & Vibration Conference & Exposition*, May 1999, Traverse City, MI, USA.

[50] X.Zhao and N.Vlahopoulos, A hybrid finite element formulation for mid-frequency analysis of systems with excitation applied on short members, *Journal of Sound and Vibration*, 237(2), 181-202, 2000.

[51] X.Zhao and N.Vlahopoulos, A basis hybrid finite element formulation for mid-frequency analysis of beams connected at an arbitrary angle. *Journal of Sound and Vibration*, 269, 135-164, 2004.

[52] Sang Bum Hong, Aimin Wang and Nickolas Vlahopoulos, A hybrid finite element formulation for a beam-plate system. *Journal of Sound and Vibration*, 298(1-2), 233-256, 2006.

[53] M.Viktorovitch, F.Thouverez, and L.Jezequel, A new random boundary element formulation applied to high-frequency phenomena, *Journal of Sound and Vibration*. 223(2), 273-296, 1999.

[54] M.Viktorovitch, F.Thouverez, and L.Jezequel, An integral formulation with random parameters adapted to the study of the vibrational behaviour of structures in the mid and high-frequency field, *Journal of Sound and Vibration*, 247(3), 431-452, 2001.

[55] M.Viktorovitch, *Formulations statistiques des structures vibrantes sur un large spectre frequentiel*, PhD Thesis, Ecole Centrale de Lyon, France, December 1998.

[56] F.J.Fahy and A.D.Mohammed, A study of uncertainty in applications of sea to coupled beam and plate systems, part I: Computational experiments, *Journal of Sound and Vibration*, 158(1), 45-67, 1992.

[57] A.J.Keane and C.S.Manohar, Energy flow variability in a pair of coupled stochastic rods, *Journal of Sound and Vibration*, 168, 253- 284, 1993.

[58] A.J.Keane and C.S.Manohar, *Statistics of Energy Flows in Spring-Coupled One-Dimensional Subsystems*, Cambridge: Cambridge University Press, 1997.

[59] K.F.Graff, *Wave motion in elastic solids*, NewYork: Dover Publications, 1991.

[60] N.Metropolis and S.Ulam, The Monte Carlo Method, *J. Amer. Stat. Assoc*, 44, 335-341, 1949.

[61] M.Abramowitz and I.A.Stegun, *Handbook of Mathematical Functions with Formulas, Graphs, and Mathematical Tables*. New York, Dover, 1965.

[62] G.C.Everstine, Finite elements formulations of structural-acoustics problems, *Computers & Structures*, 65 (3), 307-321, 1997.

[63] A.Alia and M.Souli, Simulation of vibroacoustic problem using coupled FE/BE formulation, *EURODYN 2005 Conference*, 4-7 September 2005, Paris.

[64] M.R.Spiegel, *Schaum's Mathematical Handbook of Formulas and Tables*, Paperback, 2000.

Personal publications

Conference proceedings

[1] N.Baldanzini, M. Pierini , A. Pratellesi and M. Viktorovitch, A stochastic integral formulation for mid- and high- frequency structure-borne investigations, NOVEM *Noise and Vibration: Emerging Methods International Conference* 18-21 April 2005, Saint Raphael (France).

[2] N.Baldanzini, P.Citti, M.Pierini, A.Pratellesi and M.Viktorovitch, A novel mid-frequency formulation for vibro-acoustic predictions, *FLORENCE ATA 2005 Vehicle Architectures: evolution towards improved safety, low-weight, ergonomics and flexibility*, 11-13 May 2005, Florence (Italy).

[3] N.Baldanzini, M. Pierini , A. Pratellesi and M. Viktorovitch, A novel mid-frequency formulation for vibro-acoustic predictions, *RIETER Automotive Conference*, 8-10 June 2005, Pfäffikon SZ (Switzerland).

[4] A.Pratellesi, M.Viktorovitch, M.Pierini, N.Baldanzini, A hybrid formulation for the vibro-acoustic analysis of structures in the mid-frequency domain, *ISMA International Conference on Noise & Vibration Engineering*, 18-20 September 2006, Leuven (Belgium).

[5] A.Pratellesi, M.Viktorovitch, M.Pierini, N.Baldanzini, Vibroacoustic modelling in the mid-frequency range od a 2D system for structure-borne analysis, *FISITA 2006 World Automotive Congress*, 22-27 October, Yokohama (Japan).

[6] M.Viktorovitch, A.Pratellesi, A mid-frequency formulation for structure-borne vibro-acoustic predictions, *INTERNOISE 2006*, 3-6 December 2006, Honolulu (USA).

Journals

[7] A.Pratellesi, M.Viktorovitch, N.Baldanzini, M.Pierini, A hybrid formulation for mid-frequency analysis of assembled structures, in review of the *Journal of Sound and Vibration*.